

# **Involvement of Class IA phosphoinositide 3-kinase (PI3K) in cell division and DNA repair**

by

Amit Kumar

Submitted to the Department of Molecular Biology  
in Partial Fulfilment of the Requirements for the degree of

Doctor en Biología Molecular  
por la Universidad Autónoma de Madrid

May 2009

Carried out at

Department of Immunology and Oncology  
Centro Nacional de Biotecnología  
Madrid, Spain

## ABSTRACT

The role of class I<sub>A</sub> PI3K in cell growth and cell cycle entry is well described. In addition to its activation in early G1 phase, PI3K is also activated in late G1 and is essential for G1/S phase transition. The exact mechanism of PI3K activation and the role it plays in G1/S phase transition is nonetheless poorly understood. Our observations indicate that activation of Ras and Tyr kinases is required for late G1 PI3K activation. Inhibition of late G1 PI3K activity results in low c-Myc and cyclin A expression, impaired Cdk2 activity, and reduced loading of MCM2 (minichromosome maintenance protein) onto chromatin. Conditional activation of c-Myc in late G1 or expression of a stable c-Myc mutant counteracted PI3K inhibition in late G1 and restored S phase entry. Based these findings, we concluded that Tyr kinases and Ras cooperate to induce the second PI3K activity peak in G1, which mediates initiation of DNA synthesis by inducing c-Myc stabilization.

Class I<sub>A</sub> PI3K is reported to localise to the nuclei in various cell types. We further studied the PI3K isoforms in the nucleus and their mode of translocation to the nucleus. The work presented in this thesis indicates that, of the ubiquitously expressed p110 $\alpha$  and p110 $\beta$  class I<sub>A</sub> isoforms, p110 $\beta$  was mainly nuclear, whereas p110 $\alpha$  was mostly cytoplasmic. We also found that, of the regulatory subunits p85 $\alpha$  and p85 $\beta$ , p85 $\beta$  was nuclear and p85 $\alpha$  was mostly cytoplasmic. In addition, we showed that p110 $\beta$  does not translocate to the nucleus on its own, but requires p85 $\beta$  association for nuclear translocation; this phenomenon is facilitated by a polybasic nuclear localization sequence in the p110 $\beta$  C2 domain. Nonetheless, the overexpressed p85 $\beta$ /p110 $\beta$  complexes did not show physiological nuclear staining as seen for the endogenous proteins. We identified PCNA association to p110 $\beta$ , which further helps nuclear translocation of p85 $\beta$ /p110 $\beta$  complexes.

To gain a better understanding of nuclear p110 $\beta$  function, we pulled down p110 $\beta$ -associated proteins in the nucleus. Mass spectra analysis showed DNA checkpoint proteins RAD17, RAD9, RAD50, among others. Hence, we examined the role of p110 $\beta$  in DNA repair. We observed activation of p110 $\beta$  following ultraviolet/ionizing radiation (UV/IR) exposure. We found RAD17 association to p110 $\beta$  only after UV/IR exposure. Using RNA interference in NIH3T3 cells, and knocked-out, immortalised murine embryonic fibroblasts, we demonstrate that p110 $\beta$ -deficient cells showed large numbers of chromosomes and aberrant chromosome breaks, implicating a p110 $\beta$  function in the maintenance of genomic integrity. We identified defective ATR (inactive Chk1 and reduced accumulation of p-RAD17 at DSB foci) and ATM (reduced SMC1 and  $\gamma$ -H2AX phosphorylation) signalling pathways. These defects were at the level of DNA sensor protein recruitment at the DNA damage sites, as we observed defective mobility of the DSB sensor protein NBS1 at damage sites. We also found a direct role of p110 $\beta$  in the regulation of DNA repair; p110 $\beta$  activation and its colocalisation with  $\gamma$ -H2AX at the DNA damage area imply an integrative role for p110 $\beta$  in the aftermath of DNA damage responses. In conclusion, we provide a molecular rationale as to how p110 $\beta$  integrates the regulation of different signalling pathways in response to DNA damage and show that depletion of p110 $\beta$  disrupts activation of DNA checkpoint proteins.

Thesis Supervisor: Ana Clara Carrera

Title: Professor

Dedicated with respect to the man who inspired me,  
**my grandfather**

## ACKNOWLEDGMENTS

First of all, I would like to acknowledge my thesis advisor, Ana Carrera, for giving me an opportunity to perform my doctoral thesis under her guidance. I am also grateful to her for unwavering support and sound advice as I embarked on new kinds of investigation in the lab. Her consistent encouragement and good judgement has resulted in a productive lab with a lot of good company. Working in her lab has been an invaluable experience for me; she has taught us that a lot more than good data is needed to be a mature and successful researcher.

For help, advice and their efforts, I sincerely thank the members of Ana's lab, past and present, over the last five years. In particular I would like to thank (past members) Zaira, Mónica, Domingo, Almira, Álvaro (now in lab 418) for helping me in adapting to the new change in my life. Of the present members, I thank Miriam for being a good friend and colleague, Abel and Vicen for being wonderful guys and for the discussions we had during late evening stays in the lab; both have also been good friends inside and outside the lab. Thanks are also due to Ana González, Susana, Jesús, Vir, Isabela, Lorena, Carmen and Isa for their friendliness and collaboration. Vicen and Susana also helped me in Spanish translation of part of the thesis. All these colleagues have made my stay in the lab both enjoyable and productive, and this work would not have been possible without such great support.

I would like to acknowledge Oscar Fernández-Capetillo and his lab members, who helped in conducting DNA damage experiments. In particular, thanks to Juan Lu for arranging and reserving the microscope facility at the CNIO, and Diego for performing the laser based DNA damage experiments.

I also thank all the DIO members, the CNB personnel department, the Biosecurity division, the microcomputing facility, and the security guards for their kind support; I could not have asked for more. From the department, I want to acknowledge in particular César (415), Sonia (415), Cristina (418/412/16), as well as Laura, Pilar, Bea, Borja and Oscar (all in 416), Quim (418), Jens (415), Valeria (413), Jesús Chamorro and Juanjo (413), Mohi (Genomics Facility), Antonio, Maria and Coral (Administrative department), as well as all past and current members of the DIO kitchen staff for their support and timely help. I would also like to thank Sara and Mari Carmen for their help in conducting flow cytometry analysis. Special thanks to Mario (416), Santos (415), Isabel Mérida (414) and Karel (411) for their sound advice and reagents at many junctures over the years.

A very special thanks to Cathy, who has helped me throughout these years with her critical editing, or I should say simplifying our manuscript content to make our research clear for non-native-English speakers around the world. Thank you, Cathy, for being such a wonderful person.

Most importantly, I owe thanks to all my friends outside the world of science who made my stay easier and more fun over the last five years. My biggest support has been my wife and lifeline, Rashmi. Together we have navigated through some difficult times in research and in life. Raising our daughter Tishya has been a challenging and rewarding experience. Lastly, I cannot thank enough my parents and my late grandfather, to whom I owe everything I have.



## Articles Published

1. Marqués M\*, **Kumar A\***, Poveda AM, Zuluaga S, Hernández C, Jackson S, Pasero P and Carrera AC. 2009. Specific function of phosphoinositide 3-kinase beta in the control of DNA replication. *Proc Natl Acad Sci USA* 106:7525-7530 *\*equal contribution*
2. Marqués M, **Kumar A**, Cortés I, Gonzalez-García A, Hernández C, Moreno-Ortiz MC and Carrera AC. 2008. Phosphoinositide 3-kinases p110alpha and p110beta regulate cell cycle entry, exhibiting distinct activation kinetics in G1 phase. *Mol Cell Biol* 28(8); 2803-14.
3. Alcázar I, Marqués M, **Kumar A**, Hirsch E, Wymann M, Carrera AC, Barber DF. 2007. Phosphoinositide 3-kinase gamma participates in T cell receptor-induced T cell activation. *J Exp Med* 204; 2977-87.
4. **Kumar A**, Carrera AC. 2007. New functions for PI3K in the control of cell division. *Cell Cycle*, 6; 1696-8.
5. García Z, Silio V, Marqués M, Cortés I, **Kumar A**, Hernandez C, Checa AI, Serrano A, Carrera AC. **2006**. A PI3K activity-independent function of p85 regulatory subunit in control of mammalian cytokinesis. *EMBO J* 25; 4740-51.
6. **Kumar A**, Marqués M, Carrera AC. 2006. Phosphoinositide 3-kinase activation in late G1 is required for c-Myc stabilization and S phase entry. *Mol Cell Biol* 26(23); 9116-25.
7. García Z, **Kumar A**, Marqués M, Cortés I, Carrera AC. 2006. Phosphoinositide 3-kinase controls early and late events in mammalian cell division. *EMBO J* 25(4); 655-61.
8. **Kumar A**, Vaid A, Syin C, Sharma P. 2004. PfPKB, a novel protein kinase B-like enzyme from Plasmodium falciparum: I. Identification, characterization, and possible role in parasite development. *J Biol Chem* 279(23); 24255-64.
9. **Kumar A**, Megías D, Fernandez-Capetillo O, Carrera AC. Phosphoinositide 3-kinase beta is essential for sensing DNA damage. *Manuscript in preparation*.

**Patent Application:** Carrera AC, Marqués M and **Kumar A**. Role of p110 $\beta$  in DNA repair.

## TABLE OF CONTENTS

<b>RESUMEN ESPAÑOL .....</b>	<b>7</b>
<b>Resumen.....</b>	<b>9</b>
<b>Resumen Introducción.....</b>	<b>11</b>
<b>Objetivos.....</b>	<b>15</b>
<b>Resumen Resultados.....</b>	<b>17</b>
<b>Conclusiones.....</b>	<b>19</b>
<b>Resumen Discusión.....</b>	<b>21</b>
 <b>INTRODUCTION.....</b>	 <b>25</b>
<b>SECTION 1.    Growth Factor Receptos.....</b>	<b>27</b>
1.1)    Receptor tyrosine kinases	
1.2)    G protein-coupled receptor	
 <b>SECTION 2.    Signal Transduction Proteins.....</b>	 <b>28</b>
2.1)    RAS	
2.2)    Mitogen Activated Protein Kinases	
 <b>SECTION 3.    Phosphoinositides-3 Kinases.....</b>	 <b>29</b>
3.1)    Class I PI3K	
3.1.1)    Class I <sub>A</sub> PI3K	
3.1.1.1)    PDK1	
3.1.1.2)    Protein kinase B	
3.1.2)    Class I <sub>B</sub> PI3K	
3.1.3)    PTEN	
3.2)    Class II PI3K	
3.3)    Class III PI3K	
3.4)    Class IV PI3K	
 <b>SECTION 4.    Nuclear Class I<sub>A</sub> Phosphoinositide-3-Kinase Signalling.....</b>	 <b>34</b>
4.1)    Role of nuclear Akt	
<b>SECTION 5.    Nuclear Regulatory Proteins.....</b>	<b>36</b>
5.1)    c-Myc	
<b>SECTION 6.    Cell Cycle.....</b>	<b>37</b>
6.1)    From G0 to S	
6.1.1)    Progression through G1 phase	
6.1.2)    Progression through late G1 to S phase	
6.2)    S phase entry and progression	
6.3)    G2 phase	
6.4)    Mitosis	
6.4.1)    Prophase	
6.4.2)    Metaphase	
6.4.3)    Anaphase	
6.4.4)    Telophase	
6.5)    Cytokinesis	
6.6)    Class I <sub>A</sub> PI3K and the cell cycle	
 <b>SECTION 7.    DNA Damage Response.....</b>	 <b>45</b>
7.1)    Sensors	
7.1.1)    MRN complex	
7.1.2)    Rad17-RFC and the 9-1-1 complex	
7.1.3)    ATM and ATR	
7.2)    Mediators	
7.3)    Transducers	

<b>AIMS OF THE STUDY.....</b>	<b>49</b>
<b>MATERIAL &amp; METHODS.....</b>	<b>51</b>
<b>1. Antibodies and reagents.....</b>	<b>53</b>
1.1) Antibodies	
1.2) Reagents	
<b>2. Cell Culture.....</b>	<b>54</b>
2.1) Cells and cell lines	
2.2) Transfection and retroviral transduction	
2.3) Synchronization of NIH3T3 cells	
2.4) Cell cycle analysis	
2.5) Pulse-chase assay	
2.6) Inhibitor treatment	
<b>3. DNAs, Northern blot, DNA damage, real time DNA damage.....</b>	<b>55</b>
3.1) cDNA	
3.2) mRNA analysis (Northern Blot)	
3.3) Ultraviolet and Ionizing radiation treatment	
3.4) Real-time recruitment of DNA repair proteins to the micro-laser generated sites of DNA damage	
<b>4. Biochemical Assays and Immunofluorescence.....</b>	<b>57</b>
4.1) Cell lysis, subcellular fractionation	
4.2) Immunoprecipitation and Western blotting	
4.3) PI3K assays	
4.4) Cyclin/Cdk kinase assays	
4.5) Pull-down assay	
4.6) Immunofluorescence	
<b>RESULTS.....</b>	<b>61</b>
<b>1. PI3K regulates G1/S phase transition.....</b>	<b>63</b>
1.1) Cell cycle progression	
1.2) PI3K activity in late G1 induces PKB activation that correlates with increased c-Myc protein levels	
1.3) Ras and Tyr kinases activate PI3K in late G1	
1.4) Late G1 PI3K inhibition reduces c-Myc and cyclin A levels as well as CDK2 activity	
1.5) Conditional c-Myc-ER activation rescues S phase entry in PI3K inhibitor-treated cells	
1.6) Expression of a GSK3-resistant c-Myc mutant rescues the cell cycle entry defects induced by inhibiting PI3K activity in late G1	
1.7) c-MycT58A expression rescues cyclin A expression, CDK2 activity, and MCM2 loading defects induced by PI3K inhibition in late G1	
1.8) Conclusions	
<b>2. Mechanisms controlling nuclear localisation of p110<math>\beta</math>.....</b>	<b>76</b>
2.1) Class I $\alpha$ PI3K isoforms p110 $\alpha$ and p110 $\beta$ have distinct intracellular localisation	
2.2) p110 $\beta$ localisation in the nucleus is transient and activation-dependent	
2.3) p110 $\beta$ overexpression results in cytoplasmic retention	
2.4) p85 $\beta$ promotes p110 $\beta$ nuclear localisation	
2.5) C2-domain in p110 $\beta$ contains a nuclear localisation sequence	
2.6) Preferential association of p110 $\beta$ with p85 $\beta$ compared to p85 $\alpha$	
2.7) p85 $\beta$ shuttling between nucleus and cytoplasm regulates p110 $\beta$ nuclear export	

2.8)	p85 $\beta$ N-terminal region contain a nuclear export signal	
2.9)	p85 $\beta$ /p110 $\beta$ associates with PCNA and translocates more efficiently to the nucleus	
2.10)	Conclusions	
<b>3.</b>	<b>p110<math>\beta</math> regulates DNA repair pathways.....</b>	<b>85</b>
3.1)	Cells with reduced p110 $\beta$ levels undergo apoptosis following ultraviolet radiation	
3.2)	p110 $\beta$ -deficient cells show genomic instability	
3.3)	p110 $\beta$ is activated by exposure to UV or ionising radiation	
3.4)	p110 $\beta$ associates with DNA repair protein in a radiation-dependent manner	
3.5)	p110 $\beta$ regulates the ATR pathway after UV exposure	
3.6)	p110 $\beta$ affects the ATR pathway by inactivation of its sensor protein	
3.7)	p110 $\beta$ also regulates activation of the ATM pathway	
3.8)	Rapid p110 $\beta$ translocation to the DNA damage sites	
3.9)	p110 $\beta$ controls NBS1 immobilisation at DNA damage sites	
3.10)	p110 $\beta$ regulates 53BP1 loading at DNA damage sites	
3.11)	PCNA a marker for DSB and requires p110 $\beta$ for loading at DNA damage sites	
3.12)	PCNA and NBS1 translocates simultaneously to the DNA damaged areas	
3.13)	Conclusions	
<b>CONCLUSIONS.....</b>		<b>95</b>
<b>DISCUSSION.....</b>		<b>97</b>
<b>REFERENCES.....</b>		<b>109</b>
<b>ARTICLES .....</b>		<b>133</b>



## ABBREVIATIONS

Ab	Antibody
APC	Anaphase-promoting complex
ATP	Adenosine-5'-triphosphate
BCR	Breakpoint cluster region
BSA	Bovine serum albumin
BrDU	Bromodeoxyuridine
CAK	CDK-activating kinase
CDK	Cyclin dependent kinase
dCTP	Deoxycytidine triphosphate
CHK	Check point kinase
DTT	Dithiothreitol
DMSO	Dimethyl sulphoxide
DSB	Double strand break
DAPI	4',6-diamidino-2-phenylindole
EGFR	Epidermal growth factor receptor
EDTA	Ethylene diamine tetraacetic acid
EGTA	Ethylene glycol tetraacetic acid
FBS	Foetal bovine serum
GFP	Green fluorescent protein
G1	Gap1
GPCR	G protein-coupled receptor
G2	Gap2
GTP	Guanosine-5'-triphosphate
GDP	Guanosine diphosphate
GST-tag	Tag derived from glutathione <i>S</i> -transferase
GF	Growth factor
HA-tag	Tag derived from haemagglutinin
HEPES	4-(2-hydroxyethyl)-1-piperazineethanesulfonic acid
IR	Ionising radiation
MAPK	Mitogen-activated protein kinase
MCM	Minichromosome maintenance
MEF	Mouse embryonic fibroblast
NLS	Nuclear localisation sequence
NES	Nuclear export sequence
NGF	Nerve growth factor
PAGE	Polyacrylamide gel electrophoresis
pol	Polymerase
PCR	Polymerase chain reaction
PH	Pleckstrin homology
PBS	Phosphate-buffered saline
PIP <sub>2</sub>	Phosphatidylinositol biphosphate
PIP3	Phosphatidylinositol triphosphate
PI	Phosphatidylinositol
PDGF	Platelet-derived growth factor
RFP	Red fluorescent protein
RPM	Rotations per minute
RTK	Receptor tyrosine kinase
RC	Replication complex
RBD	Ras-binding domain
SH3	Src homology 3
SH2	Src homology 2
SSC	Saline-sodium citrate buffer
SDS	Sodium dodecyl sulphate
S phase	Synthesis phase
TX-100	Triton X-100
TyrK	Tyrosine kinase
TF	Transcription factor
UV	Ultraviolet



## **RESUMEN ESPAÑOL**





## RESUMEN

El papel de la PI3K de clase I<sub>A</sub> en crecimiento y entrada en ciclo celular está bien descrito. Además de su activación en fase G1 temprana, la PI3K también se activa en fase G1 tardía y resulta esencial para la transición G1/S. Sin embargo, el mecanismo de activación y el papel que juega en la transición G1/S no se conoce y parte de nuestro trabajo ha sido estudiar la activación y función de PI3K en este proceso. Nuestras observaciones indican que Ras y Tyr- quinasas inducen la activación de PI3K en la fase G1 tardía. La inhibición de la actividad de PI3K en este estadio provoca una disminución en la expresión de c-Myc y ciclina A, alteración de la actividad Cdk2 y reducción en el reclutamiento de MCM2 a la cromatina. La activación condicional de c-Myc en fase G1 tardía o la expresión de un mutante de c-Myc resistente a degradación contrarresta la inhibición de PI3K en fase G1 tardía y restaura la entrada en fase S. Por ello concluimos que las Tyr quinasas y Ras colaboran para inducir el segundo pico de activación de PI3K en fase G1, el cual media el inicio de la síntesis de ADN estabilizando la expresión de c-Myc.

Además de su papel esencial en ciclo celular, la PI3K de clase IA ha sido descrita en el núcleo de diferentes tipos celulares. Por ello, estudiamos que isoformas localizan en el núcleo y su modo de translocación. El trabajo presentado en esta tesis indica que de las dos isoformas expresadas de manera ubicua, p110 $\alpha$  y p110 $\beta$ , solo p110 $\beta$  se localiza en gran parte en el núcleo mientras que p110 $\alpha$  es mayoritariamente citoplásmica. Hemos encontrado también que de las subunidades reguladoras p85 $\alpha$  y p85 $\beta$ , p85 $\beta$  posee una mayor localización nuclear mientras que p85 $\alpha$  es esencialmente citoplásmica. Además, observamos que p110 $\beta$  no es capaz de translocarse al núcleo por si misma necesitando de la asociación de p85 $\beta$  para la correcta translocación al núcleo y que dicho translocación se facilita por una secuencia de localización nuclear polibásica presente en el dominio C2 de p110 $\beta$ . Sin embargo, la expresión de p85 $\beta$ /p110 $\beta$  exógenos fue insuficiente para promover la traslocación al núcleo completa de p85 $\beta$ /p110 $\beta$ , sugiriendo que otras proteínas se asocian fisiológicamente a estos complejos para inducir su localización nuclear. Hemos identificado que la asociación de PCNA a p110 $\beta$  favorece la translocación nuclear de p85 $\beta$ /p110 $\beta$ .

Con objeto de tener alguna pista la función de p110 $\beta$  nuclear, hemos analizado que proteínas se asocian a p110 $\beta$  en el núcleo. Mediante análisis de espectroscopia de masas hemos encontrado entre otras, proteínas relacionadas con el control de la reparación del ADN como RAD 17, RAD9, RAD50. Hemos estudiado el posible papel de p110 $\beta$  en reparación del ADN. Tras exposición a radiación UV/IR observamos activación de p110 $\beta$ . También observamos asociación de RAD17 a p110 $\beta$ . Mediante ARN de interferencia y MEFs inmortalizadas p110 $\beta$ <sup>-/-</sup> encontramos que células deficientes para p110 $\beta$  presentan aneuploidía observándose células con un número elevado de cromosomas y roturas cromosómicas aberrantes, deduciéndose una función de p110 $\beta$  en el mantenimiento de la integridad genómica. Encontramos que p110 $\beta$  regula las vías de señalización ATR (Chk1 y p-RAD17) y ATM (SCM1 y  $\gamma$ H2AX). También identificamos que los defectos se producen a nivel de reclutamiento de las proteínas al lugar del daño en el ADN como por ejemplo la movilidad reducida de la proteína sensor de rotura doble NBS1 a los lugares de daño. En conjunto hemos determinado un papel directo de p110 $\beta$  en la regulación de la reparación del ADN; la activación de p110 $\beta$  y su colocalización con  $\gamma$ -H2AX en las zonas dañadas del ADN implican un papel integrador de p110 $\beta$  en las respuestas a daño en el ADN. Por todo ello, proporcionamos una explicación (justificación) molecular de cómo p110 $\beta$  es integradora en la regulación de las diferentes vías de señalización implicadas en la respuesta al daño en el ADN y que su depleción afecta a la activación de las proteínas de control del ADN (checkpoint proteins).



## INTRODUCCIÓN

En eucariota superiores, la división celular es un proceso fundamental para el desarrollo, el crecimiento y la renovación de células. La regulación del número de células viene determinada por un equilibrio entre división celular y muerte. Existen múltiples proteínas encargadas del control de la división celular, que pueden incluirse en cuatro categorías: factores de crecimiento y sus receptores (sección 1), transductores de señales (sección 2) y por último proteínas reguladoras nucleares. De entre las moléculas implicadas en la transducción de señales nos centraremos en la familia de las PI3K, por ser el objeto de nuestro estudio (sección 3), así como las rutas de señalización nucleares (sección 4).

La unión de los factores de crecimiento a sus respectivos receptores desencadenan la activación de estos últimos. Como consecuencia, se estimula la actividad de transductores de señales, que actúan como segundos mensajeros intracelulares. Son éstos los que regulan la función de proteínas reguladoras nucleares, impulsando la expresión génica y contribuyendo a la entrada en ciclo (sección 6). Por último se incluye una sección (7) acerca de las vías implicadas en la respuesta a daño en el DNA, ya que una parte de nuestra investigación se centra en desentrañar el posible papel de PI3K en este proceso.

## SECCIÓN 1. RECEPTORES DE FACTORES DE CRECIMIENTO

### 1.1) Receptores con actividad tirosina-quinasa

Los Receptores con actividad tirosina-quinasa (RTK) constituyen una amplia familia de proteína quinasas, que actúan a través de su unión a una gran variedad de factores de crecimiento y catalizan la fosforilación en residuos de tirosina en distintas moléculas diana. Los RTKs contienen un dominio extracelular de unión a sus respectivos ligandos, un dominio hidrofóbico transmembrana y una porción citosólica con actividad tirosina quinasa (**Hupfeld *et al.*, 2007**). Se han identificado 58 de estos receptores, clasificados en 20 subfamilias distintas, en función de las secuencia de su dominio quinasa (**Robinson *et al.*, 2000**).

### 1.2) Receptores acoplados a proteínas G

Otro grupo de receptores pertenecientes a los receptores integrales de membrana lo forman los receptores acoplados a proteínas G (GPCRs), que se unen a proteínas G heterotriméricas tras su estimulación con factores de crecimiento. El resultado consiste en el cambio conformacional de las proteínas G, lo que permite su interacción con GTPasa, estimulando la liberación de GDP.

## SECCIÓN 2. PROTEÍNAS TRANSDUCTORAS DE SEÑALES

Las proteínas transductoras de señales forman redes complejas de vías de señalización interconectadas, que permiten integrar las señales extracelulares recibidas en la membrana, regulando múltiples procesos celulares. A continuación se detallan algunas de estas proteínas:

### 2.1) Ras

Las proteínas Ras son pequeñas GTPasas ubicadas en el centro de la membrana plasmática, donde actúa como un interruptor que permite la transducción de señales extracelulares al citoplasma.

### 2.2) Proteína quinasas asociadas a microtúbulos (MAPKs)

Las MAPKs son capaces de desencadenar cambios en la expresión génica provocados por la unión de una señal extracelular a su receptor de membrana, mediante la fosforilación de diversos sustratos (**Seger & Krebs, 1995**). Dentro de este grupo destacan tres clases diferentes de MAPKs (**Gallo & Jonhson, 2002**).

- a- ERK1/2
- b- JNK1,2-3
- c- p38 ( $\alpha$ ,  $\beta$ ,  $\gamma$ ,  $\delta$ )

Las MAPKs actúan regulando la actividad de múltiples proteínas, tales como PI3K, fosfolipasa C (Rhee, 2001), proteína quinasa C (Griner & Kazanietz, 2008), así como la formación de diacilglicerol (Irving, 2003) y la liberación de  $\text{Ca}^{2+}$  (Roderick & Cook, 2008).

### SECCIÓN 3. FOSFOINOSITOL-3 QUINASA (PI3K)

Las PI3K pertenecen a una familia de las lípido quinasas que fosforilan la posición 3' del grupo hidroxilo de distintos fosfoinosítidos y regulan numerosas respuestas entre las que se incluyen la división celular, la migración etc (Serunian *et al.*, 1990; Ling *et al.*, 1992).

#### 3.1) PI3K de clase I

Las PI3K de clase I son proteínas heterodiméricas formadas por una subunidad catalítica y otra reguladora, que median la producción de  $\text{PI}(3,4,5)\text{P}_3$  y  $\text{PI}(3,4)\text{P}_2$  *in vivo*, que actúan como segundos mensajeros intracelulares. La Clase I se divide en dos subgrupos: clase  $\text{I}_A$  y clase  $\text{I}_B$  (Stoyanov *et al.*, 1995). Las isoformas catalíticas  $\text{p110}\alpha$ ,  $\beta$  y  $\delta$  pertenecen al primer grupo, mientras que el segundo estaría constituido únicamente por la subunidad  $\text{p110}\gamma$  (Hiles *et al.*, 1992; Hu *et al.*, 1993; Vanhaesebroeck *et al.*, 1997). Mientras que la clase  $\text{I}_A$  es activada por receptores con actividad tirosina quinasa,  $\text{p110}\gamma$  se activa por medio de receptores acoplados a proteínas G.

#### 3.2) Vías de señalización controladas por PI3K de clase $\text{I}_A$

La formación de  $\text{PI}(3,4,5)\text{P}_3$  y  $\text{PI}(3,4)\text{P}_2$  en la membrana plasmática desencadenada por la activación de PI3K conduce a la translocación a la membrana de distintas proteínas con dominio de homología con la pleckstrina (PH). Entre ellas encontramos a PDK1, PKB/Akt, P70S6K, PKC, cuya activación va a regular una amplia gama de funciones, tales como la captación de glucosa, el tráfico de membranas, la adhesión celular, la reorganización de actina y la proliferación. Habitualmente, la señalización intracelular de PI3K viene mediada por PDK1, una serina/treonina quinasa cuyo principal sustrato es PKB (Cohen *et al.*, 1997; Anderson *et al.*, 1998).

##### 3.2.1) PKB

PKB pertenece a la familia AGC de proteínas quinasas (Peterson *et al.*, 1999). Es el análogo en mamíferos del oncogén v-Akt (Staal, 1987). Debido a la variedad y especificidad de sus sustratos, PKB tiene un papel central en muchas de las respuestas mediadas por PI3K de clase  $\text{I}_A$ , entre las que destacan el crecimiento, la supervivencia y el metabolismo. El primer sustrato de PKB identificado fue la glicógeno sintasa quinasa (GSK, Brazil *et al.*, 2001; Datta *et al.*, 1999), de modo que su fosforilación por parte de PKB desencadena la estabilización de c-Myc, un oncogen que regula en rutas de proliferación, supervivencia y tumorigénesis (Sears *et al.*, 2000).

##### 3.2.2) PTEN

PTEN es el antagonista de la señalización de PI3K de clase I, puesto que es capaz de desfosforilar la posición 3' del anillo inosítido reduciendo los niveles de  $\text{PI}(3,4,5)\text{P}_3$  y  $\text{PI}(3,4)\text{P}_2$  (Maehama & Dixon, 1998). PTEN fue descubierta por dos grupos independientes como una molécula supresora de tumores, codificada por un gen ubicado en el locus 10q23. Estudios posteriores demostraron que se encuentra mutado frecuentemente en distintos tipos de tumores humanos (Li & Sun, 1997; Steck *et al.*, 1997).

## SECCIÓN 4. SEÑALIZACIÓN NUCLEAR MEDIADA POR PI3K

Mientras que la vías de señalización reguladas por PI3K en el citosol han sido ampliamente estudiada, se sabe menos de su papel en el núcleo, en el que PI3K podría funcionar independientemente de las vías citosólicas (Neri *et al.*, 2002). Por un lado PI3K se expresa constitutivamente en el núcleo de hepatocitos de rata (Martelli *et al.*, 1999), Neri y colaboradores detectaron por inmunohistoquímica e “immunobloting” la subunidad reguladora p85 y demostraron que la inducción de conduce a una rápida translocación de PI3K al núcleo (Neri *et al.*, 1994). Más aún, el análisis microscopía inmunoelectrónica utilizando un anticuerpo anti-p85 mostraron marcaje en la membrana nuclear y el nucleoplasma, en consonancia con otro trabajo que demostraba la presencia de PI3K en el núcleo de las células de osteosarcoma humano SAOS-2 (Zini *et al.*, 1996). Basándose en su reactividad inmunológica, Lu y colaboradores encontraron que la cantidad de PI3K existente en el núcleo de las células derivadas de hígado de rata constituía un 5% del total (Lu *et al.*, 1998). La activación de PI3K en el citosol necesita de receptores con actividad tirosina quinasa o de GTPasas como Ras, pero ninguna de esas moléculas parece estar presente en el núcleo. Por el contrario, al menos en células neuronales, se ha descrito la existencia de una GTPasa nuclear (PIKE), que es capaz de interaccionar con PI3K estimulando su actividad (Ye *et al.*, 2002). El tratamiento de estas células con NGF estimularía la translocación de PLC- $\gamma$ 1 al núcleo, donde actuaría como un GEF fisiológico de PIKE-S (Ye *et al.*, 2002), de este proceso depende la entrada de PI3K al núcleo, de una manera aún desconocida. Uno de los objetivos de este estudio es determinar el mecanismo de entrada de PI3K al núcleo celular.

## SECCIÓN 5. Proteínas Nucleares

c-myc se halla entre los primeros proto-oncogenes. Forma parte de una familia a la que también pertenecen los genes N- y L-myc. Las proteínas derivadas de estos genes se localizan principalmente en el núcleo y su expresión, generalmente, se correlaciona con la proliferación celular. Las células que expresan constitutivamente elevados niveles de c-myc reducen sus requerimientos de factores de crecimiento (Kaczmarek *et al.*, 1985; Sorrentino *et al.*, 1986; Stern *et al.*, 1986), presentan una fase G1 más corta y no entran en G0 tras deprivación de suero (Kohl & Ruley, 1987). c-myc regula la expresión de múltiples genes, alguno de los cuales son esenciales durante el intervalo G0/S (Ponzielli *et al.*, 2005; Dang *et al.*, 1999). Se trata de un gen de respuesta rápida indispensable para una rápida progresión de G0 a G1 y a través de esta última fase (Schorl 2003; Mateyak *et al.*, 1997; Amati *et al.*, 1998).

c-myc es una proteína muy inestable, de modo que su expresión se encuentra muy controlada a lo largo del ciclo celular. La regulación de su estabilidad se lleva a cabo por medio de su fosforilación, siendo los residuos implicados en este proceso la Thr58 y la Ser62. El primero es fosforilado por MAPK y el segundo por GSK3 $\beta$ . La proteína fosforilada es susceptible de degradación por el proteasoma (Yeh *et al.*, 2004).

## SECCIÓN 6. CICLO CELULAR

El ciclo celular es uno de los procesos biológicos estudiados con mayor profundidad, debido a su relevancia en el crecimiento celular y el desarrollo de los procesos fisiológicos normales de un individuo y también en muchas de las enfermedades humanas (Fig. 1). Los eventos clave del ciclo celular, tales como la replicación del DNA y la división del citosol, ocurren durante interfase y citocinesis respectivamente. La interfase se puede dividir en cuatro etapas: G1, S, G2 y fase M. Durante G1 tiene lugar un aumento de la masa y una serie de eventos moleculares que permiten a la célula estar preparada para la replicación del DNA. En G1, la célula determina si puede seguir adelante (en presencia de factores de crecimiento y nutrientes), o si entra en fase de quiescencia (G0). Una vez que la célula pasa del punto de restricción en G1 avanzado (Pardee, 1989) ésta se

vuelve refractaria a las señales extracelulares que regulan el crecimiento y queda comprometida a completar el ciclo celular (**Garcia *et al.*, 2006**).

A lo largo de la fase S se desencadenan una serie de complejos eventos que permiten la duplicación de los cromosomas, Tras la replicación del DNA la célula transita a través de la fase G2, una etapa en la que la célula se prepara para la división nuclear (mitosis) y la citoquinesis. En mitosis tiene lugar la separación de los cromosomas en dos núcleos diferentes, tras este proceso se divide el citosol, formándose dos células separadas. Una vez terminada la citoquinesis, la exposición a factores de crecimiento determinará si las células hijas continúan dividiéndose o salen del ciclo, para entrar en un estado especial, denominado G0.

El ciclo celular está controlado por las CDKs (cyclin dependent kinases). Se trata de serina/treonina quinasas que forman complejos con unas subunidades reguladoras denominadas ciclinas, que se expresan transitoriamente a lo largo del ciclo. La constitución de los complejos ciclina D (D1, D2 y D3)/Cdk6 o Cdk4 es necesaria para la progresión de G1; mientras que para la entrada en fase S se requiere la constitución de complejos ciclina E/Cdk2 y ciclina A/Cdk2. En mitosis son esenciales la formación de complejos ciclina A/Cdk1 y ciclina B/Cdk1 (**Ekholm *et al.*, 2000**). La formación de diferentes complejos a lo largo del ciclo permite la activación de sustratos específicos implicados en su regulación temporal. En la fase G2 se sintetiza una serie de proteínas que permite a la célula asegurarse de que la copia del DNA realizada carece de errores en su secuencia y responde al daño en el DNA. Cuando se produce este daño se puede desencadenar varios procesos, como la parada del ciclo, la iniciación de la reparación del DNA, la activación de un programa de transcripción, la entrada en senescencia o la muerte por apoptosis (**Khanna & Jackson, 2001; Zhou & Bartek, 2004**). Los puntos de restricción no sólo paran el ciclo en respuesta a daño en el DNA, sino que también controlan la activación de rutas de reparación y regulan el movimiento de estas proteínas al sitio adecuado en el DNA (**Rouse & Jackson, 2002**).

## SECCIÓN 7. RESPUESTA A DAÑO

Existen distintos tipos de daño en el DNA que pueden conducir a la activación de proteínas de control del DNA. Producen una parada temporal del ciclo que permite la reparación del DNA. Las proteínas ATM y ATR pertenecientes a la clase IV de las PI3K se activan rápidamente en respuesta a radiación UV e ionizantes, dando paso a la reparación del DNA.

Las proteínas implicadas en respuesta a estrés genotóxico se pueden dividir en sensores, transductores y mediadores. Parte de nuestro trabajo se centra en examinar el efecto de eliminar las isoformas de PI3K de clase IA en las respuestas a estrés por radiación.

## OBJECTIVOS DEL ESTUDIO

La activación de la PI3K de clase IA tras activación de receptores para factores de crecimiento es necesaria para el crecimiento celular (aumento de la masa) y la entrada en ciclo celular. Además, la expresión de mutaciones activadoras y la sobre expresión de las isoformas PI3K de clase IA produce un aumento en la señalización de la vía PI3K, lo cual se asocia con transformación celular y cáncer. La activación de PI3K mediada por factores de crecimiento ocurre a dos tiempos diferentes durante la fase G1 del ciclo celular. El primer pico de activación se observa rápidamente tras la adición de los factores de crecimiento, mientras que el segundo pico de activación se produce en la fase G1 tardía, justo antes de la entrada en fase S. Este segundo pico de activación es esencial para la replicación del ADN. Sin embargo, los mecanismos y la función de la activación de PI3K en la entrada de fase S son desconocidos.

Recientemente se ha encontrado que una fracción de la PI3K de clase IA se encuentra en el núcleo. El papel de PI3K nuclear está relacionado con supervivencia celular, mitosis, diferenciación, etc. a través de su principal efector PKB. Sin embargo, se desconoce que isoformas de PI3K se localizan en el núcleo. Las isoformas de clase IA ubicuas p110 $\alpha$  y p110 $\beta$  exhiben distintas y importantes funciones en la división celular, por tanto es importante estudiar cual es la localización intracelular de las distintas subunidades catalíticas y reguladoras de clase IA. Además, es también necesario determinar el modo de su translocación al núcleo.

La delección genética de p110a y p110b en ratones provoca letalidad embrionaria. Además, p110a ha sido claramente implicada en cáncer ya que se han descrito distintas mutaciones que provocan un incremento en su actividad quinasa y están presentes en tumores humanos. La sobre expresión de p110b también ha sido descrita en diferentes tipos de tumor, sin embargo, no hay mutaciones funcionales descritas en el gen PIK3CB. El ratón deficiente condicional para p110b mostró un papel independiente de la actividad quinasa en desarrollo, de cualquier forma, la función de p110b está poco clara.

Para abordar estas cuestiones, los principales objetivos de mi tesis fueron:

- 1) Investigar los mecanismos de activación y el papel de la actividad de PI3K de clase IA en fase G1 tardía
- 2) Identificar que isoformas de PI3K de clase IA localizan en el núcleo y investigar los mecanismos implicados en su translocación al núcleo
- 3) Investigar la participación de p110 $\beta$  en las respuestas a daño en el ADN





## RESULTADOS

La fosfoinosítido 3-quinasa (PI3K) es una de las moléculas de señalización temprana inducida por estimulación de receptores para factores de crecimiento, la cual es necesaria para el crecimiento celular y entrada en ciclo celular. La activación de PI3K ocurre a dos tiempos diferentes durante la fase G1. El primer pico de activación tiene lugar inmediatamente tras la adición de los factores de crecimiento, y el segundo en la fase G1 tardía, antes de la entrada en fase S. Este segundo pico de actividad es esencial para la transición desde G1 a S; sin embargo, el mecanismo por el cual este pico de actividad se induce y regula la entrada en fase S se desconoce. En este trabajo hemos estudiado el mecanismo de activación y la función de la actividad PI3K en fase G1 tardía. La activación de PI3K en G1 induce activación de PKB y expresión de c-Myc (Fig. 2). Nosotros hemos observado la activación de TyrK y Ras en la fase G1 tardía (Fig. 3) es esencial para la activación de PI3K y de sus efectores en la fase G1 tardía (Fig. 4, 5).

La inhibición de la actividad PI3K en dicha fase produce una baja expresión de c-Myc, ciclina D2, Cdk4 (Fig. 6). Para estudiar por qué se produce esta reducción de los niveles proteicos de c-Myc tras la inhibición de la actividad de PI3K en G1 tardía, realizamos Northern blot analizando el efecto sobre los niveles de mRNA y ensayos de pulso y caza para ver el efecto sobre estabilidad de la proteína c-Myc (Fig. 7, 8). Observamos mayor bajada de niveles de proteína que de ARNm cuando inhibimos la actividad PI3K en G1 tardía. La inhibición de la actividad PI3K en G1 tardía también provoca una bajada de niveles de ciclina D3, ciclina A, e hipo-fosforilación de Rb (Fig. 9) alterando además, la actividad Cdk2 debida a la presencia de mayores niveles del inhibidor p27<sup>Kip1</sup> (Fig. 10). Esta bajada de Cdk2 produjo un descenso en el reclutamiento del complejo MCM (mantenimiento de minicromosoma) a la cromatina (Fig. 11).

La consecuencia más importante de inhibir PI3K en fase G1 tardía fue la desestabilización de c-Myc. Para demostrar esto usamos un vector condicional de c-myc fusionado a ER que responde a 4-OHT y induce el desplazamiento de c-Myc al núcleo. También usamos un mutante c-MycT58A, que no depende de GSK3 $\beta$ . La activación condicional de c-Myc en fase G1 avanzada o la expresión estable del mutante c-Myc rescataron los defectos de la inhibición PI3K y restaurando la entrada en fase S (Fig. 12, 14); corrigiendo los niveles de cyclin A, actividad de ciclina E/CDK2, ciclina A/CK2 y el reclutamiento de MCM2 a cromatina (Fig 15, 16, 17, 19). Estos resultados muestran que las tirosina quinasas y Ras cooperan a la hora de inducir el segundo pico de actividad PI3K en G1 que induce la iniciación de la síntesis de ADN por estabilización de c-Myc.

La localización nuclear de la PI3K de clase IA se ha descrito con anterioridad. Sin embargo, que isoformas se localizan en el núcleo se desconocen. Comparando la localización de las isoformas ubicuas p110 $\alpha$  y p110 $\beta$ , determinamos que la mayoría de p110 $\beta$  localiza en el núcleo mientras que p110 $\alpha$  es mayoritariamente citoplásmica (Fig. 20). También observamos la localización de p110 $\beta$  en el núcleo de otras líneas celulares (Fig. 21). Por otro lado, hemos observado que durante la progresión del ciclo celular p110 $\beta$  se desplaza entre el núcleo y el citoplasma y que se produce una gran concentración nuclear durante la fase S (Fig. 22A). El incremento en la localización nuclear coincidió con la activación de p110 $\beta$  en el núcleo (Fig. 22B). Estas observaciones nos permiten concluir que la actividad quinasa de p110 $\beta$  es importante para su translocación nuclear, un aspecto que requiere futuros análisis.

Para estudiar la función de p110 $\beta$  en núcleo, transfectamos p110 $\beta$  en varias líneas celulares y observamos que el p110 $\beta$  sobreexpresado no se localiza correctamente, dando lugar a una expresión citoplásmica (Fig. 23). Nosotros describimos parte de los mecanismos implicados en la translocación de p110 $\beta$ . Concluimos que p110 $\beta$  no se transloca al núcleo por sí misma y que necesita de la asociación con p85 $\beta$ , y no con p85 $\alpha$ . Dicha asociación facilita la localización nuclear de p110 $\beta$ . Cuando transfectamos p110 $\alpha$  con p85 $\alpha$  o p85 $\beta$ , p110 $\alpha$  permaneció en el

citoplasma al igual que p85 $\alpha$  y al igual que la mayoría de p85 $\beta$  (Fig24 A). Además, hemos identificado una secuencia de localización nuclear en el dominio C2 de p110 $\beta$ , que cuando se muta inhibe la translocación al núcleo del complejo p85 $\beta$ /p110 $\beta$ . Estos resultados fueron inesperados; aunque se considera que ambas subunidades reguladoras tienen papeles similares, ya que solo p85 $\beta$  (no p85 $\alpha$ ) facilitó de manera reproducible la translocación nuclear de p110 $\beta$ . Una posibilidad es la unión preferencial de p110 $\beta$  a p85 $\beta$  y de p110 $\alpha$  a p85 $\alpha$ . Para examinar esta posibilidad fusionamos el NLS a p85 $\beta$  y cotransfectamos p110 $\alpha$  o p110 $\beta$  con p85 $\beta$ -NLS (“nuclear localization signal”). p85 $\beta$  mostró una completa localización nuclear debido a la secuencia NLS (de SV40), lo cual también se tradujo en la localización de p110 $\beta$  en el núcleo; sin embargo, en el caso de p110 $\alpha$ , una gran fracción permaneció en el citoplasma (Fig. 26).

A parte del papel de p85 $\beta$  en la translocación nuclear de p110 $\beta$ , p85 $\beta$  también controla su exclusión nuclear (Fig. 27). Identificamos que los primeros 41 aminoácidos en la región N-terminal de p85 $\beta$  regulan la exportación nuclear de esta proteína (Fig.28). Observamos que p85 $\beta$  no fue suficiente para completar la translocación nuclear de p110 $\beta$  a niveles semejantes al endógeno. Hemos observado que la unión de PCNA a p110 $\beta$  (Fig. 29) incrementa la localización nuclear de p110 $\beta$  Fig3.

Tras determinar la localización nuclear de p110 $\beta$  y su papel en la regulación de la replicación del ADN, estudiamos su función en el núcleo. La exposición de células con niveles reducidos de p110 $\beta$  a UV, indujo apoptosis (Fig. 31). p110 $\beta$  KO MEF mostraron un número de cromosomas muy superior a lo normal y roturas cromosómicas aberrantes, implicando una función de p110 $\beta$  en el mantenimiento de la integridad genómica (Fig 32).

Posteriormente analizamos dos vías de señalización de reparación activadas tras daño al ADN como son las iniciadas por ATR y ATM. Se observó una señalización defectuosa a través de ATR, una menor activación de Chk1 y una acumulación reducida de p-RAD17 (Fig. 35, 36). Además, también encontramos que la delección de p110 $\beta$  provoca defectos en la vía ATM donde se producen alteraciones en la activación de ATM y sus efectores p-SMC1, p-Chk2 y  $\gamma$ -H2AX (Fig 37). La colocalización de p110 $\beta$  con  $\gamma$ H2AX, en los puntos de daño al el ADN implica un papel integrador de p110 $\beta$  en las respuestas a daño en el ADN (Fig. 38). Por otro lado, encontramos que p110 $\beta$  regula la movilidad de la proteína “sensor” NBS1 a los puntos de daño. p110 $\beta$ <sup>-/-</sup> MEF presentan defectos en la movilización de NBS1 y 53BP1 en respuesta a daño en el ADN inducido por láser UV (Fig. 39, 40). Estas observaciones nos llevan a concluir que p110 $\beta$  actúa antes que las proteínas “sensor” de daño en el ADN. Dado que anteriormente identificamos que p110 $\beta$  asocia con PCNA, examinamos si PCNA localiza en las áreas dañadas y observamos inmovilización de PCNA con cinéticas similares a las de NBS1(Fig. 41), infiriendo por tanto que PCNA puede tener un papel como proteína sensor además de su papel en la replicación de AND y que es dependiente de p110 $\beta$ .

## CONCLUSIONES

### ***Objetivo 1. Investigar el mecanismo de activación y función de PI3K en G1 tardía***

- 1,1) La activación de Ras y Tyr quinasas son necesarios para la activación de PI3K en G1 tardía.
- 1,2) La actividad PI3K en G1 tardía regula los niveles de c-Myc y en consecuencia los niveles de ciclina A, la actividad Cdk2 y la unión de MCM2 a la cromatina. La expresión de c-Myc rescata los defectos provocados por la inhibición de PI3K en G1 tardía y la entrada en fase S.

### ***Objetivo 2. Investigar el mecanismo de localización de p110 $\beta$ en el núcleo***

- 2,1) La mayoría de p110  $\beta$  es nuclear mientras p110  $\alpha$  es principalmente citosólico. Además, p110  $\beta$  se mueve entre el núcleo y el citosol durante la progresión del ciclo celular y es principalmente nuclear en la fase S; el aumento de la localización nuclear de p110  $\beta$  coincide con la activación de PI3K nuclear.
- 2,2) La localización nuclear de p110  $\beta$  requiere de su asociación con p85  $\beta$  . La subunidad reguladora p85  $\beta$  también determina la salida del núcleo de p110  $\beta$ , los primeros 41 aa p85  $\beta$  contienen una región que actúa como secuencia de exporte nuclear.
- 2,3) p110 $\beta$  contiene una señal de localización nuclear en el dominio C2.
- 2,4) p110  $\beta$  se asocia con PCNA; este complejo aumenta la localización nuclear de p110 $\beta$ .

### ***Objetivo 3. Investigar la participación de p110 $\beta$ en la reparación del ADN.***

- 3.1) La reducción de los niveles p110 $\beta$  celulares interfiere con los mecanismos de reparación del ADN provocando inestabilidad genómica.
- 3.2) La radiación ionizante y la luz ultravioleta activan p110  $\beta$ .
- 3,3) p110  $\beta$  asocia RAD17 de forma dependiente de la radiación. p110 $\beta$  también regula la activación de ATR y de ATM.
- 3,4) p110  $\beta$  transloca a las roturas de ADN; la deficiencia en p110 $\beta$  impide el posterior reclutamiento de NBS1, 53BP1 y PCNA al sitio de daño al ADN.



## DISCUSIÓN

### La activación de PI3K de clase IA en fase G1 tardía se requiere para la estabilización de c-Myc y la entrada en fase S

La activación de PI3K en la fase G1 tardía es esencial para la entrada en fase S (**García *et al.*, 2006**; **Jones *et al.*, 2001**). En este trabajo examinamos las señales implicadas en la activación de PI3K en la fase G1 tardía y los mecanismos por lo cuales PI3K controla la transición G1/S. Encontramos que las tirosina quinasas y Ras también se activan en fase G1 tardía. De hecho, la inhibición simultánea de las tirosina quinasas y Ras en fase G1 tardía anuló por completo el segundo pico de activación de PI3K. Estos resultados sugieren que la activación de PI3K en la fase G1 tardía es dependiente de la actividad tirosina quinasa y es además controlada por Ras.

También demostramos que la estabilización de c-Myc es la principal función de la activación de PI3K en la fase G1 tardía, basándonos en la observación de que la inhibición de PI3K en fase G1 tardía reduce los niveles de c-Myc y ciclina A. La inhibición de PI3K en este momento también incrementó la expresión de p27kip y redujo la actividad quinasa asociada a ciclinaE/CDK2 y ciclinaA/CDK2. Nuestros resultados son consistentes con lo observado en células deficientes para c-Myc, las cuales muestran defectos similares (**Vlach *et al.*, 1996**; **Mateyak *et al.*, 1999**). Nosotros demostramos esto usando un mutante de c-Myc (MycT58A, **Hemann *et al.*, 2005**) resistente a la acción de GSK3 $\beta$ , o alternativamente, expresando una forma inducible de c-Myc en fase G1 tardía se restaura la entrada en ciclo celular contrarrestando la inhibición de PI3K en todos los parámetros estudiados. Estos incluyen la síntesis de ADN, la expresión de ciclina A, la actividad de ciclina E/CDK2 y ciclina A/CDK2, así como la separación de p27kip de ciclinaE/CDK2. La activación de PI3K en fase G1 tardía por lo tanto regula los niveles de la proteína c-Myc.

Un aspecto muy interesante de nuestras observaciones es que aunque la actividad de PI3K en fase G1 tardía es casi paralela a la de c-Myc y de hecho la activación de PI3K puede sustituirse por la expresión de una forma estable de c-Myc, en la transición G0 a G1, c-Myc y PI3K tienen funciones bien distintas y ambas son necesarias para inducir el paso a fase G1 (**Jones *et al.*, 2001**), sugiriendo distintas funciones de PI3K en fase G1 temprana y tardía. La activación de PKB mediada por PI3K es también requerida para la inactivación del factor de transcripción (FT) FoxO. En un estado desfosforilado, FoxO inhibe la inducción de varias dianas de c-Myc, proporcionando un mecanismo para la acción sinérgica de c-Myc y PI3K en la progresión del ciclo celular (**Bouchard *et al.*, 2004**). La activación inmediata de PI3K tras estimulación de receptores de factores de crecimiento podría explicar esta aparente contradicción, ya que la actividad PI3K en fase G1 temprana es esencial para el crecimiento celular (**Álvarez *et al.*, 2003**) y para la inactivación de FoxO (**Álvarez *et al.*, 2001**).

Las proteínas de mantenimiento del minicromosoma (MCM) están implicadas en la replicación y forman un complejo del cual se piensa que es la helicasa replicativa en organismos eucariota. El complejo MCM se mantiene con el complejo de replicación hasta que dicho proceso de replicación se completa, y varias proteínas MCM están reguladas a través de fosforilación CDK (**Tye, 1999**). Nosotros hipotetizamos que, desde que la inhibición de la actividad PI3K en fase G1 tardía provocó un descenso en la actividad ciclina/CDK2 (**Geng *et al.*, 2003**), esta inhibición podría afectar al reclutamiento del complejo MCM a la cromatina. Hemos examinado el reclutamiento a la cromatina cerca de la transición G1/S mientras inhibimos la actividad PI3K. Encontramos que la actividad PI3K en fase tardía G1 es requerida para un correcto reclutamiento de MCM2, otro evento crucial para una correcta inducción de la síntesis de ADN.

Después de examinar el papel de la PI3K en la fase G1 tardía, identificamos la isoforma de clase IA PI3K responsable de la transición G1/S. Nuestro grupo recientemente describió que tanto p110 $\alpha$  y p110 $\beta$  se activan en fase G1 tardía, aunque a tiempos distintos (**Marques *et al.*, 2008**). p110 $\alpha$  se activa a mitad de fase G1, mientras que p110 $\beta$  se activa más tarde en G1 (en la entrada en fase S) concluyéndose que p110 $\beta$  tiene un papel diferente de p110 $\alpha$ , dado que p110 $\beta$  regula la progresión de la fase S.

## La asociación a p85 $\beta$ media la translocación nuclear de p110 $\beta$

Se exploraron las bases del papel de p110 $\beta$  en progresión de la fase S. Usando inmunomarcaje (immunostaining) y inmunofijación (immunoblotting) de la subunidad reguladora p85, Neri y colaboradores mostraron que la PI3K de clase IA localiza en el núcleo de diferentes tipos celulares (Neri *et al.*, 2002). Nosotros encontramos distintas localizaciones intracelulares para p110 $\alpha$  y p110 $\beta$  en células NIH3T3; mientras que p110 $\alpha$  se concentraba principalmente en el citoplasma, la mayoría de p110 $\beta$  se localizó en el núcleo. En células HeLa y en fibroblastos embrionarios de ratón (MEF), también observamos la localización nuclear de p110 $\beta$ . Estas observaciones sugieren que p110 $\beta$  aparece en el núcleo como un fenómeno general, indistintamente del tipo celular y de la especie de mamífero. Algunos trabajos recientes documentan la aparición de PI3K en núcleo y un posible papel diferente de PI3K en núcleo y citoplasma (Martelli *et al.*, 2007). El mecanismo por el cual p110 $\beta$  se transloca al núcleo se desconocía.

Mostramos que tras re-estimular células paradas en G0 en medio sin suero, una fracción de p110 $\beta$  se desplaza entre el citoplasma y el núcleo durante la fase G1. Además, la cinética de activación nuclear de PI3K fue en paralelo a las translocación de p110 $\beta$  al núcleo. p110 $\beta$  nuclear fue máxima cerca de la transición de fases G1/S. También, encontramos p85 $\beta$  nuclear, mientras que p85 $\alpha$  se localizó mayoritariamente en el citoplasma.

Mientras estudiábamos el papel de p110 $\beta$  nuclear, observamos que su sobreexpresión inducía una localización citoplásmica. Por ello consideramos que la transcripción y traducción continua de ADNc en las células podría provocar la acumulación del p110 $\beta$  sintetizado *de novo* en los polisomas del retículo endoplásmico. En este sentido, la inhibición de la expresión de proteínas con ciclohexamida durante 3 h antes del análisis de inmunofluorescencia no cambió la localización citosólica de p110 $\beta$  recombinante. Una posibilidad alternativa es que p110 $\beta$  requiere asociación con otras proteínas celulares para su translocación nuclear.

p110 $\alpha$  y p110 $\beta$  son considerados compañeros obligados de sus subunidades reguladoras p85 (Geering *et al.*, 2007). Nosotros determinamos que la expresión de p85 $\beta$ , y no la de p85 $\alpha$ , facilita la localización nuclear de p110 $\beta$ , y no la de p110 $\alpha$ . Cuando p85 $\beta$  fue expresado solo, provocó un ligero marcaje nuclear en las células transfectadas. Cuando las células son cotransfectadas con p85 $\beta$ /p110 $\beta$ , el marcaje nuclear de p85 $\beta$  fue observado en el 22% de las células. Además p110 $\beta$  también se localizó en el núcleo en estas células, mostrando que p85 $\beta$ /p110 $\beta$  es el heterodímero que se localiza en el núcleo. Cuando p110 $\alpha$  fue cotransfectada con p85 $\alpha$  o p85 $\beta$ , p110 $\alpha$  permaneció en el citoplasma al igual que p85 $\alpha$  y la mayoría de p85 $\beta$ . Estos resultados fueron inesperados; ya que se considera que ambas subunidades reguladoras tienen papeles similares y solo p85 $\beta$  (no p85 $\alpha$ ) facilitó de manera reproducible la translocación nuclear de p110 $\beta$  (no p110 $\alpha$ ).

La unión de p85 $\beta$  a p110 $\beta$  podría provocar cambios conformacionales en el complejo, o en la activación del complejo; cualquiera de estos eventos podría promover la translocación nuclear. Otra posibilidad es la unión preferencial de p110 $\beta$  a p85 $\beta$  y de p110 $\alpha$  a p85 $\alpha$ . Examinamos esta posibilidad fusionando el NLS a p85 $\beta$  y cotransfectando p110 $\alpha$  y p110 $\beta$  con p85 $\alpha$  y p85 $\beta$ -NLS (Fig. 26). p85 $\beta$ -NLS mostró una completa localización nuclear debido a la SV40 NLS, lo cual también se tradujo en un p110 $\beta$  nuclear; sin embargo, en el caso de p110 $\alpha$  una gran fracción permaneció en el citoplasma al igual que p85 $\alpha$ . Con estos datos parece que existe una unión preferencial de p110 $\beta$  a p85 $\beta$  aunque el análisis bioquímico (futuro) es necesario para confirmar esta posibilidad.

Tras determinar la localización de estos complejos en el núcleo, buscamos si existían NLS clásicos en p85 $\beta$  o en p110 $\beta$ . Encontramos una región potencial polibásica NLS en p85 $\beta$  y la mutamos reemplazando dichos residuos básicos por los correspondientes en la misma región de p85 $\alpha$ . Sin embargo no observamos una localización de los complejos mutantes distinta de la de los complejos control p85 $\beta$ /p110 $\beta$ . De estas observaciones concluimos que la potencial polibásica en p85 $\beta$  no funciona como un NLS.

Además, detectamos tres NLS potenciales en p110 $\beta$ , las cuales fueron mutadas con residuos no básicos. Dos de estas mutaciones no tuvieron efecto en la localización nuclear de los complejos mutantes p85 $\beta$ /p110 $\beta$ , mientras la mutación en el NLS putativo en el dominio C2 de p110 $\beta$  inhibió la translocación nuclear del complejo p85 $\beta$ /p110 $\beta$ . Estas observaciones nos permitieron hipotetizar que la conformación del complejo p85 $\beta$ /p110 $\beta$  abre la región polibásica en el dominio C2 para asociar la maquinaria de importación nuclear para su translocación como complejo (Fig. 2).

Para determinar si p85 $\beta$  o p110 $\beta$  tienen una señal de exportación nuclear (NES), examinamos el efecto del tratamiento con Leptomomicina B en la localización de p85 $\beta$ , p110 $\beta$  o p85 $\beta$ /p110 $\beta$ . Dicho tratamiento resultó en una localización nuclear constitutiva de p85 $\beta$  transfectada y en una retención parcial nuclear del p110 $\beta$  cotransfectado con p85 $\beta$ . Estos resultados sugieren la presencia de un NES en p85 $\beta$ . De hecho, identificamos una región NES en sus N-41 aminoácidos (NT41aa).

Incluso cuando p85 $\beta$  fue coexpresada con p110 $\beta$ , no todas las células que coexpresaron estas dos subunidades mostraron un fenotipo de localización nuclear tan completo como el exhibido por los complejos endógenos. Nosotros identificamos asociación de p110 $\beta$  con PCNA, la cual podría ayudar en la translocación de p85 $\beta$ /p110 $\beta$ . Aunque PCNA no tiene un NLS, se trata de una proteína constitutivamente nuclear. Se ha sugerido que CDK2 controla la translocación de PCNA al núcleo (Koundrioukoff *et al.*, 2000). Se requieren estudios futuros que ayuden a identificar proteínas que contribuyen a en la translocación de p110 $\beta$ . En cualquier caso nuestros datos sugieren que la asociación de PCNA a p85 $\beta$ /p110 $\beta$  incrementa su localización nuclear.

### **p110 $\beta$ es necesaria para la estabilidad genómica y activación de la respuesta a daño del ADN tras exposición a UV e IR**

p110 $\beta$  regula la reparación del ADN. Esta hipótesis fue confirmada por la observación de células transfectadas con shARN de p110 $\beta$  y exposición a UV lo que provocó muerte celular (en fase sub-G1). Nuestros resultados también indicaron que la delección de p110 $\beta$  en células con defectos en apoptosis (defectos en la ruta de p53) provoca inestabilidad genómica, con roturas cromosómicas y alteración de los cromosomas debido a uniones aberrantes. Además, encontramos aneuploidias en MEFs p110 $\beta^{-/-}$ /DNp53 con una media de 100-150 cromosomas. Esto nos permitió examinar el papel de p110 $\beta$  en reparación del ADN. Aquí mostramos que p110 $\beta$  es esencial para la correcta activación de los mecanismos de reparación del ADN inducidos por UV e IR. La activación de dichos mecanismos implica a una compleja red de proteínas de control que ejercen distintas funciones en reparación de DNA y son activadas por ATM o ATR. Los diferentes requerimientos para la activación de ATM y ATR, así como otras proteínas relacionadas con estas vías de señalización permanecen por esclarecer. Nosotros observamos asociación de p110 $\beta$  con RAD17 dependiente de radiación, sugiriendo un papel específico para los complejos p110 $\beta$ /RAD17 en reparación del ADN.

Un incremento en la actividad quinasas de p110 $\beta$  tras exposición a UV o IR muestra que el daño en el ADN induce actividad de p110 $\beta$ . Recientemente Bouzic *et al.* describieron activación de PKB en respuesta a DNA DSB (Bozulic *et al.*, 2008). Ellos concluyeron que PKB $\alpha$  actúa en niveles inferiores de la vía de señalización de DNA-PK en DDR (DNA Damage Response), donde DNA-PK fosforila PKB en Ser473; además, ellos observaron un incremento en la fosforilación de Thr308 que es estrictamente dependiente de PI3K. Por tanto es posible que la activación de p110 $\beta$  regula la activación de PKB tras DSB.

Nuestros estudios indican activación defectuosa de la vía ATR en células deleccionadas de p110 $\beta$ ; hubo una disminución en la fosforilación de Chk1 y RAD 17 en dichas células tras exposición a UV o IR. Nosotros también observamos una disminución en la acumulación de p-RAD17 y formación de focos tanto en células depleccionadas de p110 $\beta$  y células tratadas con inhibidores de p110 $\beta$ , aunque el efecto fue mucho más fuerte en células p110 $\beta^{-/-}$ . Esto podría deberse a la activación ya descrita de ATR mediada por RAD17/9-1-1, donde el complejo



RAD17-9-1-1 recluta a la proteína activadora de ATR, TopBP1 a los lugares de daño en el ADN (**Kumagai *et al.*, 2006; Delacroix *et al.*, 2007; Lee *et al.*, 2007**).

Por otro lado, se observó que p110 $\beta$  regula la autofosforilación de ATM, la cual a su vez controla la DDR tras exposición IR. Después de exponer células p110 $\beta^{-/-}$  a radiación gamma, observamos activación defectuosa de ATM, Chk2 y SMC1, como resultado de la disminución de los eventos superiores en la vía de señalización de ATM. También identificamos que los defectos se produjeron a nivel del reclutamiento de las proteínas sensor al daño en el ADN como así ocurrió en el caso de la proteína sensor NBS1. También observamos inmovilización defectuosa a los lugares de daño del ADN en el caso de GFP-53BP1 tras inducción de daño en el ADN mediante láser UV lo cual corresponde con una defectuosa DDR, pues 53BP1 está implicada en la respuesta celular temprana a DSB (**Schultz *et al.*, 2000**) y contribuye a la activación de los puntos de control tras su reclutamiento (**Wang B. *et al.*, 2002**).

También hemos determinado un papel directo de p110 $\beta$  en la regulación del proceso reparación del ADN; la activación de p110 $\beta$  y su colocalización con gamma-H2AX en las áreas de daño del ADN, implican un papel integrador de p110 $\beta$  en las respuestas a daño.

Holmes y colaboradores sugirieron que PCNA es un requerimiento para el reclutamiento de proteínas de recombinación a los puntos de reparación del ADN (**Holmes MA, and Haber JE, 1999**). De acuerdo con esta idea, nuestros análisis de imágenes *in vivo* tras exposición a UV-láser en células vivas, mostraron movilización simultánea de PCNA y NBS1 a los lugares de daño del ADN. Examinamos el efecto de p110 $\beta$  en la translocación de PCNA al punto de daño del ADN, y encontramos que la inhibición de la actividad quinasa de p110 $\beta$  retardó la movilidad de PCNA; la delección de p110 $\beta$  alteró mas aún la localización de PCNA en los puntos de daño. Concluimos que p110 $\beta$  actúa como andamio molecular regulando el reclutamiento de PCNA a la cromatina en los lugares de daño en el ADN. Por tanto, concluimos que p110 $\beta$  regula ambas ramas de las vías de señalización relacionadas con DSB. Como la PI3K tiene actividad proteína y lípido quinasa (**Dhand *et al.*, 1994; Foukas *et al.*, 2004; Foukas & Shepherd, 2004**), estudios futuros ayudarán a esclarecer el papel de p110 $\beta$  (como proteína o lípido quinasa) tras activación inducida por IR/UV.

## **INTRODUCTION**



In higher eukaryotes, cell division is a fundamental process for development, growth, and replacement of worn-out cells. A balance is always maintained between cell division and cell death to regulate cell number. In a normal setting, division and death are tightly regulated through complex mechanisms, as deregulation of either can result in unrestrained cell proliferation, leading to tumourigenesis. Such deregulation can be due to the changes in cell cycle machinery caused by hyperactive proto-oncogenes or by tumour suppressor genes that no longer respond to normal control of cell proliferation. Cell cycle deregulation associated with hyperproliferation occurs through the overexpression or mutation of proteins with a pivotal role in different cell cycle phases. These proteins exploit the mechanisms they regulate to shorten cell cycle length, and to bypass checkpoint and DNA replication defects.

These cell division regulatory proteins can be grouped into four classes: growth factors, growth factor receptors (section 1), signal transducers (section 2), and nuclear regulatory proteins. Among signal transducers, we will introduce in more detail the PI3K signalling pathway, which constitutes the objective of our study (section 3), as well as signalling pathways in the nucleus (section 4). Receptor activation by growth factors (GF) triggers signal transducers, which act on secondary messengers. These secondary messengers control nuclear regulatory proteins (section 5) to initiate gene expression, which contributes to the triggering of cell cycle entry (section 6). An introduction to DNA damage response-mediated pathways is included (section 7), as part of our research refers to the role of the PI3K pathway in DNA damage repair.

## SECTION 1. GROWTH FACTOR RECEPTORS

Addition of growth factors stimulates GF receptors, some of which are described below.

### 1.1) Receptor tyrosine kinases

The receptor tyrosine kinases (RTK) form a large family of protein kinases, which act upon extracellular signals through a variety of growth factors and catalyse the phosphorylation of tyrosines on various target molecules. RTK comprise an extracellular ligand-binding domain, a transmembrane hydrophobic  $\alpha$  helix, and a cytosolic domain with protein-tyrosine kinase activity (**Hupfeld *et al.*, 2007**). Of 90 known tyrosine kinases, 58 are RTK; they are further classified into 20 subfamilies, depending on the sequence of the kinase domain (**Robinson *et al.*, 2000**). Some of these subfamilies are EGF (epidermal GF), insulin, PDGF (platelet-derived GF), FGF (fibroblast GF), VEGF (vascular endothelial GF), and HGF (hepatocyte GF).

Following GF stimulation, distinct protein ligands bind to their respective receptors on the extracellular domain, triggering dimerisation with adjacent homologous RTK. This dimerisation leads to activation of the cytoplasmic side of the receptor by autophosphorylation of its tyrosine residues or through cytoplasmic tyrosine kinases, such as Src kinases, that phosphorylate the receptor. The resulting phosphotyrosines serve as docking sites for adaptor proteins containing Src homology 2 (SH2) or PTB (phosphotyrosine-binding) domains (**Schlessinger, 2000; Hubbard & Till, 2000**).

Adaptor proteins can act in two different ways: they either directly phosphorylate effector molecules following activation or, if they lack kinase activity, they facilitate the association of activated tyrosine receptors to their partners. These SH2- and PTB-containing signalling proteins are modular in nature (**Schlessinger & Lemmon, 2003**). A large family of SH2 domain-containing proteins have intrinsic enzymatic activities such as protein tyrosine kinases (PTK; examples are the Src kinases), protein tyrosine phosphatase (PTP; Shp2), phospholipase C (PLC $\gamma$ ), or Ras-GAP. Another family of proteins that have only SH2 or SH3 domains use these domains to mediate the interaction of different proteins involved in signal transduction (**Pawson, 1995**). Whereas RTK are

signal transduction initiators, adaptor proteins act to transmit the signal induced by GF addition to the cell.

## 1.2) G protein-coupled receptors

Another prominent group of receptors belongs to the integral membrane receptors family. These are the G protein-coupled receptors (GPCR), which bind to heterotrimeric G proteins and are activated following stimulation (for example, by growth factors) to transduce extracellular signals into intracellular changes through secondary messenger cascades. GPCR act on the heterotrimeric G proteins as guanine-nucleotide exchange factors. Stimulation thus results in conformational changes in the G protein complex, which allow it to interact with GTPases, leading to GDP release. The GTP-bound form of the G protein  $\alpha$ -subunit dissociates from the receptor and from the stable  $\beta\gamma$ -dimer, initiating a signalling cascade. Hydrolysis of  $\alpha$ -subunit-bound GTP through its intrinsic GTPase activity results in its inactivation (**Dupré *et al.*, 2009**).

Many reports suggest that RTK can use proximally located G protein/GPCR signalling components in an integrated manner to induce activation of key regulatory pathways linked to cellular processes such as proliferation and differentiation. RTK (e.g., receptors for PDGF, insulin, EGF) appear to form associated complexes with GPCR, which in some cases supply G protein for use by the RTK for downstream signalling. In addition, certain RTK (e.g., IGF-1R) appear to associate directly with and activate heterotrimeric G protein (**Malbon, 2004; Alcántara-Hernández *et al.*, 2008**).

## SECTION 2. SIGNAL TRANSDUCTION PROTEINS

Signal transduction proteins form complex networks of highly interconnected and redundant signalling pathways to implement intra- and extracellular signals for distinct cell processes. Many proteins participate in signal transduction pathways downstream of GF receptors to mediate various cell responses; we will introduce a few of these below.

### 2.1) RAS

Ras proteins are G proteins (small GTPases) positioned at the inner leaflet of the plasma membrane, where they serve as binary molecular switches to transduce extracellular ligand-mediated stimuli into the cytoplasm. Ras shuttles between two conformations – an active (RAS-GTP) and inactive form (RAS-GDP). Guanine nucleotide exchange factors (GEF) activate Ras by releasing GDP from Ras and allowing GTP to bind to it. Allosteric changes in Ras after GTP binding increase its affinity for its effectors, to generate intracellular signals, whereas Ras is inactivated by GTPase-activating proteins (RAS-GAP), which hydrolyse the RAS-bound GTP to GDP while releasing an inorganic phosphate. This activation/inactivation cycle is associated with the transduction of an upstream signal to downstream effectors to regulate Ras-mediated cell processes.

In addition to the regulation of Ras family proteins by their GTP- or GDP-bound status, Ras GTPases undergo post-translational modifications that regulate protein-protein interactions, stability, as well as membrane attachment and thus, subcellular localisation and function (Fig. 1). The Ras carboxy terminus has a membrane targeting sequence (CAAX motif), which is a substrate for a series of post-translational modifications that create a lipidated hydrophobic domain; this mediates attachment to specific proteins and membranes (**Karnoub *et al.*, 2008**). Post-translationally modified active Ras translocates to the plasma membrane, where Ras interacts and activates its downstream effector proteins.

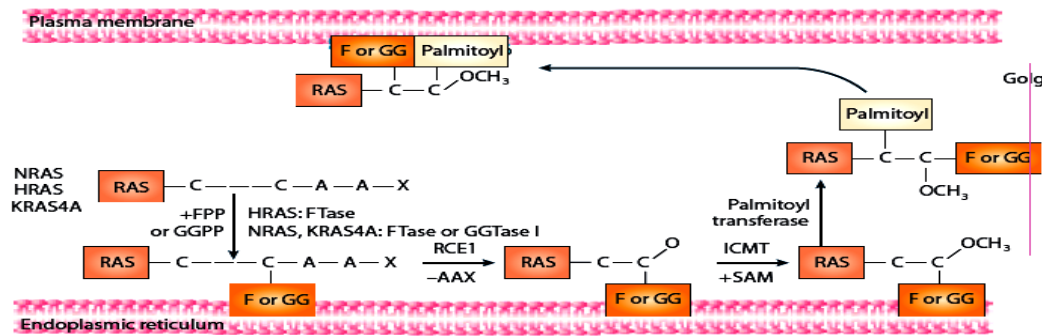


**Figure 1. Prenylation and post-prenylation reactions of RAS GTPases.** Newly synthesized RAS is a cytosolic protein. HRAS, NRAS and KRAS4A are prenylated (HRAS is only farnesylated, whereas NRAS and KRAS4A can be farnesylated or geranylgeranylated) before proteolytic removal of the AAX tripeptide by RAS-converting enzyme 1 (RCE1) and carboxymethylation by isoprenylcysteine carboxymethyltransferase (ICMT) in the endoplasmic reticulum. They are subsequently palmitoylated in the Golgi and transferred to the plasma membrane, to which they attach through their farnesyl (F) or geranylgeranyl (GG), and palmitoyl moieties. (Adapted from Konstantinopoulos *et al.*, 2007).

## 2.2) Mitogen-activated protein kinases

The mitogen-activated protein kinase (MAPK) pathway regulates cell processes by transmitting extracellular signals from cell surface receptors to downstream factors in the nucleus to regulate gene expression through phosphorylation (Seger & Krebs, 1995). The MAPK signalling cascades are composed of a wide array of specialized molecules that include transmembrane receptors, guanosine triphosphatase (GTPases), adaptors, kinases, phosphatases, scaffolds, and transcription factors (Gaestel, 2006). There are three major classes of MAPK: extracellular signal-regulated kinases (ERK1/2), c-Jun N-terminal kinases (JNK1, JNK2 and JNK3; often called the stress-activated protein kinase) and p38 kinases ( $\alpha$ ,  $\beta$ ,  $\gamma$ ,  $\delta$ ) (Gallo & Johnson, 2002).

Activation of these kinases requires phosphorylation by upstream kinases. The ERK MAP kinases are activated by the MAPK kinases (MKK) MKK1 and MKK2; the p38 MAPK are activated by MKK3, MKK4, and MKK6, and the JNK pathway is activated by MKK4 and MKK7. These MAPK kinases are activated in turn by several different MAPK kinase kinases (MKKK). Activation of ERK1/2 has been linked to cell survival, whereas JNK and p38 are associated primarily to apoptosis induction, although some studies report a role in cell survival (Alvarado-Kristensson *et al.*, 2004; Gallo & Johnson, 2002). JNK phosphorylate Jun proteins, thereby enhancing their ability to activate transcription without affecting DNA binding. The role of p38 MAPK signalling in cell responses is diverse, depending on cell type and stimulus.

Signalling pathways vital for a variety of cellular responses include phosphoinositide-3-kinase (PI3K), phosphoinositide-specific phospholipase C (PLC) (Rhee, 2001), protein kinase C (PKC) (Griner & Kazanietz, 2007), diacylglycerol (DAG) (Irvine, 2003), and  $\text{Ca}^{2+}$  release (Roderick & Cook, 2008). Of these, the PI3K constitute the centre of our research; a detailed description of this pathway is presented in section 3.

## SECTION 3. PHOSPHOINOSITIDE-3-KINASES

The PI3K family of lipid kinases are one of the signal transducers required for transformation of mammalian cells (Serunian *et al.*, 1990; Ling *et al.*, 1992). PI3K belongs to the family of lipid kinases that phosphorylate the 3'-hydroxyl group of phosphoinositides (PI, PI4P, PI5P, PI(4,5)P2). In normal cells,  $\text{PIP}_3$  {phosphatidylinositol (3,4,5)-triphosphate} can be detected transiently after stimulation by a variety of growth factors (Whitman *et al.*, 1988; Varticovski *et al.*, 1989).  $\text{PIP}_3$  levels can increase by more than 50-fold, peaking between 10-60 sec after PDGF

stimulation and lasting for 30-60 min (Auger *et al.*, 1989). The PDGF receptor was the first receptor shown to associate with (Kaplan *et al.*, 1987) and activate PI3K (Auger *et al.*, 1989).

PI3K was discovered as a Rous sarcoma virus protein associated with polyoma middle-T transformation (Whitman *et al.*, 1985). Later, Whitman *et al.* (1988) identified that the D-3 site on the inositol ring is phosphorylated by type I PI3K. With time, many PI3K homologues were found and grouped into four classes according to sequence homology and substrate specificity. All PI3K isoforms have similar Ras-binding (except class III), C2, PIK and catalytic domains, with maximum similarity in these last. These four classes contribute to a variety of cell responses such as division (Garcia *et al.*, 2006), survival, migration (Katso *et al.*, 2001; Datta *et al.*, 1999), polarity (Wang F. *et al.*, 2002), cytoskeletal organisation (Sasaki *et al.*, 2004; Reif *et al.*, 1996; Toker & Cantley, 1997), vesicle trafficking (Siddhanta *et al.*, 1998), glucose transport (Toker & Cantley, 1997), platelet function (Jackson *et al.*, 2004), autoimmunity (Katso *et al.*, 2001), angiogenesis (Katso *et al.*, 2001; Graupera *et al.*, 2008), apoptosis (Franke *et al.*, 2003) and DNA repair (Sancar *et al.*, 2004). A brief introduction to the four PI3K classes is given below.

### 3.1) Class I PI3K

The class I PI3K are heterodimeric proteins consisting of one catalytic and one associated regulatory subunit, which catalyze the *in vivo* production of PI (3,4,5) P3 and PI(3,4)P2, which act as second messengers for the activation of many PI3K effectors. The regulatory subunits modulate the kinase activity of the enzyme and its subcellular localisation (Garcia *et al.*, 2006). In addition their role as lipid kinases, class I PI3K also exhibit limited protein kinase activity.

Depending on their mode of activation and their association to different receptors, class I PI3K are further divided into two subgroups, class I<sub>A</sub> and class I<sub>B</sub> PI3K (Stoyanov *et al.*, 1995). Class I<sub>B</sub> PI3K is composed of a single gene product, PIK3G (PI3K $\gamma$ ), and is activated by GPCR. In mammals, three genes have been identified that code for the class I<sub>A</sub> catalytic isoforms, namely p110 $\alpha$ , p110 $\beta$  and p110 $\delta$  (Hiles *et al.*, 1992; Hu *et al.*, 1993; Vanhaesebroeck *et al.*, 1997), encoded by *PIK3CA*, *PIK3CB* and *PIK3CD*, respectively. There are five p85-related regulatory subunits (p85 $\alpha$ , p85 $\beta$ , p55 $\alpha$ , p50 $\alpha$  and p55 $\gamma$ ), of which p55 $\gamma$  and p85 $\beta$  are encoded by *PIKR3* and *PIKR2*, whereas p85 $\alpha$ , p55 $\alpha$  and p50 $\alpha$  are encoded by *PIK3R1* through alternative splicing (Koyasu, 2003). Of the three class I<sub>A</sub> catalytic subunits, p110 $\alpha$  and p110 $\beta$  are expressed ubiquitously, whereas p110 $\delta$  is abundant in haematopoietic cells.

While class I<sub>B</sub> PI3K is activated by GPCR, class I<sub>A</sub> PI3K are activated mainly by RTK growth factor receptors. This subfamily is also activated through cytosolic tyrosine kinases such as Src family members, which phosphorylate the p85 subunit of the heterodimer. Ras can further enhance class I<sub>A</sub> activity after initial activation through RTK (Downward, 2003). As an exception, the p110 $\beta$ /p85 complex can also be activated through GPCR and can function redundantly in the absence of class I<sub>B</sub> to mediate GPCR signals (Garcia *et al.*, 2006).

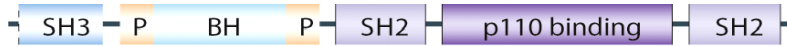
The p85 regulatory subunits  $\alpha$  and  $\beta$ , which are encoded by different but related genes, have two carboxy-terminal SH2 domains separated by an inter-SH2 region that forms the binding site for the catalytic subunits p110 $\alpha$ , p110 $\beta$  and p110 $\delta$ . In addition, p85 $\alpha$  and p85 $\beta$  have an amino-terminal proline-binding SH3 and a breakpoint cluster region (BCR) homology domains. Finally, the BCR homology domains are flanked by two proline-rich domains (Fig. 2A) (Wymann & Pirola, 1998).

The p110 catalytic subunits are also organized in a modular manner, containing an N-terminal p85-binding domain (25-173), a Ras-binding domain, a membrane-binding C2 domain, a helical region and catalytic subunit at the C-terminal (Fig. 2B). The ribbon crystal structure of p110 $\alpha$  with the p85 $\alpha$  region is shown in Fig. 2C.

A)



B)



C)

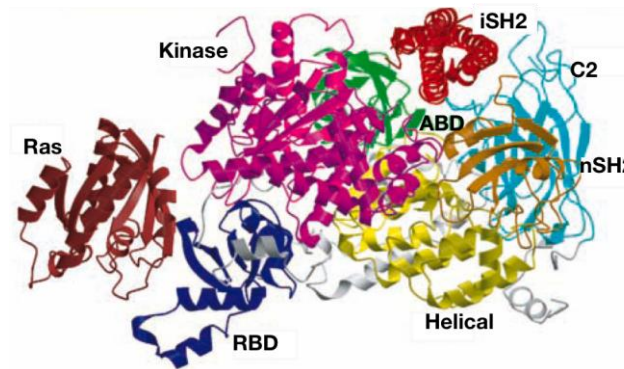


**Figure 2. Domain structure of class I<sub>A</sub> PI3K catalytic and regulatory isoforms.** A) Structure of the catalytic subunit p110 with the N-terminal p85-binding domain, Ras-binding region, a C2 domain, PIK domain and a C-terminal catalytic domain. B) Structure of p85 proteins with SH3, polyproline, BCR region, polyproline, N-terminal SH2 followed by an iSH2 p110-binding region and a C-terminal SH2 domain. C) Ribbon structure of p110 $\alpha$  binding to p85 inter-SH2 domain while in subsequent association with Ras (figure adapted from [Huang \*et al.\*, 2007](#)).

### 3.1.1) Signalling pathways controlled by class I<sub>A</sub> PI3K

The class I<sub>A</sub> PI3K are activated by a variety of RTK such as PDGF-R, IGF and Ras. *In vitro* studies using PI3K-binding mutants of the PDGF receptor show that PI3K is responsible for PDGF-induced cell proliferation, survival and migration ([Valius & Kazlauskas, 1993](#); [Bazenet & Kazlauskas, 1994](#); [Joly \*et al.\*, 1994](#)) (Fig. 3). Active PI3K catalyzes production of the phospholipid messenger PIP<sub>3</sub>. Production of PIP<sub>3</sub> results in membrane translocation of some of its effectors through the specific pleckstrin homology (PH) domain, which following activation transduces PI3K signals to many downstream effectors. The finding that RTK activation of PKB (protein kinase B) is blocked by the PI3K inhibitors wortmannin and LY294002 indicates that PI3K activity is necessary for PKB activation ([Chan \*et al.\*, 1999](#)). The many proteins that bind to these lipids, such as phosphoinositide-dependent kinase 1 (PDK1), PKB, p70S6k, Bruton's tyrosine kinase, protein kinase C (PKC) have diverse physiological functions ([Toker & Cantley, 1997](#)) including glucose uptake, cell trafficking, adhesion, actin rearrangement, and proliferation.

Activation of PI3K downstream kinases in the cytosol is often mediated by PDK1, a serine/threonine kinase originally identified as critical for PKB activation loop phosphorylation and its activation ([Cohen \*et al.\*, 1997](#); [Anderson \*et al.\*, 1998](#)).



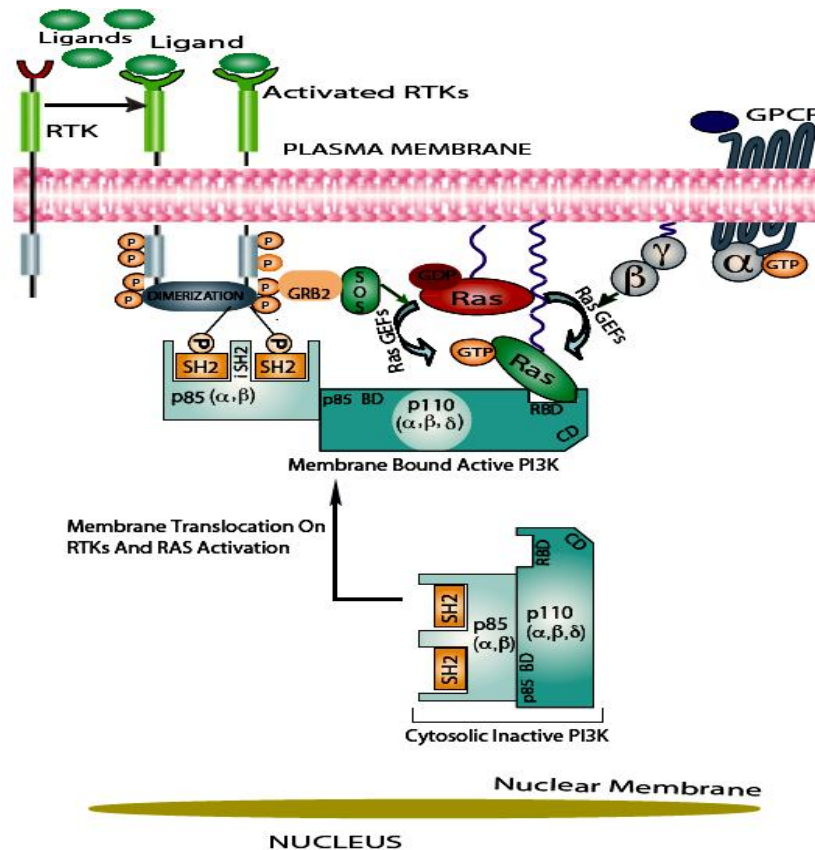


**Figure 3. Activation of class I<sub>A</sub> PI3K after growth factor-mediated stimulation.** In response to extracellular stimuli, the catalytic subunit of PI3K (p110) is recruited through its regulatory subunit (p85) to RTK or GPCR at the membrane where it phosphorylates PIP<sub>2</sub> to generate PIP<sub>3</sub>.

### 3.1.1.1) PDK1

PDK1 is a 63 kDa protein kinase, which consists of an N-terminal kinase domain and a C-terminal PH domain. The PH domain of PDK1 binds to the PI3K products PIP<sub>3</sub> and PIP<sub>2</sub>, which target PDK1 to the plasma membrane; for this reason, it was termed 3-phosphoinositide-dependent kinase-1 (Alessi *et al.*, 1997). PDK1 is activated by phosphorylation in the activation loop (Ser241 in human and Ser244 in the mouse) (Casamayor *et al.* 1999; Wick *et al.*, 2002; Wick *et al.*, 2003). In addition to phosphorylation, PDK1 function is regulated by protein-protein interactions (Makris *et al.*, 2002), and it regulates many AGC super family protein kinases, including protein kinase A (PKA), PKC and RAC-PK (Williams *et al.*, 2000; Dutil *et al.*, 1998; Le Good *et al.*, 1998), the ribosomal S6kK, and S6K1 kinases (Toker & Newton, 2000; Vanhaesebroeck & Alessi, 2000).

### 3.1.1.2) PKB

PKB belongs to the AGC family of protein kinases (Peterson *et al.*, 1999). Mammalian PKB is a homologue of the *v-Akt* oncogene (acute transforming retrovirus in mice) (Staal, 1987). Following PI3K activation, the PKB PH domain binds to PIP<sub>2</sub> and PIP<sub>3</sub>, which induces translocation of cytoplasmic PKB to the plasma membrane (Frech *et al.*, 1997; Franke *et al.*, 1997). After membrane translocation, PKB is phosphorylated at Thr308 by PDK1, which facilitates Ser473 phosphorylation by the mTOR complex 2 or by DNA-PK (Fig. 4). Phosphorylation at Ser473 results in fully activated PKB (Alessi *et al.*, 1996).



**Figure 4. PKB structure and mechanism of activation.** The N-terminal PH domain of PKB is followed by the catalytic domain. Active PDK1 phosphorylates Thr308, making Ser473 available for phosphorylation by mTOR or DNA-PK. After phosphorylation at Ser473, PKB is fully activated.

Due to the variety and specificity of its substrates, PKB has a central role in many PI3K class I<sub>A</sub>-mediated cell responses such as growth, survival and metabolism. PKB substrates have a common consensus sequence, RXRXXS/T, where X is any amino acid and S/T are the phosphorylation sites. Glycogen synthase kinase (GSK) was the first substrate identified for PKB and the consensus substrate sequence was derived from it (**Brazil *et al.*, 2001**; **Datta *et al.*, 1999**). GSK inactivates glycogen synthase after stimulation and regulates glycogen synthesis. PKB phosphorylates GSK3- $\beta$  at Ser9 and indirectly regulates the stability of c-Myc, an oncogene implicated in a number of cell growth, survival and tumourigenic pathways (**Sears *et al.*, 2000**). PKB has been implicated in regulating the apoptotic pathway specifically through control of the phosphorylation and inhibition of apoptotic mediators such as the FOXO family (**Brunet *et al.*, 1999**), the Bcl-2 family, BAD (**Datta *et al.*, 1997**), GSK3- $\beta$  and IKK- $\beta$ , and through inhibition the apoptosis-promoting JNK pathway. PKB is also important in neurobiology, as it modulates neuronal synapse activity and neurodegeneration (**Dudek *et al.*, 1997**).

### 3.1.2) Class IB PI3K

The class I<sub>B</sub> subgroup is a heterodimer composed of one catalytic p110 $\gamma$  subunit (Fig. 5) that associates with p101 or p87 regulatory subunits of class IB PI3K (**Walker *et al.*, 1999**; **Pacold *et al.*, 2000**). GPCR are major activators of class IB PI3K; as one more exception, this class can be activated by tyrosine kinases (**Alcazar *et al.*, 2008**).



**Figure 5. Domain structure of the class I<sub>B</sub> p110 $\gamma$  catalytic subunit.** Ras-binding domain, C2 domain, PIK region and catalytic domain.

### 3.1.3) Phosphatase and tensin homologue deleted on chromosome 10 (PTEN)

PTEN is an antagonist of class I PI3K signalling that directly opposes the activity of PI3K by dephosphorylating the third position of the inositol ring of poly-phosphoinositols (**Maehama & Dixon, 1998**). *PTEN* was first discovered by two independent groups and recognized as a tumour suppressor gene on human chromosome 10q23, a locus that is highly susceptible to mutation in primary human cancers (**Li & Sun, 1997**; **Steck *et al.*, 1997**).

## 3.2) Class II PI3K

These enzymes mainly catalyse the production of PI(3)P, but to a lesser extent can also produce PI(3,4)P<sub>2</sub> after activation. Class II PI3K have roles in regulating cytoskeleton organization, cell migration, membrane trafficking and exocytosis (**Gaidarov *et al.*, 2001**; **Engelman *et al.*,**

2006). This class is comprised by three isoforms, PI3KC2 $\alpha$ , PI3KC2 $\beta$  and PI3KC2 $\gamma$ . Class II PI3K are catalytic subunit monomers, as they do not associate with a regulatory subunit (Fig. 6). PI3K C2 $\alpha$  is located in the nucleus of some cell types, and can regulate mRNA transcription (Didichenko & Thelen, 2001).



Figure 6. Domain structure of the class II catalytic subunit. Ras-binding domain, C2 domain, PIK region, catalytic domain, PX, C-terminal C2 domain.

### 3.3) Class III PI3K

This PI3K class comprises only one isoform, the vacuolar protein-sorting defective 34 (Vps34). It is a heterodimer of the 101 kDa catalytic subunit (Fig. 7) and a 150 kDa regulatory subunit (Vps15p/p150). Vps15p/p150 has an N-terminal myristylation signal, a serine/threonine kinase domain, a series of leucine-rich repeats, and C-terminal WD motifs (tryptophan-aspartate repeat). Vps34 preferentially catalyzes phosphorylation of PI to produce PI3P. The primary function of Vps34 was shown to be vesicle trafficking, but it might have additional roles in controlling cell growth, as it is reported to regulate the mammalian target of rapamycin (mTOR) (Nobukuni *et al.*, 2005), and in autophagy (Wurmser & Emr, 2002; Vieira *et al.*, 2001).



Figure 7. Domain structure of the Vps34 catalytic subunit. C2 domain, PIK region and catalytic domain.

### 3.4) Class IV PI3K

This is a distinct class of the PI3K family, which act as serine/threonine kinases and lack lipid kinase activity. This class comprises four isoforms: ataxia telangiectasia mutant (ATM), ataxia telangiectasia and Rad3-related (ATR), DNA-PK and mTOR (Engelman *et al.*, 2006). ATM, ATR and DNA-PK are implicated in DNA repair, where they recruit DNA damage sensor proteins to the site of DNA damage and induce the cell cycle checkpoint through various means (Sancar *et al.*, 2004). Of these isoforms, ATR and ATM are activated by cell exposure to ultraviolet (UV) light or ionizing radiation (IR), after which they are recruited to the DNA damage sites. Activation of ATM (by autophosphorylation at Ser1981) or ATR kinases activates checkpoint kinases 1 (Chk1) and 2 (Chk2) through phosphorylation. Activated Chk1 and Chk2 regulate several proteins that promote DNA repair, some of which cause cell cycle arrest due to DNA damage (Su, 2006).

## SECTION 4. NUCLEAR CLASS I $\alpha$ PI3K SIGNALLING

Whereas PI3K signalling in the cytosol is well documented as an essential pathway for transducing signals from the plasma membrane to the nucleus, evidence suggests that the nucleus-specific phosphoinositide signalling pathway works independently of the cytoplasm (Neri *et al.*, 2002). PI3K and its effectors involved in PI3K signalling, such as PDK1 (Lim *et al.*, 2003), PKB, and PTEN are localised partially to the nucleus (Chan *et al.*, 1999; Neri *et al.*, 2002; Planchon *et al.*, 2008). The purpose of these signals is thought to be the activation of specific chromatin-remodelling complexes (Rando *et al.*, 2002; Zhao *et al.*, 1998), specific gene transcription, and inhibition of apoptotic pathways (Martelli *et al.*, 1999).

Whereas PI3K is constitutively expressed in the nucleus of rat hepatocytes (Martelli *et al.*, 1999), Neri *et al.* used immunostaining and immunoblotting of the p85 regulatory subunit to show that nerve growth factor (NGF) stimulation of PC-12 rat pheochromocytoma cells results in rapid PI3K translocation to the nucleus (Neri *et al.*, 1994). PI3K activity was identified in isolated rat liver nuclei (Lu *et al.*, 1998). Furthermore, analysis with an antibody to the regulatory subunit (p85 $\alpha$ ) and immunoelectron microscopy demonstrated immunolabelling of both the nuclear membrane and the nucleoplasm, in agreement with a report showing the intranuclear presence of PI3K in Saos-2 human osteosarcoma cells (Zini *et al.*, 1996). Based on its immunological reactivity, nuclear rat liver PI3K was found to constitute approximately 5% of total cellular PI3K (Lu *et al.*, 1998).

Cytoplasmic PI3K activation requires activated RTK or GTPase proteins such as Ras. Nevertheless, none of these PI3K activators is known to be present in the nucleus. A novel brain-specific nuclear GTPase, phosphoinositide 3-kinase enhancer (PIKE), interacts with PI3K to stimulate its lipid kinase activity (Ye *et al.*, 2000) in neurons. NGF treatment elicits PIKE-S activation by triggering the nuclear translocation of PLC- $\gamma$ 1, which acts as a physiological GEF for PIKE-S through its SH3 domain (Ye *et al.*, 2002); this effect is independent of its lipase catalytic activity. Nuclear PI3K is also implicated in RNA processing and transport (Boronenkov *et al.*, 1998; Bunney *et al.*, 2000). NGF elicits the translocation of PI3K and its downstream effectors into the nucleus, although the mode of nuclear PI3K translocation and its biological functions in the nucleus remain elusive. One goal of this study was to determine the mechanism of PI3K translocation to the nucleus.

#### 4.1) Role of nuclear PKB

In NIH3T3 cells, v-Akt is distributed equally between cell membrane, cytosol, and the nucleus (Ahmed, 1993). Both v-Akt and PKB localize in the nucleus (Chan *et al.*, 1999). After insulin stimulation in 293T cells, PKB translocation to the plasma membrane was followed by its nuclear translocation (Andjelkovic *et al.*, 1997; Meier *et al.*, 1997). Nuclear phosphorylated PKB has been reported in lung, breast, prostate, and thyroid cancers, as well as in acute myeloid leukaemia (Lee *et al.*, 2002; Brandts *et al.*, 2005; Nicholson *et al.*, 2003; Vasko *et al.*, 2004; Capellini *et al.*, 2003; Van de Sande *et al.*, 2005). All three PKB isoforms (PKB-1, -2, -3) have a classic leucine-rich, leptomycin-sensitive nuclear export sequence (NES) (Saji *et al.*, 2005). PKB-1 overexpression with a non-functional NES results in constitutive nuclear localisation of PKB-1 and enhanced *in vitro* migration of PKB-1<sup>-/-</sup> fibroblasts (Saji *et al.*, 2005). These findings suggest that PKB nuclear localisation is involved in tumourigenesis. It was also reported that in PC12 cells, PIP<sub>3</sub> generated in the nucleus by PI3K after NGF stimulation regulates the nuclear translocation of PKC- $\zeta$  (Neri *et al.*, 1999); following nuclear translocation, PKC- $\zeta$  phosphorylates nucleolin (Zhou *et al.*, 1997) involved in rRNA synthesis, metabolism and transport (Ginisty *et al.*, 1999) (Fig. 8). Nucleolin also acts as a stabilizing agent for the anti-apoptotic protein Bcl-2 (Sengupta *et al.*, 2004; Kito *et al.*, 2003). Recent reports propose that nuclear PKB activity promotes cell survival (Lee *et al.*, 2008).

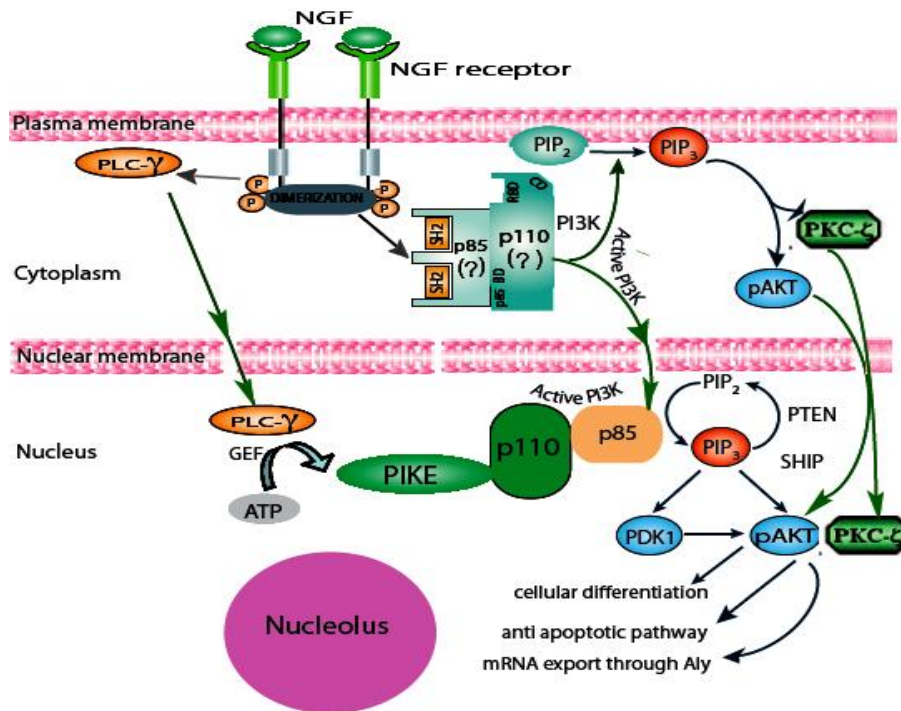


**Figure 8. Nuclear PI3K signalling.** NGF binding to its receptor stimulates translocation of both PI-PLC- $\gamma$  and PI3K class I (p85/p110) to the nucleus. Catalytically inactive PI-PLC- $\gamma$  acts as a GEF and activates a nuclear GTPase called PIKE. PIKE stimulates the activity of the nuclear PI3K, which phosphorylates PtdIns(4,5)P<sub>2</sub> into PtdIns(3,4,5)P<sub>3</sub>. PtdIns(3,4,5)P<sub>3</sub> attracts PKC- $\zeta$  and p-PKB that, after activation, translocate from cytoplasm to the nucleus and phosphorylate their nuclear substrates. The nuclear PI3K pathway inhibits the DNA fragmentation activity of caspase-activating DNase (CAD), promotes cell differentiation and assists mRNA export through Aly, a recently identified targets of the activated nuclear PI3K pathway.

## SECTION 5. NUCLEAR REGULATORY PROTEINS

A number of nuclear proteins are intimately involved in the sequential expression of genes that regulate variety of cellular processes. Many have the ability to bind DNA and thereby influence the expression of other genes. Of these, c-Myc constitutes the main interest of our study and is introduced below.

### 5.1) c-Myc

c-Myc was one of the first proto-oncogenes discovered; it belongs to the MYC family that also includes *N-myc* and *L-myc* genes, which encode related proteins. The proteins (c-Myc) encoded by MYC family genes localize predominantly to the cell nucleus, and their expression generally correlates with cell proliferation. The c-myc gene was first isolated as the chicken cellular homologue of v-myc (Vennstrom *et al.*, 1982). c-Myc is frequently elevated in human cancers (Little *et al.*, 1983; Mariani-Costantini *et al.*, 1988; Munzel *et al.*, 1991; Erisman *et al.*, 1985); its overexpression is strictly dependent on mitogenic signals and is suppressed by growth-inhibitory signals (Alexandrow *et al.*, 1995).

c-Myc is important for proliferation and apoptosis in response to appropriate stimuli, and itself acts as a strong mitogenic and apoptotic stimulus (Grandori *et al.*, 2000). Mouse embryos in which both *c-myc* alleles have been deleted by homologous recombination lack primitive haematopoiesis and die early in development (Davis *et al.*, 1993). Targeted gene replacement of endogenous *c-myc* with *N-myc* during embryogenesis allows normal development, indicating that *N-myc* has functional activities largely equivalent to those of *c-myc* (Malynn *et al.*, 2000; Landay

*et al.*, 2000). *L-myc*-null mice are healthy and do not have a phenotype distinct from their wild-type littermates, suggesting that *L-myc* is not required for embryogenesis (Hatton *et al.*, 1996). Downregulation of c-Myc expression leads to a marked decrease or absence of proliferation and cell viability (Shi *et al.*, 1993).

The study of the proteins that interact with c-Myc led to identification of the Max protein. Max interacts specifically with all MYC family proteins, and the resulting heterocomplexes recognize the hexameric DNA sequence CACGTG (belonging to the larger class of sequences known as E-boxes, CANNTG) (Prendergast & Ziff, 1991). c-Myc requires Max to activate transcription of genes containing E-box-binding sites (Amati *et al.*, 1992). c-Myc-Max binding to E-boxes is associated predominantly with gene activation, a finding consistent with c-Myc's ability to recruit multiple co-activator complexes (Grandori *et al.*, 2000; Adhikary & Eilers, 2005; Cole & Nikiforov, 2006). c-Myc has also been associated with transcriptional repression. While there are several modes of Myc repression, at least one mechanism involves specific binding and inhibition of the transcriptional activator Miz-1 (Kleine-Kohlbrecher *et al.*, 2006). Deregulated ARF, p53, and Bcl-xL interact with c-Myc to increase cell growth by inhibiting c-Myc-induced pro-apoptotic pathways (Seoane *et al.*, 2002; Lawlor *et al.*, 2006). c-Myc also regulates expression of genes that block cell cycle progression (e.g., cyclin-dependent kinase inhibitors (CKI) (Knoepfler *et al.*, 2002; Staller *et al.*, 2001; Herold *et al.*, 2002), inhibit signal transduction pathways (Berwanger *et al.*, 2002), and reduce cell contact and adhesion (Frye *et al.*, 2003; Wilson *et al.*, 2004; Gebhardt *et al.*, 2006). The ability of mammalian c-Myc to abrogate the influence of proliferation arrest genes is a crucial aspect of c-Myc function in normal development (Zindy *et al.*, 2006) and in tumourigenesis (Seoane *et al.*, 2002; Oskarsson *et al.*, 2006). Proteins of the Mxd family (formerly known as the Mad family) of transcriptional repressors contain c-Myc-related bHLHZ domains, heterodimerise with Max, and bind E-box sequences to restrict c-Myc binding and antagonize c-Myc function (Grinberg *et al.*, 2004; Hooker and Hurlin 2006; Rottmann and Luscher, 2006).

In general, *c-myc* expression correlates with the proliferative potential of the cell. Cells that constitutively express high c-Myc levels have reduced requirements for GF (Kaczmarek *et al.*, 1985; Sorrentino *et al.*, 1986; Stern *et al.*, 1986), spend less time in G1 phase (Karn *et al.*, 1989), and cannot become quiescent (Kohl & Ruley, 1987). c-Myc regulates expression of a large number of genes, some of which play an essential role in the G0/S interval (Ponzielli *et al.*, 2005; Dang *et al.*, 1999). *c-myc* is an early response gene whose rapid induction is essential for cell progression from G0 to G1 and for progress through early G1 (Schorl 2003; Mateyak *et al.*, 1997; Amati *et al.*, 1998). c-Myc expression is induced within minutes of cell exposure to GF, and contributes to control of cyclin D and cyclin E expression. Moreover, c-Myc is essential for cyclin-A expression (Vlach *et al.*, 1996; Mateyak *et al.*, 1999). c-Myc also regulates CDK kinase activity by controlling p27<sup>Kip1</sup> expression, and in addition, can restrain p27<sup>Kip1</sup> association to cyclinE/CDK2 and cyclinA/CDK2 (Vlach *et al.*, 1996; Perez-Rogers *et al.*, 1997). c-Myc levels also increase in two waves that coincide temporally with PI3K activation (Ponzielli *et al.*, 2005; Jones *et al.*, 2001). c-Myc is a very unstable protein; regulation of its stability is therefore controlled temporally throughout the cell cycle. Phosphorylation-dependent regulation of c-Myc stability involves two key residues, Thr58 and Ser62; the former is mediated by MAPK and the latter by GSK3 $\beta$ , which targets c-Myc for degradation (Yeh *et al.*, 2004).

## SECTION 6. CELL CYCLE

The cell cycle is one of the most comprehensively studied biological processes, given its importance for cell growth and development in normal physiology and in many human disorders. Research on yeast, mammals, flies, worms and frog reveals a universal picture of the regulation of



basic cell cycle machinery. The time required to complete one cell cycle is organism-specific. For example, bacteria require as little as 20 min for cell division, single-celled yeast take 90-120 min, whereas mammalian cells need about 24 h to complete the cell cycle. The fundamental cell cycle events such as DNA replication and cell division occur during interphase and cytokinesis, respectively. In interphase, the cell's mass increases, followed by duplication of cytoplasmic components and of chromosomes. The interphase can be further classified into four primary stages, G<sub>1</sub>, S, G<sub>2</sub> and M phases (Fig. 10). A brief review of the different interphase stages is given below, followed by a detailed description of each phase.

The G<sub>1</sub> phase represents the collective events needed by the cell to prepare for the process of DNA replication. In G<sub>1</sub>, the cell also determines its fate to stop, proceed or exit the cell cycle, depending on mitogen or growth inhibitory signals. After proceeding to a state in G<sub>1</sub> termed the “restriction point” (Pardee, 1989), the cell becomes refractory to extracellular growth regulatory signals and is committed to completion of the cell cycle (Garcia *et al.*, 2006). After completion of DNA replication, cells transit to G<sub>2</sub> or Gap 2 phase, an interval in which a cell prepares itself to undergo successful nuclear division, termed mitosis. The mitosis or M phase represents the group of complex events through which the replicated chromosomes are segregated into separate nuclei, after which the cell proceeds to cytokinesis for cytosolic division into two independent daughter cells. Following successful cytokinesis, growth factors determine whether the daughter cells continue the cell cycle process or leave the cycle to enter the specialized resting phase known as G<sub>0</sub>. Defects in G<sub>1</sub> control are universal in tumours. Appropriate stimulation leads cells to leave G<sub>0</sub> (quiescence), and re-enter the cell cycle through the G<sub>1</sub> phase; hence, the division program is cyclical (Vermeulen *et al.*, 2003; Norbury & Nurse 1992; King & Cidlowski, 1998).

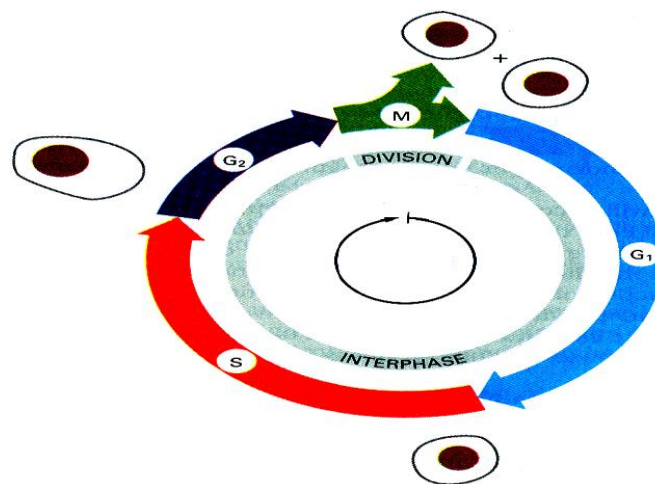


**Figure 10. Cell cycle image illustrating different phases of the cell cycle.** The cell cycle is composed of four distinct phases: the first gap phase (G<sub>1</sub>); the DNA synthesis phase (S); the second gap phase (G<sub>2</sub>); and finally, mitosis (M). A normal cell requires approximately 24 h for duplication, and the daughter cells generated re-enter the cell cycle in G<sub>1</sub> (figure adapted from Alberts *et al.*, 2004).

A model system widely used to study cell proliferation and cell cycle progression is the stimulation of serum-starved cells with growth factors, after which the events leading to transition and progression from one phase into another are followed.

### 6.1) From G<sub>0</sub> to S

In many cell types, serum starvation results in quiescence (G<sub>0</sub>). The quiescent state represents the total inactivation and stalling of the machineries that promote cell proliferation,

through elevated expression and activation of various cell cycle inhibitors (**Deng *et al.*, 2004**). To proliferate, these cell types must first begin the cell cycle by entering G1 phase. In G0 phase, however, cells express limited numbers of receptors for their ligands and low levels of cyclins. After stimulation, these ligands bind to and activate their respective receptors, which become competent to respond to further stimuli following the expression of new receptors. Expression and activation of new growth factor receptors also results in expression and activation of cell cycle regulatory proteins, leading to the G0/G1 transition, which is accompanied by an increase in cellular metabolism (**Sherr, 1994**).

### 6.1.1) Progression through G1 phase

Mitogen stimulation leads to G1 entry by activating RTK, GPCR and Ras, which use various means to control G1 phase-regulating proteins at the level of transcription and translation, and downstream signalling pathways (**Jones & Kazlauskas, 2000**).

In unicellular eukaryotes, cell cycle progression is governed mainly by CDK (cyclin-dependent kinase) Ser/Thr kinases that pair with cell cycle-specific regulatory subunits known as cyclins, due to their transient expression during cell cycle progression. There is a series of critical criteria that must be met during G1 for cells to proceed to S phase. These criteria, and those for cell re-entry into the cell cycle through G1, are governed by the sequential assembly and activation of different sets of cyclin-Cdk complexes. Although initially discovered in yeast, cyclins are now known to be the universal cell cycle regulators in all eukaryotes. In multicellular eukaryotes, cell cycle control is more complex; several CDK and cyclins are required for cell cycle progression. The D cyclins (D1, D2, D3) and Cdk4 or Cdk6 are needed for G1 progression; cyclin E and Cdk2, or cyclin A and Cdk2 are necessary for entering S phase, and cyclinA/CDK2 as well as cyclinA/CDK1 and cyclinB/CDK1 for progression through mitosis (**Ekholm *et al.*, 2000**). Different cyclins impart distinct substrate specificity to CDK for temporal regulation of cell division. G1 events can be further subdivided into early, mid and late G1 phase.

Growth factor addition initiates the first wave of signalling in G0/G1 transition and early G1, which continues for 60-90 min post-stimulation and then returns to basal levels. The first wave of GF mediates signalling through activation of tyrosine kinases, GPCR, and Ras. This results in a substantial increase in cyclin D1, D2 and D3 expression, which is strictly GF stimulation-dependent (**Assoian & Zhu, 1997**). These cyclins interact with their catalytic partners CDK4 and CDK6 to form cyclinD/CDK4 and cyclinD/CDK6 complexes; they can phosphorylate many substrates to activate or inactivate them, and are essential for G1 entry (**Sherr, 1994**). In contrast to cyclin D proteins, CDK protein levels remain relatively stable throughout the cell cycle. In addition to cyclin-dependent CDK activation, the catalytic activity of CDK can be counteracted by phosphorylation on tyrosine and threonine residues (Tyr15 and Thr14) or through binding to the inhibitory subunit INK4 family of CKI (cyclin kinase inhibitor). These CKI form stable complexes with CDK before cyclin binding, preventing association with cyclin D (**Carnero & Hannon, 1998**). In contrast, the other class of cell cycle inhibitors, p21<sup>Cip1</sup> and p27<sup>Kip1</sup>, although they bind and inhibit CDK2, also bind to cyclinD/CDK4 or cyclinD/CDK6 complexes, but do not inhibit their kinase activity (**Blain *et al.*, 1997**; **LaBaer *et al.*, 1997**). Indeed, association of p21<sup>Cip1</sup> and p27<sup>Kip1</sup> contribute to the formation of stable cyclinD/CDK4 or cyclinD/CDK6 complexes during early cell cycle phases (**Blain *et al.*, 1997**; **LaBaer *et al.*, 1997**; **Cheng *et al.*, 1999**) and target them to the nucleus. CyclinD/CDK complexes can also be activated by threonine phosphorylation (Thr177 in CDK6 and Thr172 in CDK4) by CDK-activating kinase (CAK).

In addition to the biochemical modulation through different cell cycle inhibitors, continuous stimulation is required to maintain cyclin D levels, which sustains CDK kinase activity, as these proteins have short half-lives. When cyclinD/CDK4 or cyclinD/CDK6 complexes are active, the



target proteins are phosphorylated on CDK consensus sites. A critical target of cyclinD/CDK4 and cyclinD/CDK6 is the product of the retinoblastoma tumour suppressor gene (Rb). Rb is a 110 kDa nuclear phosphoprotein that belongs to the family of pocket proteins, due to its pocket-like structure; it binds to cell proteins in G1 and blocks cell cycle progression (**Tamrakar *et al.*, 2000; Harbour & Dean, 2000; Lukas *et al.*, 1995**). Growth suppression by Rb is considered to be a consequence of its ability to bind E2F and HDAC (histone deacetylase protein); Rb acts as a transcriptional repressor of the E2F target genes needed for cell cycle progression. During early G1, Rb is phosphorylated at Ser795, leading to its partial dissociation from HDAC and E2F, which then transcribes proteins needed for later cell cycle phases.

In addition to inducing cyclinD-associated CDK kinase activity, early G1 signals also inactivate the FOXO transcription factors. These factors negatively regulate cell cycle progression by inhibiting cyclin D1 and D2 expression (**Brunet *et al.*, 2002**) and by promoting transcription of cyclin inhibitors such as p18<sup>INK4c</sup>, p27<sup>Kip1</sup> and p21<sup>Cip1</sup> (**Schmidt *et al.*, 2002; Dijkers *et al.*, 2000; Medema *et al.*, 2000**). Cell cycle-promoting signals also stimulate downregulation and degradation of cell cycle inhibitors such as p27<sup>Kip1</sup> and p16<sup>INK4a</sup>. In these conditions, expression of D-type cyclins activates the CDK kinase activities, which inhibit transcription of cell cycle inhibitor proteins and activate other transcription factors.

### 6.1.2) Progression through late G1 to S phase

While D type cyclins, in association with CDK4 and CDK6, regulate early and mid-G1 phase progression, cyclinE/CDK2 acts in the G1-to-S phase transition. The progression from G1 to S phase requires the *de novo* expression of genes that encode proteins and enzymes involved in DNA replication. Regulation of these S phase genes is therefore an important component of the biological program during late G1 progression. S phase genes are silenced in quiescent and early G1 cells, and are activated at the G1/S transition. Indeed, late G1 signalling mechanisms require induction of a second wave of activation of signalling molecules in late G1 (**Jones & Kazlauskas, 2000; Jones & Kazlauskas, 2001**). The two waves of GF-dependent signalling events are necessary for a proliferative response. The first is an acute burst of signalling that takes place immediately after GF stimulation, lasts for 60-90 min, and is essential to trigger cell growth and cyclin D synthesis; the second occurs in late G1 (7-12 h post-stimulation) and the mechanism that triggers its induction is unknown. RTK and Ras are activated during the second signalling wave, and inhibition of either of these abrogates cell cycle progression (**Jones *et al.*, 1999; Takuwa & Takuwa, 1997, 2001**). The second signalling wave in late G1 induces cyclin E expression, which in turn increases its associated CDK2 protein kinase activity. The active cyclinE/CDK2 complex hyperphosphorylates pRb at various positions, inactivating it completely. CyclinE/CDK2 kinase activity is negatively regulated by the Cip/Kip family of cell cycle inhibitor proteins. p21<sup>Cip1</sup> (**Harper *et al.*, 1995**), p27<sup>Kip1</sup> and p57<sup>Kip2</sup> (**Nakayama & Nakayama, 1998**) form inactive complexes with cyclinE/CDK2, which no longer allow CAK phosphorylation of CDK2 at Thr160. In addition, p21<sup>Cip1</sup> and p27<sup>Kip1</sup> have separate binding sites for cyclins and CDK, which regulate cyclinE/CDK2 complex formation and interfere with the ATP binding site in the catalytic cleft of the complex. p27<sup>Kip1</sup> appears to be a primary negative regulator during normal cell proliferation in a variety of cell types (**Sherr & Roberts, 1999**).

At the G1/S boundary, pools of cyclinE/CDK2 are liberated from the inactive ternary complex and phosphorylate p27<sup>Kip1</sup> at Thr187; this phosphorylation provides a recognition motif for an E3 ligase (SCF<sup>Skp2</sup>) that targets phosphorylated p27<sup>Kip1</sup> for ubiquitination. Ubiquitinated p27<sup>Kip1</sup> is targeted for proteosomal degradation (**Elledge and Harper 1998; Bloom & Pagano 2003**). p27<sup>Kip1</sup> is phosphorylated only when the cyclinE/CDK2 concentration exceeds that of p27<sup>Kip1</sup> (**Vlach *et al.*, 1997; Sheaff *et al.*, 1997**). As p27<sup>Kip1</sup> is degraded, positive-feedback dynamics lead to rapid phosphorylation and destruction of the remaining p27<sup>Kip1</sup> pool. There are

additional mechanisms by which  $p27^{Kip1}$  binding to the cyclin/CDK complex is regulated; these include MAPK and direct c-Myc-mediated inhibition of  $p27^{Kip1}$  binding (Vlach *et al.*, 1996). Sequential pRb phosphorylation by many cyclin/CDK complexes in late G1 results in complete activation of E2F and chromatin-remodelling proteins following their release from the Rb complex, promoting entry into S phase. This pRB inactivation is also considered the sensor of restriction point. In other words, the restriction point switch from GF-dependent early G1 to the subsequent mitogen-independent phases reflects the induction of broad transcriptional programmes that are regulated by the parallel Rb and c-Myc pathways, which regulate genes critical for G1/S transition and initiation of S phase progression. Activated E2F contributes to both the silencing and the activation of S phase genes. E2F1 positively regulates the transcription of genes whose products are required for late G1 progression and S phase entry, including cyclin A, cyclin E and Cdc25 (Buchkovich *et al.*, 1989; Brehm *et al.*, 1998). A schematic diagram of G1-to-S progression, the temporal relationship between the two G1 control points, and the components that influence cell cycle, with their approximate position, is shown in Fig. 11.

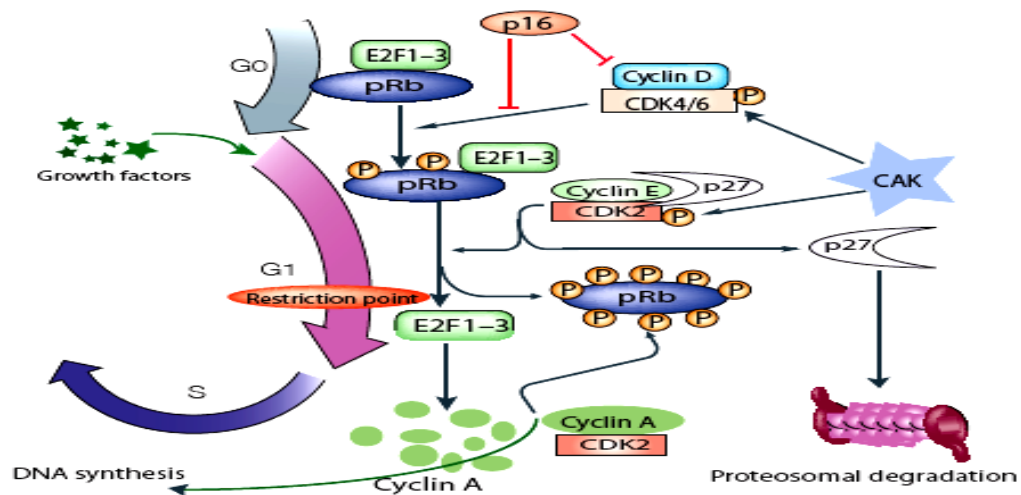


**Figure 11. G1 progression with cyclins, cyclin inhibitors and restriction point clearance.** Quiescent cells (G0) entering the cell cycle after growth factor addition are driven by the activities of different cyclin/CDK complexes, which hyperphosphorylate Rb and  $p27^{Kip1}$ , thereby blocking their growth-inhibitory functions and permitting cell cycle progression. Progression through G1 phase is facilitated by cyclinD/CDK4, cyclinD/CDK6 and cyclinE/CDK2. CyclinD/CDK4 and cyclinE/CDK2 complexes are active after phosphorylation by CAK. Following activation, the cyclinE/CDK2 complex mediates  $p27^{Kip1}$  proteosomal degradation and release of E2F transcription factors from the Rb complex. Released E2F induces expression of cyclinA and induces cyclinA/CDK2 activity, promoting S phase entry and DNA replication.

## 6.2) S phase entry and progression

The function of cyclinE/CDK2 is not completely restricted to G1 phase regulation. In S phase, the E-type cyclins and their catalytic partner CDK2 phosphorylate substrates directly involved in cell duplication, such as replication origin components and proteins involved in origin firing, thereby participating in establishment of the pre-replication complex (pre-RC) and its licensing, which is determined by the binding of the minichromosome maintenance protein complex (MCM) to the replication complex (Yu & Sicinski, 2004). The cyclinE/CDK2 complex is considered indispensable for S phase initiation. At the G1/S boundary, cyclin A is expressed, binds to CDK2, and regulates S phase progression. CyclinA/CDK2 is activated in late G1; this activation increases steadily as cells begin DNA replication, and it is required for S phase

completion (**Girard *et al.*, 1991**). The increased activities of cyclinE/CDK2 and cyclinA/CDK2 maintain p27<sup>Kip1</sup> levels low in S phase through phosphorylation-triggered proteolysis (**Malek *et al.*, 2001**).

Replication in eukaryotic cells is initiated from many replication origins, and a large network of proteins is required to regulate DNA replication. A two-step mechanism governs the initiation of DNA replication, ensuring that the entire genome is precisely duplicated in each cell cycle. In the first step, Cdc6 and Cdt1 collaborate with the origin recognition complex (ORC) to load the replicative hexameric helicase MCM2-7 complex, which has ATPase activity, into pre-RC at replication origins (Fig. 12, **Cvetič & Walter, 2006**). Once the MCM proteins have been loaded on chromatin, ORC and Cdc6p can be removed from chromatin without preventing subsequent DNA replication, which suggests that the primary role of the pre-RC is MCM loading (**Rowles *et al.*, 1999; Hua & Newport, 1998**). CyclinE/CDK2 is crucial for MCM2 loading onto chromatin, as it cooperates with Cdc6 in pre-RC assembly. Cells lacking cyclin E fail to load MCM2 replicative helicase onto replication origins while re-entering the cell cycle from quiescence (**Geng *et al.*, 2003**). Inhibition of the MCM2-7 complex causes its dissociation from chromatin, resulting in a rapid halt of DNA replication.

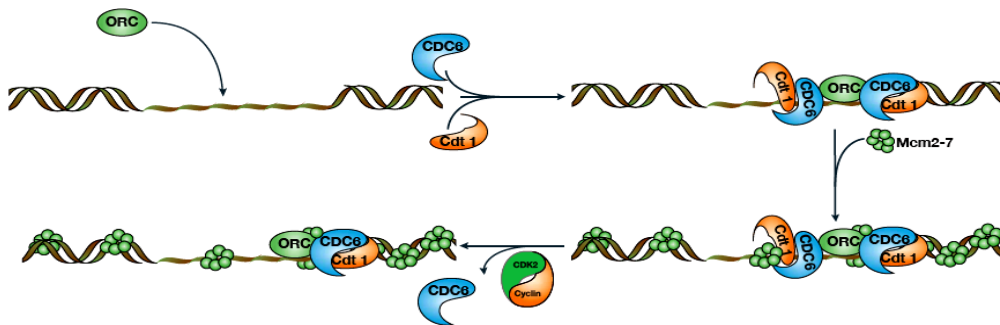


**Figure 12. A model for pre-replicative complex formation.** Current information concerning pre-RC formation in eukaryotes. The stoichiometry of the components is unknown. The apparent overabundance of MCM2–7 relative to other components is illustrated as additional MCM2–7 complexes associated with adjacent chromatin (figure adapted from **Bell & Dutta, 2002**).

DNA duplication occurs once per cell cycle due to pre-RC assembly only in late mitosis and G1; once cells enter S phase, pre-RC can no longer assemble. Cell cycle regulation is critical to ensure that origins fire once and only once during each cell cycle. CDK2- and CDK1-associated activity thus prevents pre-RC formation by phosphorylating pre-RC components (ORC, Cdc6p and the MCM), although the mechanism by which it prevents re-initiation is unknown (**Nguyen *et al.*, 2001**). Cdc6 phosphorylation leads to its degradation (**Calzada *et al.*, 2000; Drury *et al.*, 2001**). Phosphorylation of the MCM2-7 complex leads to its export from the nucleus once released from the chromatin (**Labib *et al.*, 1999; Nguyen *et al.*, 2000**). Although Cdt1 itself may not be phosphorylated, it is exported with MCM (**Tanaka & Diffley, 2002**). Whereas the same proteins are regulated by CDK phosphorylation in all organisms, the details differ. Metazoans have a CDK-independent mechanism to control re-replication, the Cdt1 inhibitor protein geminin (**Wohlschlegel *et al.*, 2000; Tada *et al.*, 2001**). Geminin is present from S through M phase, and is degraded by the anaphase-promoting complex (APC) at the metaphase-to-anaphase transition (**McGarry & Kirschner, 1998**). Pre-RC formation marks potential sites for the initiation of DNA replication; hence, the regulation of complex formation at origins is essential to ensure that large eukaryotic genomes are faithfully duplicated. These proteins include regulatory factors as well as components of the DNA replication fork.

The next step in the process of DNA duplication is activation of the origins through formation of a replication fork. Cdc7/ASK protein kinase complex then convert pre-RC into bidirectional replisomes at each origin. The MCM helicase is activated at this point, unwinds the DNA duplex, and the resulting single-stranded DNA is stabilized through binding of multiple copies of the heterotrimeric single-strand binding protein RPA. This results in formation of a bidirectional replication fork. DNA strands are replicated continuously through the 5'→3' polymerase activity of DNA polymerases. After the initiation of DNA replication by the formation of small newly synthesised oligonucleotides by DNA polymerase- $\alpha$ , replication factor C (RFC, chaperone-like complex) specifically bind to the template primers at the 3' ends and catalyzes the subsequent binding of the ring-shaped homotrimer replication factor PCNA that encircles DNA, displacing DNA polymerase- $\alpha$  and recruiting polymerase- $\delta$  to replace RFC in the replicative complex; this enables rapid, progressive synthesis of both leading and lagging strands at the replication fork (Fig. 13) (Johnson & O'Donnell, 2005; Barsky & Venclovas, 2005).

PCNA belongs to the family of DNA sliding clamps ( $\beta$ -clamps), which are structurally and functionally conserved (Kelman, 1997). They form ring-shaped complexes with pseudo-hexameric symmetry, which encircle the DNA and are able to slide freely in both directions. On the verge of DNA replication completion, the DNA Pol $\delta$  or  $\eta$  holoenzyme meets the 5' end of the RNA portion of the previously synthesised fragment, specialised proteins are recruited that remove the RNA part, fill the gap. Finally, Lig1 associates with PCNA and performs the final ligation step, sealing the nick and finishing the process (Moldovan *et al.*, 2007).

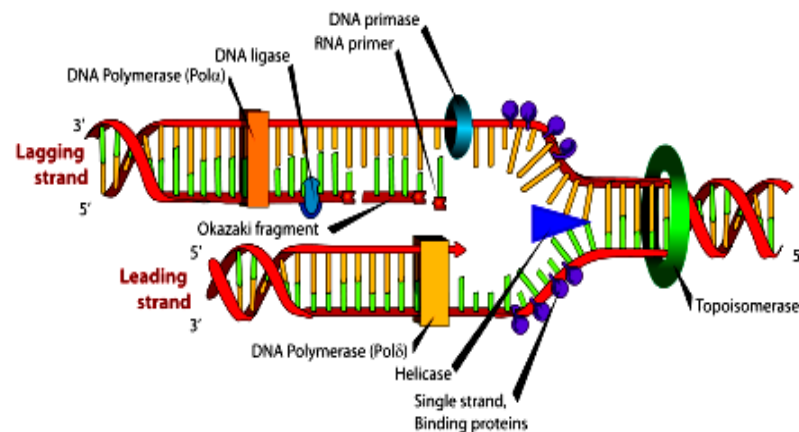


**Figure 13. DNA replication.** During S phase, DNA replication begins with local decondensation and separation of the double DNA helices, so that the DNA molecule becomes accessible for enzymes to make a complementary copy of each strand. (figure from M. Ruiz, Wikipedia [accessed 22-04-09]).

### 6.3) G2 phase

Similar to G1, G2 is an intermediate gap phase. After genome duplication in S phase, cells transit through G2, where they prepare for mitosis. In this phase, cell cycle regulatory proteins ensure that the copied DNA is error-free (Lukas *et al.*, 2004), and respond to DNA damage (similar checkpoints are found in other cell cycle phases). The DNA damage response results in one of several possible cell fate decisions: induction of cell cycle arrest, initiation of DNA repair, activation of transcription programs, and either apoptosis or cell senescence (Khanna & Jackson, 2001; Zhou & Bartek, 2004). The DNA damage response causes a delay to allow DNA repair before entry into mitosis. The DNA damage checkpoints are not unique pathways activated by DNA damage, but rather are biochemical pathways that operate under normal growth conditions that are amplified by an increase in damage. These checkpoints not only arrest the cell cycle in

response to DNA damage, but also control activation of DNA repair pathways and regulate the movement of DNA repair proteins at the damage site (section 7).

Apart from checking and correcting potential DNA errors, proteins that are needed for mitosis are synthesised and assembled during the G2 phase, including mitotic cyclins, Plk, and the Aurora kinases.

#### **6.4) Mitosis**

Mitosis is the final phase of the cell cycle. Mitosis can be further divided in four stages: prophase, metaphase, anaphase and telophase.

##### **6.4.1) Prophase**

Prophase is the beginning of mitosis, in which the cyclinA/CDK1 and cyclinB/CDK1 complexes are activated to drive events, such as chromosome condensation and resolution, nuclear envelope breakdown, and assembly of the mitotic spindle (composed of cytoplasmic microtubules and other proteins). In prophase, microtubules move one pair of centrioles to the opposite poles of the cell.

##### **6.4.2) Metaphase**

The prophase to metaphase transition involves the cyclinA,B/CDK1-mediated bi-orientation of all sister chromatid pairs on the spindle. The sister chromatids are pulled towards the poles, but held together by sister chromatid cohesion. When all the chromosomes are aligned at the cell equator halfway between the poles in metaphase, the anaphase-promoting complex (APC) activates and promotes degradation of the cohesins, permitting progression to anaphase. Cyclin A is destroyed during prometaphase and cyclin B promotes the completion of chromosome condensation and spindle assembly: cyclin B is destroyed later in anaphase.

##### **6.4.3) Anaphase**

CDK activity drives cell cycle progression until metaphase, when its inactivation coincides with dephosphorylation of CDK substrates and activation of the APC, cohesions degradation permits chromosome separation and movement and spindle stability (Nigg, 2001; Miel, 2004). Progression into anaphase and beyond therefore depends on the ubiquitin-protein ligase called the anaphase-promoting complex (APC) or cyclosome, which ubiquitinates several regulatory proteins, thereby targeting them to the proteosomes for destruction. APC activity oscillates in response to changes in APC association with the activating subunits CDC20 or CDH1. In anaphase, sister chromatids separate and move toward opposite poles of the cell through the spindle apparatus. At the end of anaphase, each pole of the spindle located has a complete set of chromosomes and the cell is ready to transit to telophase.

##### **6.4.4) Telophase**

Telophase begins when chromosomes arrive at the poles and begin to decondense. The nuclear envelope forms from the fusion of small vesicles. At this point DNA division (mitosis) is complete.

#### **6.5) Cytokinesis**

Cytokinesis is the final stage in eukaryotic cell division. It is achieved by the equatorial constriction of the mother cell through an actomyosin-based contractile ring, dividing the cytoplasm into the daughter cells. This process is precisely regulated in space and time.

## 6.6) Class IA PI3K and the cell cycle

The early embryonic lethality of p110 $\alpha$ - or p110 $\beta$ -null mice indicates that these isoforms have distinct, essential functions in embryonic development and possibly in cell division (**Bi *et al.*, 1999; Bi *et al.*, 2002**). In normal cells, PIP<sub>3</sub> can be detected transiently following stimulation with growth factors (**Whitman *et al.*, 1988; Varticovski *et al.*, 1989**). Class I<sub>A</sub> PI3K mediates the GF-stimulated pathways, such as PKB activation, that initiate cell division. Enhanced PIP<sub>3</sub> production after GF receptor binding accelerates cell cycle entry, whereas PIP<sub>3</sub> reduction diminishes this process (**Álvarez *et al.*, 2003**). PI3K activity increases within minutes of GF receptor stimulation (first peak), with a second PI3K peak in mid-G1, which is essential for transition to S phase (**Jones & Kazlaukas, 2001**). Neutralizing PI3K antibodies block S phase entry when they are microinjected in mid- to late G1 (**Roche *et al.*, 1994**). Indeed, inhibition of PI3K activity abrogates cell cycle progression (**Garcia *et al.*, 2006**). A role for PKB in cell cycle regulation was observed in the phenotype of MyrPKB-expressing cells, in which increased *c-Myc* and Bcl-2 expression were found even in the absence of GF (**Brennan *et al.*, 1997**). PKB helps to transduce PI3K-dependent GF signals that end in Rb hyperphosphorylation, thereby promoting E2F activation. PKB also phosphorylates FOXO transcription factors, inducing their sequestration in the cytosol and reducing FOXO TF-mediated expression of cyclin G2 and p27<sup>Kip1</sup>, which in turn inhibit CDK and regulate p53 intracellular levels through MDM2 (**Medema *et al.*, 2000**). PI3K also controls the G0/G1 transition through PKB, promoting cyclin D synthesis through the PI3K effectors Rac and Cdc42; cyclin D then activates CDK4 or CDK6 in G1. Phosphorylation of Rb by PKB-transduced signals could result from a combination of mechanisms, including downregulation of the cyclin-dependent kinase inhibitor p27<sup>Kip1</sup> by directly phosphorylation of p27<sup>Kip1</sup> on Thr157; this results in nuclear exclusion of p27<sup>Kip1</sup> and later degradation through ubiquitination (**Sheaff *et al.*, 1997; Nguyen *et al.*, 1999**). PKB also inhibits *c-Myc* and cyclin D degradation by inactivating GSK-3 $\beta$ . Therefore, all these mechanisms contribute to explain how PI3K regulate G0>G1 transition. Nevertheless, the mechanism involved in PI3K activation in late G1 and its role in S phase entry remains unknown. Here we used an alternative approach, inhibition of late G1 PI3K activity, to address the precise requirements for PI3K activation in late G1, and we analysed the effect of this inhibition on cell cycle.

PI3K also influences the G2/M phase. There is an additional minor PI3K activity peak at M phase entry. Release of epithelial cell lines from S phase arrest shows a basal PI3K activity during S phase and activity peak at M phase entry (**Garcia *et al.*, 2006**). This second activation peak is not as strong as that observed during cell cycle entry, but PI3K inhibition in late S phase blocks mitosis entry in MDCK cells, whereas it delays this transition in HeLa and NIH3T3 cells (**Shtivelman *et al.*, 2002**). These studies show that PI3K regulates mitosis entry with a distinct relative contribution depending on cell type. Finally, PI3K activity must be downregulated for completion of mitosis, as fibroblasts expressing constitutive active PI3K/PKB forms show delayed G2/M progression and defective cell cycle exit (**Álvarez *et al.*, 2001**).

## 7. THE DNA DAMAGE RESPONSE

Several types of DNA damage can trigger activation of the DNA checkpoint proteins. Activation of these checkpoint proteins temporarily blocks cell cycle progression to allow repair of the damaged DNA. The class IV PI3K proteins ATM and ATR are among the most proximal players triggered by IR- and UV-induced DNA damage that initiate a rapid response, allowing DNA repair. The proteins that participate in the cell response to genotoxic stress can be grouped as **sensors, mediators and transducers** (Fig. 14).

## 7.1) Sensors

Three groups of proteins are known as checkpoint-specific damage sensors: the MRN complex (*MRE 11-Rad50-Nbs1 complex*) (Lee & Paull, 2005), the RFC/PCNA (clamp loader/polymerase clamp)-related *Rad17-RFC/9-1-1 complex* (Melo & Toczyski, 2002) and the two phosphoinositide 3-kinase-like kinase (PIKK) or class IV PI3K family members, *ATM and ATR* (Durocher & Jackson, 2001).

### 7.1.1) Mre11-Rad50-Nbs1 complex

The MRN complex is a heterotrimeric complex consisting of Mre1, Rad50 and Nbs1 proteins. After formation of DSB (double-strand break), this complex binds to DNA and resects the double strand, exposing ssDNA to proteins involved in repair (Falck *et al.*, 2005; Mirozoeva *et al.*, 2001; Carney, 1998). MRN complexes can activate ATM by independently promoting both monomerisation and autophosphorylation.

### 7.1.2) Rad17-RFC and the 9-1-1 complex

The Rad17-RFC complex is a checkpoint-specific structural homologue of the RFC replication factor, where Rad17 interacts with four RFC subunits (Rfc2, Rfc3, Rfc4 and Rfc5) to form a pentameric complex. After checkpoint activation, the 9-1-1 (Rad9-Rad1-Hus1) complex functions as a clamp loader, similar to PCNA (Bartek J *et al.*, 2004; Parrilla-Castellar *et al.*, 2004; Bartek & Lukas, 2003). *In vitro* experiments suggest that Rad17 recruits the 9-1-1 complex to DNA damage sites (Bermudez *et al.*, 2003). After DNA damage, however, phosphorylation of Rad17 by ATR is necessary for the DNA damage checkpoint response (Bao *et al.*, 2001). Replication protein A (RPA) mediates the recruitment of ATR/ATRIP, Rad17, and 9-1-1 complexes to ssDNA and stimulates the kinase activity of ATR toward Rad17 (Zhou & Elledge, 2000; Zou *et al.*, 2003). When IR induces the DNA damage, Rad 17 phosphorylation relies more heavily on ATM activation (Bao *et al.*, 2001).

### 7.1.3) ATM and ATR

ATM and ATR are among the most proximal proteins that carry out a variety of cell processes in response to DNA damage (Sancar *et al.*, 2004; Tibbetts *et al.*, 1999; de Klein *et al.*, 2000). ATM is a 350 kDa oligomeric protein, whereas ATR (ATM- and Rad3-related) is a 303 kDa protein. Both ATM and ATR show considerable sequence similarity to PI3K family proteins (Engelman *et al.*, 2006), although ATM and ATR lack lipid kinase activity and are protein kinases activated following DNA DSB formation.

After cell exposure to ionizing radiation, ATM, which is normally found in the nucleus as a resting homodimer, is activated through intermolecular autophosphorylation on Ser1981. This results in the dissociation of ATM homodimers and localisation of monomeric ATM to damage sites on the DNA (Bakkenist & Kastan, 2003). Activated ATM in turn phosphorylates many proteins, including Chk2 at Thr68 (Matsuoka *et al.*, 2000; Zhou *et al.*, 2000; Bartek & Lukas, 2003), p53 at Ser15 (Caspary, 2000), NBS1 (Lim *et al.*, 2000) and BRCA1 (Cortez *et al.*, 1999).

ATR must associate with ATRIP (ATR-interacting protein) for its function, and is activated preferentially after generation of single strand breaks (UV irradiation) (Cortez *et al.*, 2001; Sancar *et al.*, 2004). Following activation, ATR phosphorylates the same proteins as ATM, as well as another set of substrates after UV irradiation. ATR is also activated in response to IR, although probably later and not as strongly as ATM. In the absence of ATM, ATR can partially compensate for ATM function by phosphorylating and activating common downstream targets (Cliby *et al.*, 1998; Kim *et al.*, 1999). In the absence of ATR, ATM is unable to compensate, and ATR<sup>-/-</sup> mutants are embryonic lethal (de Klein *et al.*, 2000). DNA synthesis defects induce mainly the ATR pathway.



## 7.2) Mediators

Mediator proteins associate simultaneously with damage sensors and help to provide signal transduction specificity. Mediator proteins include histone 2AX (H2AX), Rad9, p53-binding protein (53BP1) (Schultz *et al.*, 2000; Wang *et al.*, 2002), the topoisomerase-binding protein (TopBP1) (Yamane *et al.*, 2002), mediator of DNA damage checkpoint 1 (MDC1) (Goldberg *et al.*, 2003; Stewart *et al.*, 2003), and structural maintenance of chromatin 1 (SMC1). These proteins interact with damage sensors such as ATM, ATR, RAD17 and the MRN complex, signal transducers such as Chk2, and effector molecules such as p53. H2AX phosphorylation is one of the first measurable responses to DSB (Fernandez-Capetillo *et al.*, 2003). It is phosphorylated on Ser139 and is loaded into a 2 Mb region surrounding a break and can be visualized (Burma *et al.*, 2001; Banath & Olive, 2003; Friesner *et al.*, 2005). The DNA damage checkpoint response is abrogated in cells that have decreased levels of or lack of these proteins.

## 7.3) Transducers

Two kinases, Chk1 and Chk2, have a strict signal transduction function in cell cycle regulation and checkpoint responses; both are Ser/Thr kinases with limited substrate specificity. In mammalian cells, the DSB signal sensed by ATM is transduced by Chk2 (Hirao *et al.*, 2000), and the UV damage signal sensed by ATR is transduced by Chk1 (Abraham, 2001); there is nonetheless some functional overlap between these two proteins.

A part of our research examined the consequences of knockdown of the class I<sub>A</sub> PI3K isoform on checkpoint responses following radiation stress.

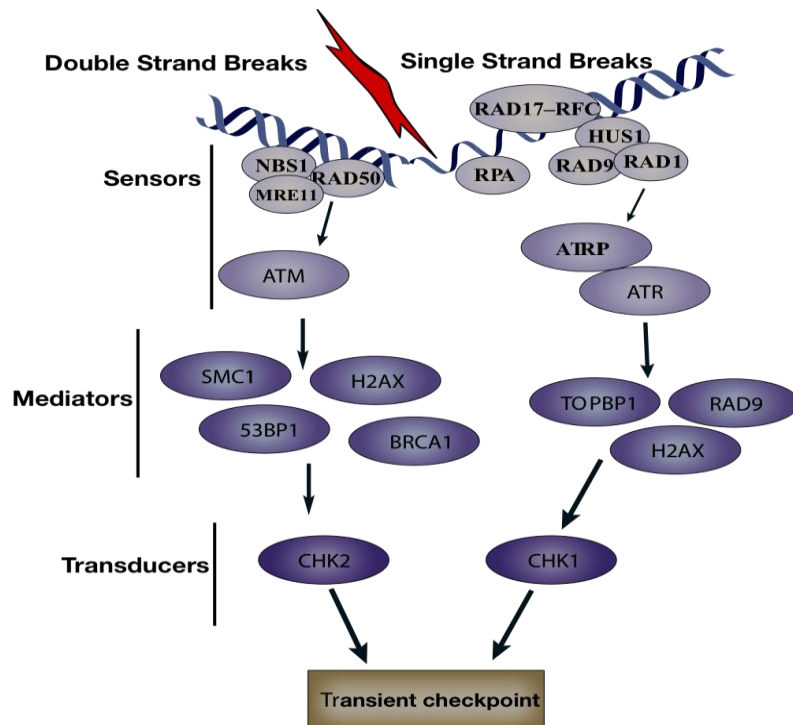


**Figure 14. The DNA damage response (DDR).** The DDR is robustly activated by DNA double strand breaks (DSB) and/or exposure of RPA-coated single-stranded DNA (ssDNA). DSB are sensed by MRN complex, and the C terminus of NBS1 recruits the apical protein kinase ATM, which undergoes autophosphorylation. Chk2 localizes transiently at DNA damage sites to be phosphorylated and activated by ATM. The exposure of modified histone residues further boosts accumulation of the DNA damage mediator 53BP1 at the damage site. In the case of single strand breaks, once ssDNA forms, RPA-coated ssDNA recruits the heterodimeric complex that comprises ATR (a paralogue of ATM), its DNA-binding subunit ATRIP, and the RAD17-9-1-1 complex. ATR activity is boosted by the 9-1-1 and RAD17-RFC complexes. In addition, ATR activity is stimulated by TOPBP1, which is necessary for CHK1 phosphorylation.





## AIMS OF THE STUDY

Activation of class I<sub>A</sub> PI3K is necessary for cell growth and cell cycle entry downstream of growth factor receptors. Moreover, mutational activation or overexpression of class I<sub>A</sub> PI3K isoforms result in enhanced PI3K signalling, which is associated with cell transformation and cancer. Growth factor-mediated PI3K activation occurs at two distinct time points during the G1 cell cycle phase. The first activation peak is observed immediately after growth factor addition, whereas the second peak of activation occurs in late G1, before S phase entry. This second activity peak is essential for DNA replication; nonetheless, the mechanism and function of PI3K activation at the onset of S phase entry is poorly understood.

A fraction of class I<sub>A</sub> PI3K was recently described to reside in the cell nucleus. The role of nuclear PI3K is linked to cell survival, mitogenesis, and differentiation through its principle effector, PKB. Which PI3K isoforms are nuclear nonetheless remains unclear. The different class I<sub>A</sub> PI3K isoforms p110 $\alpha$  and p110 $\beta$  exhibit distinct, important functions in cell division. It is therefore necessary to study the intracellular localisation of the class I<sub>A</sub> PI3K catalytic and regulatory subunits, as well as the mode of their nuclear translocation.

Genetic deletion of p110 $\alpha$  and p110 $\beta$  in mice leads to embryonic lethality. In addition, p110 $\alpha$  has been clearly implicated in cancer, as multiple mutations lead to an increase in its kinase activity. Overexpression of p110 $\beta$  is also reported in various types of tumours, although no functional mutations are known in the *PIK3CB* gene. A recent study of conditional knockout mice for p110 $\beta$  showed a kinase-independent role in development; nonetheless, the p110 $\beta$  function is presently unclear.

To address these issues, the main objectives of my thesis work were:

- 1) Investigate the mechanism of activation and the role of class I<sub>A</sub> PI3K activity in late G1
- 2) Identify which isoforms of class I<sub>A</sub> PI3K localise in the nucleus and study the mechanism for their nuclear translocation
- 3) Investigate p110 $\beta$  involvement in DNA damage responses



## **MATERIALS AND METHODS**



## 1. Antibodies and reagents

### 1.1) Antibodies

Antibody	Supplier
c-Myc (C-19)	Santa Cruz Biotechnology
Cyclin E (M-20)	Santa Cruz Biotechnology
Oestrogen receptor alpha (ER) (MC-20)	Santa Cruz Biotechnology
Pan-Ras	Oncogene Research
Tubulin	Oncogene Research
p-PKB(473)	Cell Signaling Technologies
Cyclin D3	BD Biosciences
p27 <sup>Kip</sup>	BD Biosciences
MCM2	BD Biosciences
Rb	Zymed Laboratories
Phospho(T58/S62)-c-Myc	Cell Signaling Technologies
Myc-tag (9B11)	Cell Signaling Technologies
Cyclin A	Upstate Biotechnology
Phosphotyrosine	Upstate Biotechnology
$\beta$ -actin	Sigma
Histone	Chemicon International
Cyclin D2	Santa Cruz Biotechnology
CDK4	Santa Cruz Biotechnology
p110 $\beta$ (for immunofluorescence)	Santa Cruz Biotechnology
p110 $\beta$ (WB, IP)	Cell Signaling Technologies
p110 $\alpha$ (immunofluorescence)	Klippel <i>et al.</i> , 1998
p110 $\alpha$ (WB, IP)	Cell Signaling
p-Chk1 (Ser345)	Cell Signaling
Chk1	Novocastra
Chk2	Upstate
p-ATM (1981)	Rockland Immunochemicals, Inc
p85 $\beta$	Donated by Isabel Cortes, DIO, CNB
PCNA	BD transduction Lab.
RAD17(IP)	Santa Cruz Biotechnology
RAD17(WB)	Abcam
p-RAD17	Abcam
p-p38	Cell Signaling Technologies
p38	Cell Signaling Technologies
p-SMC1	Abcam
$\gamma$ -H2AX	Millipore
HRP-conjugated second antibodies	Dako
Anti-rabbit second Ab-Alexa 488	Molecular Probes
Anti-rabbit second Ab-Cy3	Jackson Laboratories
Anti-rabbit second Ab-Cy5	Jackson Laboratories
Anti-mouse second Ab-Alexa 488	Molecular Probes
Anti-mouse second Ab-Cy3	Jackson Laboratories
Anti-mouse second Ab-Cy5	Jackson Laboratories

## 1.2) Reagents

Enhanced chemiluminescence, L-[<sup>35</sup>S]methionine, [<sup>32</sup>P]dCTP, and [<sup>32</sup>P]ATP were from Amersham Biosciences. Lovastatin, herbimycin, and Ly294002 were from Calbiochem. PIK75 and TGX221 (Knight *et al.* 2006; Jackson *et al.* 2005) were synthesised in the Australian Centre for Blood Diseases (Melbourne, Australia). Hoechst 33258 was purchased from Molecular Probes. Cyclohexamide, leptomycin B, and all remaining reagents were bought from Sigma

## 2. Cell Culture

### 2.1) Cells and Cell lines

The different cell lines were maintained in Dulbecco's modified Eagle's medium (DMEM; Gibco-BRL) supplemented with 10% (vol/vol) foetal bovine serum (FBS), 2 mM glutamine, 10 mM HEPES, 100 U/ml penicillin, and 100 µg/ml streptomycin in a humidified atmosphere (5% CO<sub>2</sub>, 37°C).

Cell lines used:

- NIH 3T3 mouse fibroblast line
- HeLa epithelial cell line derived from human cervical cancer
- Saos-2 human epithelial-like osteosarcoma cell line
- Phoenix cells are second-generation retrovirus producer lines for the generation of helper free ecotropic and amphotropic retroviruses
- 293T cells expressing gag-pol and envelope protein (for ecotropic and amphotropic viruses) were also used in some retroviral infections

Mouse embryonic fibroblasts (MEF):

MEF were isolated from mouse embryos at day 14 of gestation, and maintained in tissue culture medium with 20% FBS. Immortalized p110β KO, KR and WT MEF were donated by Drs. JJ Zhao and TM Roberts (Dana Farber Cancer Institute, Boston, MA).

### 2.2) Transfection and retroviral transduction

We used JetPei (Genycell) to transfect cell lines. In some cases, transfected cells (p110β shRNA) were selected for 2 days in medium containing 2 µg/ml puromycin (Sigma). For retroviral transduction, Phoenix cells were transfected using JetPei-NaCl (Polyplus transfection) according to manufacturer's protocols; after 10 h, cells were washed and placed in DMEM-10% FBS. At 48 h post-transfection, the supernatant from transfected phoenix cells was filtered through a 0.45 µm filter and polybrene added to a final concentration of 5 µg/ml. Cells to be infected were supplemented with viral supernatant and polybrene, and were centrifuged (1800 rpm, 90 min, 37°C). To improve infection, the procedure was repeated 3 times at 8-10 h intervals. Infected NIH3T3 (c-MycER) cells were selected for 2 days in medium containing 2 µg/ml puromycin.

### 2.3) Synchronization of NIH3T3 cells

**Synchronization in G<sub>0</sub>.** To monitor the G<sub>0</sub>-to-S transition accurately, we established a standard time course protocol for all experiments (Martinez-Gac *et al.* 2004). Exponentially growing cells were seeded into dishes and rendered quiescent by incubation in DMEM-0.1% FBS (19 h). Under these conditions, cells showed a G<sub>0</sub> phenotype, examined as described (Martinez-Gac *et al.* 2004).

**Synchronization in metaphase.** NIH3T3 cells were arrested in mitosis by maintaining cells in medium containing 75 ng/ml colcemid (KaryoMAX, 12 h).

### 2.4) Cell cycle analysis

**Propidium iodide** staining for cell cycle analysis. Quiescent cultures were rinsed with serum-free medium and synchronous cell cycle entry was stimulated by serum re-addition (10% final

concentration). Some samples were harvested immediately before serum addition (time zero); other cells were harvested at various times after serum stimulation. DNA synthesis was studied by DNA staining with propidium iodide and analysed in a flow cytometer (Beckman-Coulter) as described (Álvarez *et al.*, 2001).

**BrdU incorporation.** Cells were incubated with 10  $\mu$ M BrdU (90 min) and harvested at indicated time points using trypsin-EDTA (see Fig. 4). Cells were washed twice with phosphate-buffered saline (PBS)-1% FBS and fixed in ice-cold 80% methanol overnight. Cells were then washed twice and resuspended in PBS containing 1% FBS and 0.1 mg/ml RNase (30 min, room temperature). To extract histones and denature cellular DNA, we incubated cells with 1.5 N HCl and 0.5% Triton X-100 (30 min, room temperature). For direct immunofluorescence staining, cells were incubated (1 h) with fluorescein isothiocyanate-conjugated anti-BrdU antibody (Becton Dickinson). After washing (PBS-1% FBS), cells were resuspended in 500  $\mu$ l PBS (with 0.1 mg/ml RNase, 0.1% NP-40, 5  $\mu$ g/ml propidium iodide). DNA synthesis was studied as percent BrdU incorporation and analysed by flow cytometry (Beckman-Coulter).

### 2.5) Pulse-chase assay

NIH3T3 cells were incubated in DMEM-0.1% FBS for 19 h (as above); medium was then replaced with Met-free RPMI (Gibco) containing 10% dialyzed FBS (9 h), with 0.75 mCi [ $^{35}$ S]Met (per p100 dish) included for the last 6 h. At 8.5 h after serum addition, some samples were treated with Ly294002 (10  $\mu$ M). After the 9-h pulse, the [ $^{35}$ S]Met-containing medium was washed and replaced by DMEM-10% FBS containing 200  $\mu$ M cold Met and Cys alone, or with Ly294002 (10  $\mu$ M) and maintained until 12 h and 16 h after serum addition (chase).

### 2.6) Inhibitor treatment

To activate c-MycER, we added 4-hydroxytamoxifen (4-OHT; 200 nM, Sigma) 6.5 h after serum stimulation. In some cases, cells were treated with 0.1% dimethylsulphoxide (control), lovastatin (10  $\mu$ M), herbimycin (2  $\mu$ M), or Ly294002 (10  $\mu$ M). When samples were collected at time zero, inhibitors were added 30 min before serum addition; otherwise, inhibitors were added 4, 6, or 7 h after serum stimulation. Cycloheximide (20  $\mu$ g/ml) was used to inhibit translation in intact cells. In DNA repair experiments, cells were TGX221-treated (indicated) to inhibit p110 $\beta$  kinase activity.

## 3. DNA, Northern blot, DNA damage, real-time DNA damage

### 3.1) cDNA

The table below shows the different constructs used for experiments. Myc-tagged-p110 $\beta$ , originally cloned in pCMV, was subcloned into the PSG5 *EcoRI* site using the restriction enzyme *EcoRI* at both ends. pEBG-GST-p110 $\beta$  was generated by inserting p110 $\beta$  in the C-terminus of GST in pEBG. To construct pEBG-GST-p110 $\beta$ -NLS, the SV40 NLS sequence PKKKRKV was inserted 3' of p110 $\beta$ . pSG5-p85 $\beta$ -NLS was generated in a similar manner, where amplified p85 $\beta$ -NLS was inserted in pSG5. pEGFP-C1-p110 $\beta$  was generated by amplifying p110 $\beta$  and inserting it in pEGFP-C1. The mutants pSG5-p110 $\beta$  Mut1, pSG5-p110 $\beta$  Mut2 and pSG5-p110 $\beta$  Mut3 were generated using the Quik site-directed mutagenesis kit (Stratagene) with primers described below.

For preparation of the p85 $\beta$  chimera, the p85 $\beta$  fragment from amino acids 77 to 343 was replaced by the corresponding amino acids from p85 $\alpha$ .

$\Delta$ 41-p85 $\beta$  was generated by deletion of the first 41 amino acids by PCR amplification and was subcloned in the pSG5 vector.  $\Delta$ 100-p85 $\beta$  was generated similarly. shRNA for p110 $\beta$  was purchased from Origene Technology.



Plasmid	Reference
pSG5-Myc-p110 $\alpha$ bovine	Jiménez <i>et al.</i> , 1998
pCDNA3-His-p110 $\beta$ human	B. Vanhaesebroeck (Ludwig Inst Cancer Research, UK)
pSG5-Myc-p110 $\beta$ human	Described in above
pEBG-GST-p110 $\beta$	Described in above
pEBG-GST-p110 $\beta$ -NLS	Described above
pSG5-p110 $\beta$ Mut1	Described above
pSG5-p110 $\beta$ Mut2	Described above
pSG5-p110 $\beta$ Mut3	Described above
pSG5-HA-p85 $\beta$	I. Cortés, DIO, CNB, Madrid
pSG5-HA-p85 $\alpha$	I. Cortés, DIO, CNB, Madrid
pSG5-HA-p85 $\beta$ -NLS	Described above
pSG5-HA-p65 $\beta$	I. Cortés, DIO, CNB, Madrid
pSG5- $\Delta$ 1-p85 $\beta$	Described above
pSG5- $\Delta$ 2-p85 $\beta$	Described above
pCMV-c-Myc-WT/T58A	S. Lowe (Cold Spring Harbor Laboratory, NY)
pBabe puro c-Myc-ER	G. Evan (Cancer Research Institute, UCSF, CA)
pEGFP-NBS1	O. Fernández Capetillo, CNIO, Madrid
pEGFP-53BP1	O. Fernández Capetillo, CNIO, Madrid
RFP-PCNA	M.C. Cardoso, MDC, Berlin

### 3.2) mRNA analysis (Northern blot)

Total RNA was isolated from serum-starved, 9 h-serum stimulated, or LY-treated cells using the Trizol reagent kit. Total RNA (20  $\mu$ g) was separated by electrophoresis in denaturing formaldehyde-1% agarose gels and transferred overnight to a nylon membrane (Zeta-Probe; Bio-Rad) followed by UV crosslinking. The c-Myc probes were [ $^{32}$ P]dCTP-labelled by random priming with the Prime-It II labelling kit (Stratagene). Hybridization was performed with ExpressHyb solution (BD Biosciences; 1 h, 60°C) in the presence of 10  $\mu$ g/ml sheared salmon sperm DNA (Sigma). The membrane was washed three times in 2x SSC (150 mM NaCl, 15 mM sodium citrate, pH 7.0) with 0.05% sodium dodecyl sulphate (SDS) at room temperature, and once in 0.1x SSC plus 0.1% SDS (52°C). Murine c-Myc (1.4 kb) was used as probe.

### 3.3) Ultraviolet and ionizing radiation treatment

NIH3T3 cells were transfected with p110 $\beta$  shRNA or control plasmid. After 30 h transfection, cells were selected for 2 days in medium containing 2  $\mu$ g/ml puromycin and exposed to ultraviolet or ionizing radiation at the doses given in Results. IR was delivered by the X-ray generator (MARK 1-30, Shephard & Associates).

### 3.4) Real-time recruitment of DNA repair proteins to microlaser-generated DNA damage sites

NIH3T3 cells transfected with p110 $\beta$  shRNA or control plasmid were incubated with 2  $\mu$ g/ml puromycin after 30 h transfection. After selection for 12 h, transfected cells were seeded on 6-well Petri plates with puromycin-containing medium. At 10 h post-plating, cells were transfected with fluorescent-tagged plasmids (indicated) using the JetPei/NaCl method. After 24 h, cells were again seeded on Petri plates for live study using confocal microscopy (Leica). Some control plates were incubated with TGX221. Before laser treatment, medium was changed to phenol red-free DMEM (Invitrogen). DNA intercalating dye Hoechst 33258 was added at 10  $\mu$ g/ml and incubated for 20 min at 37°C. Cells were irradiated with a 351-nm laser along a user-defined path to generate localized DSBs. The UV laser output was set to 50%, the minimum dose required to generate a clearly detectable DSB response (in a Hoechst-dependent manner) strictly within the laser-exposed

nuclear compartments. The total time of single-cell exposure to the laser beam did not exceed 1 sec. In these conditions, cells showed no morphological or cytotoxic effects. Immediately after microirradiation, the same field was subjected to repeated image acquisition via the confocal unit integrated into the microscope using LCS software version 2.61. The first images were consistently recorded ~5 - 6 sec after DSB generation with a gap of 1.6 sec. per image .

#### **4. Biochemical assays and immunofluorescence**

##### **4.1) Cell lysis, subcellular fractionation**

**Cell lysis.** Total cell lysates were prepared in RIPA lysis buffer (20 mM Tris-HCl pH 8.0, 137 mM NaCl, 1 mM MgCl<sub>2</sub>, 1 mM CaCl<sub>2</sub>, 10% glycerol, 1% NP-40, 0.5% sodium deoxycholate, 0.1% SDS and protease inhibitors (1 mM PMSF, 1 mM Na<sub>3</sub>VO<sub>4</sub>, 10 µg/ml leupeptin, 10 µg/ml aprotinin, 5 mM NaF, 10 mM okadaic acid, 1 mM EDTA).

**Subcellular fractionation.** For analysis of MCM2 loading onto chromatin, cells were fractionated into cytosol, nucleosol and chromatin using the lysis buffers in the following sequence.

- For extraction of the cytoplasmic fraction, cells were resuspended in buffer A (10 mM Hepes pH 7.9, 10 mM KCl, 1.5 mM MgCl<sub>2</sub>, 340 mM sucrose, 10% glycerol, 1 mM DTT, 0.1% TX-100 with protease inhibitors mentioned above) for 5 min on ice, then centrifuged (3500 rpm, 5 min). The supernatant constitutes the cytoplasmic fraction.
- The remaining pellet contains the intact nuclei of the lysed cells, which were washed once in buffer A without TX-100 and centrifuged as above. Pellets were then resuspended in buffer B (3 mM EDTA, 0.2 mM EGTA with protease inhibitors) and incubated (30 min, on ice, with mixing every 10 min). The lysates were then centrifuged (3500 rpm, 5 min). The supernatant constitutes the nuclear soluble fraction and the pellet contains the chromatin fraction.
- Pellets were resuspended in 2x Laemmli sample buffer for electrophoresis and boiled (5 min, 95°C). These samples were sonicated to resuspend DNA aggregates.

To examine protein-protein interactions, cells were fractionated into cytosolic and nuclear fractions using the lysis buffers below sequentially (NP-40 protocol).

- For extraction of the cytoplasmic fraction, cells were resuspended in buffer A (10 mM Hepes pH 7.5, 10 mM KCl, 5 mM MgCl<sub>2</sub> with protease inhibitors mentioned above) and incubated (15 min, on ice), after which NP-40 was added to a final concentration of 0.3%, followed by incubation (10 min, on ice). Lysates were centrifuged (3500 rpm, 5 min). The supernatant constitutes the cytoplasmic fraction.
- Pellets (nuclear fraction) were resuspended in buffer B (20 mM Hepes pH 7.5, 200 mM NaCl, 1% NP-40 containing protease inhibitors and DNase 2-3U/µl) and incubated (30 min, 37°C). Lysates were then centrifuged (14000 rpm, 20 min) and the supernatant was collected as total nuclear extract.

##### **4.2). Immunoprecipitation and Western blotting**

For PCNA association with p110α and p110β, NIH3T3 cells were co-transfected either with pSG5-Myc-p110β plus pSG5-HA-p85β-NLS or pSG5-Myc-p110α plus pSG5-HA-p85β-NLS. Transfected cells were fractionated into cytoplasmic and nuclear fractions using the NP-40 protocol. Total protein concentration was measured with the Micro BCA kit (Pierce). Immunoprecipitation was performed by incubating lysates (4°C, 3-4 h) with the appropriate antibody, followed by incubation with 30 µl of 50% protein A-Sepharose slurry (Amersham Biosciences) for 1 h. Protein (800 µg) from the nuclear fraction was used to immunoprecipitate p110, and 200 µg nuclear lysate was used for control immunoprecipitations. Immunoprecipitates were washed three times with lysis buffer, twice with 50 mM Tris-HCl, pH 7.5.

Immunoprecipitated proteins were resolved by SDS-PAGE, then transferred to nitrocellulose for Western blot analysis.

RAD17 association with p110 $\beta$  was examined in control cells or cells irradiated with UV or IR; at 1 h post-exposure, cells were harvested and fractionated as cytoplasmic and nuclear extracts using the NP40 protocol. Anti-p110 $\beta$  Ab (Cell Signaling) was used to immunoprecipitate p110 $\beta$  from 800  $\mu$ g nuclear lysate, whereas RAD17 was immunoprecipitated from 200  $\mu$ g (control) using anti-RAD17 Ab (Santa Cruz). Western blot to analyse associations were developed with anti-RAD17 and anti-pan p85 for controls.

#### 4.3) PI3K assays

Different PI3K isoforms were immunoprecipitated from the distinct subcellular fractions using appropriate antibodies (see Results). Immunopurified PI3K was resuspended in 20  $\mu$ l 50 mM Hepes containing phosphoinositide4,5-bisphosphate (PIP2; 10 mg/ml; Sigma) as substrate. The kinase reaction was initiated by adding 5  $\mu$ l of kinase buffer containing 10  $\mu$ Ci [ $^{32}$ P]ATP, 100 mM MgCl<sub>2</sub>, and 100  $\mu$ M cold ATP (37°C, 5 min). The reaction was terminated by adding 100  $\mu$ l 1 M HCl and 200  $\mu$ l of methanol/chloroform (1:1 v/v). The extracted phospholipids were resolved by thin layer chromatography (Silica Gel 60; Merck) on 1% potassium oxalate-coated plates and developed in glacial acetic acid/H<sub>2</sub>O/*n*-propyl alcohol (4:31:65 v/v/v). The radioactive products were visualized by autoradiography.

#### 4.4) Cyclin/Cdk kinase assays

NIH 3T3 cells were incubated in DMEM-0.1% FBS for 19 h (see above), after which medium was replaced with DMEM containing 10% FBS for 9, 12 and 16 h. At 7 h post-serum addition, some samples were treated with Ly294002 (20  $\mu$ M). Cells were harvested at indicated times (see Results) and lysed. We used 200  $\mu$ g of total lysate to immunoprecipitate cyclin E or cyclin A using appropriate antibodies. Antibodies were incubated with total lysates overnight (4°C) followed by protein A (blocked with 3% milk in 1x PBS) incubation (2 h, 4°C). Bead-bound immunoprecipitated protein was washed three times with lysis buffer, twice with 50 mM Tris/HCl pH 7.5 and twice with kinase buffer. The kinase reaction was performed in kinase buffer (20 mM Tris/HCl pH 8.0, 10 mM MgCl<sub>2</sub>, 1 mM EGTA, 1 mM DTT, 5  $\mu$ Ci  $\gamma$ -ATP with protease inhibitors) and incubated (30 min, 30°C). Reactions were terminated by boiling the reaction mixture in 1x Laemmli buffer (10 min, 95°C), resolved in SDS-PAGE, and the radioactive products were visualized by autoradiography.

#### 4.5) Pull-down assay

**Ras pull-down assay.** Ras-GTP was purified from cell extracts on Sepharose-Gex2T-RBD (the Ras-binding domain of Raf-1). Briefly, NIH3T3 cells were harvested, lysed with glutathione S-transferase fluorescent *in situ* hybridization buffer (50 mM Tris-HCl, pH 7.5, 2 mM EDTA, 100 mM NaCl, 2 mM MgCl<sub>2</sub>, 1% [vol/vol] NP-40, 5 mM NaF, 10% [vol/vol] glycerol, 1 mM phenylmethylsulphonyl fluoride, 1  $\mu$ g/ml aprotinin, and 10  $\mu$ g/ml leupeptin). Protein concentration, determined using the Micro BCA kit, was normalized and lysates were incubated (1 h, 4°C) with glutathione-Sepharose beads coupled with glutathione S-transferase-RBD. Beads were washed three times in lysis buffer, and bound Ras-GTP was solubilised in 30  $\mu$ l Laemmli buffer. Ras-GTP levels were analysed by Western blot

**GST-p110 $\beta$  pull-down.** NIH3T3 cells were transfected with pEBG-GST or pEBG-p110 $\beta$ -NLS. Cells were harvested and fractionated into cytoplasmic and nuclear extracts. Lysates (1 mg) were incubated (2 h, 4°C) with glutathione beads. Beads were washed twice with lysis buffer, once with 50 mM Tris/HCl pH 7.5, bound p110 $\beta$  was resuspended in 2x Laemmli buffer and resolved in SDS-PAGE. The gel was stained using a silver staining kit (Amersham). Stained proteins were cut into small pieces and analysed by mass spectrometry. p110 $\beta$ -associated proteins was identified

by comparison of peptide sequences with the database.

#### **4.6) Immunofluorescence**

Cell lines and MEF were fixed with 4% formaldehyde (1x PBS; 10 min, room temperature) after the indicated treatments. The cells were then blocked using 1x PBS staining solution and permeabilised with 0.3% TX-100 PBS (10 min). Cells were incubated with appropriate primary antibodies (1 h, room temperature, with end-to-end rocking), followed by three washes with blocking buffer. Appropriate secondary antibodies were added to samples and incubated (1 h, room temperature), followed by three washes with blocking buffer. Cells were then mounted using mounting medium containing DAPI (VectaShield) and visualized under the microscope the confocal or fluorescence microscope.



## **RESULTS**



## 1. PI3K REGULATES G1/S TRANSITION

### 1.1) Cell cycle progression

There are several methods to study cell division, such as monitoring the increase in cell number over time or examining cells visually under a microscope. The use of specific analysis in flow cytometry (such as staining of phospho-histone H3 for mitosis detection) provides additional means of estimating cell division, as does determination of the cell doubling time and of the percentage of cells in different phases of the cell cycle. For this last method we measure DNA cell content with propidium iodide. NIH3T3 cells, used here to study the cell cycle, were arrested in G0-phase by serum starvation (**Martinez *et al.*, 2004**). Serum-starved cells were stimulated with 10% FBS to trigger cell cycle entry, after which they progressed synchronously through the distinct phases of the cell cycle. Following stimulation, cells were harvested at different time points to determine by FACS the time needed to reach a specific cell cycle phase. NIH3T3 cells showed a smooth progression through the cell cycle after stimulation of serum-starved cells (Fig. 1). The G1-to-S phase transition occurred at ~9 h, and progressed through S phase until 16 h post-stimulation. At 18 h, cells showed a synchronized transition into G2/M phase.

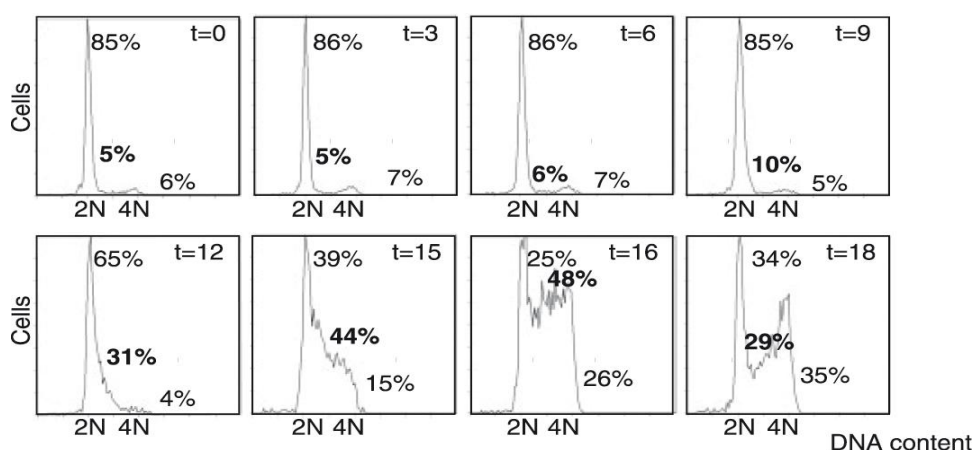


**Figure 1.** Quiescent NIH3T3 cells enter S phase between 9 to 12 h post-stimulation. DNA content in cell cycle profiles of NIH3T3 cells arrested in G0 by serum deprivation, then released for different periods (indicated) to allow synchronous cell cycle entry. Percentage of cells in G0/G1, S (in bold) and G2/M phases is indicated.

### 1.2) PI3K activity in late G1 induces PKB activation that correlates with increased c-Myc protein levels

Initiation of cell division requires exposure of resting quiescent cells to growth factors (GF) (**Sherr, 1994**). Cells cultured in the continuous presence of GF undergo two waves of intracellular signalling molecules activation, the first occurs within one hour after GF addition and the second at 7-to-9 h after serum addition; the two signalling waves include activation of PI3K, Ras and MAPK (**Jones *et al.*, 1999**). PI3K is activated in late G1 (**Jones *et al.*, 2001**); this activity peak is essential for S phase entry, since PI3K inhibition in late G1 blocks S phase entry, and PIP<sub>3</sub> addition in late G1 induces cell cycle entry in the absence of serum (**del Real *et al.*, 2004**; **García *et al.*, 2006**). Prolonged and continuous contact with GF is required to commit cells to cell cycle entry. Indeed, GF are needed until the cells pass the so called restriction point (in advance G1 phase), after which GF can be eliminated and the cells proceed to S phase even in the absence of GF (**García *et al.*, 2006**). However, the continuous presence of GF can be substituted by addition of GF in early and late G1 with an intermediate serum deprivation (**Jones *et al.*, 2001**). We first checked that incubation with serum-containing medium for just 9h was sufficient to trigger cell cycle entry (not shown).



In cells entering the cell cycle synchronously, we confirmed early G1 (1 h) and late G1 (~9 to 15 h) PI3K activity peaks (Fig. 2A), as determined by examining phosphorylation of the PI3K effector PKB (pPKB) (**Bouchard *et al.*, 2004**). We also examined c-Myc expression levels and found that they paralleled the PI3K activity peaks (Fig. 2B).

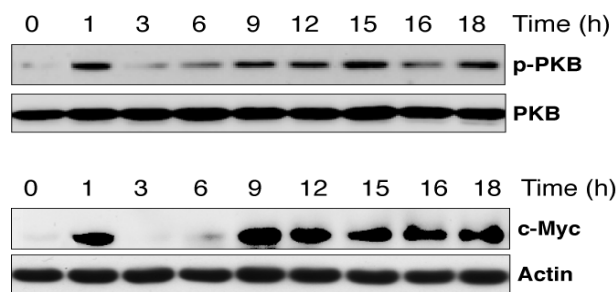


**Figure 2. The late G1 PI3K activity peak induces PKB activation and c-Myc expression.** Western blot (WB) analysis of the cells in Fig. 1 using anti-phospho-S473-PKB (pPKB), -PKB, -c-Myc and -actin antibodies.

### 1.3) Ras and Tyr kinases activate PI3K in late G1

It has been extensively examined how induction of the first signalling wave occurs immediately after acute cell stimulation (**Marques *et al.*, 2008**). In contrast, nothing is known regarding the molecular events by which the second wave of signalling molecules occurs. Whether the mechanisms by which the signalling enzymes are activated during the first and second wave of signalling are identical or distinct is thus unknown. Growth factors activate tyrosine kinases (TyrK) and Ras needed for cell cycle entry. PI3K activation at the G0/G1 transition is known to be triggered following activation by TyrK and Ras activities (**Blow & Dutta, 2005; Schmidt *et al.*, 2002**). We thus investigated whether TyrK and Ras were also induced in late G1. We examined TyrK activation using an anti-pTyr antibody in WB, and Ras activity in pull-down assays. We observed that after growth factor addition, total TyrK activity increased transiently at 1 h, and again between 9 and 16 h (Fig. 3A). Some of the Tyr-phosphorylated bands that appeared at 1 h differed from those visible at ~9 h, suggesting that more than one TyrK is activated during G1. Ras activation was also observed in early and late G1, as Ras-GTP increased at ~1 h and again at 9-12 h post-serum stimulation; the second Ras activity peak was greater than that at early G1 (Fig. 3B).

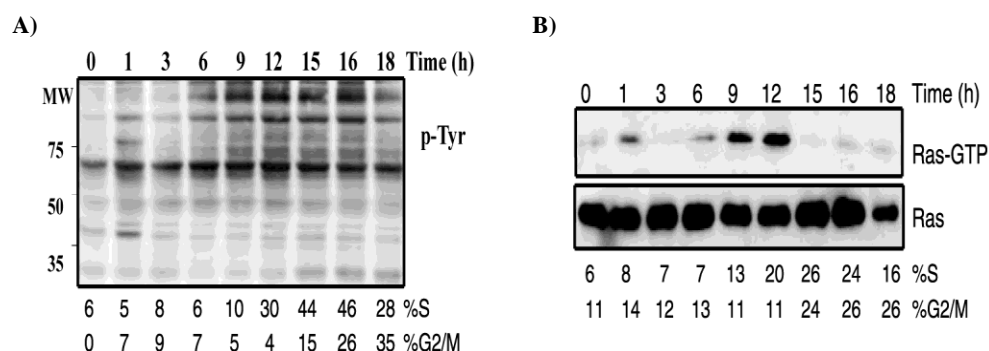


**Figure 3. PKB activation in late G1 correlates with TyrK and Ras activation.** A) Activation of TyrK in cells entering cycle, as determined in WB using anti-p-Tyr antibody. B) Ras-GTP was examined in whole cell extracts. Total Ras and Ras-GTP were examined by WB. The figure shows representative experiments of at least four with similar results.

PDGF receptor activation results in recruitment of p85/p110 from cytosol to the plasma membrane *via* p85 SH2 domains binding to phosphotyrosine residues on the PDGF receptor (Cantley *et al.*, 1991). To determine whether TyrK or Ras stimulation was necessary for PI3K activation in late G1, we used the small molecule inhibitors: herbimycin for TyrK inhibition (Serrano *et al.*, 1997) and lovastatin for Ras inhibition (Schorl & Sedivy, 2003), and examined the effects on PI3K activity in extracts from synchronous cell cultures. At 4 h post-serum addition, treatment with lovastatin, herbimycin, or both resulted in reduced PI3K activity at 7 to 8 h post-serum addition (Fig. 4).

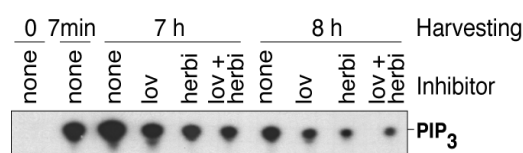


**Figure 4. Ras and TyrK contribute to PI3K activation in late G1.** PI3K was immunoprecipitated from cell extracts (see Methods) and its activity assayed *in vitro*. The inhibitors lovastatin (lov), lovastatin plus mevalonate (lov+mev) or herbimycin (herbi) were added to some samples at the time of serum addition ( $t = 0$ ) or at 4 h post-serum addition, and cell extracts collected at the time points indicated. Lipids were extracted and resolved by TLC.

As PI3K activity regulates pPKB, c-Myc and cyclin levels, we also examined the effects of lovastatin and herbimycin on PI3K effectors. Lovastatin addition at 0, 4 or 6 h reduced pPKB levels at 9 and 12 h after serum stimulation (Fig. 5A), suggesting that Ras activation is involved in late G1 PI3K activation. Addition of mevalonate, a lovastatin substrate, restored PKB phosphorylation (Fig. 5A). Herbimycin also reduced PKB activation at 9 and 12 h (Fig. 5A), whereas genistein, an inhibitor with high specificity for EGFR (Uckun *et al.*, 1998), did not affect the second PI3K activity peak in late G1 (not shown). Combination of lovastatin and herbimycin treatments yielded a greater reduction in pPKB (Fig. 5A).

*In conclusion, examination of the PI3K effector PKB confirmed that TyrK and Ras are involved in late-G1 PI3K activation.* The decrease in pPKB levels correlated with a reduction in both c-Myc content and in the number of cells entering S phase at 12 h (Fig. 5A). We also examined the effect of lovastatin and herbimycin on cyclin D3, E and A levels. Inhibition of both TyrK and Ras reduced the levels of these cyclins, with a more marked effect on cyclin A (Fig. 5A). Since c-Myc-action is critical for Cyclin A expression, *we concluded that one of the most prominent defects of PI3K inhibition on late G1 was the reduction of c-Myc levels and in turn the defective Cyclin A expression.* TyrK and Ras thus cooperate to induce the second PI3K activity peak, which in turn regulates c-Myc and cyclins levels in G1, as well as S phase entry. The activity of the inhibitors in blocking TyrK and Ras activation was confirmed in WB; herbimycin reduced cell phospho-Tyr levels (Fig. 5B), and lovastatin reduced the active Ras fraction, an effect that was reversed by mevalonate addition (Fig. 5C).



To examine whether reduced c-Myc protein levels were caused by PI3K inhibition of c-Myc transcription or protein stability, we performed Northern blot for *c-myc* mRNA. Cells were synchronized as above and the PI3K inhibitor Ly294002 was added 7 h after serum stimulation; cells were harvested at 9 h. This analysis showed that late G1 PI3K inhibition induced a reduction in *c-myc* mRNA levels of about  $15 \pm 5\%$  (at 9 h; mean of three experiments, Fig. 7B), whereas the reduction in c-Myc protein was systematically  $>50\%$  (Fig. 7A).

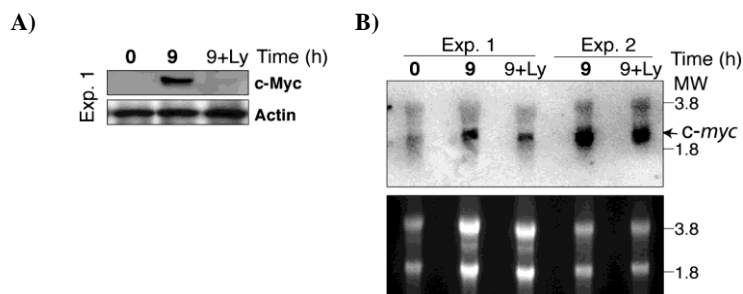


**Figure 7. PI3K inhibition in late G1 reduces c-Myc protein but not mRNA levels.** Total RNA and protein extracts were prepared from cells entering the cell cycle synchronously. Ly294002 was added at 7 h post-serum addition; cells were harvested at  $t = 0$  and 9 h. Samples were examined in WB (A) and in Northern blot (B) using a *c-myc* probe or anti-Myc antibody, respectively (B). The Northern blot corresponds to two different experiments.

We further examined the effect of PI3K inhibition in late G1 on c-Myc protein stability in  $^{35}\text{S}$ -Met pulse-chase assays. Inhibition of PI3K activity in early G1 (3 h post-serum stimulation) blocked protein synthesis (not shown). For pulse-chase, we synchronized cells, labelled them with  $^{35}\text{S}$ -Met between 3 to 9 h post-serum addition, and harvested them at 9 h. At this time, the medium was exchanged for non-radiolabelled Met/Cys-rich medium, alone or with Ly294002, and cells were collected at 12 and 16 h (Fig. 8). For the 9 h time point with Ly294002, the inhibitor was added 30 min prior to cell harvest. PI3K inhibition greatly reduced c-Myc stability, an effect that was already evident by 30 min after enzyme inhibition (Fig. 8).

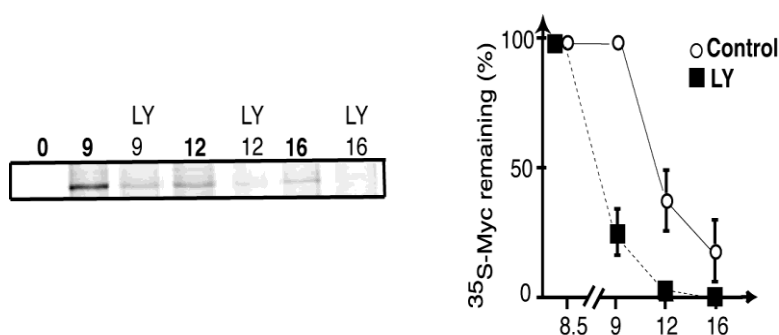


**Figure 8. PI3K activity in late G1 regulates c-Myc protein stability.** Synchronized cells were  $^{35}\text{S}$ -Met labelled during the first 9 h post-serum addition and medium was changed to unlabelled Met/Cys-rich medium, alone or with Ly294002 (LY; 10  $\mu\text{M}$ ), and cells were collected at 12 and 16 h. For the 9 h with Ly294002, the inhibitor was added 30 min before harvest.  $^{35}\text{S}$ -c-Myc was examined by autoradiography. Quantitative analysis of three experiments is shown.

To further define the role of the second G1 PI3K activity peak in S phase entry, cells were synchronized in G0/G1 and PI3K was inhibited at 7 h post-serum stimulation; we examined the consequences for G1 phase cyclin levels at different time points. Inhibition of late G1 PI3K activity greatly reduced cyclin A protein levels at 9 h, whereas cyclin D3 and E levels were more affected when Ly294002 was present for prolonged periods (Fig. 9). The Ras inhibitor lovastatin had a greater effect than Ly294002 on reducing cyclin D3 levels (Fig. 5, 9); this is probably due to the reported Ras/MAPK dependence for cyclin D synthesis (Jirmanova *et al.*, 2002). We next

tested the effect of PI3K inhibition on CDK2 activity. The CDK2 substrate retinoblastoma protein (Rb) was hyperphosphorylated in late G1 and this phosphorylation was markedly reduced by PI3K inhibition (Fig. 9).

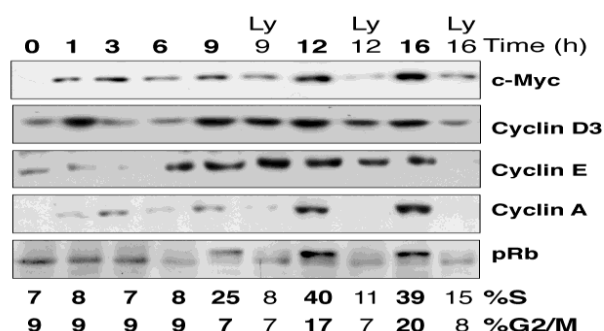


**Figure 9. Inhibition of PI3K activity in late G1 downregulates cyclin A levels and hypophosphorylation of retinoblastoma protein.** Cell extracts as Fig. 6 were examined by WB using anti-c-Myc, -cyclin D3, -E, and -A, as well as anti-Rb antibodies. The percentage of cells in S and G2/M phases is indicated beneath the blots.

Moreover, both cyclinE/CDK2 and cyclinA/CDK2 kinase activities were consistently decreased after PI3K inhibition (Fig. 10 A). The decrease in cyclin A expression (Fig. 9) paralleled the reduction in cyclinA/CDK2 activity. Nonetheless, PI3K inhibition in late G1 affected cyclinE/CDK2 activity more markedly than cyclin E levels. Considering that we also observed an increase in p27<sup>kip1</sup> expression after PI3K inhibition in late G1 (Fig. 10 B), a possible explanation for the defect could be that the increased p27<sup>kip1</sup> levels resulted in an enhanced association of p27<sup>kip1</sup> to cyclinE/CDK2 complex, thereby reducing its kinase activity.

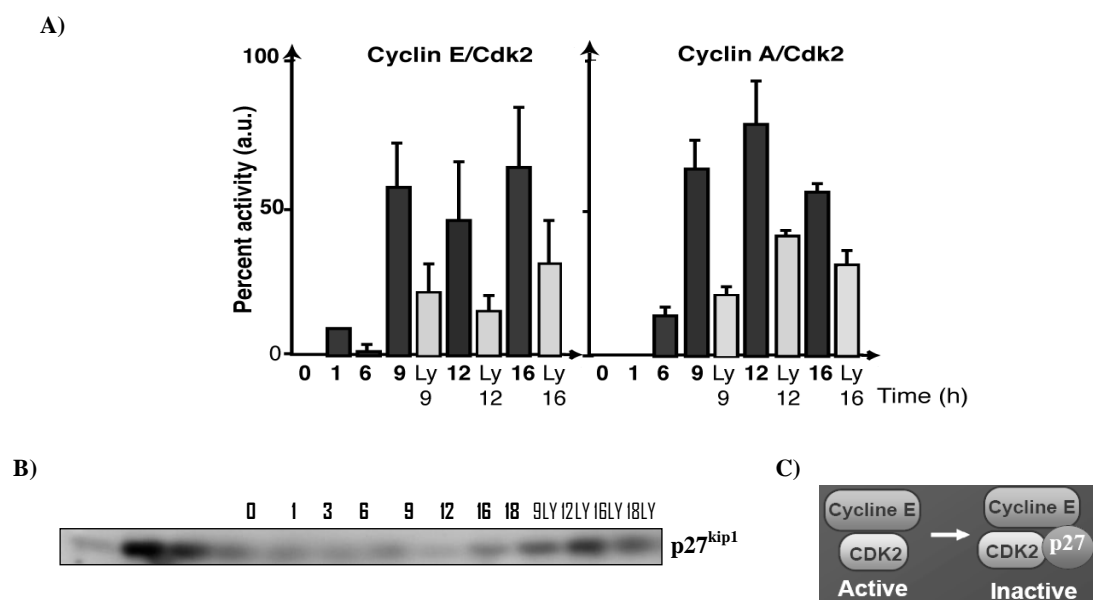


**Figure 10. PI3K activity in late G1 regulates cyclin E/A-associated CDK2 kinase activity.** (A) Downregulation of cyclin E/CDK2 and cyclin A/CDK2 kinase activities in cyclin E and cyclin A immunoprecipitates, respectively, from cell extracts. Histone H1 (5  $\mu$ g) served as substrate. <sup>32</sup>P-histone was quantitated and the activity represented (in arbitrary units). Mean  $\pm$  SD of three experiments. (B) Upregulation of p27 protein levels after inhibition of PI3K activity in late G1. (C) Scheme representing the cause of downregulation of cyclin E/A-associated kinase activities on the inhibition of PI3K activity in late G1.

We examined whether PI3K inhibition reduced cyclin E/CDK2 activity by enhancing its association with p27<sup>kip1</sup>. PI3K inhibition increased the amount of p27<sup>kip1</sup> bound to CDK2 (see

below), which explained the reduction in cyclin E/CDK2 activity by late G1 PI3K inhibition. Cyclin E/CDK2 activity is required for minichromosome maintenance protein complex (MCM2) loading onto chromatin (Ekholm-Reed *et al.*, 2004; Geng *et al.*, 2003). Accordingly, PI3K inhibition in advanced G1 resulted in a notable reduction in the amount of chromatin-bound MCM2 (Fig. 11).

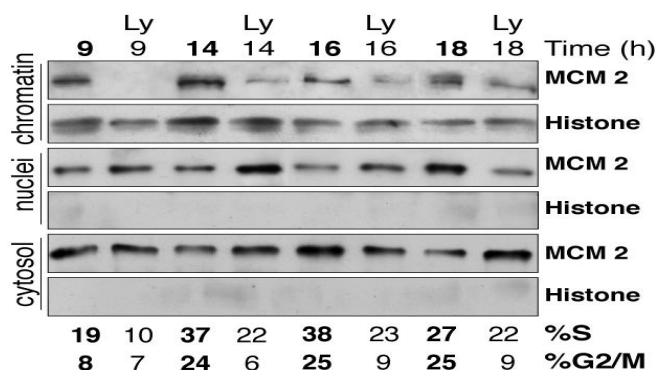


**Figure 11. Inhibition of PI3K activity in late G1 reduces MCM2 association to chromatin.** Cells entering the cell cycle synchronously, treated as in Fig. 6 were fractionated into cytosolic, nuclear and chromatin fractions, which were examined in WB using anti-MCM2 and -histone antibodies. A representative experiment is shown of three with similar results.

### 1.5) Conditional c-Myc-ER activation rescues S phase entry in PI3K inhibitor-treated cells

PI3K inhibition reduced cyclin A levels and CDK2 activity. c-Myc regulates G1 cyclin expression, especially that of cyclin A, and the association of p27<sup>kip</sup> with cyclin/CDK2 (Mateyak *et al.*, 1997; Perez-Roger *et al.*, 1997; Vlach *et al.*, 1996). We thus hypothesized that the main function of PI3K activity in late G1 is to regulate c-Myc levels. To test this possibility, we used a c-Myc-oestrogen receptor fusion protein (c-Myc-ER) that translocates to the nucleus after addition of an estrogen analogue 4-OHT (Littlewood *et al.*, 1995; Fig. 12A). We examined whether the S phase entry defects induced by late G1 PI3K inhibition were counteracted by c-Myc-ER induction. Cells were infected with c-Myc-ER-expressing viruses (Fig. 12B), arrested in G0, and released by serum addition. Some of the cells were treated with 4-OHT alone (at 6.5 h), with Ly294002 (at 7 h post-serum addition), or with both. We collected cells at different times and examined S phase entry.

c-Myc-ER induction corrected the defects in S phase entry, cyclin A expression, and Rb phosphorylation induced by late-G<sub>1</sub> PI3K inhibition (Fig. 12 C). c-Myc-ER expression did not trigger S phase entry in the absence of serum (Fig. 12D, E). After serum addition, c-Myc-ER expression caused a slight increase in S phase entry compared to that in control cells, which was moderately enhanced by 4-OHT addition (Fig. 12 D, E). We found no notable differences when 4-OHT was added at 0 or at 6.5 h (not shown). Ly294002 treatment reduced the proportion of cells in S phase by 50% in both c-Myc-ER and control ER vector-expressing cells (Fig. 12E). Nonetheless, c-Myc-ER induction at 6.5 h in cells treated with Ly294002 in advanced G1 (7 h) showed almost normal S phase entry levels (85% recovery) compared to Ly294002-treated controls (Fig. 12D, F). Induction of c-Myc-ER failed to compensate for the action of PI3K in S phase entry when PI3K was inhibited in early G1 (0 to 4 h post-stimulation; Fig. 12E and not shown). Examination of BrdU incorporation confirmed that c-Myc induction at 6.5 h counteracted S phase entry defects in cells treated with Ly294002 in advanced G1 (Fig. 12F). Results were comparable using the PI3K inhibitor wortmannin (not shown). *These data suggest that the main function of PI3K activity in late G1 is to regulate c-Myc protein levels.*

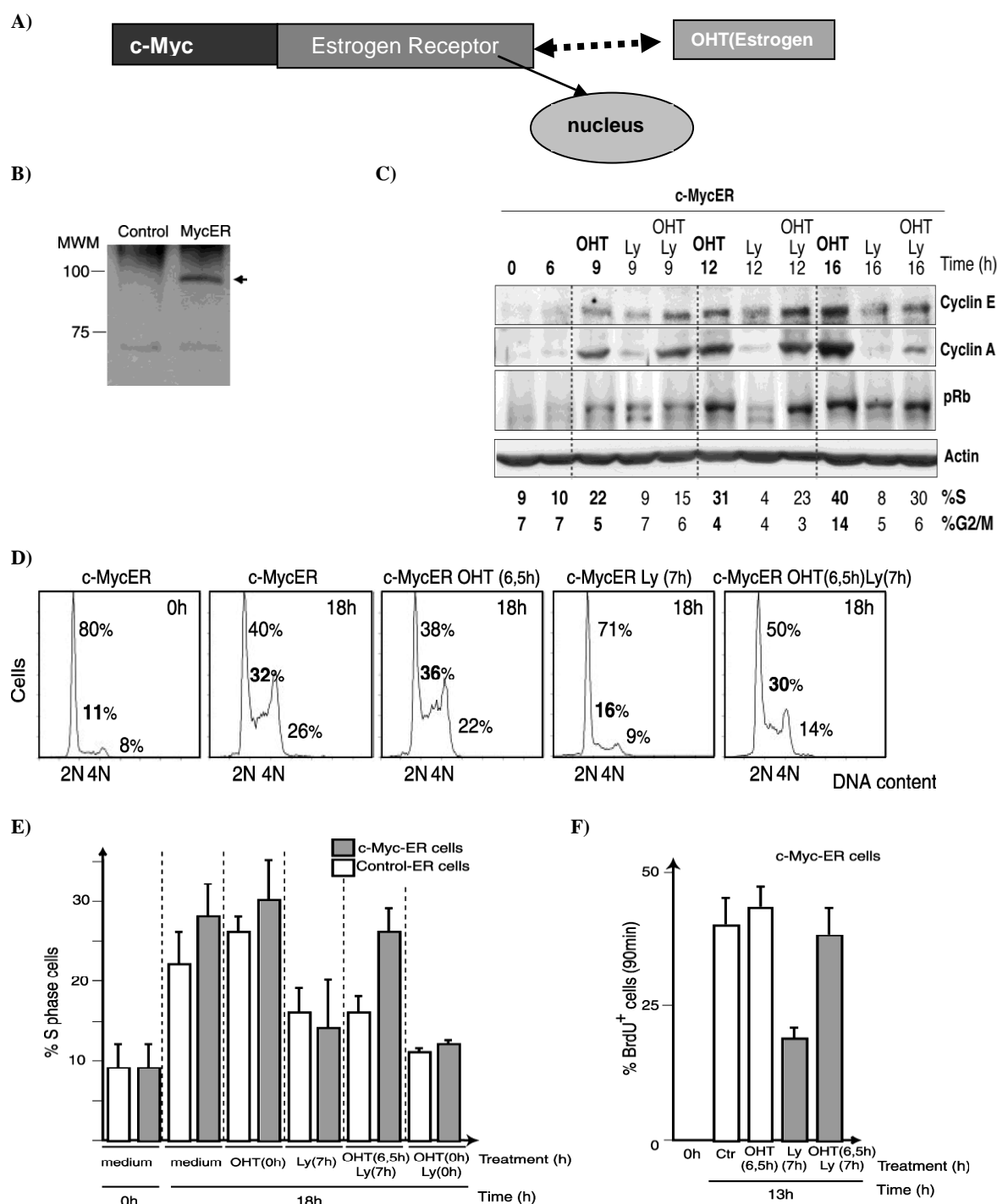


**Figure 12. Conditional activation of c-Myc-ER rescues S phase entry blockade induced by PI3K inhibition in late G1.** **A)** Myc-ER, a chimaeric protein of c-Myc fused with the estrogen receptor, Myc-ER complexed with Hsp90 is localized in the cytoplasm in the absence of 4-OHT. Following 4-OHT addition, Myc-ER is translocated into the nucleus to be activated. **B)** c-Myc-ER expression was examined in c-Myc-ER-infected NIH3T3 cells by WB using anti-Myc antibody. **C)** Synchronized c-Myc-ER-expressing cells were treated with 4-OHT (at 6.5 h), Ly294002 (at 7 h), or both simultaneously; cells were collected at different time points (indicated). Cyclin E, cyclin A, pRb, and actin levels were examined by WB. **D)** Cell cycle profiles of c-Myc-ER cells in quiescence ( $t = 0$ ) or at 18 h post-serum addition, alone or in the presence of 4-OHT (200 nM; added at  $t = 6.5$  h) and/or Ly294002 (10  $\mu$ M; added at  $t = 7$  h post-serum addition). The figure illustrates a representative experiment of three performed. **E)** Percentage of c-Myc-ER and control cells in S phase. Cells were treated as in (C). A sample of cells treated with 4-OHT and Ly294002 as above at the time of serum addition ( $t = 0$  h) is included. The figure shows the mean of three experiments. **F)** BrdU incorporation in c-Myc-ER-infected NIH3T3 cells entering cell cycle synchronously as in (C) and collected at 13 h after serum addition. BrdU (10  $\mu$ M) was present for the last 90 min. Mean  $\pm$  SD of three experiments.

### 1.6) Expression of a GSK3-resistant c-Myc mutant rescues the cell cycle entry defects induced by inhibiting PI3K activity in late G1

PI3K/PKB inactivate GSK3 $\beta$ , an enzyme that targets c-Myc for degradation (Yeh *et al.*, 2004; Fig. 13). To confirm that c-Myc stabilization is the main role of PI3K activity in late G1, we examined the effect of inhibiting PI3K in cells expressing the c-MycT58A substitution mutant, which is resistant to GSK3 $\beta$  action (Hemann *et al.*, 2005).

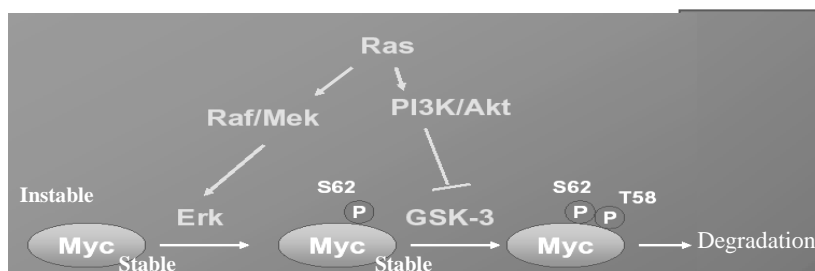


**Figure 13. Mechanism of PI3K mediated c-Myc stabilization.** Activation of PI3K and ERK pathway through Ras. Activated PI3K inhibits GSK-3 $\beta$  activity to stop c-Myc phosphorylation at Thr 58. Phosphorylation at Thr 58 targets c-Myc for proteosomal degradation.

Cells were transfected with GFP control vector or with cDNAs encoding GFP fused to WT c-Myc or c-MycT58A (Fig. 14A). Transfected cells were sorted, the cell cultures were synchronized, released from arrest, and treated with Ly294002 at 7 h after serum addition. Cells were harvested at different time points. Overexpression of either WT c-Myc or c-MycT58A induced apoptosis and cell cycle entry in the absence of serum (Fig. 14B). Late G1 PI3K inhibition reduced cell cycle entry in control cells and, to a lesser extent, in cells overexpressing WT c-Myc; nevertheless, c-MycT58A expression largely restored cell cycle entry in cells treated with LY (Fig. 14B).

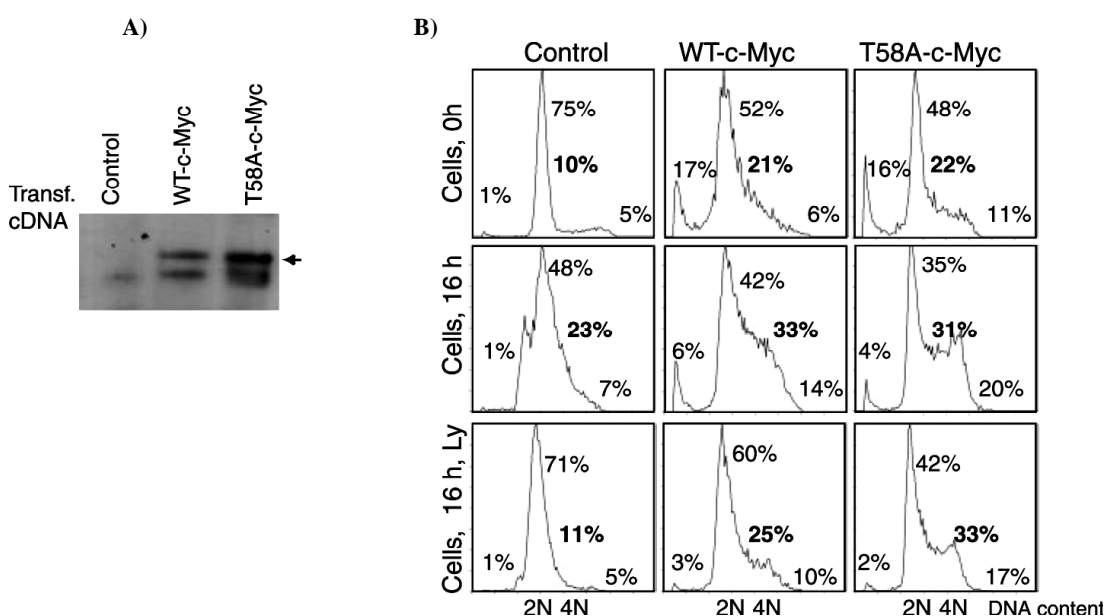


**Figure 14. Expression of c-Myc T58A and WT c-Myc rescues cell cycle entry defects induced by PI3K inhibition in late G1.** A) WT-c-Myc and c-MycT58A expression in NIH3T3 cells, tested in WB using anti-Myc antibody. B) DNA content in representative NIH3T3 cells transfected with a control vector or cDNA encoding WT-c-Myc or c-MycT58A. Cells were arrested by serum deprivation ( $t = 0$ ) and released by serum addition for 16 h. Some samples were incubated with Ly294002 added 7 h post-serum stimulation.



In the previous experiment (Fig. 14), we observed that overexpression of c-Myc (WT or c-MycT58A) induced apoptosis and cell cycle entry even in the absence of serum. To reduce c-Myc expression levels we used infection with virus encoding c-MycT58A, which yield lower expression levels than transfection. Under these conditions, c-MycT58A did not markedly induce cell cycle entry in the absence of serum (Fig. 15). Synchronous cultures of infected cells were treated with Ly294002 at 7 h after serum addition and harvested at different time points. PI3K inhibition blocked cell cycle entry in controls, but cell cycle entry was nearly normal in cells expressing c-MycT58A (Fig. 15). Again, expression of c-MycT58A restored S-phase entry in cells treated with LY. These results confirm that a stable form of c-Myc substitutes for PI3K action in late G1.

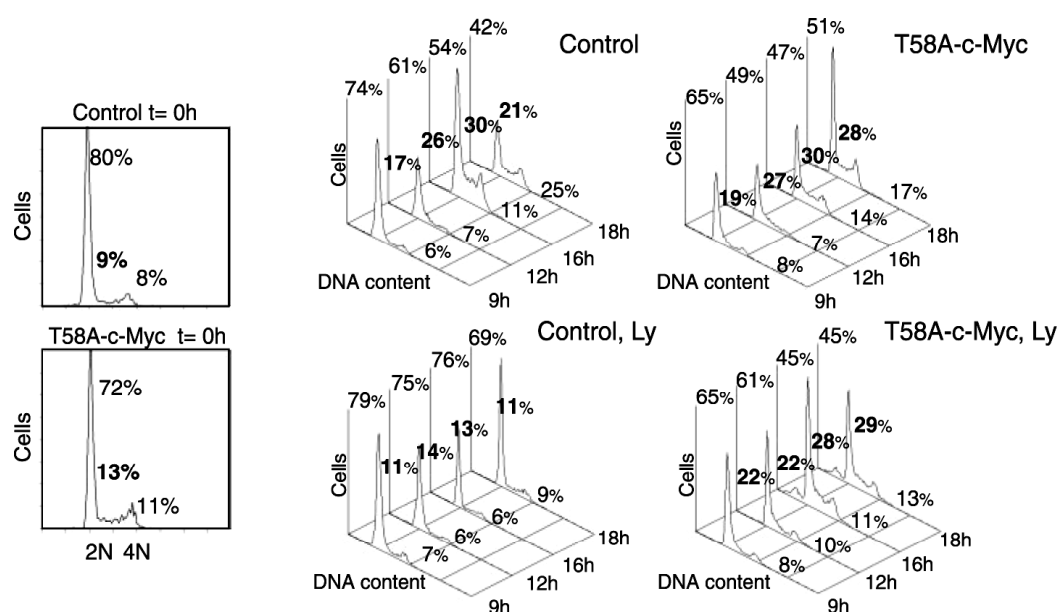


**Figure 15. Expression of c-MycT58A rescues cell cycle entry defects induced by PI3K inhibition in late G1.** DNA content in representative NIH3T3 cells infected with a control virus or a virus encoding c-MycT58A. Infected cells were arrested by serum deprivation, or arrested and then released by serum addition for 9, 12, 16 and 18 h. Some samples were incubated with Ly294002 added 7 h after serum stimulation. A representative experiment is shown of four with similar results. Percent of cells in G0/G1, S (in bold) and G2/M phases is indicated.

### 1.7) c-MycT58A expression rescues cyclin A expression, CDK2 activity, and MCM2 loading defects induced by PI3K inhibition in late G1

To confirm that the primary effect of PI3K activity in advanced G1 is to stabilize c-Myc, we tested whether c-MycT58A expression compensated for the cell cycle entry defects induced by late G1 PI3K inhibition. PI3K inhibition moderately affected cyclin D3 and E expression levels (see above). Similarly, c-MycT58A expression did not markedly alter cyclin D3 (not shown) or cyclin E levels (Fig. 16). In contrast, cyclin A levels were greatly reduced by PI3K inhibition in late G1 (Fig. 16). c-MycT58A expression increased cyclin A expression in Ly294002-treated cells and moderately increased basal cyclin A levels (Fig. 16). Results were similar to c-Myc-ER-expressing cells treated with 4-OHT (at 6.5 h), Ly294002 (at 7 h), or both simultaneously (Fig. 12 C).

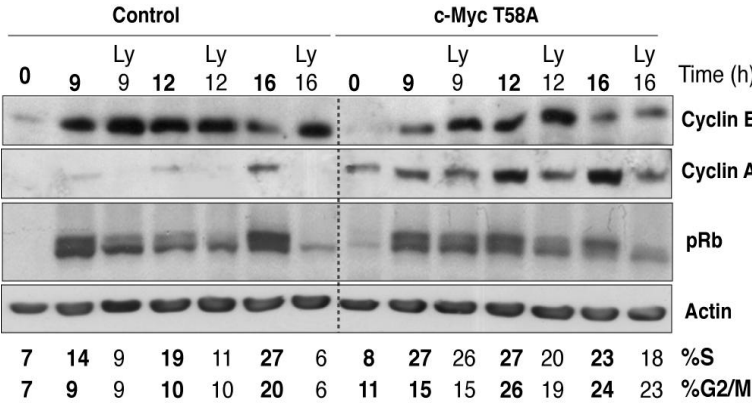


**Figure 16. c-MycT58A expression counteracts cyclin A expression induced by PI3K inhibition in late G1.** Control and c-MycT58A-expressing cells were arrested in G0, then released and treated with LY294002 at 7 h post-serum addition. Cells were harvested at different time points (indicated) and extracts examined by WB using anti-cyclin E, -cyclin A, -actin and -Rb antibodies.

Moreover, whereas levels of hyperphosphorylated Rb and cyclinE/CDK2 and cyclinA/CDK2 kinase activities were reduced by late G1 PI3K inhibition in control cells, they were virtually unaffected in c-MycT58A-expressing cells (Fig. 17).

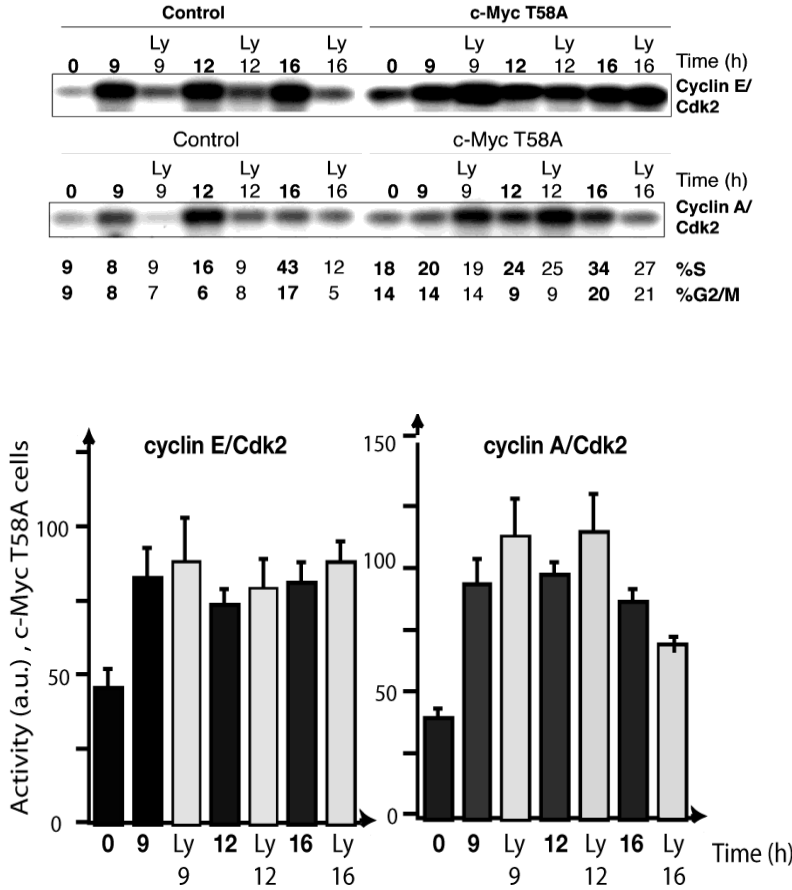


**Figure 17. c-MycT58A expression counteracts CDK2 activity defects induced by PI3K inhibition in late G1.** Cyclin E/CDK2 and cyclin A/CDK2 kinase activity in cyclin E and cyclin A immunoprecipitates, respectively, of cell extracts from control and c-MycT58A-expressing cells treated as in Fig. 16. CDK2 activity was measured as in Fig. 10. Cyclin E/CDK2 and cyclin A/CDK2 activity in c-MycT58A-expressing cells was examined by *in vitro* kinase assays performed as in Fig. 10. Data shown are means ± standard deviation of three experiments.

Finally, we examined p27<sup>kip</sup> binding to the cyclinE/CDK2 complex. Ly294002 treatment at 7 h in synchronous cell cultures increased p27<sup>kip</sup> association with cyclinE/CDK2 in controls, but association was lower and resistant to PI3K inhibition in c-MycT58A-expressing cells (Fig. 18). Thus, p27<sup>kip</sup>-CDK2 association was reduced upon c-MycT58A expression in LY-treated cells.

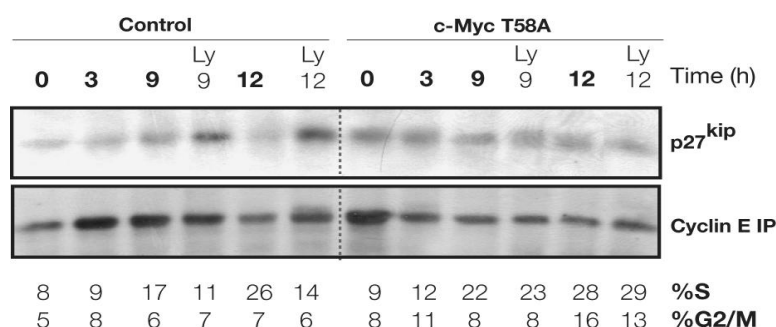


**Fig. 18. c-MycT58A expression inhibits p27 binding to the cyclinE/CDK 2 complex.** Synchronized cells in different cell cycle phases were lysed and cyclin E was immunoprecipitated from lysates (200  $\mu$ g). Samples were resolved and examined by WB using anti-p27<sup>kip</sup> or anti-cyclin E antibody.

We also examined the result of expressing c-MycT58A on MCM2 loading onto chromatin. In control cells, MCM2 loading was still low at 9 h (similar to that observed at 0 h), increased at 12 to 16 h, and was blocked by PI3K inhibition. In contrast, in c-MycT58A cells, MCM2 loading increased by 9 h in c-MycT58A-expressing cells and remained insensitive to late G1 PI3K inhibition (Fig. 19).

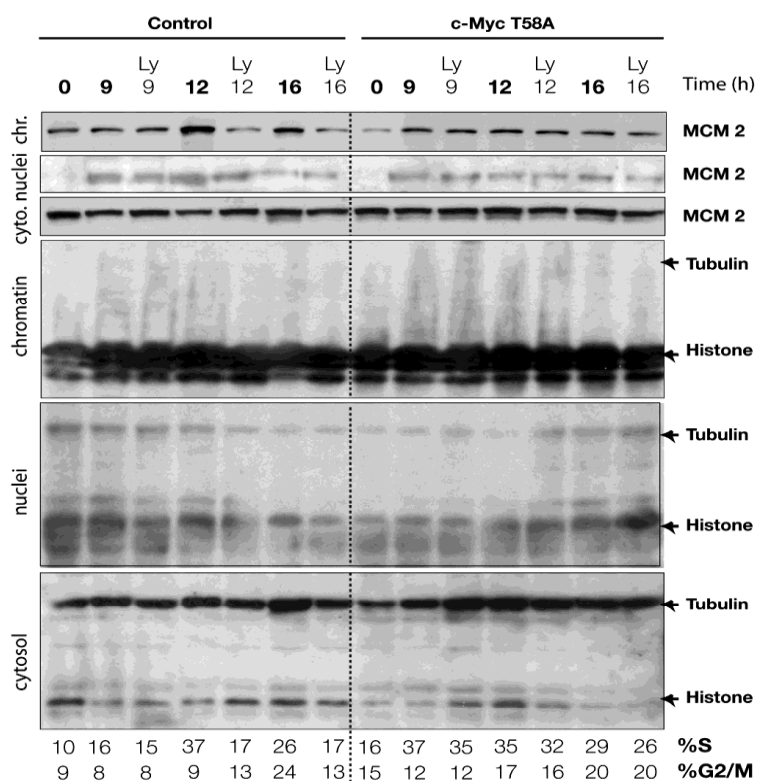


**Figure 19. c-MycT58A expression counteracts the reduced MCM2 chromatin loading induced by PI3K inhibition in late G1.** Western blots documenting MCM2 protein levels in different subcellular fractions (as in Fig. 3F) of cells treated as in Fig. 6A. WB using anti-tubulin and -histone antibodies were used as controls of fraction purity.

## 1.8) Conclusions

Phosphoinositide 3-kinase (PI3K) is one of the early signalling molecules induced by growth factor receptor (GFR) stimulation that is necessary for cell growth and cell cycle entry. PI3K activation occurs at two distinct time points during G1 phase. The first peak is observed immediately following GF addition, and the second in late-G1, before S phase entry. This second activity peak is essential for transition from G1 to S phase; nonetheless, the mechanism by which this peak is induced and regulates S phase entry was poorly understood. We have examined the mechanism of activation and the function of PI3K activity in late G1. *We conclude that activation of Ras and Tyr kinases are required for late-G1 PI3K activation.* Inhibition of late-G1 PI3K activity results in low c-Myc and cyclin A expression, impaired Cdk2 activity, and reduced MCM2 (minichromosome maintenance) loading onto chromatin. *The primary consequence of inhibiting late-G1 PI3K was c-Myc destabilization, as conditional activation of c-Myc in advanced G1 as well as expression of a stable c-Myc mutant rescued all of these defects, restoring S phase entry.* These results show that Tyr kinases and Ras cooperate to induce the second PI3K activity peak in G1, which mediates initiation of DNA synthesis by inducing c-Myc stabilization.

## 2. MECHANISMS CONTROLLING p110 $\beta$ NUCLEAR LOCALISATION

### 2.1) Class I<sub>A</sub> PI3K isoforms p110 $\alpha$ and p110 $\beta$ have distinct intracellular localisation

The main function of class I<sub>A</sub> PI3K in cells is thought to be its ability to produce PIP<sub>3</sub> at the plasma membrane. Nonetheless, class I<sub>A</sub> is also found in the nucleus of various cell types (Neri *et al.*, 2002). p110 $\beta$  selectively controls DNA replication, whereas p110 $\alpha$  had a minor function in this process (Marques *et al.*, 2009). Since DNA replication occurs in the nucleus, we considered that p110 $\beta$  might exhibit a subcellular localisation distinct from that of p110 $\alpha$ .

We studied the localisation of p110 catalytic and p85 regulatory subunits in NIH3T3 cells by immunostaining with specific anti-p110 $\beta$ , -p110 $\alpha$ , -p85 $\alpha$  and -p85 $\beta$  antibodies. We found that p110 $\beta$  catalytic and p85 $\beta$  regulatory subunits localised mainly in the nucleus, whereas p110 $\alpha$  and p85 $\alpha$  subunits concentrated mainly in cytoplasm (Fig. 20A). We examined the specificity of the antibodies used for p110 $\alpha$  and p110 $\beta$  immunostaining by transfecting shRNA for p110 $\alpha$  and p110 $\beta$ , respectively, which reduced the detection of the corresponding p110 isoforms (Fig. 20B).

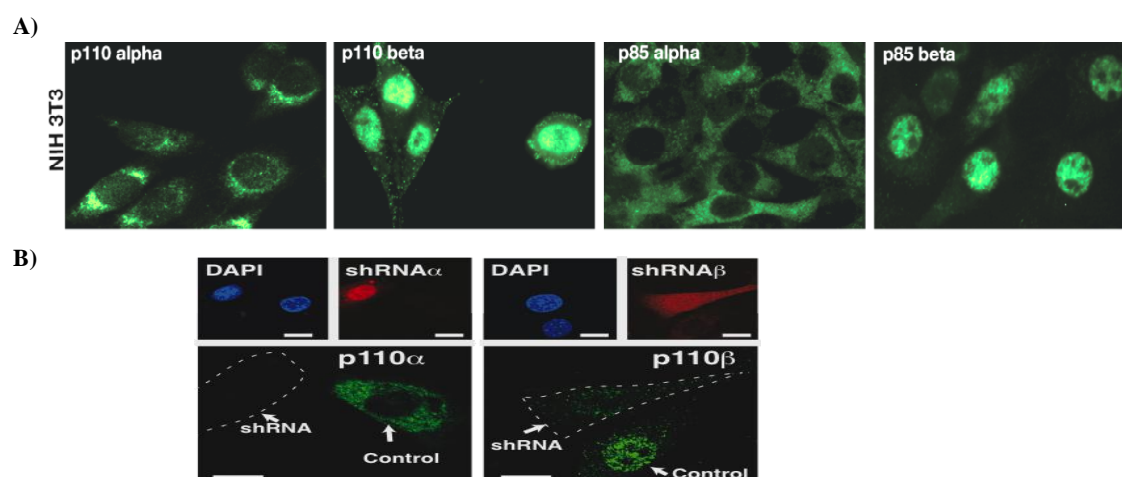


**Figure 20.** Cellular localisation of different class IA PI3K proteins in NIH3T3 cells. **A)** Immunofluorescence (indirect) in exponential growing cells, using specific anti-p110 $\alpha$ , -p110 $\beta$ , -p85 $\alpha$  and -p85 $\beta$  antibodies developed with Alexa488-secondary antibody. **B)** NIH3T3 cells were cotransfected with red fluorescence protein (RFP) and control, p110 $\alpha$  or - $\beta$  shRNA; p110 localisation was examined by immunofluorescence. DAPI nuclear staining is shown in insets.

We also determined p110 $\beta$  localisation in other cell types and found that p110 $\beta$  localizes in the nuclei in HeLa, MEF and SAOS-2 cells (Fig. 21). *p110 $\beta$  nuclear localisation is therefore not restricted to the murine NIH3T3 cell line, but is also present in many mammalian cells.*

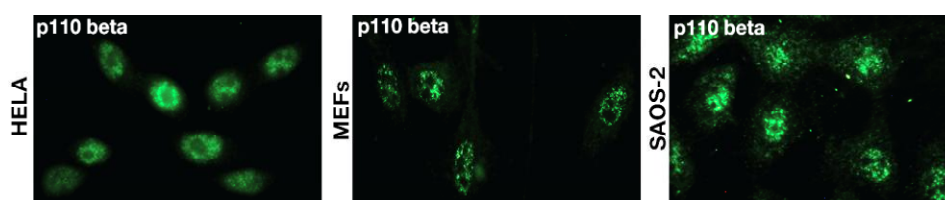


**Figure 21.** Cellular localisation of PI3K p110 $\beta$  protein in different cells. Indirect immunofluorescence of p110 $\beta$  staining in HeLa, MEF and SAOS-2 cells, treated as above (Fig. 20 A).

### 2.2) p110 $\beta$ localisation in the nucleus is transient and activation-dependent

These observations suggested that p110 $\beta$  localisation in the nucleus is a phenomenon common to various cell types. Our group described p110 $\beta$  activation at different times during G1, which is necessary for cell transit through G1/S (Marques *et al.*, 2008). Based on our findings, we

considered that p110 $\beta$  intracellular localisation might be important for its role in S phase; we thus examined p110 $\beta$  localisation and subcellular activity during cell progression through G1.

Quiescent NIH3T3 cells were stimulated, fixed at different times and stained with anti-p110 $\beta$  antibody. Although quiescent cells showed diffuse p110 $\beta$  staining throughout the cell, 30 min serum stimulation induced its complete nuclear translocation. At 45 and 90 min post-serum stimulation, some p110 $\beta$  returned to the cytoplasm. At later times (4.5 h), p110 $\beta$  again began to concentrate in the nucleus, with maximum nuclear localisation at 8.5 h post-stimulation (Fig. 22A). We prepared cytoplasmic and nuclear subcellular fractions of cells at different times in G1, then immunoprecipitated with anti-p85 Ab (as p110 $\beta$  is the only nuclear isoform observed), followed by an *in vitro* PI3K kinase assay using PI as substrate. In cytoplasmic fractions, PI3K was activated at 5 min post-stimulation; this activity later returned to basal levels. In contrast, the second PI3K activity peak (Jones *et al.*, 2001) was observed at 7-10 h post-serum stimulation (Fig. 22B). In the nucleus, however, PI3K activation was observed at 30 min post-stimulation, with a second peak at 8.5 h that remained even at 10 h post-stimulation. The kinetics of p110 $\beta$  nuclear localisation parallels nuclear PI3K activity, suggesting that p110 $\beta$  might enter the nucleus in its active state.

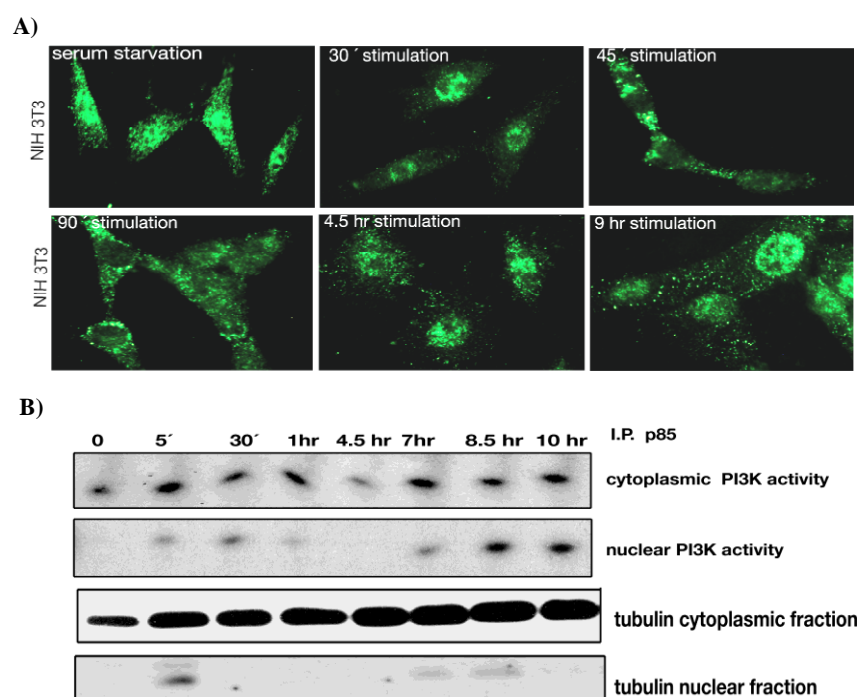


**Figure 22.** p110 $\beta$  shows parallel intracellular localisation and activation kinetics during the cell cycle. A) Intracellular p110 $\beta$  staining using anti-p110 $\beta$  antibody at different times after serum stimulation of quiescent cells. B) *In vitro* PI3K kinase assay using PI as substrate to detect PI3K activity in cytoplasm and nuclear fractions of cells harvested at the indicated times post-stimulation. After the kinase reaction, the substrate was resolved on thin layer chromatography (upper panels). Anti-tubulin antibody was used to control purity of the two subcellular fractions of these samples (tubulin is an exclusively cytoplasmic protein) (lower panels).

### 2.3) p110 $\beta$ overexpression results in cytoplasmic retention

To elucidate the role of PI3K p110 $\beta$  in the nucleus, we transfected p110 $\beta$  into several cell lines. p110 $\beta$  overexpression resulted in cytoplasmic accumulation of this protein in all cell types tested (Fig. 23A). To exclude the possibility that protein overexpression caused an accumulation of newly synthesized protein in the endoplasmic reticulum (ER), we inhibited translation using cyclohexamide in the last 2-3h of the 24h transfection period. Despite inhibition of protein synthesis, p110 $\beta$  remained cytoplasmic (Fig. 23B). We also tested the localisation of overexpressed p110 $\alpha$ , p85 $\alpha$  and p85 $\beta$ . As predicted, p110 $\alpha$  and p85 $\alpha$  were overexpressed in

cytoplasm, as is the case for endogenous proteins, whereas overexpressed p85 $\beta$  showed diffused cytoplasmic and nuclear staining (Fig. 23C).

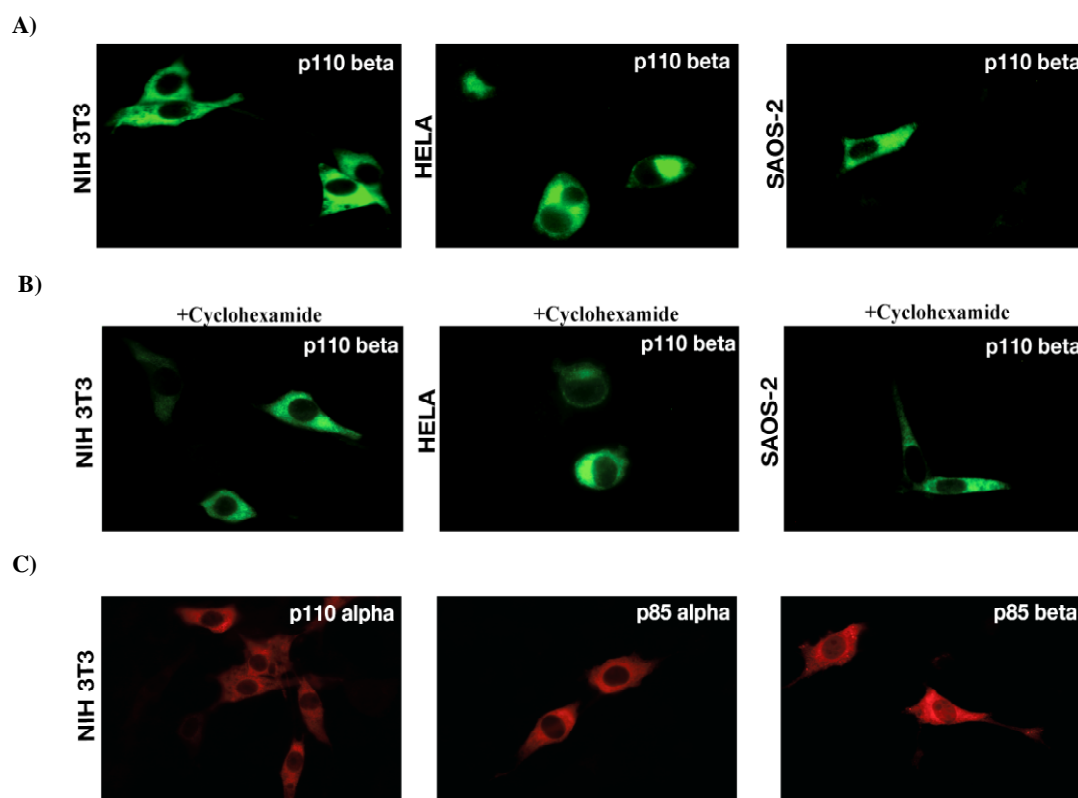


**Figure 23. p110 $\beta$  overexpression results in cytoplasmic localisation as for p110 $\alpha$ .** A) NIH3T3, HeLa and SAOS-2 cells were transfected with p110 $\beta$  plasmid and stained with anti-p110 $\beta$  antibody at 48 h post- transfection. B) p110 $\beta$ -transfected NIH3T3, HeLa and SAOS-2 cells were cyclohexamide-treated (30  $\mu$ g/ml, 3 h) before being fixed for staining. Cells were stained with anti-p110 $\beta$  antibody for indirect immunofluorescence. C) Myc-tagged p110 $\alpha$ , HA-p85 $\alpha$  and HA-p85 $\beta$  were transfected individually into NIH3T3 cells and processed for indirect immunostaining using appropriate tag-specific antibodies to examine intracellular localisation.

## 2.4) p85 $\beta$ promotes p110 $\beta$ nuclear localisation

The regulation of subcellular localisation has emerged as a major mechanism that governs several cell processes (Reynisdottir *et al.*, 1997; Zhou *et al.* 2001). Based on the report by Geering *et al.*, showing that class I $_A$  catalytic and regulatory subunits are obligatory heterodimers and are not physiologically available as single subunits (Geering *et al.*, 2007), we determined whether regulatory subunits might influence subcellular localisation of the class I $_A$  catalytic isoforms. We cotransfected combinations of catalytic p110 $\alpha$  and p110 $\beta$  subunits with the regulatory p85 $\alpha$  and p85 $\beta$  subunits, and found that only the p110 $\beta$ /p85 $\beta$  combination showed nuclear localisation (Fig. 24A). The p110 $\beta$ /p85 $\alpha$ , p110 $\alpha$ /p85 $\alpha$  and p110 $\alpha$ /p85 $\beta$  concentrated in cytoplasm (Fig. 24A); a fraction of p85 $\beta$  was always seen in the nucleus (possibly in combination with endogenous p110 $\beta$ ). Therefore, p110 $\alpha$  bound to either p85 $\alpha$  or p85 $\beta$  is cytosolic, whereas p110 $\beta$  translocates to the nucleus in association with p85 $\beta$ .

The finding that p110 $\beta$ /p85 $\beta$  coexpression caused nuclear localisation, and that this did not occur with p110 $\beta$ /p85 $\alpha$  complexes prompted us to determine the molecular basis for this difference. We examined the sequence homology of p85 $\alpha$  and p85 $\beta$ , although we did not find a clear nuclear localisation sequence (NLS) in p85 $\beta$ , we found a basic region between the BCR and N-SH2 region in p85 $\beta$  that was not present in p85 $\alpha$ . To test the role of this sequence in p85 nuclear localisation, we constructed a chimera in which we replaced this region in p85 $\beta$  (77-351 aa) with the corresponding p85 $\alpha$  sequence (Fig. 24B). We cotransfected this chimera with p110 $\beta$  and observed no difference between p110 $\beta$  / p85 $\beta$  and p110 $\beta$  / p85 $\beta$ - $\alpha$  chimera localisation. The p85 $\beta$ -

$\alpha$  chimera still co-localized with p110 $\beta$  in the nucleus (Fig. 24C). *These results suggest that polybasic sequence between BCR and N-SH2 in p85 $\beta$  does not act as a nuclear localisation region.*

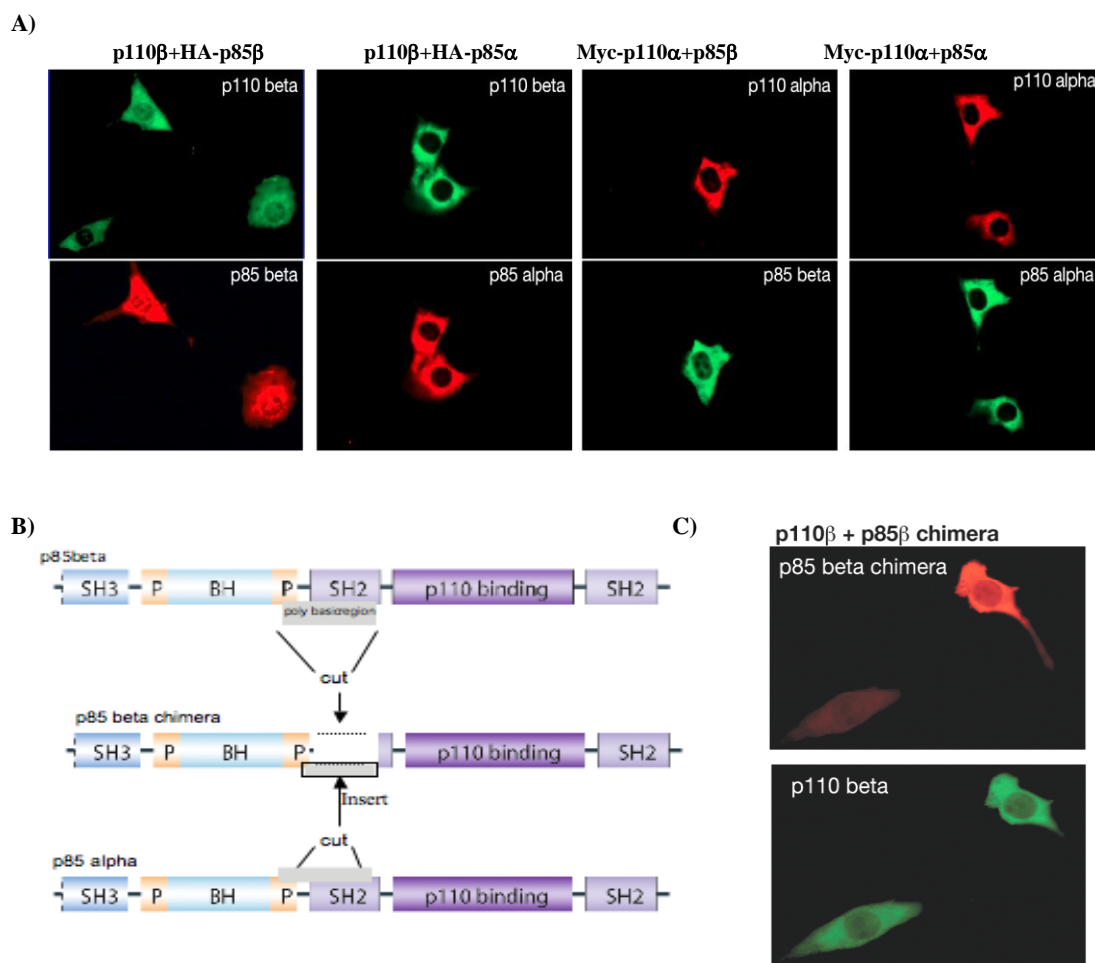


**Figure 24. Intracellular localisation of p110 $\alpha$  and p110 $\beta$  in combination with different regulatory subunits.** A) NIH3T3 cells were transfected with p110 $\beta$  in combination with HA-p85 $\beta$  or HA-p85 $\alpha$ , or with Myc-p110 $\alpha$  combined with HA-p85 $\alpha$  or HA-p85 $\beta$ . In cells cotransfected with p110 $\beta$ /p85 $\beta$  or p110 $\beta$ /p85 $\alpha$ , we identified transfected proteins using anti-p110 $\beta$  (green), -HA for p85 $\alpha$  (red), and -p85 $\beta$  (red). In cells cotransfected with p110 $\alpha$ /p85 $\alpha$  or p110 $\alpha$ /p85 $\beta$ , we identified transfected proteins using anti-Myc tag for p110 $\alpha$  (red), -HA for p85 $\alpha$  (green), and -p85 $\beta$  (green). B) Scheme of p85 $\beta$ -chimera formation. The p85 $\beta$  region between amino acids 78 to 351 was removed and replaced with amino acids 77-363 from p85 $\alpha$ . C) NIH3T3 cells were transfected with the HA-p85 $\beta$  chimera with the p110 $\beta$  plasmid and stained with anti-p110 $\beta$  (green) and -HA antibodies (red).

## 2.5) C2-domain in p110 $\beta$ contains a nuclear localisation sequence

Since we did not find any NLS in p85 $\beta$ , we sought to identify if NLS were present in p110 $\beta$  that would explain the nuclear localisation of p110 $\beta$ /p85 $\beta$  complexes. We identified three putative NLS motifs with polybasic residues in p110 $\beta$  (**KVKTKRSTK**, **RRKMRK** and **RRH**). We proceed to substitute their basic residues with non-basic residues **KVNTTRSTK** (mutant 1), **RRNMRN** (mutant 2) and **RGH** (mutant 3) (Fig. 25). We did not find any obvious effect of mutant 2 and mutant 3 mutations in nuclear localisation of p110 $\beta$  co-expressed with p85 $\beta$  suggesting that these sequences do not determine the nuclear localisation of p85 $\beta$ /p110 $\beta$  complexes. On the other hand, expression of mutant 1 with p85 $\beta$  could not enter nucleus, suggesting that **KVKTKRSTK** acts as the nuclear localisation of p85 $\beta$ /p110 $\beta$  complex.



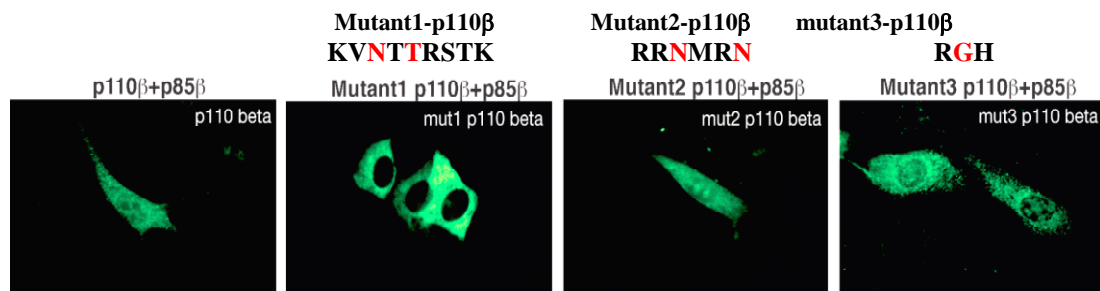


**Figure 25. NLS motif in p110β.** Amino acid substitutions were made to generate mutant with non-basic residues (in red). p110β and three distinct mutant of p110β were cotransfected with p85β and processed and stained for indirect fluorescence with anti-p110β.

## 2.6) Preferential association of p110β with p85β compared to p85α

Based on the role of the p85α and p85β regulatory subunits in the distinct cellular localisation of p110β and p110α, we tested whether there is preferential complex formation when the regulatory subunits are coexpressed in conjunction with either catalytic subunit (p85α+p85β with p110β or p110α). We fused the SV40 NLS at the p85β N-terminus. Coexpression of p85β-NLS with p110β or p110α resulted in constitutive nuclear localisation of p110α and p110β (Fig. 26, upper panel). In contrast, when p85β-NLS+p85α were coexpressed with p110β or p110α, most p110β was nuclear, whereas p110α concentrated mainly in cytoplasm (Fig. 26, lower panel). This suggests that p110β associates preferentially with p85β and not p85α, and that p110α prefers p85α to p85β. We will attempt to confirm this observation biochemically in the future.

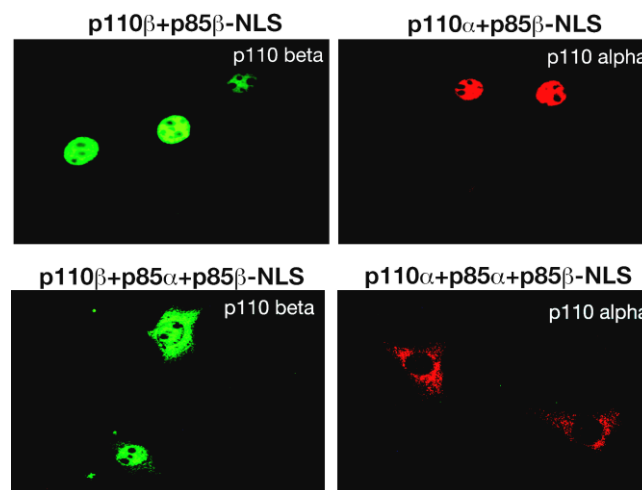


**Figure 26. Association of regulatory subunits determines the cellular localisation of catalytic subunits.** NIH3T3 cells were cotransfected with HA-p85β-NLS and p110β or Myc-p110α (upper panel), or in triple cotransfections with HA-p85β-NLS and HA-p85α with p110β or p110α (lower panel). Samples were processed and stained for indirect fluorescence using anti-p110β (green) or -Myc tag for p110α (red).

## 2.7) p85β shuttling between nucleus and cytoplasm regulates p110β nuclear export

After determining that p85β facilitates p110β translocation to the nucleus, we sought the mechanism for transient nuclear-cytoplasm localisation during cell cycle progression. p110β was found in cytoplasm by 90 min post-serum stimulation in quiescent cells (Fig. 22A). Various means of nuclear export have been documented (Kaffman and O'Shea, 1999). One common mechanism is a conserved leucine-rich nuclear export signal (NES) that binds the nuclear export protein CRM1 (Fornerod *et al.* 1997; Kudo *et al.* 1998). We used leptomycin B to inhibit CRM1 binding to the cargo protein, which retains NES-containing protein in the nucleus. After leptomycin B treatment of p110α-, p110β-, p85α- and p85β-transfected cells, only p85β-expressing cells showed a strong

increase in the amount of recombinant protein in the nucleus; p110 $\beta$  also had moderately enhanced nuclear localisation (Fig. 27A), suggesting strong CRM1 dependence for nuclear export of p85. We examined the effect of leptomycin B on cellular localisation of the p85 $\beta$  chimera (overexpressed) and of p65 $\beta$  (a mutant similar to p65 $\alpha$ ; **Jiménez *et al.*, 1998**). p65 $\beta$  lacks the 562-to-723 C-terminal fragment. Both the p85 $\beta$  chimera and p65 $\beta$  were found in cytosol and nucleus, and both showed increased nuclear localization after leptomycin B treatment (Fig. 27B). As we had observed that p85 $\beta$  facilitates p110 $\beta$  nuclear entry, we tested the leptomycin B effect on p110 $\beta$  localisation when coexpressed with p85 $\beta$ . Leptomycin B-mediated inhibition of p85 $\beta$  nuclear export led to p110 $\beta$  accumulation in the nucleus (Fig. 27C). Results were similar after leptomycin B treatment when p110 $\beta$  was coexpressed with the p85 $\beta$  chimera or p65 $\beta$  (Fig. 27D). We concluded that p85 $\beta$  has an important role in both nuclear export and import of p110 $\beta$ .

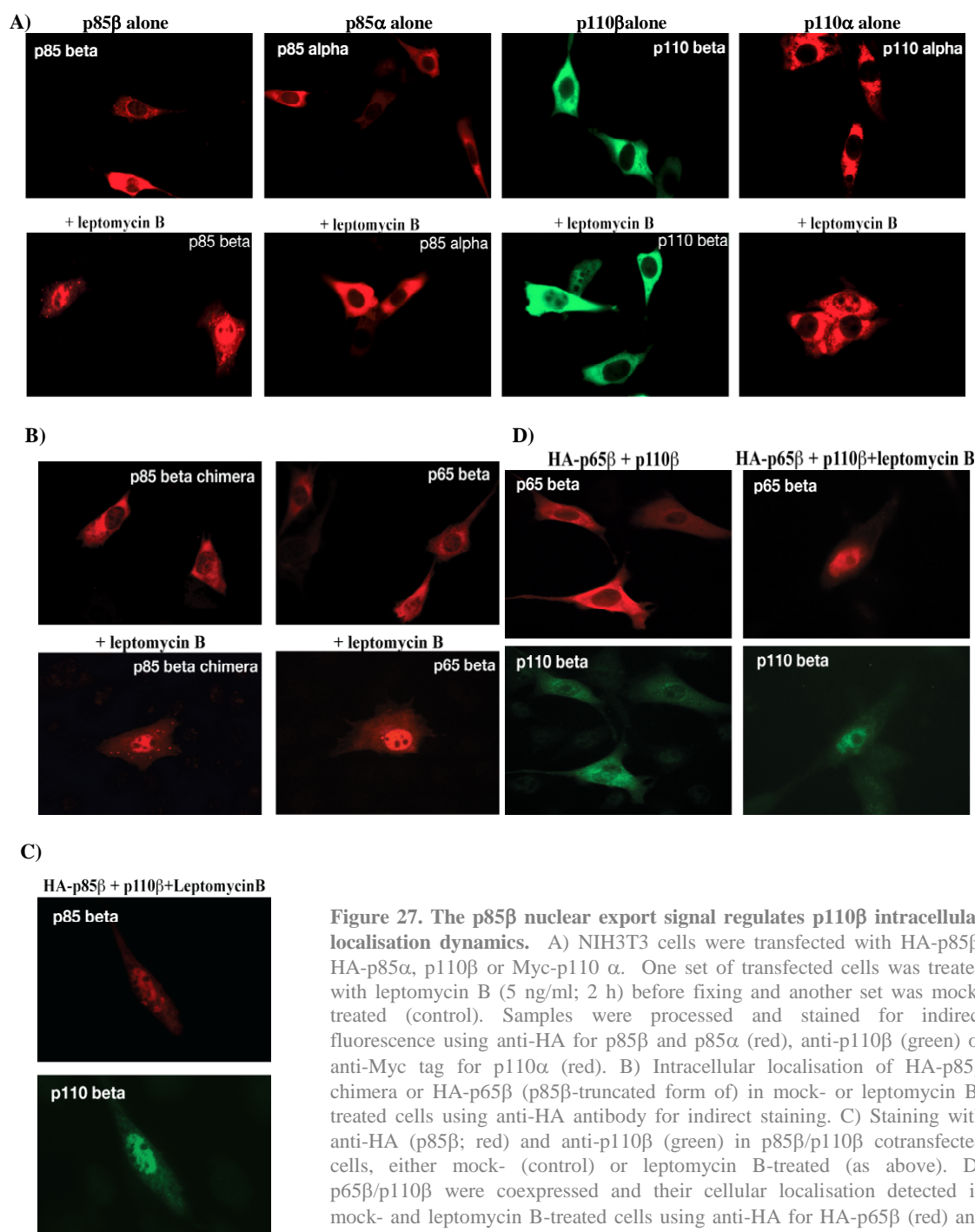


**Figure 27. The p85 $\beta$  nuclear export signal regulates p110 $\beta$  intracellular localisation dynamics.** A) NIH3T3 cells were transfected with HA-p85 $\beta$ , HA-p85 $\alpha$ , p110 $\beta$  or Myc-p110  $\alpha$ . One set of transfected cells was treated with leptomycin B (5 ng/ml; 2 h) before fixing and another set was mock-treated (control). Samples were processed and stained for indirect fluorescence using anti-HA for p85 $\beta$  and p85 $\alpha$  (red), anti-p110 $\beta$  (green) or anti-Myc tag for p110 $\alpha$  (red). B) Intracellular localisation of HA-p85 $\beta$  chimera or HA-p65 $\beta$  (p85 $\beta$ -truncated form of) in mock- or leptomycin B-treated cells using anti-HA antibody for indirect staining. C) Staining with anti-HA (p85 $\beta$ ; red) and anti-p110 $\beta$  (green) in p85 $\beta$ /p110 $\beta$  cotransfected cells, either mock- (control) or leptomycin B-treated (as above). D) p65 $\beta$ /p110 $\beta$  were coexpressed and their cellular localisation detected in mock- and leptomycin B-treated cells using anti-HA for HA-p65 $\beta$  (red) and anti-p110 $\beta$  for p110 $\beta$  (green).

## 2.8) The p85 $\beta$ N-terminal region contains a nuclear export signal

p85 $\beta$  regulates p110 $\beta$  nuclear export. We next investigated which region in p85 $\beta$  is responsible for p85 $\beta$ /p110 $\beta$  nuclear export. The p65 $\beta$  mutant lacks the 562-to-723 CT terminal fragment of p85 $\beta$  (Jiménez *et al.*, 1998) and localized similarly than p85 $\beta$  (Fig. 28). Replacement of the region between BCR and N-SH2 (77-to-351 aa) in p85 $\beta$  for the ones corresponding in p85 $\alpha$  also did not affect nuclear localisation (Fig. 24). Moreover, both the p85 $\beta$  chimera and p65 $\beta$  responded to leptomycin treatment implying that they include the potential NES of p85 $\beta$ . Then neither the 77-to-351 region nor the 562-to-723 region contained the NES.

We generated two additional truncated p85 $\beta$  constructs, one in which the first N-terminal 41 amino acids were deleted and a second in which the N-terminal 100 amino acids were deleted. Both the p85 $\beta$  lacking 41 N-terminal amino acids ( $\Delta$ 1p85 $\beta$ ) and p85 $\beta$  lacking 100 N-terminal amino acids ( $\Delta$ 2p85 $\beta$ ) concentrated predominantly in the nucleus (Fig. 28A). This indicates that first 41 N-terminal amino acids of p85 $\beta$  are necessary for its nuclear export. We examined the effect of these truncated p85 $\beta$  forms on p110 $\beta$  localisation after coexpression. p85 $\beta$  lacking the 41 N-terminal amino acids remained in the nucleus, whereas p110 $\beta$  localized mainly in cytoplasm. The localisation of p85 $\beta$  lacking the 100 N-terminal amino acids was similar to that of p110 $\beta$  (Fig. 28B). These data shows that the NES is located within the first 41 NT- residues of p110 $\beta$  and implies that truncation of these residues affects formation of p85 $\beta$ /p110 $\beta$  complexes. We will examine this biochemically in the future.

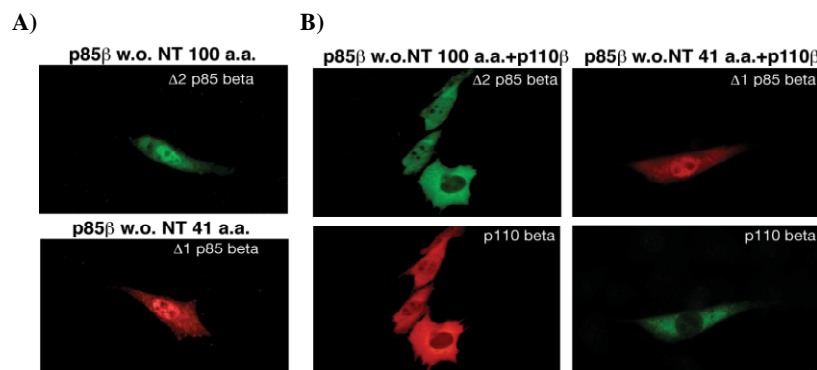


**Figure 28.** The p85 $\beta$  N-terminal region has a CRM1-dependent nuclear export signal, and p110 $\beta$  intracellular localisation varies after its coexpression of distinct truncated p85 $\beta$  forms. A) NIH3T3 cells were transfected with truncated p85 $\beta$  constructs alone ( $\Delta$ 1, lacking 41, or  $\Delta$ 2, lacking 100 N-terminal amino acids). B) cells cotransfected with truncated p85 $\beta$ /Myc-p110 $\beta$ . Cells were fixed after 48 h and processed for indirect immunofluorescence with anti-p85 $\beta$  (green) and -Myc tag (red) antibodies in  $\Delta$ 2 p85 $\beta$ /myc-p110 $\beta$  transfected cells and with anti-HA (red) and p110 $\beta$  (green) in  $\Delta$ 1HA-p85 $\beta$ /p110 $\beta$  transfected samples.

## 2.9) p85 $\beta$ /p110 $\beta$ associates with PCNA and translocates more efficiently to the nucleus

Although we identified the NLS in p110 $\beta$  and export domain in p85 $\beta$  that facilitates shuttling of p85 $\beta$ /p110 $\beta$  complex in and out of nucleus, we were unable to get the overexpressed-p110 $\beta$  concentrated in the nucleus as we find the endogenous p110 $\beta$ . Our group described a direct p110 $\beta$  role in DNA replication (Marques *et al.*, 2009) by regulating PCNA (proliferating cell nuclear antigen) loading onto chromatin. Considering that PCNA is a nuclear resident protein, we postulated that PCNA might associate with p110 $\beta$ , and influence its nuclear localisation. We examined p110 $\beta$  association with PCNA.

To this end, we examined cells in S phase, as most p110 $\beta$  is in the nucleus in this phase (Fig. 22). Cells were serum starved for 19 h to induce quiescence, then stimulated with 10% FBS for 14 h to drive the majority of cells into S phase; cells were then harvested and lysed. We

immunoprecipitated p110 $\beta$  and examined the presence of associated PCNA in WB (Fig. 29A); PCNA immunoprecipitated with anti-PCNA antibody was used positive control.

To determine whether the selective association of PCNA with p110 $\beta$  was due to a p110 $\beta$ -specific structural feature or to its subcellular distribution, we modify the subcellular localization of p110 by coexpressing it with a p85 molecule-fused to a strong NLS. Under these conditions, NLS-p85 cotransfection with Myc-WT-p110 $\alpha$  or - $\beta$ , which increased the nuclear localisation of both p110 $\beta$  and  $\alpha$  (Fig. 26). Both nuclear p110 $\beta$  and  $\alpha$  associated with PCNA, although p110 $\beta$  association to PCNA was greater than that of nuclear p110 $\alpha$  (Fig 29B).

We also immunoprecipitated p110 $\alpha$  and p110 $\beta$  from plasmid-transfected cells using anti-Myc tag antibody and examined their PCNA association by blotting with anti-PCNA antibody (Fig. 29C). PCNA showed higher affinity for p110 $\beta$  than for p110 $\alpha$ . These observations led us to conclude that PCNA preferentially binds to p110 $\beta$  and this association depends on the physiological p110 $\beta$  localisation in the nucleus. *Therefore, in addition to its subcellular distribution, p110 $\beta$  has a structural advantage for association to PCNA.*

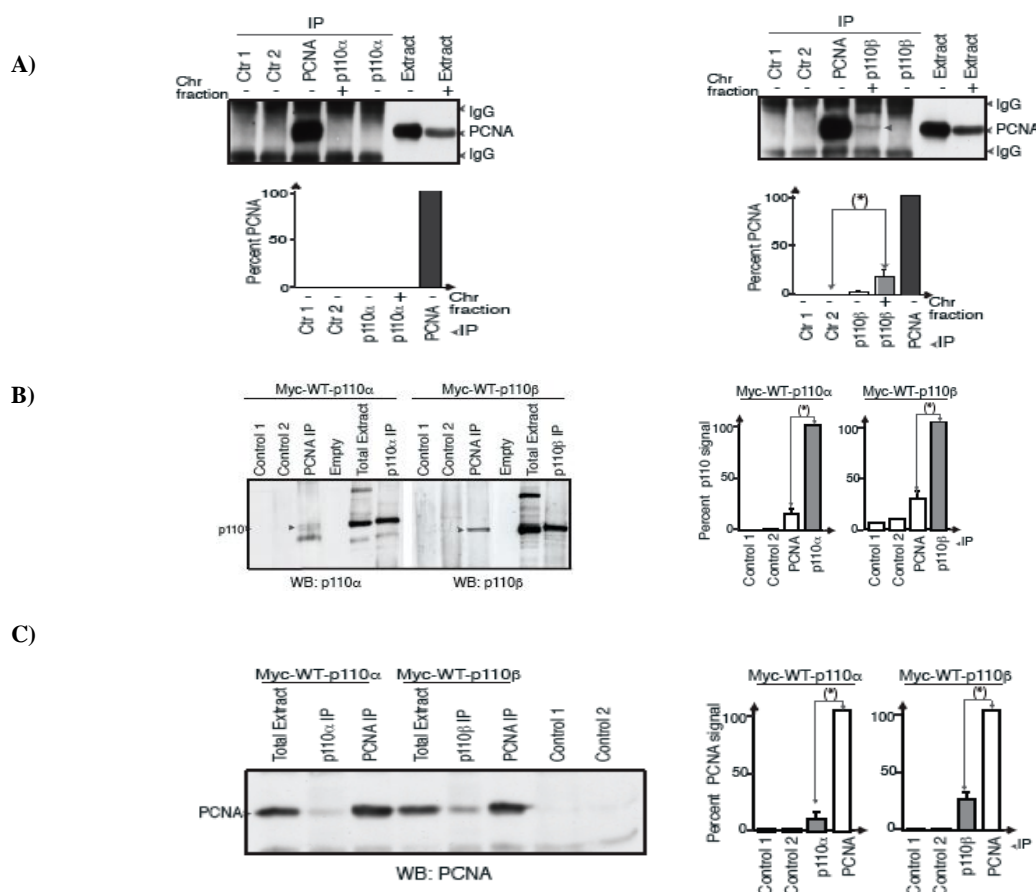


**Figure 29. PCNA associates with p110 $\beta$  and coexpression increases its nuclear localisation.** A) Synchronized NIH3T3 cell cultures were collected at 14 h post-serum addition and chromatin fractions were obtained. PCNA or p110 immunoprecipitates were analysed in western blot using anti-PCNA antibody. As controls, protein A was incubated with antibody alone or with lysate alone. Graphs show the percent PCNA signal in p110 $\alpha$  and p110 $\beta$  immunoprecipitates, where 100% = signal in PCNA immunoprecipitates from a similar amount of lysate. B, C) NIH3T3 cells were transfected with Myc-p110 $\alpha$  or - $\beta$  in combination with p85 $\beta$ -NLS. Cells were synchronized at 24 h post-transfection and collected at 14 h post-serum release. The chromatin fraction was immunoprecipitated with anti-Myc-tag (100  $\mu$ g) or -PCNA (800  $\mu$ g) antibodies. p110 $\alpha$  or p110 $\beta$  association to PCNA was tested in western blot using anti-Myc-tag antibody. Extracts were also immunoprecipitated with anti-Myc-tag (400  $\mu$ g) or -PCNA (100  $\mu$ g) antibodies, then examined in western blot using anti-PCNA antibody. The graphs show the mean percentage of p110 bound to PCNA, normalized to p110 levels in p110 immunoprecipitates, or the percentage of PCNA bound to p110 compared to PCNA levels in PCNA immunoprecipitates.

We then determined whether PCNA affects the cellular localisation of class I<sub>A</sub> PI3K regulatory and catalytic subunits when coexpressed. p85 $\beta$  localisation to the nucleus increased when it was coexpressed with PCNA, whereas p85 $\alpha$  remained in cytoplasm when expressed alone or with PCNA. Nonetheless, coexpression of p110 $\alpha$  with PCNA did not alter its cytoplasmic localisation, whereas p110 $\beta$  coexpression with PCNA increased p110 $\beta$  nuclear translocation (Fig. 30). These findings suggest that contributes to determine the nuclear localisation of p110 $\beta$ /p85 $\beta$ .

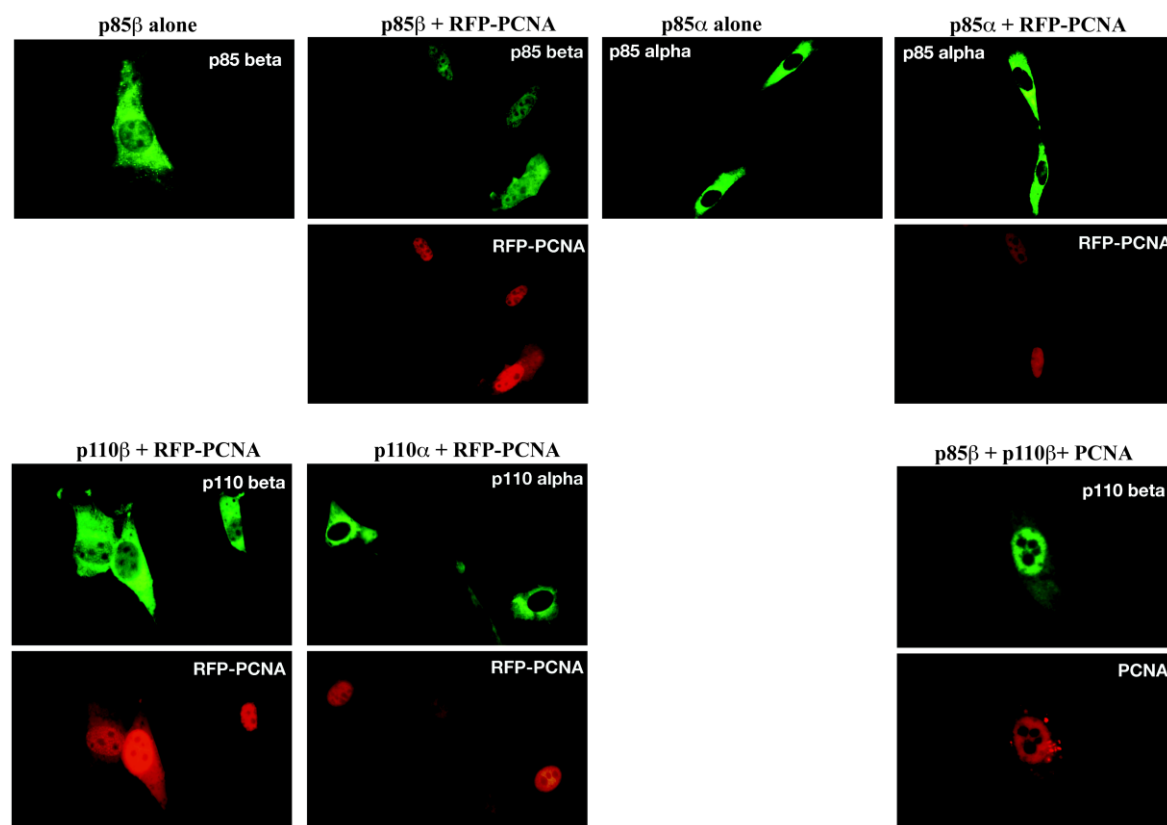


**Figure 30. Coexpression of PCNA with p110 $\beta$  increases p110 $\beta$  nuclear localisation.** RFP-PCNA was cotransfected with p85 $\beta$ , p85 $\alpha$ , p110 $\beta$ , or p110 $\alpha$  (upper panel and lower left panel), PCNA was cotransfected with p85 $\beta$  and p110 $\beta$  (lower right panel) processed for indirect fluorescence at 48 h post-transfection using anti-PCNA (red) and anti-p110 $\beta$  (green). Only p85 $\beta$  and p110 $\beta$  showed increased nuclear localisation when coexpressed with PCNA.

## 2.10) Conclusions

Nuclear localisation of class I<sub>A</sub> PI3K was described previously, although the specific isoforms that located to the nucleus remained unclear. Here we determined that of the PI3K ubiquitous isoforms p110 $\alpha$  and p110 $\beta$ , *the majority of p110 $\beta$  localizes in the nucleus, whereas p110 $\alpha$  is found mainly in cytoplasm.* We also determined that during cell cycle progression, p110 $\beta$  shuttles between the nucleus and cytosol and that major nuclear concentration occurs in S phase. The increase in nuclear localisation coincided with p110 $\beta$  activation in the nucleus. These observations led us to conclude that p110 $\beta$  kinase activity is important for its nuclear translocation, an aspect that requires future analysis. We dissected part of the mechanism for p110 $\beta$  nuclear translocation, and report that *p110 $\beta$  does not translocate to the nucleus by itself, but must associate to p85 $\beta$ .* In addition to its role in nuclear translocation of p110 $\beta$ , *p85 $\beta$  also controls p110 $\beta$  nuclear exclusion.* We determined that the first 41 N-terminal amino acids of p85 $\beta$  regulate nuclear export of this protein. In addition, we identified a nuclear localisation sequence in the p110 $\beta$  C2 domain, which when mutated inhibits nuclear translocation of the p85 $\beta$ /p110 $\beta$  complex. Finally, we observed that p85 $\beta$  was not sufficient for complete nuclear localisation of p110 $\beta$ , and that PCNA binds to p110 $\beta$  and increases p110 $\beta$  nuclear localisation.



### 3. P110 $\beta$ REGULATES DNA REPAIR PATHWAYS

#### 3.1) Cells with reduced p110 $\beta$ levels undergo apoptosis following ultraviolet radiation

We previously shown that p110 $\beta$  regulates DNA replication (Marques *et al.*, 2009), we next examined p110 $\beta$  control of DNA repair. To determine the role of p110 $\beta$  in DNA damage response, we first examined whether reduced expression of p110 $\beta$  affect the recovery of cells following radiation stress. We used p110 $\beta$ -specific shRNA. At 30 h post-transfection with p110 $\beta$  shRNA, we selected the cells transfected with p110 $\beta$  shRNA using puromycin (48 h). Cells were then harvested and lysed, then analysed in western blot for p110 $\beta$  and actin. All three shRNA tested reduced the levels of p110 $\beta$  to approximately 60% of those for endogenous p110 $\beta$  (Fig. 31A). p110 $\alpha$  shRNA also reduced p110 $\alpha$  expression (Fig. 31A) p110 $\alpha$  shRNA, p110 $\beta$  shRNA and vector-transfected cells were exposed to UV light and 12 h after UV exposure, we observed a greater apoptosis in cultures of p110 $\beta$ -depleted cells than in vector-transfected control cells or p110 $\alpha$ -depleted cells. At 30 h post-UV exposure, more p110 $\beta$ -depleted cells were found in sub-G1 than p110 $\alpha$ -deleted or control cells (Fig. 31B), suggesting that reduction of p110 $\beta$  levels interferes with the cellular mechanisms that correct the DNA damage inducing cell death.

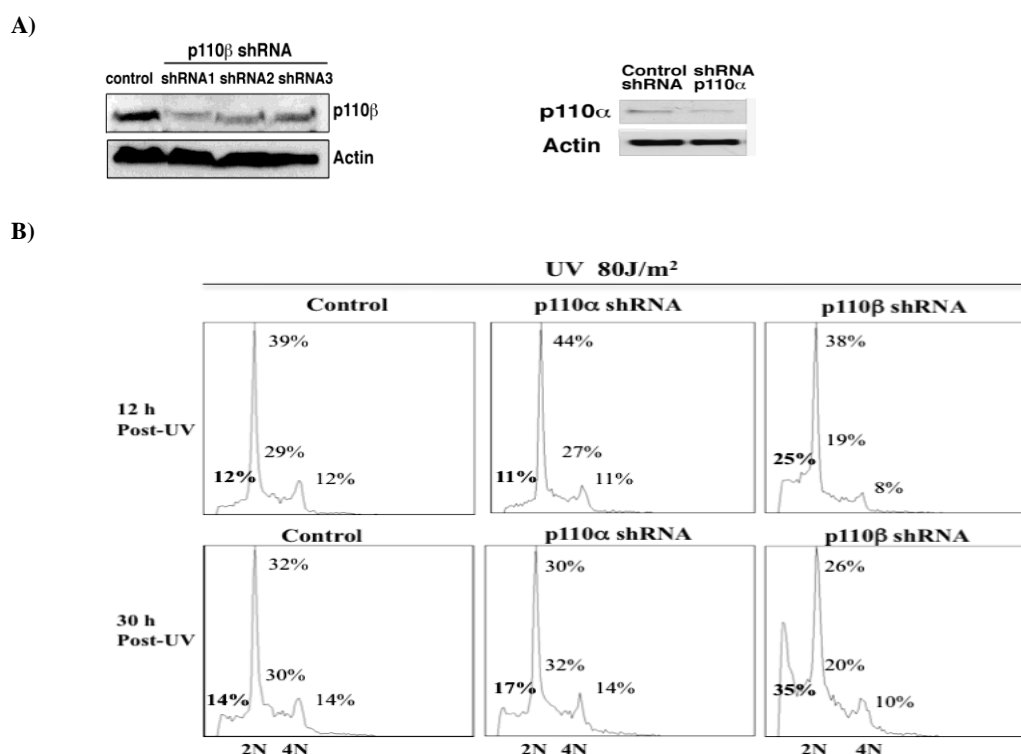


**Figure 31. Downregulation of p110 $\beta$ , but not of p110 $\alpha$  results in cell death following UV exposure.** A) (left panel) NIH3T3 cells transfected with vector or three different p110 $\beta$  shRNA were selected with puromycin (2  $\mu$ M; 48 h) at 48 h post-transfection; lysates were then analysed for p110 $\beta$  in western blot, (right panel) vector or p110 $\alpha$  shRNA transfected in NIH3T3 cells, 48 h post transfection cell were lysed and p110 $\alpha$  protein levels were determined in western blot using anti p110 $\alpha$  antibody, actin was used as loading control. B) Propidium iodide FACS analysis of vector, p110 $\alpha$ - and p110 $\beta$ -deleted cells at different times post-UV (80 J/m<sup>2</sup>) exposure. Percentage of cells in Sub G1 (dead, in Bold), G0/G1, S and G2/M phases is indicated.

#### 3.2) p110 $\beta$ -deficient cells show genomic instability

The recently described conditional p110 $\beta$ <sup>-/-</sup> mouse phenotype and that of inactive p110 $\beta$  knock-in mice indicate that p110 $\beta$  kinase activity regulates mouse and tumour growth and that p110 $\beta$  has a kinase-independent function essential for embryonic development (Jia *et al.*, 2008;

**Ciraolo *et al.*, 2008**). Kinase-independent functions often reflect the ability of a protein to associate a necessary partner, as is the case for PI3K $\gamma$  in the control of cardiac stress response (**Patrucco *et al.*, 2004**). To this end, we compared metaphases of p110 $\beta$ <sup>-/-</sup> immortalized mouse embryonic fibroblasts (MEF) with p110 $\beta$ <sup>-/-</sup> MEF reconstituted with WT-p110 $\beta$  (**Jia *et al.*, 2008**). Most p110 $\beta$ <sup>-/-</sup> immortalized cells had aberrant chromosome numbers (Fig. 33), including highly aneuploid cells containing 100-150 chromosomes. Chromosome breaks and non-disjunction figures were also observed in almost all p110 $\beta$ -deficient metaphase cells analysed.

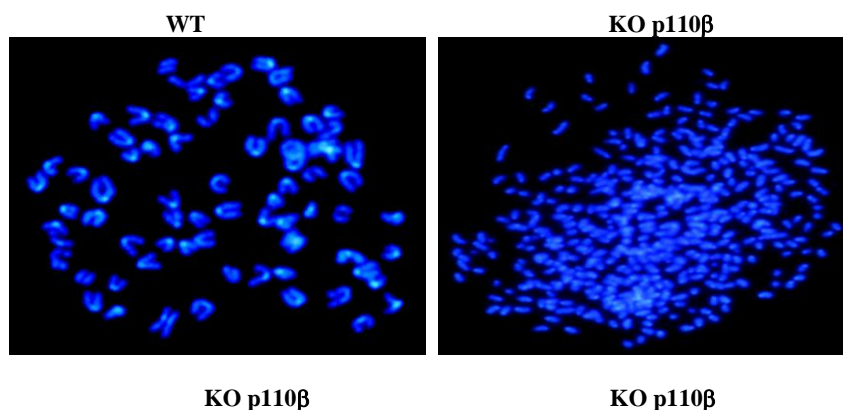


**Figure 32. Genomic instability in p110 $\beta$ <sup>-/-</sup> cells.** DAPI staining of wild type and p110 $\beta$ <sup>-/-</sup> immortalized MEF showing chromosome breaks and non-disjunction structures (arrowheads).

### 3.3) p110 $\beta$ is activated by exposure to UV or ionising radiation

To determine whether p110 $\beta$  activation is induced following DNA damage, we exposed NIH3T3 cells to UV or IR. NIH3T3 cells were harvested at different time points after UV or IR exposure and we examined p110 $\beta$  PI3K activity following immunoprecipitation with anti-p110 $\beta$  antibody in an *in-vitro* kinase assay using PI as substrate. Maximum p110 $\beta$  activation was observed at 15 min post-UV exposure, whereas p110 $\beta$  activation peaked at 30 min after IR exposure; serum-stimulated (1 h) NIH3T3 cells (**Marques *et al.*, 2008**) were used as positive control for p110 $\beta$  activity (Fig. 33).

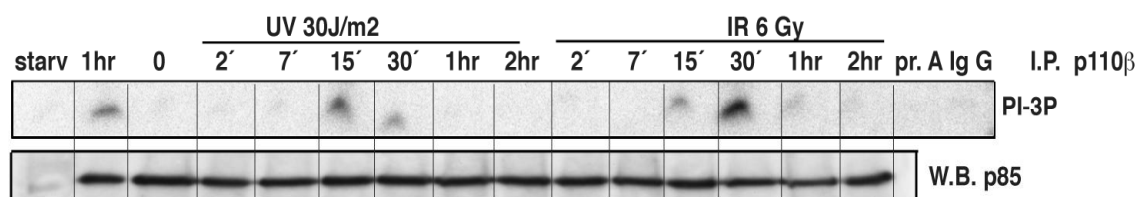


**Figure 33. p110 $\beta$  is activated by UV or  $\gamma$ -irradiation.** NIH3T3 cells in exponential growth were exposed to UV (30 J/m<sup>2</sup>) or  $\gamma$ -irradiation (6 Gy) and harvested at different times post-irradiation. Lysates were quantified and an *in vitro* PI3K lipid kinase assay performed using lysates (800  $\mu$ g) from mock, UV- and IR-treated cells, immunoprecipitated with anti-p110 $\beta$  antibody and PI as substrate. As controls, protein A was incubated with antibody alone or with lysate alone.

### 3.4) p110 $\beta$ associates with DNA repair protein in a radiation-dependent manner

To dissect the mechanism of p110 $\beta$  action after UV and IR exposure, we analysed p110 $\beta$  association with the DNA repair machinery. We expressed GST-p110 $\beta$  in the nuclei by fusing NLS at the N-terminus of GST-p110 $\beta$ . We isolated GST alone and GST-p110 $\beta$  from the nuclear fraction using glutathione Sepharose columns, and associated proteins were resolved in SDS-PAGE. GST-p110 $\beta$ -bound fraction-specific bands were excised and analysed by mass spectrometry. The DNA repair protein RAD17 was pulled down with p110 $\beta$  (Fig. 34A). We then tested whether p110 $\beta$  and RAD17 form a complex in intact cells. NIH3T3 cells were harvested 1 h after exposure to mock-, UV- or  $\gamma$ -irradiation, then fractionated into cytoplasmic and nuclear fractions. p110 $\beta$  and RAD17 interaction was studied in coimmunoprecipitation experiments using the nuclear fraction from irradiated NIH3T3 cells. Anti-p110 $\beta$  immunoprecipitates analysed in Western blot with anti-RAD17 Ab showed that RAD17 coimmunoprecipitates with p110 $\beta$  (Fig. 34B). p110 $\beta$  association with RAD17 was not constitutive, but induced by irradiation (Fig. 34B). Both UV- and IR-irradiation induced strong p110 $\beta$ -RAD17 association. The presence of p110 $\beta$ /RAD17 complexes only in irradiated cells suggests a role for p110 $\beta$  in DNA repair. We also identified RAD9B, RAD50 in the pull-down assay, but did not confirm their association to p110 $\beta$  in intact cells.

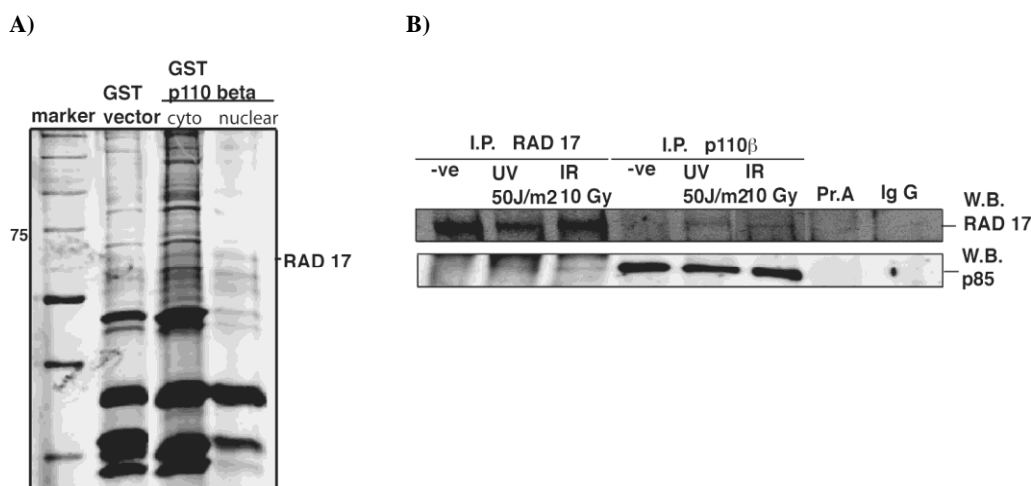


**Figure 34. UV and  $\gamma$ -irradiation induced p110 $\beta$ /RAD17 association.** A) NIH3T3 cells were transfected with GST or GST-p110 $\beta$ -NLS. The GST fusion proteins were purified from nuclear extracts in glutathione-agarose columns and resolved in SDS-PAGE. Gels were silver-stained, stained differential bands sliced and analysed by mass spectrometry. RAD17, RAD9B and RAD50 were identified. B) Anti-RAD17 western blot of anti-p110 $\beta$  or -RAD17 immunoprecipitates from NIH3T3 cells, untreated or UV- or IR-exposed as indicated.

### 3.5) p110 $\beta$ regulates ATR pathway activation after UV exposure

The observation that p110 $\beta$  binds to RAD17 after irradiation was of interest, as RAD17 is one of the first sensor proteins to recognize damaged DNA, and has an important role in functional activation of the ATR pathway of DNA repair (Zou *et al.*, 2002). We studied phosphorylation of the ATR effector protein Chk1, which is phosphorylated by ATR after UV exposure. We also examined phosphorylation of p38, as cells undergo apoptosis through activation of the p38 pathway after UV exposure (Bulavin *et al.*, 1999). After UV exposure, Chk1 phosphorylation was severely affected in p110 $\beta$  shRNA-transfected cells compared to control vector-transfected cells (Fig. 35). We tested whether total Chk1 protein was affected by p110 $\beta$  depletion, and found no change in Chk1 levels in p110 $\beta$  shRNA cells compared to controls. There was no change in p38 phosphorylation in p110 $\beta$  shRNA-transfected cells after UV radiation, indicating that this pathway is not controlled through p110 $\beta$  (Fig. 35). These findings suggest that apoptosis of p110 $\beta$  shRNA-transfected cells following UV exposure is not mediated by the p38 pathway, as phospho-p38



levels were unaltered in p110 $\beta$  shRNA and control cells. The reduction in Chk1 (S345) phosphorylation nonetheless suggested a defective ATR pathway in p110 $\beta$ -depleted cells.

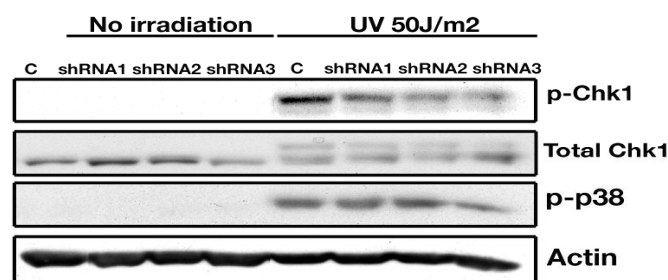
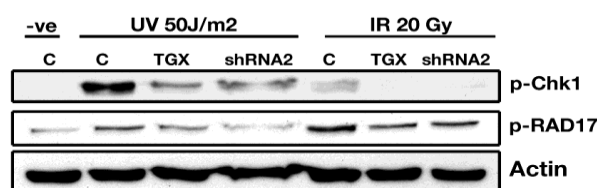


**Figure 35. p110 $\beta$  depletion reduces Chk1 phosphorylation.** Three different p110 $\beta$  shRNA or a control vector were transfected individually into NIH3T3 cells; after 48 h, cells were puromycin-selected (48 h). Cells were then plated in duplicate; one group was UV-exposed and the other was not-irradiated. Cells were harvested at 1 h post-treatment, lysed, and analysed by western blot using anti p-Chk1(S345), -Chk1 and -p-p38; anti-actin was used as control.

### 3.6) p110 $\beta$ affects the ATR pathway by inactivation of its sensor protein

We examined the mechanism by which p110 $\beta$  regulates activation of the ATR pathway following UV or IR treatment of cells, and examined whether p110 $\beta$  kinase activity has a role in ATR pathway activation. We treated the cells with a p110 $\beta$  specific inhibitor TGX221 (**Jackson *et al.*, 2005**) and subsequently irradiated them with UV or IR. We found that inhibition of p110 $\beta$  kinase activity resulted in a defective ATR pathway activation (Fig. 36). The phosphorylation defect was more evident in p110 $\beta$  shRNA cells than TGX-treated cells, suggesting that in addition to kinase-mediated regulation, p110 $\beta$  might have a kinase-independent role in ATR pathway activation. We examined the phosphorylation state of RAD17, an upstream protein that also acts as a sensor protein. RAD17 phosphorylation is required for functional activation of the ATR pathway (**Lee *et al.*, 2007**). Inhibition of kinase activity or p110 $\beta$  depletion led to RAD17 inactivation, even at high radiation doses, actin was used as a protein loading control (Fig. 36A). This observation suggests that p110 $\beta$  is upstream of RAD17 in ATR pathway activation during DNA repair. We also examined phospho-RAD17 by immunofluorescence after IR exposure in vector (control)- or p110 $\beta$  shRNA-transfected cells (Fig. 36B). This analysis confirmed the profound defect in RAD17 phosphorylation in cells expressing reduced p110 $\beta$  levels.

A)



B)

3Gy, 15min

**Figure 36. p110 $\beta$  depletion results in defective activation of the RAD17 sensor protein.** NIH3T3 cells were transfected with p110 $\beta$  shRNA or control vector; after 48 h, cells were puromycin-selected (48 h). A) The p110 $\beta$  shRNA or vector-transfected cells that had been DMSO- or TGX21-treated (4 h) were UV- or IR-exposed, and harvested after 1 h. Lysates were resolved in SDS-PAGE and probed in western blot with anti p-Chk1 and -p-RAD17 antibodies, with anti-actin as loading control. B) At 48 h post-puromycin selection, vector and p110 $\beta$  shRNA cells were plated on coverslips; after 24 h, cells were exposed to IR, fixed after 15 min, and processed for indirect immunofluorescence using anti-phospho-RAD17 antibody and Alexa 488-secondary antibody.

### 3.7) p110 $\beta$ also regulates activation of the ATM pathway

After determining the role of p110 $\beta$  in radiation-induced ATR pathway activation, we examined whether p110 $\beta$  acts as a general regulator of DNA repair pathways. Because ATM

participates in cellular responses to DNA DSB, we investigated whether activation of the ATM pathway is p110 $\beta$ -dependent. We examined ATM pathway activation in p110 $\beta$ -depleted, p110 $\beta$  kinase-inactive (TGX-treated) and control NIH3T3 cells after UV or IR exposure. Inhibition of p110 $\beta$  kinase activity or a reduction in p110 $\beta$  protein reduced ATM phosphorylation at S1981 in UV- or IR-treated cells (Fig 37A). Structural maintenance of chromatin 1 (SMC1), Chk2 and  $\gamma$ H2AX protein phosphorylation were downregulated due to inactivation of the ATM pathway (Fig 35A). In a complementary experiment, p110 $\beta$  knockdown or inactivation markedly decreased p-ATM and  $\gamma$ H2AX accumulation at IR-induced DSB foci (Fig 37B, C). Together these data suggested that, both as a kinase and as a protein, p110 $\beta$  regulates activation of the ATM DNA repair pathway.

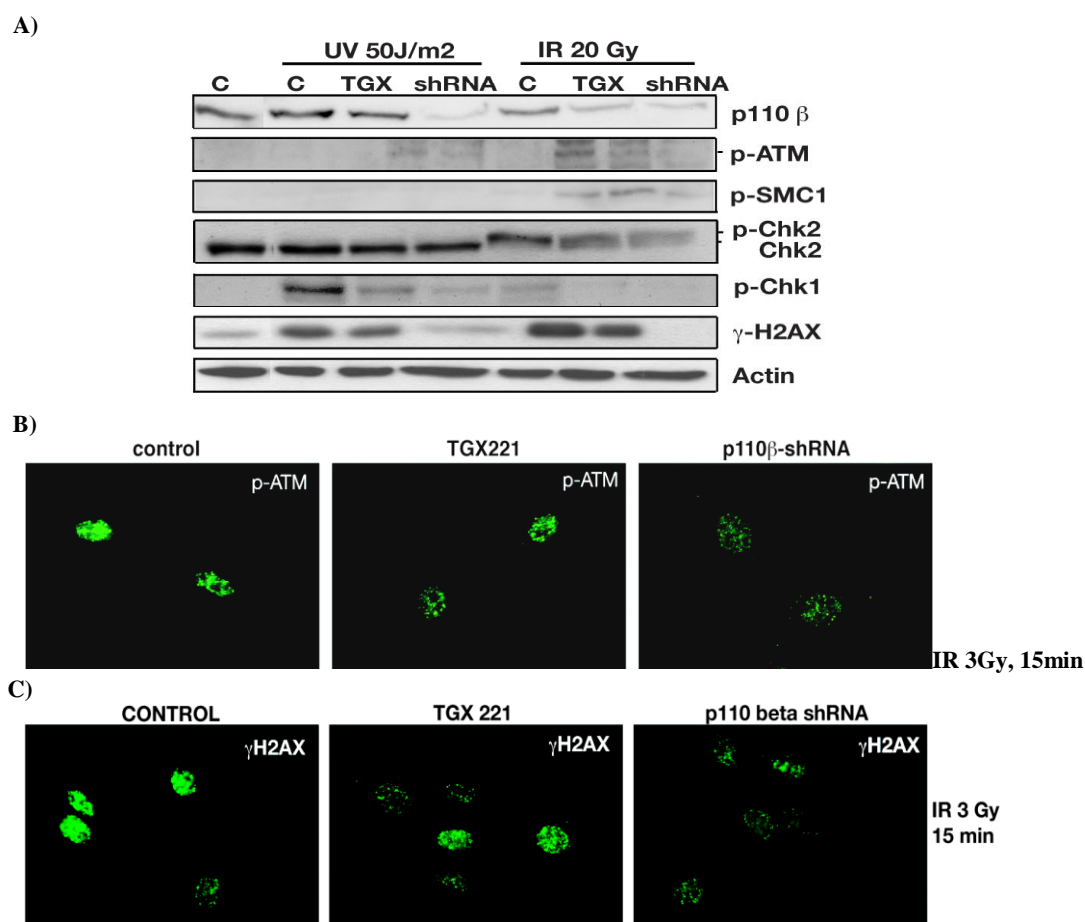


**Figure 37. ATM pathway downregulation following p110 $\beta$  deletion.** A) NIH3T3 cells were transfected and selected as in Fig. 36. A) The p110 $\beta$  shRNA or vector-transfected cells that had been DMSO- or TGX21-treated (4 h) were UV- or IR-exposed, and harvested after 1 h. Lysates were resolved in SDS-PAGE and probed in western blot with anti-p-Chk1, -Chk2, -p-ATM, -p110 $\beta$  and  $\gamma$ H2AX; actin was used as loading control. B) At 48 h post-puromycin selection, vector and p110 $\beta$  shRNA cells were plated on cover slips; after 24 h, cells were exposed to IR, fixed after 15 min, and processed for indirect immunofluorescence using anti-phospho-ATM 1981 antibody and Alexa 488-secondary antibody. C) At 48 h post-puromycin selection, vector, TGX treated cells and p110 $\beta$  shRNA expressing cells were plated on cover slips; after 24 h, cells were exposed to UV (upper panel) or IR (lower panel), fixed after 15 min, and processed for indirect immunofluorescence using anti-phospho-H2AX antibody and Alexa 488-secondary antibody.

### 3.8) Rapid p110 $\beta$ translocation to DNA damage sites

Biochemical fractionation of cells (Mendez *et al.*, 2002) showed that p110 $\beta$  appears in chromatin fraction (our data not shown). To elucidate the role of p110 $\beta$  in regulation of DNA repair pathways, we examined whether inhibition or deletion of p110 $\beta$  affects translocation of DNA damage mediator proteins to the DSB.

We cotransfected NIH3T3 cells with GFP-p110 $\beta$  and p85 $\beta$ -NLS for constitutive

translocation of p110 $\beta$  to the nucleus. Cells were then irradiated by a micro-laser in conditions that generate limited DNA strand breaks in defined nuclear volumes. We followed GFP-p110 $\beta$  protein mobility in time by fluorescence after photobleaching at the irradiated portion in individual nuclei. GFP-p110 $\beta$  moved to the laser-generated DSB sites, suggesting integration of p110 $\beta$  in the DNA repair machinery (Fig. 38A). We also examined the intranuclear localisation of p110 $\beta$  following IR irradiation. We observed a dramatic increase in the p110 $\beta$  accumulation at DSB sites in comparison with control (non-irradiated) cells (Fig. 38B). The concentration of p110 $\beta$  at specific points in mock treated cells could be due to its role in DNA replication, where it is shown to associate PCNA (Fig. 29). Accumulation of p110 $\beta$  in IR-induced foci was confirmed by co-immunostaining with  $\gamma$ -H2AX (Fig. 38C; **Pilch *et al.*, 2003**).

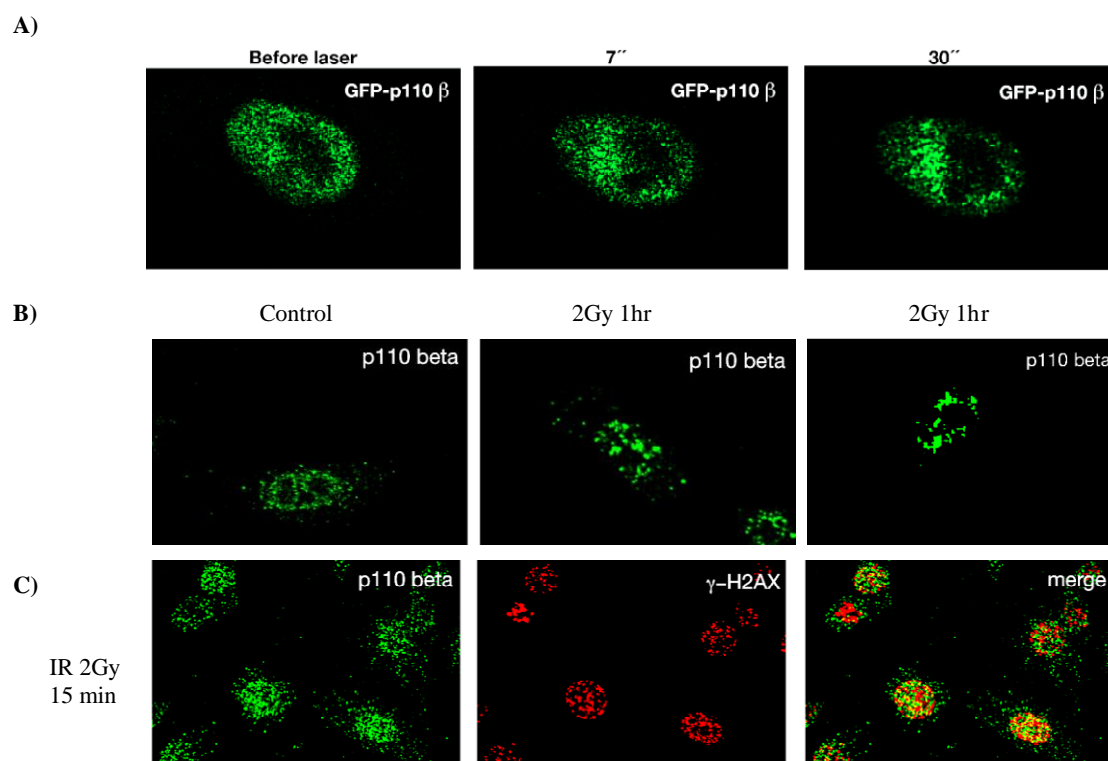


**Figure 38. p110 $\beta$  mobilizes to UV laser-induced DNA breaks.** A) NIH3T3 cells were cotransfected with GFP-p110 $\beta$  and p85 $\beta$ -NLS; after 24 h, cells were plated and part of the nucleus was micro-irradiated, after which GFP-p110 $\beta$  loading was observed under a confocal microscope. B) NIH3T3 cells were exposed to IR (2Gy), fixed after 1hr, and processed for indirect immunofluorescence using anti-p110 $\beta$  antibody. C) NIH3T3 cells were exposed to IR (2Gy), fixed after 15 min, and processed for indirect immunofluorescence using anti-phospho-H2AX (red) and anti-p110 $\beta$  (green) antibody.

### 3.9) p110 $\beta$ controls NBS1 immobilisation at DNA damage sites

To test the importance of the p110 $\beta$ -controlled events for the DNA damage response, and to elucidate whether p110 $\beta$  is integrated in or operates in parallel to known DNA repair pathways, GFP-NBS1 was transfected in WT, KR and KO p110 $\beta$  MEF. A part of the nucleus in GFP-NBS1-transfected cells was micro-irradiated using a UV laser, and GFP-NBS1 mobility was examined (**Bekker-Jensen *et al.*, 2005**; **Lukas *et al.*, 2003**; **Lukas *et al.*, 2004**).

NBS1 accumulation at the micro-irradiated zone was slower and less intense in p110 $\beta$ -KR than in WT cells, whereas the NBS1 mobility defects were more pronounced in p110 $\beta$ -KO cells (Fig. 39). These results show that p110 $\beta$  acts upstream in the activation of the ATM pathway in response to DNA breaks.

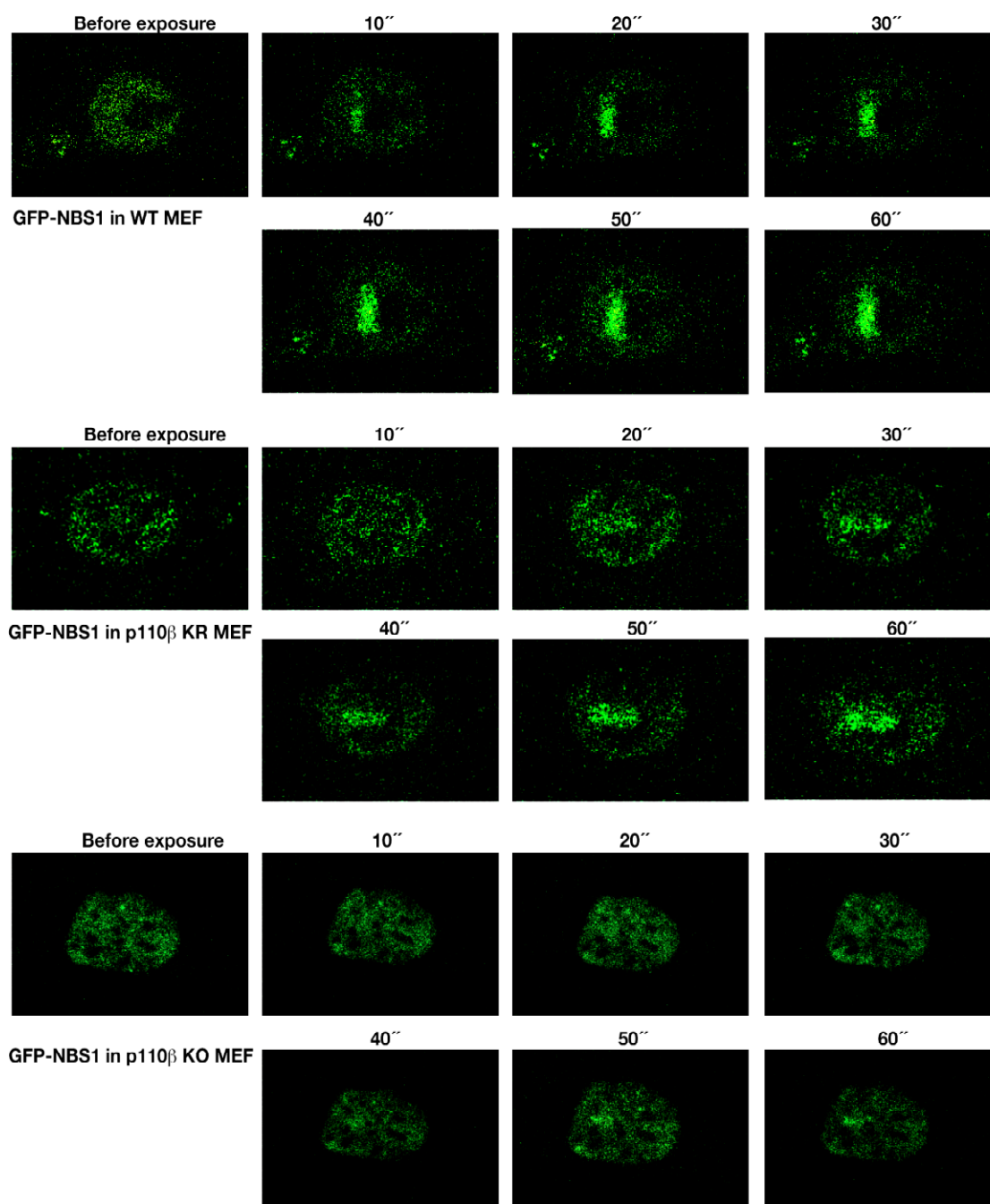


**Figure 39. p110 $\beta$ <sup>-/-</sup> MEF showed defective NBS1 mobility at DNA damage sites.** Immortalized WT, KR and KO MEF were transfected with GFP-NBS1; after 24 h, cells were plated. A UV laser was applied to part of the nucleus, after which GFP-NBS1 mobility to the irradiated site was followed under a confocal microscope.

### 3.10) p110 $\beta$ regulates 53BP1 loading at DNA damage sites

To confirm the role of the p110 $\beta$  pathway in the regulation of DNA repair in live cells, we examined the DNA repair protein 53BP1 (an ATM substrate in the homologous DNA repair pathway; Wang *et al.*, 2002). GFP-53BP1 loading at the DNA damage sites was less intense and was delayed in samples in which p110 $\beta$  kinase activity had been inhibited using TGX221, as compared to control DMSO-treated cells. Moreover, 53BP1 mobility to the micro-irradiated area was absent in p110 $\beta$  knockdown cells (Fig. 40). These data further supported that p110 $\beta$  is essential for activation of DNA damage responses.

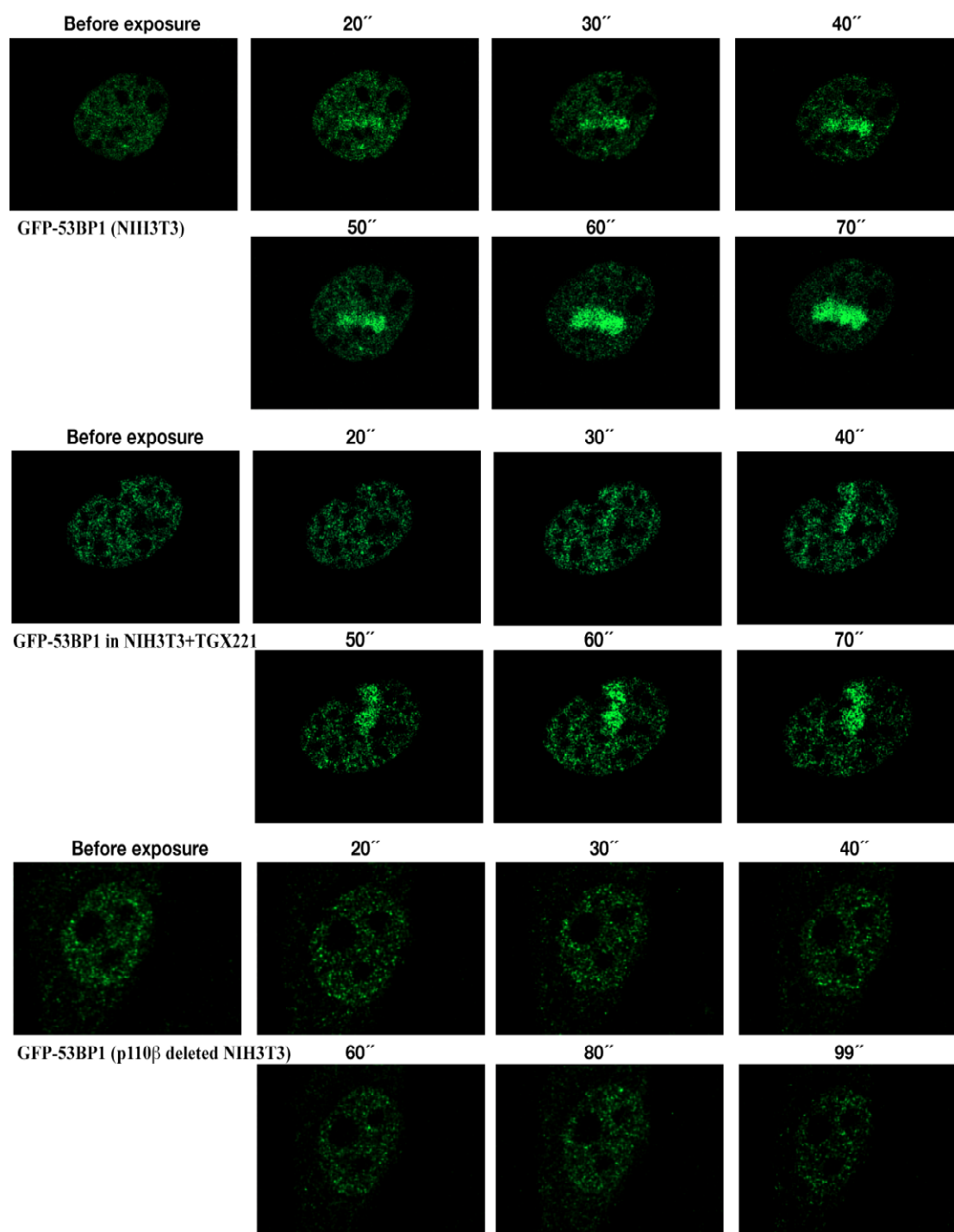


**Figure. 40. Inhibition of p110 $\beta$  kinase activity resulted in defective 53BP1 loading at DNA damage sites.** NIH3T3 cells were treated as in Fig. 36, cells were also transfected with GFP-53BP1. After 24 h, p110 $\beta$  shRNA or vector-transfected cells that had been DMSO- or TGX21-treated (4 h) were micro-irradiated using UV laser; the exchange rate of the GFP-tagged proteins at the DSB sites was determined by live imaging under confocal.

### 3.11) PCNA is a marker for DSB and requires p110 $\beta$ for loading at DNA damage sites

PCNA is a known DNA replication marker and also has an important role in mismatch and nuclear excision repair (Jonsson *et al.*, 1997). Since we observed a physical association of p110 $\beta$  with PCNA, and that p110 $\beta$  activates following DNA damage and regulates DNA repair machinery, we analysed whether PCNA translocates at the nicks formed using a UV laser scissor.

We found that *PCNA translocated rapidly to DNA breaks* and remained there for long periods. After confirming PCNA loading at DNA nicks, we examined the role of p110 $\beta$  in PCNA loading at DNA breaks (Fig. 41). RFP-PCNA was transfected into control vector- or p110 $\beta$  shRNA-transfected NIH3T3 cells; we also examined cells in which p110 $\beta$  kinase activity was inhibited with TGX221 (20  $\mu$ M). Cells were passed through a UV laser scissor and RFP-PCNA translocation to the damage site was followed. We concluded that *p110 $\beta$  kinase regulates PCNA localization at damage sites. Moreover expression of p110 $\beta$  protein is critical for PCNA loading at DNA damage sites* (Fig. 41).

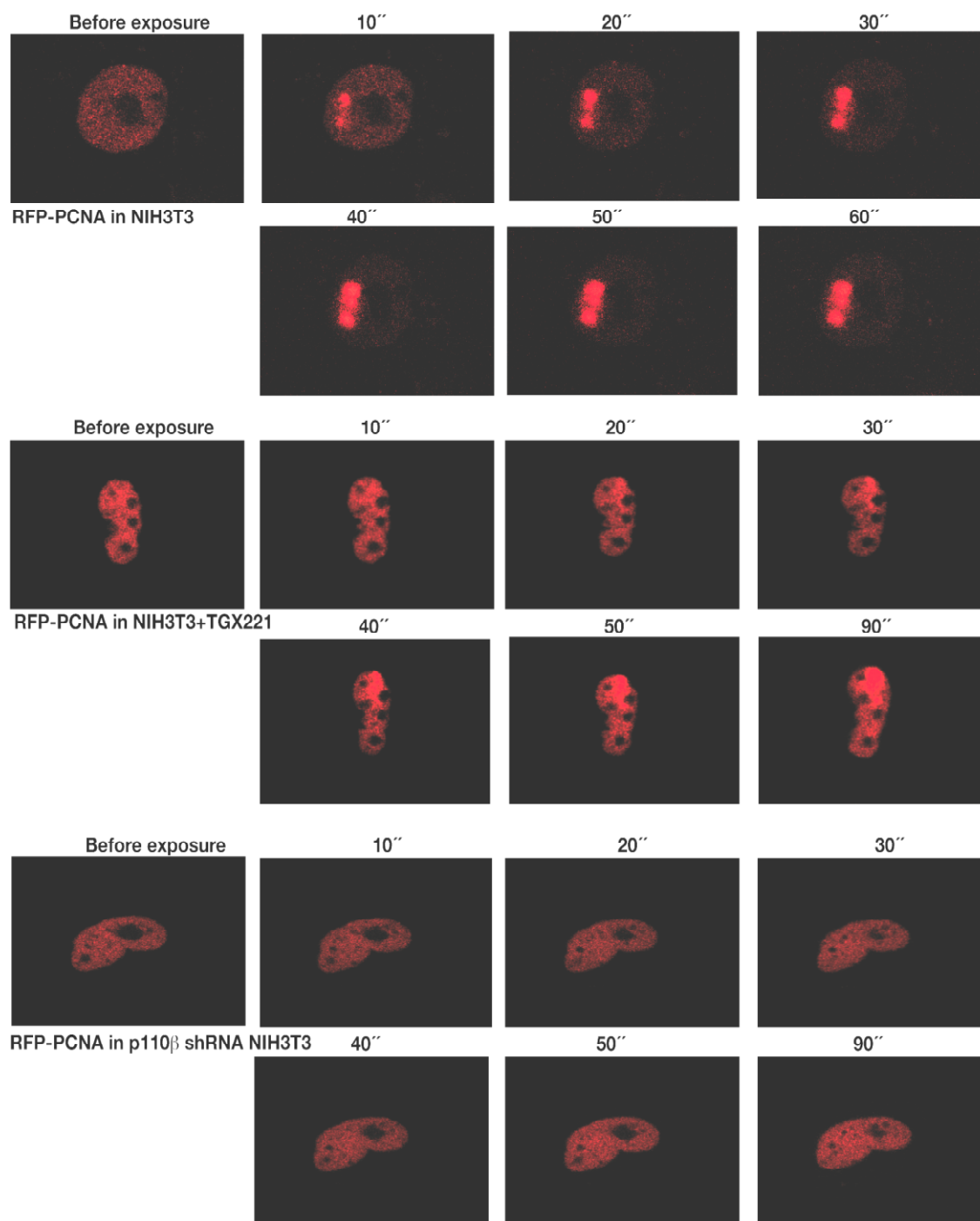


**Figure 41. p110 $\beta$  regulates PCNA loading at DNA damage sites .** NIH3T3 cells were transfected and selected as in Fig. 36, transfected with RFP-PCNA. After 24 h, The p110 $\beta$  shRNA or vector-transfected cells that had been DMSO- or TGX21-treated (4 h) were micro-irradiated using UV laser, the exchange rate of the RFP-tagged-PCNA at the DSB sites was determined by live imaging under confocal microscope.



### 3.12) PCNA and NBS1 translocates simultaneously at damaged areas

Having identified PCNA mobility on micro-irradiated sites, we tested whether it translocates to DNA damaged sites in parallel to NBS1 translocation after micro-irradiation induced DSBs. Indeed, we found simultaneous translocation of both PCNA and NBS1 at DSB suggesting that PCNA acts as a sensor protein at DSB sites.

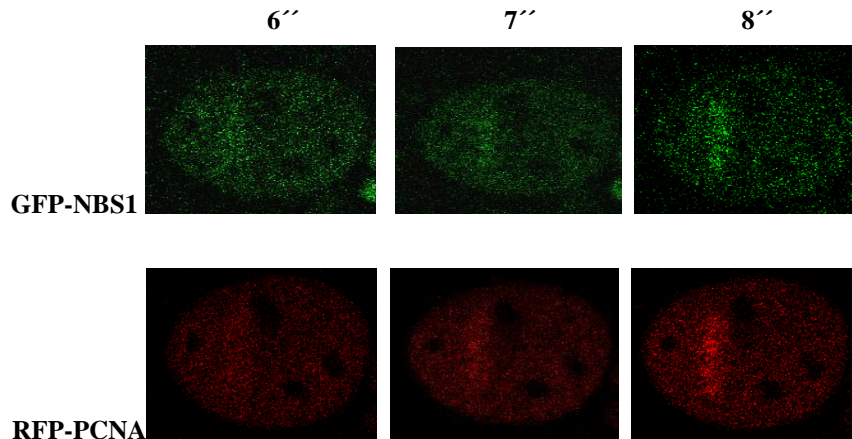


**Figure 42. Identical NBS1 and PCNA translocation kinetics at micro-irradiated sites.** NIH3T3 cells were transfected with NBS1 and RFP-PCNA. After 48 h, were micro-irradiated using UV laser, the mobility rate of the RFP-tagged-PCNA and GFP-tagged-NBS1 at the DSB sites was determined under confocal microscope.

### 3.13) Conclusions

After determining the nuclear localization of p110 $\beta$  and its role in regulation of DNA replication, we examined whether p110 $\beta$  participates in the regulation of DNA repair pathways, an important cell process required for maintaining genomic stability, proliferation and survival. p110 $\beta$  knockout mice are embryonic lethal, and recent reports indicated that p110 $\beta$  kinase activity regulates mouse growth, as well as tumour development. A kinase-independent role in embryonic development is also described. The UV exposure of cells with reduced p110 $\beta$  levels resulted in apoptosis. We examined the possibility of greater p38 pathway activation in these cells compared to controls. The similar phospho-p38 levels detected led us to study the DNA repair pathways in p110 $\beta$ -depleted cells. p110 $\beta$ -deficient cells showed larger numbers of chromosomes and aberrant chromosomal breaks, implicating *a p110 $\beta$  function in the maintenance of genomic integrity*. We further analysed two pathways that regulate activation of DNA damage responses and DNA repair machinery, the ATR and ATM pathways. We observed a defective ATR pathway, with inactive Chk1 and reduced p-RAD17 accumulation. In addition, we found that deletion of p110 $\beta$  also resulted in a defective ATM pathway, in which we found downregulation of activation of ATM and its downstream effectors. We also determined the direct role of p110 $\beta$  in regulation of DNA repair; p110 $\beta$  activation and its colocalisation with  $\gamma$ -H2AX at the DNA damage area, implying an integrative role for p110 $\beta$  in the aftermath of DNA damage. *We found that p110 $\beta$  regulates the mobility of the DSB sensor protein NBS1 at damage sites, and conclude that p110 $\beta$  acts upstream of DNA damage sensor proteins.* We also showed that PCNA localizes at the DNA damage area with similar kinetics over time as NBS1, and infer that PCNA could be a sensor protein in addition to its role in DNA replication and its dependence on p110 $\beta$ .

## CONCLUSIONS

### ***Objective 1. Investigate the mechanism of activation and the function of PI3K activity in late G1***

- 1.1) Activation of Ras and Tyr kinases are required for late-G1 PI3K activation and this late-G1 PI3K activity regulates c-Myc levels and in turn cyclin A expression, Cdk2 activity, and MCM2 loading onto chromatin
- 1.2) The primary function of late-G1 PI3K is c-Myc stabilization, as conditional activation of c-Myc in advanced G1 as well as expression of a stable c-Myc mutant rescued the defects induced by late G1 PI3K inhibition and S phase entry

### ***Objective 2. Investigate the mechanism for p110 $\beta$ nuclear localisation***

- 2.1) The majority of p110 $\beta$  is nuclear while p110 $\alpha$  is mainly cytosolic. In addition p110 $\beta$  shuttles between nucleus and cytosol during cell cycle progression and is mainly nuclear in S phase; p110 $\beta$  increased nuclear localisation is coincident with activation of nuclear PI3K activity
- 2.2) p85 $\beta$  association with p110 $\beta$  is required for the localisation of p110 $\beta$  in the nucleus. In addition p85 $\beta$  also determines p110 $\beta$  exit from the nucleus; the first 41NT-residues contain the NES of p85 $\beta$
- 2.3) The C2 domain of p110 $\beta$  contains a NLS
- 2.4) p110 $\beta$  associates with PCNA; this complex further increases p110 $\beta$  nuclear localisation

### ***Objective 3. Investigate the involvement of p110 $\beta$ in DNA repair***

- 3.1) Reduction of p110 $\beta$  cellular levels interferes with the cellular mechanisms that counteract DNA damage; these cells undergo cell death upon UV irradiation. p110 $\beta$  deficiency also induces genomic instability
- 3.2) UV and IR activates irradiation p110 $\beta$
- 3.3) p110 $\beta$  associates RAD17 in a radiation-dependent manner and regulates ATR and ATM pathway activation
- 3.4) p110 $\beta$  translocates to DNA damage sites and controls NBS1, 53BP1 and PCNA recruitment to these sites





## **DISCUSSION**



Studies in *Caenorhabditis elegans* and *Drosophila melanogaster* have been a useful source of knowledge regarding PI3K regulation, as these species have a single class I<sub>A</sub> PI3K. Class I<sub>A</sub> PI3K mediates cell growth and metabolism control downstream of the IGF-R (Engelman *et al.*, 2006). Due to the many effectors PI3K pathway and to the various growth factors that transmit signals through PI3K, its signalling in mammals is more complex. Of this family, only class I PI3K is implicated in cancer; class II and class III PI3K (Vps34p) have no described role in oncogenesis. The distinct roles of the different PI3K classes could be due to their specific substrate preference and to the products they catalyze. In general, overexpression and mutational activation of class I PI3K and inactivation of PTEN result in oncogenic cell transformation and cancer (Cantley, 2002; Wishart & Dixon, 2002; Bachman *et al.*, 2004; Broderick *et al.*, 2004; Campbell *et al.*, 2004; Fruman, 2004; Leslie & Downes, 2004; Cully *et al.*, 2006; Vogt *et al.*, 2007; Salmena *et al.*, 2008). The signalling pathways by which activated class I<sub>A</sub> PI3K isoforms control cell growth and contribute to cell transformation are therefore of considerable and continuing interest.

The study of cell cycle regulation is fundamental for understanding the mechanisms of cell proliferation. Cells plated at low cell density in serum-containing medium progress through the four cell cycle phases: G1, S, G2 and M. The initial phase of growth factor-stimulated signalling facilitates entry into the cell cycle; the majority of these signalling events do not persist much longer than 60 min. In normal cells, class I PI3K activity is precisely controlled. Activation of transmembrane receptors recruit cytosolic PI3K to the plasma membrane; this relocation is mediated by interactions with RTK (Skolnik *et al.*, 1991) or GPCR (Stephens *et al.*, 1994). The PI3K products accumulate within minutes of growth factor stimulation, and return to near-basal levels by 30 min. Fibroblasts nonetheless require 8-10 h of continuous exposure to growth factor to pass the restriction point (Pardee, 1989; Stiles *et al.*, 1979). Jones *et al.* demonstrated that the early signalling burst is insufficient for cell cycle progression, and that there is additional growth factor input at later times before S phase entry (Jones *et al.*, 2001). One goal of the studies presented here was to further understand the purpose and mechanism of PI3K activation near the G1/S transition.

### **Class I<sub>A</sub> PI3K activation in late G1 is required for c-Myc stabilization and S phase entry**

PI3K activation in late G1 is essential for cell cycle entry (García *et al.*, 2006; Jones *et al.*, 2001). Here we examined the signals involved in late G1 PI3K activation and the mechanisms by which PI3K controls the G1/S transition. We found that tyrosine kinases and Ras activation are both necessary to activate PI3K in late G1 phase. Specific inhibition of tyrosine kinases or Ras in late G1 resulted in downregulation of PI3K-associated lipid kinase activity. Simultaneous inhibition of tyrosine kinase/Ras in late G1 completely abrogated PI3K activity. The results suggest that PI3K activation in late G1 is tyrosine kinase-dependent and is further controlled by Ras. We also demonstrate that c-Myc stabilization is a major function of PI3K activation in the late G1 phase, based on the observation that PI3K inhibition in late G1 reduces c-Myc and cyclin A levels. PI3K inhibition in late G1 also increased p27<sup>kip</sup> expression and reduced cyclinE/CDK2- and cyclinA/CDK2-associated kinase activity. Our results are consistent with observations in c-Myc-deficient cells, which show similar defects (Vlach *et al.*, 1996; Mateyak *et al.*, 1999). Oscillations in cyclin-dependent kinase (CDK) activities dictate orderly progression through the cell cycle; downregulation of CDK activity due to PI3K inhibition abrogated cell cycling. As PI3K/PKB inactivates GSK3 $\beta$ , the enzyme that targets c-Myc for degradation (van Weeren *et al.*, 1998; Yeh *et al.*, 2004), we hypothesised that late G1 PI3K activation is essential for c-Myc stabilization. We demonstrated this using a c-Myc mutant (MycT58A, Hemann *et al.*, 2005) resistant to GSK3 $\beta$  action, and by induction of c-Myc in late G1. MycT58A expression or tamoxifen activation of c-Myc ER expression in late G1 restored cell cycle entry by counteracting PI3K inhibition in all

parameters studied, which included those related to DNA synthesis, cyclin A expression, cyclinE/CDK2 and cyclinA/CDK2 activity, as well as p27<sup>kip</sup> association to cyclinE/CDK2. PI3K activation in late G1 therefore regulates c-Myc protein levels.

Due to the relatively short half-lives of *c-Myc* mRNA and protein, c-Myc levels are tightly controlled in normal cells. The average half-life is 20-30 min for *c-Myc* RNA and 20-40 min for the protein (Thompson *et al.*, 1998; Ponzielli *et al.*, 2005). To achieve the c-Myc protein expression levels necessary for cell cycle entry (Mateyak *et al.*, 1997), the stability of c-Myc must be regulated during G1. We found that late G1 PI3K activation stabilizes c-Myc, which is further supported by our findings using interfering RNA and constitutive active mutants of class I<sub>A</sub> PI3K isoforms (Marques *et al.*, 2008). Although these tools do not allow distinction between the first and second PI3K activity peaks in the G1 phase, they confirm the role of PI3K in cell cycle entry and in c-Myc expression control. Whereas PI3K activation accelerates cell cycle entry and increases c-Myc levels, downregulation of PI3K levels reduces S phase entry and c-Myc levels (Marques *et al.*, 2008).

The regulation of c-Myc stability involves the phosphorylation of two key residues, Thr58 and Ser62. MAPK mediates phosphorylation of Ser62, which is necessary for subsequent Thr58 phosphorylation by GSK3 $\beta$  (Yeh *et al.*, 2004). Thr58 phosphorylation destabilizes c-Myc protein, and represents a major mutation hotspot in Burkitt's lymphomas (Hemann *et al.*, 2005). Since Ser62 phosphorylation is a prerequisite for Thr58 phosphorylation, c-Myc might be phosphorylated *in vivo* by MAPK in late G1. The concomitant activation of MAPK and PI3K in late G1 supports this possibility. We also observed an increase in c-Myc phosphorylation at Thr58 after inhibition of PI3K activity in late G1 phase, which is consistent with previous reports (Domínguez-Cáceres *et al.*, 2004).

Although the main role of PI3K in late G1 appears to be c-Myc stabilization, the functions of c-Myc and PI3K are otherwise unrelated. c-Myc function is linked to its transcription factor activity, which is required for its transforming capacity (Ponzielli *et al.*, 2005; Dang *et al.*, 1999; Amati *et al.*, 1998). c-Myc regulates transcription by associating to the Max protein (Cole & Nikiforov, 2006). c-Myc/Max-regulated gene expression involves several complex mechanisms, including chromatin remodelling due to c-Myc association with TRRAP, an ATM-related protein that interacts with histone acetyl-transferase (HAT) (Dang, 1999). c-Myc also associates with CREB-binding protein (CBP), providing a link between c-Myc and transcription activation. In addition c-Myc associates with the chromatin remodelling regulators TIP48 and TIP49 (Dang, 1999). Finally, c-Myc interacts with components of the SWI/SNF complex, which control transcription through nucleosome repositioning (Dang, 1999). Local chromatin remodelling as well as recruitment of RNA polymerases and transcription elongation factors forms part of the mechanism by which c-Myc controls gene expression of its targets (Dang, 1999; Pelengaris *et al.*, 2002). c-Myc regulates a large number of target genes, including all those containing E-box consensus binding sites in their promoters; many of these are required for cell cycle progression, including cyclins D, E and A (Dang, 1999). The first c-Myc expression peak occurs ~1 h after serum stimulation; since c-Myc promotes cyclin D and E expression (Mateyak *et al.*, 1999, and results shown here), this regulation would take place in early G1. c-Myc is also essential for cyclin A expression, as well as for p27<sup>kip</sup> inhibition (Perez-Rogers *et al.*, 1997; Vlach *et al.*, 1996; Mateyak *et al.*, 1999). Our observations suggest that the second c-Myc expression peak (coincident with Rb hyperphosphorylation) is necessary for cyclin A expression and p27<sup>kip</sup> inhibition.

One intriguing aspect of our observations is that although PI3K activity in late G1 is nearly parallel to that of c-Myc, c-Myc and PI3K cooperate in cell cycle entry, at G0→G1 transition (Jones *et al.*, 2001), suggesting distinct functions in early and late G1. PI3K-mediated

PKB activation is also needed for FoxO TF inactivation. In an unphosphorylated state, FoxO TF inhibit induction of several c-Myc targets, providing a mechanism for the synergistic action of c-Myc and PI3K in cell cycle progression (**Bouchard *et al.*, 2004**). PI3K activation shortly after GFR stimulation might explain this apparent contradiction, as PI3K activity in early G1 is essential for cell growth (**Álvarez *et al.*, 2003**) and for FoxO TF inactivation (**Álvarez *et al.*, 2001**). We found that c-Myc does not compensate the first PI3K activity peak, since inhibition of PI3K in early G1 (during the first 6 h) impaired cell cycle entry, even in cells expressing WT or T58A c-Myc. Indeed, c-Myc induction in early G1 after tamoxifen addition did not compensate for the loss of PI3K, and resulted in inhibition of cell cycle progression; this was not the case when PI3K was inhibited in late G1. It is possible that the action of PI3K at stimulating cell growth pathways is not compensated by c-Myc and *vice versa*. We thus propose that PI3K and c-Myc cooperate early in G1, but the principal late G1 PI3K activity is to stabilize c-Myc protein levels.

A number of enzymes show discontinuous activation during the G1 phase. Incubation of G0-arrested fibroblasts with PDGF for 30 min, and again at 8 h after serum addition, induces cell cycle entry similar to that of continuous PDGF exposure. Moreover, MAPK activation combined with c-Myc overexpression substitutes for the first PDGF pulse, whereas PIP<sub>3</sub> addition substitutes for the second pulse (**Jones *et al.*, 2001**). In view of our findings, we propose that PIP<sub>3</sub> addition at 8 h probably results in c-Myc stabilization and initiation of further downstream events.

During a normal somatic cell cycle, early G1 signals trigger cell growth as well as cyclin D synthesis and stabilization. MAPK and c-Myc activation are essential for synthesis of cyclin D (**Mateyak *et al.*, 1999**; **Jirmanova *et al.*, 2002**). Early G1 PI3K activity is crucial for cell growth promotion via the mTOR pathway and for FoxO TF inactivation (**Medema *et al.*, 2000**; **Álvarez *et al.*, 2001**; **Martinez-Gac *et al.*, 2004**). When cyclin D reaches optimal levels and p27<sup>kip</sup> expression decreases, cyclinD/CDK drives Rb phosphorylation, followed by E2F activation, which is necessary for cyclin E synthesis (**Geng *et al.*, 1996**). This initial signalling wave is transient, probably due to the short-lived action of phosphatases; nonetheless, TyrK, Ras, MAPK and PI3K are later reactivated and drive CDK2 activation. During this second signalling wave, the main PI3K function is c-Myc stabilization, as PI3K can be replaced by GSK-3 $\beta$ -resistant c-Myc. Stabilized c-Myc in turn contributes to triggering cyclin A synthesis, p27<sup>kip</sup> inactivation, and cyclinE/CDK2 activation.

The mini-chromosome maintenance proteins (MCM) are implicated in replication and form a complex that is thought to be the replicative helicase in eukaryotic organisms. The MCM complex remains with the replication complex until replication is complete, and several MCM proteins are regulated by CDK phosphorylation (**Tye, 1999**). Details of MCM regulation differ among organisms, but in all cases, several of these proteins are degraded through ubiquitin-dependent pathways, are excluded from the nucleus, or are otherwise prevented from performing their replication function (**DePamphilis, 2003**). We hypothesised that, since inhibition of PI3K activity in late G1 resulted in downregulation of cyclinE/CDK2 activity, this inhibition would affect MCM complex loading on chromatin. We examined MCM2 protein, as it is defective in cyclin E knockout mice (**Geng *et al.*, 2003**), and tested chromatin loading near the G1/S transition while inhibiting PI3K activity. We found that the late G1 PI3K activity is required for MCM2 loading, and that all of these events are crucial for DNA synthesis induction. Our results are consistent with the previously reported inactivation of MCM2, which resulted in nuclear export (**Yamaguchi & Newport, 2003**). This led us to conclude that inhibition of the late PI3K activity peak inhibits S phase entry in this manner.

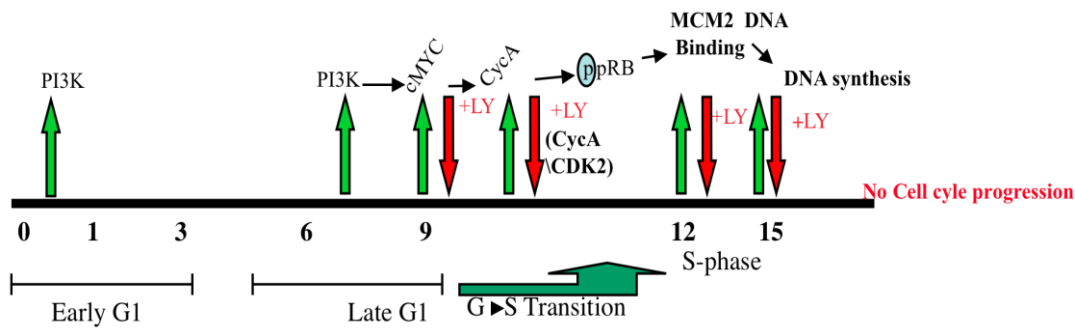


**Figure 1. Mechanism of DNA replication inhibition after inactivation of PI3K in late G1.** An early burst of signalling results in activation of the PI3K pathway following stimulation of serum-starved cells; signalling continues for 60-90 min, and then returns to basal levels. The second wave of signalling is observed around late G1 (7-9 h post-stimulation); it activates the PI3K pathway, whose primary role is to stabilize c-Myc. This in turn regulates cyclinA expression, Rb hyperphosphorylation and DNA replication. Inhibition of late G1 PI3K using LY294002 blocks the pathway and abrogates G1/S transition.

After determining the role of PI3K in late G1, we sought to identify the class I<sub>A</sub> PI3K isoform responsible for G1/S transition. Our group recently reported that both p110 $\alpha$  and p110 $\beta$  are activated in late G1, although the timing differs (Marques *et al.*, 2008). p110 $\alpha$  is activated at about mid-G1, whereas p110 $\beta$  is activated near late G1 (G1/S phase entry). The distinct activation times of these isoforms indicates separate roles in the G1-to-S phase transition. Marques *et al.* also described distinct p110 $\alpha$  and p110 $\beta$  requirements during late G1 and S phases. When p110 $\alpha$  and p110 $\beta$  constitutive active stable cell lines reached confluence and were released to observe cell cycle progression, control and p110 $\alpha$  cells were arrested in G1, whereas some p110 $\beta$  cells progressed slowly into S phase. They concluded that p110 $\beta$  has a different role from that of p110 $\alpha$ , as it regulates S phase progression and hence DNA replication (Marques *et al.*, 2009).

### p85 $\beta$ association mediates nuclear translocation of p110 $\beta$

We explored the basis of the role of p110 $\beta$  in S phase progression. Using immunostaining and immunoblotting of the p85 regulatory subunit, Neri and colleagues showed that class I<sub>A</sub> PI3K localizes in the nucleus of various cell types (Neri *et al.*, 2002). We found distinct intracellular localisation for different p110 $\alpha$  and p110 $\beta$  class I<sub>A</sub> PI3K isoforms of in NIH3T3 cells; whereas p110 $\alpha$  is concentrated mainly in cytoplasm, most p110 $\beta$  is found in the nucleus. In HeLa and mouse embryonic fibroblasts (MEF), we also observed nuclear localisation of p110 $\beta$ . These observations suggest that nuclear p110 $\beta$  is a general phenomenon, irrespective of cell type and mammalian species. A few recent reports document PI3K isoforms in nucleus and a distinct role from their cytoplasmic counterparts (Martelli *et al.*, 2007), although the mechanism of p110 $\beta$  nuclear translocation remains unclear.

To dissect the role of nuclear p110 $\beta$  and to define its function in DNA replication, we used the NIH3T3 cell line and determined the intracellular localisation of p110 $\beta$  at different times during G1 phase. We showed that following cell release from serum starvation, a fraction of p110 $\beta$  shuttles between the cytoplasm and the nucleus during G1. In addition, the nuclear kinetics of PI3K activation paralleled the nuclear translocation of p110 $\beta$ . p110 $\beta$  nuclear localisation was maximal near the G1/S phase transition. We also found p85 $\beta$  nuclear localisation, whereas the p85 $\alpha$  regulatory subunit was mainly cytoplasmic.

While studying the role of nuclear p110 $\beta$ , we observed that p110 $\beta$  overexpression resulted in its cytoplasmic localisation. In view of this result, we sequenced cDNA for human

PIK3CB and murine pik3cb. Although their primary sequences were correct, expression of recombinant p110 $\beta$  resulted in cytoplasmic localisation of exogenous protein in murine as well as in human cells. We considered that the continuous transcription and translation of cDNA in cells could result in accumulation of *de novo* synthesised p110 $\beta$  in the polysomes of the endoplasmic reticulum. Moreover, inhibition of protein expression with cyclohexamide 3 h before immunofluorescence analysis did not change the cytosolic localisation of recombinant p110 $\beta$ . An alternative possibility is that p110 $\beta$  requires association with other cell proteins for its nuclear translocation.

p110 $\alpha$  and p110 $\beta$  are considered obligatory partners of their regulatory p85 subunits (Geering *et al.*, 2007). We found that expression of p85 $\beta$ , but not of p85 $\alpha$  facilitates nuclear localisation of p110 $\beta$  but not of p110 $\alpha$ . When p85 $\beta$  was expressed alone, it showed slight nuclear staining in all transfected cells. When cells were cotransfected with p85 $\beta$ /p110 $\beta$ , p85 $\beta$  nuclear staining was observed in ~22% of the cells. p110 $\beta$  also localized to the nucleus in these cells, showing that p85 $\beta$ /p110 $\beta$  is the heterodimer that localizes to the nucleus. When p110 $\alpha$  was cotransfected with p85 $\alpha$  or p85 $\beta$ , p110 $\alpha$  remained cytoplasmic similarly than p85 $\alpha$  and most of p85 $\beta$ . These results were unexpected; although both regulatory subunits are considered to have similar roles, p85 $\beta$  subunit and not p85 $\alpha$  reproducibly facilitated nuclear translocation of p110 $\beta$ , but not that of p110 $\alpha$ .

p85 $\beta$  binding to p110 $\beta$  might result in conformational changes in the complex, or in complex activation; either of these events could promote nuclear translocation. Another possibility is preferential binding of p110 $\beta$  to p85 $\beta$  and of p110 $\alpha$  to p85 $\alpha$ . We examined this possibility by fusing the NLS to p85 $\beta$  and cotransfecting p110 $\alpha$  or p110 $\beta$  with p85 $\alpha$  and p85 $\beta$ -NLS (Fig. 26). p85 $\beta$  showed complete nuclear localisation due to the SV40 NLS, which also rendered p110 $\beta$  nuclear; however, even in this case, a large fraction of p110 $\alpha$  remained cytoplasmic, similar to p85 $\alpha$ . Until further data have been accumulated, we cannot rule out the possibility of preferential binding of p85 $\beta$  to p110 $\beta$  or selective exposure of NLS in the p85 $\beta$ /p110 $\beta$  complex.

After determining the localisation of complexes to the nucleus, we searched for classical NLS in p85 $\beta$  and p110 $\beta$ . We found a potential polybasic NLS region in p85 $\beta$  and mutated it by replacing the basic residues from the same region in p85 $\alpha$ . We observed no change in localisation of the p85 $\beta$ /p110 $\beta$  mutant complex, and the p85 $\beta$  chimera expressed alone also retained its intracellular localisation. In addition, we detected three potential NLS in p110 $\beta$  and mutated them with non-basic residues. Two of these mutations had no effect on nuclear localisation of p85 $\beta$ /p110 $\beta$  mutant complexes, whereas mutation in the putative NLS in the p110 $\beta$  C2 domain inhibited nuclear translocation of the p85 $\beta$ /p110 $\beta$  complex. These observations led us to hypothesize that the p85 $\beta$ /p110 $\beta$  complex conformation opens up the polybasic region in the C2 domain to associate the nuclear import machinery for nuclear translocation as a complex (Fig. 2).

To determine whether p85 $\beta$  or p110 $\beta$  has a nuclear export signal (NES), we examined the effect of leptomycin B treatment on p85 $\beta$ , p110 $\beta$  or p85 $\beta$ /p110 $\beta$  localisation. Leptomycin B alkylates and inhibits CRM1 (a protein required for nuclear export of NES-containing proteins). Leptomycin B treatment resulted in constitutive nuclear localisation of transfected p85 $\beta$  and in partial nuclear retention of p110 $\beta$ . In contrast, p110 $\alpha$  and p85 $\alpha$  localisation were unchanged after leptomycin B treatment; these isoforms did not localize to the nucleus and the inhibitor did not alter their localisation. These results suggested the presence of a NES in p85 $\beta$ . We indeed identified the NES-containing region in the initial 41 N-terminal amino acids (NT41aa). Interestingly, when p110 $\beta$  was coexpressed with a p85 $\beta$  mutated form that lacked NT41aa, truncated p85 $\beta$  localized mainly to the nucleus, whereas p110 $\beta$  was found in cytoplasm. This shows that the NES is found in the first 41 amino acids of p85 $\beta$ , but also that this mutation impairs p85 $\beta$ /p110 $\beta$  complex formation. We also examined the localisation of p110 $\beta$  coexpressed with p85 $\beta$  lacking NT100aa,



and detected these complexes distributed throughout the cell. This implies that the p85 $\beta$  NT41aa region could have a role in certain conformational changes in the complex that affect its localisation.

Even when p85 $\beta$  was coexpressed with p110 $\beta$ , not all the cells coexpressing these two subunits showed as complete a nuclear localisation phenotype as that exhibited by endogenous complexes. We hypothesised that p110 $\beta$  might associate with additional partners. To identify such potential partners, we fused the NLS from SV40 large T-antigen to the p110 $\beta$  C-terminal and examined the associated proteins by pull-down assays. We observed the association of several proteins, among them the DNA repair-associated protein RAD17. RAD17 forms part of the 9-1-1 complex, which behaves as a clamp loader, similarly to a PCNA trimmer. We therefore analysed the binding of nuclear p110 $\beta$  to PCNA. As anti-p110 $\beta$  antibody was poorly efficient in immunoprecipitation, we performed a reciprocal assay in cells transfected with Myc-p110 $\alpha$  or -p110 $\beta$ , which were expressed at levels similar to those of endogenous p110. A small fraction of endogenous PCNA associated to Myc-p110 $\beta$  in the nuclear fraction; PCNA association to p110 $\alpha$  was barely detectable. These observations were confirmed by immunoprecipitating Myc-tagged-p110 $\alpha$  and -p110 $\beta$ ; PCNA affinity for p110 $\beta$  was much higher than for p110 $\alpha$ , suggesting that p110 $\beta$  localisation in the nucleus determines its association to PCNA. In addition, we found that PCNA assists p110 $\beta$ /p85 $\beta$  nuclear entry. The p85 $\beta$ /p110 $\beta$  complex showed an increase in nuclear localisation, whereas cotransfection with PCNA rendered this complex completely nuclear (Fig. 31, results). A scheme on the mode of p110 $\beta$  nuclear translocation is presented (Fig. 2). Although PCNA does not have a NLS, it is a constitutively nuclear protein. CDK2 has been suggested to control PCNA translocation to the nucleus (**Koundrioukoff *et al.*, 2000**). Further study will increase understanding of the mechanism or identify other proteins that contribute to p110 $\beta$  nuclear translocation.

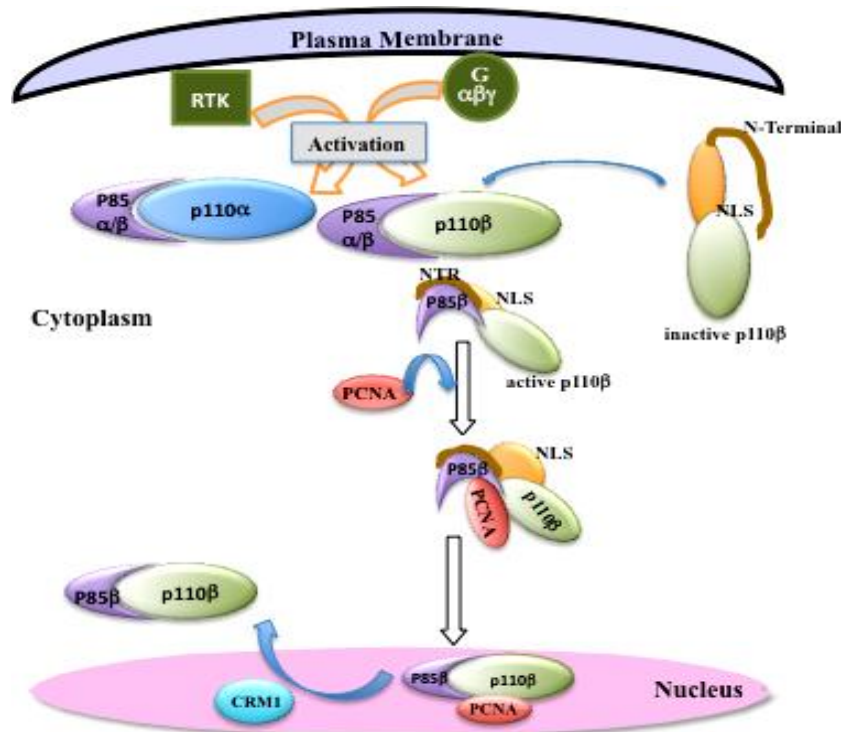


**Figure 2.** Model explaining possible mechanism of p110 $\beta$  nuclear localisation. Growth factor mediated activation of p85 $\beta$ /p110 $\beta$  results nuclear localisation aided by C2-domain NLS in p110 $\beta$ . The association of PCNA to p85 $\beta$ /p110 $\beta$  further enhances their nuclear translocation.

### **p110 $\beta$ is necessary for genomic stability and for activation of the DNA damage response after UV or IR exposure**

Our results indicated that p110 $\beta$  deletion gives rise to genomic instability, with chromosome breaks and altered chromosome structures due to aberrant junction. In addition, we found aneuploidy in p110 $\beta^{-/-}$  MEF, with an average chromosome number of 100-150. This led us to examine the role of p110 $\beta$  in DNA repair. Although several molecules that participate in the DNA damage response have been identified, the full spectrum of proteins that act in the cell response to DNA damage remains to be discovered. Here we show that p110 $\beta$  is essential for correct activation of the DNA repair pathway induced by UV and IR. DNA damage response (DDR) pathways coordinate a multi-step cascade, interactions among a multitude of proteins, DNA-protein complexes and checkpoint controls. Activation of the DNA repair pathway involves a complex network of checkpoint signalling molecules downstream of ATM and ATR. The differing requirements for ATM and ATR activation, as well as later differences in signalling partnerships remain unclear. We found radiation-dependent p110 $\beta$  association with RAD17, suggesting a specific role for p110 $\beta$ /RAD17 complexes in DNA repair. This hypothesis was further strengthened by the observation that in p110 $\beta$  shRNA-transfected cells, UV exposure led to cell death (in sub-G1 phase).

UV-induced activation of p38 MAPK signalling promotes cell death through regulation of p53 activity, by directly targeting p53 residues for phosphorylation (**Bulavin *et al.*, 1999**). Nonetheless, comparable levels of p38 pathway activation in control and p110 $\beta$  shRNA-transfected cells suggested the involvement of additional signalling pathways regulated by p110 $\beta$  in DNA repair. An increase in p110 $\beta$  kinase activity after UV or IR exposure shows that DNA damage induces p110 $\beta$  activity. **Bozulic *et al.*** recently reported PKB activation in response to DNA DSB (**Bozulic *et al.*, 2008**). They concluded that PKB $\alpha$  acts downstream of DNA-PK in DDR, where DNA-PK phosphorylates PKB at Ser473; in addition, they reported an increase in phosphorylation at Thr308 that is strictly PI3K-dependent. It is therefore possible that p110 $\beta$  activation regulates PKB activation following DSB.

Deletion of Chk1 results in hyperactivation of initiation of DNA replication (**Syljuåsen *et al.*, 2005**), a phenotype that correlates with hyperactivation of replication origins (**Maya-Mendoza *et al.*, 2007**). Results were similar in cells in which p110 $\beta$  kinase activity was inhibited, with hyperactivation of initiation of DNA replication and defective DNA elongation (**Marques *et al.*, 2009**). In addition, both ATR $^{-/-}$  and p110 $\beta^{-/-}$  mice are embryonic lethal, implying that ATR and p110 $\beta$  are essential for embryonic development (**Brown & Baltimore, 2000; Bi *et al.*, 2002**). As these defects were similar in both phenotypes, we postulated that p110 $\beta$  might regulate the ATR pathway.

Our studies indicate impaired activation of the ATR pathway in p110 $\beta$ -depleted cells; Chk1 and RAD17 phosphorylation was downregulated in these cells following UV or IR exposure. We also observed a diminished pRAD17 accumulation and focus formation in both p110 $\beta$ -inhibited and -depleted cells, although the effect was more profound in p110 $\beta$ -depleted cells. This could be due to the reported RAD17/9-1-1-mediated activation of ATR, where the RAD17-9-1-1 complex recruits the ATR-activating protein TopBP1 to DNA damage sites (**Kumagai *et al.*, 2006; Delacroix *et al.*, 2007; Lee *et al.*, 2007**).

We observed that p110 $\beta$  also regulates ATM autophosphorylation, which in turn controls the DDR after IR exposure. Following exposure of p110 $\beta$ -depleted cells to  $\gamma$ -irradiation, we observed defective ATM, Chk2 and SMC1 activation, resulting from the downregulation of upstream events in the ATM pathway. Indeed, IR-induced pATM focus formation was largely abolished in p110 $\beta$ -depleted cells; the remaining cellular pATM showed diffuse staining and rarely

formed distinctive foci. To further analyze whether p110 $\beta$  regulates upstream events in the ATM pathway, we examined immobilisation of NBS1 (a regulatory protein that acts early in the ATM pathway) at DNA damage areas and found defective migration of this protein. Formation of the MRN complex (Mre11, Rad50 and Nbs1) plays a critical role in DNA damage sensing, signalling and repair mechanisms, as well as in maintenance of the chromosomal integrity of the cell (**van den Bosch *et al.*, 2003; Kanaar & Wyman, 2008**). Our results indicated that defective NBS1 loading at DNA damage sites in p110 $\beta$ -depleted cells inactivated the ATM pathway. Previous studies showed that NBS1 associates with the p110 $\alpha$ , p110 $\beta$ , and p110 $\delta$  catalytic subunits of class I<sub>A</sub> PI3K (**Chen Y-C *et al.* 2008**). We propose that, of these, only the p110 $\beta$ /NBS1 complex resides in the nucleus. IR-induced  $\gamma$ -H2AX focus formation was barely detectable in p110 $\beta$ -depleted cells. In cells in which p110 $\beta$  kinase activity was inhibited using TGX221,  $\gamma$ -H2AX levels decreased, although less markedly than in p110 $\beta$ -depleted cells. We thus concluded that p110 $\beta$  is necessary for ATM pathway activation at the DNA damage-sensing stage, irrespective of the type of radiation exposure. p110 $\beta$  mobility to the micro-irradiated sites further demonstrated an integral role for p110 $\beta$  in the initiation of DNA damage responses.

p53-binding protein 1 (53BP1) participates in the cell response to DNA DSB, where it associates with various DNA repair proteins in a ATM-dependent manner (**Wang *et al.*, 2002; DiTullio *et al.*, 2002**). In our study, manipulation of the p110 $\beta$  signalling pathway resulted in defective 53BP1 recruitment to DNA damage sites. Translocation of 53BP1 to the damage sites was more severely affected in p110 $\beta$ -depleted than p110 $\beta$ -inhibited cells. The defect observed in GFP-53BP1 immobilisation in UV laser-induced DNA damage is in accordance with a defective DDR, as 53BP1 is an early participant in the cell response to DNA DSB (**Schultz *et al.*, 2000**) and contributes to activation of the checkpoint following recruitment (**Wang B. *et al.*, 2002**).

PCNA is a major factor in many features of DNA metabolism, such as DNA replication, NER (nucleotide excision repair), MMR (mismatch repair) and BER (base excision repair) (**Jónsson & Hübscher, 1997**). Here we showed rapid PCNA accumulation at UV laser-microirradiated sites, suggesting a role for PCNA in DSB repair. Our data are consistent with the previous observation that PCNA is needed for filling a single-strand DNA gap (**Torres-Ramos *et al.*, 1996**). PCNA might therefore be necessary for recruiting DNA polymerases or repair proteins to the DNA damage site, and not only for processive replication by DNA polymerases. In addition, Holmes and colleagues suggested that PCNA is a requirement for recruiting recombination proteins to DNA repair sites (**Holmes & Haber, 1999**). In support of this idea, our live imaging analysis in cells showed simultaneous mobilization of PCNA and NBS1 to the DNA damage sites following UV-laser treatment. We examined the effect of p110 $\beta$  on PCNA translocation to DNA damage system, and found that inhibition of p110 $\beta$  kinase activity retarded PCNA mobility. Moreover, p110 $\beta$  depletion greatly impaired PCNA localisation at DNA damage sites. We concluded that p110 $\beta$  acts as a scaffold to regulate PCNA loading onto chromatin following DNA damage.

Both p110 $\alpha$  and p110 $\beta$  knockout mice are reported to be non-viable. p110 $\alpha$ <sup>-/-</sup> mice die at embryonic day E9 (**Bi *et al.*, 1999,2002**) and p110 $\alpha$  kinase-dead (PIK3CA<sup>D933A/D933A</sup>) knock-in mice die at E10 (**Foukas *et al.*, 2006**). Like p110 $\alpha$ <sup>-/-</sup> mice, p110 $\alpha$  kinase-dead heterozygous mice (PIK3CA<sup>D933A/D933</sup>) not only show no oncogenic effects, but also in fact have proliferation defects (**Foukas *et al.*, 2006**). p110 $\alpha$  is described as the principal isoform responsible for cell hyperproliferation, as many human cancer types show miss-sense mutation hot spots in the p110 $\alpha$  gene (**Kang *et al.*, 2005; Samuels & Ericson, 2006**). These results indicate a kinase-dependent role for p110 $\alpha$ . Although their hypothesis remains to be confirmed, Irarrazabal *et al.* proposed that IR-mediated changes in chromatin structure could activate nuclear PI3K, leading in turn to ATM activation (**Irarrazabal *et al.*, 2006**). p110 $\beta$ <sup>-/-</sup> mice die very early (E3.5), which has been linked to a cell proliferation defect (**Bi *et al.*, 2002**). Jia *et al.* recently reported similar results, with a

description of retarded cell growth in p110 $\beta$ <sup>-/-</sup> MEF (Jia *et al.*, 2008). The p110 $\beta$  kinase-dead allele (PIK3CB<sup>K805R/K805R</sup>) (Ciraolo *et al.*, 2008) yields two distinct phenotypes. Viable mice show normal proliferation and high PIK3CB<sup>K805R/K805R</sup> protein expression; whereas mice with low PIK3CB<sup>K805R/K805R</sup> expression levels were embryonic lethal, demonstrating that p110 $\beta$  acts as a scaffold protein rather than as a kinase (Jia *et al.*, 2008).

The class I<sub>A</sub> p110 $\alpha$  catalytic isoform exhibit point mutations at hot spots in many tumour types, supporting the kinase-dependent function of p110 $\alpha$  (Kang *et al.*, 2005). p110 $\alpha$  mutations at amino acids E542K, E545K and H1047R are considered oncogenic gain-of-function mutations (Kang *et al.*, 2005; Zhao *et al.*, 2005). p110 $\beta$  overexpression is described in some tumours, but no mutations were found in the protein, which places in doubt the role of p110 $\beta$  as an oncogene (Benistant *et al.*, 2000; Knobbe & Reifemberger, 2003; Zhao *et al.*, 2005). Zhao *et al.* showed that p110 $\beta$  could be oncogenic, as addition of a myristoylation tag to p110 $\beta$  resulted in cell hyperproliferation (Zhao *et al.*, 2005). It is clear from our studies that p110 $\beta$  regulates both branches of the DSB response pathways. As class I PI3K have both lipid and protein kinase activities (Dhand *et al.*, 1994; Foukas *et al.*, 2004; Foukas & Shepherd, 2004), further study will help determine the role of p110 $\beta$  (as protein or lipid kinase) after IR/UV-induced activation.

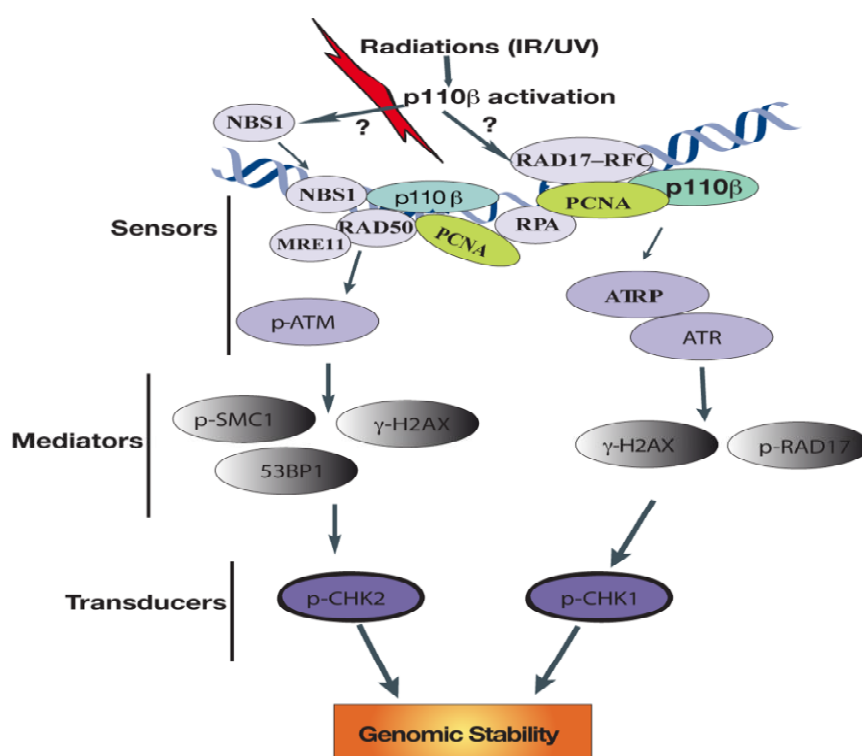


**Figure 3. Proposed model for p110 $\beta$ -mediated activation of ATR and ATM pathways in the DNA damage response (DDR).** p110 $\beta$  is activated by DNA double strand breaks (DSB), loads itself at the DNA damage sites immediately, and helps to recruit DNA sensor proteins NBS1 and PCNA simultaneously; these in turn recruit the apical protein kinase ATM, which undergoes autophosphorylation. Chk2 localizes transiently at DNA damage sites to be phosphorylated and activated by ATM. ATM translocation at damage sites stimulates various mediators, leading to Chk2 translocation to the damage area, where it is phosphorylated by ATM. H2AX phosphorylation further boosts accumulation of the DNA damage mediator 53BP1 at the damage site. Recruitment of p110 $\beta$  can also activate ATR pathway, where it regulates RAD17 phosphorylation. In addition, we propose that PCNA is recruited and might be able to replace 9-1-1 complex function, boosting ATR pathway activation and Chk1 phosphorylation.



## REFERENCES



- Abraham RT.** 2001. Cell cycle checkpoint signaling through the ATM and ATR kinases. *Genes & Development*, **15**; 2177-2198.
- Adhikary S and Eilers M.** 2005. Transcriptional regulation and transformation by Myc proteins. *Nat Rev Mol Cell Biol*, **6**(8); 635-45.
- Ahmed NN, Franke TF, Bellacosa A, Datta K, Gonzalez PM, Taguchi T, Testa JR and Tsichlis PN.** 1993. The proteins encoded by c-akt and v-akt differ in post-translational modification, subcellular localization and oncogenic potential. *Oncogene*, **8**; 1957-63.
- Alcántara-Hernández R, Casas-González P and García-Sáinz JA.** 2008. Roles of c-Src in alpha1B-adrenoceptor phosphorylation and desensitization. *Auton Autacoid Pharmacol*, **28**; 29-39.
- Alcázar I, Marqués M, Kumar A, Hirsch E, Wymann M, Carrera AC and Barber DF.** 2007. Phosphoinositide 3-kinase gamma participates in T cell receptor-induced T cell activation. *J Exp Med*, **204**; 2977-87.
- Álvarez B, Martínez AC, Burgering BM and Carrera AC.** 2001. Forkhead transcription factors contribute to execution of the mitotic programme in mammals. *Nature*, **413**; 744-747.
- Álvarez B, Garrido F, Garcia-Sanz JA and Carrera AC.** 2003. Phosphoinositide 3-kinase activation regulates cell division time by coordinated control of cell mass and cell cycle progression rate. *J. Biol. Chem*, **278**; 26466- 26473.
- Alvarado-Kristensson M, Melander F, Leandersson K, Rönnstrand L, Wernstedt C and Andersson T.** 2004. p38-MAPK signals survival by phosphorylation of caspase-8 and caspase-3 in human neutrophils. *J Exp Med*, **199**(4); 449-58.
- Alessi DR, Andjelkovic M, Caudwell B, Cron P, Morrice N, Cohen P and Hemmings BA.** 1996. Mechanism of activation of protein kinase B by insulin and IGF-1. *EMBO J*, **15**; 6541-51.
- Alessi DR, James SR, Dowens CP, Holmes AB, Gaffney PR, Reese CB and Cohen P.** 1997. Characterization of a 3-phosphoinositide-dependent protein kinase which phosphorylates and activates protein kinase Balpha. *Curr Biol*, **7**; 261-9.
- Alessi DR, Deak M, Casamayor A, Caudwell FB, Morrice N, Norman DG, Gaffney P, Reese CB, MacDougall CN, Harbison D, Ashworth A and Bownes M.** 1997. 3-Phosphoinositide-dependent protein kinase-1 (PDK1): structural and functional homology with the Drosophila DSTPK61 kinase. *Curr. Biol*, **7**; 776-789
- Alexandrow MG, Kawabata M, Aakre M and Moses HL.** 1995. Overexpression of the c-Myc oncoprotein blocks the growth-inhibitory response but is required for the mitogenic effects of transforming growth factor beta 1. *Proc. Natl Acad. Sci. USA*, **92**; 3239-3243.
- Alberts B, Johnson A, Lewis J, Raff M, Roberts K and Walter P.** 2004. *Molecular Biology of cell*, 4<sup>th</sup> edition, Garland Sciences.
- Alcántara-Hernández R, Casas-González P and García-Sáinz JA.** 2008. Roles of c-Src in alpha1B-adrenoceptor phosphorylation and desensitization. *Auton Autacoid Pharmacol*, **28**; 29-39.
- Amati B, Dalton S, Brooks MW, Littlewood TD, Evan GI and Land H.** 1992. Transcriptional activation by the human c-Myc oncoprotein in yeast requires interaction with Max. *Nature*, **359**(6394); 423-6.
- Amati B, Alevizopoulos BK and Vlach J.** 1998. Myc and the cell cycle. *Front. Biosci*, **3**; 250-268.



- Anderson KE, Coadwell J, Stephens LR and Hawkins PT.** 1998. Translocation of PDK-1 to the plasma membrane is important in allowing PDK-1 to activate protein kinase B. *Curr Biol*, **8**; 684-691.
- Andjelkovic M, Alessi DR, Meier R, Fernandez A, Lamb NJ, Frech M, Cron P, Cohen P, Lucocq JM and Hemmings BA.** 1997. Role of translocation in the activation and function of protein kinase B. *J. Biol.Chem*, **272**; 31515-24.
- Assoian RK and Zhu X.** 1997. Cell anchorage and the cytoskeleton as partners in growth factor dependent cell cycle progression. *Curr. Opin. Cell Biol*, **9**(1); 93-8.
- Auger KR, Serunian LA, Soltoff SP, Lobby P and Cantley LC.** 1989. PDGF-dependent tyrosine phosphorylation stimulates production of novel polyphosphoinositides in intact cells. *Cell*, **57**(1); 167-75.
- Bachman KE, Argani P, Samuels Y, Silliman N, Ptak J, Szabo S, Konishi H, Karakas B, Blair BG, Lin C, Peters BA, Velculescu VE, Park BH.** 2004. The PIK3CA gene is mutated with high frequency in human breast cancers. *Cancer Biol Ther*, **3**; 772-775.
- Bakkenist CJ, and Kastan MB.** 2003. DNA damage activates ATM through intermolecular autophosphorylation and dimer dissociation. *Nature*, **421**(6922); 499-506.
- Ban  th JP and Olive PL.** 2003. Expression of phosphorylated histone H2AX as a surrogate of cell killing by drugs that create DNA double-strand breaks. *Cancer Res*, **63**(15); 4347-50.
- Bao S, Tibbetts RS, Brumbaugh KM, Fang Y, Richardson DA, Ali A, Chen SM, Abraham RT, Wang XF.** 2001. ATR/ATM-mediated phosphorylation of human Rad17 is required for genotoxic stress responses. *Nature*, **411**; 969-74.
- Barone MV and Courtneidge S.** 1995. Myc but not Fos rescue of a PDGF signalling block by kinase-inactive Src. *Nature*, **378**; 509- 12.
- Bartek J and Lukas J.** 2003. DNA repair; Damage alert. *Nature*, **421**; 486-488.
- Barsky D, Venclovas C.** 2005. DNA sliding clamps; just the right twist to load onto DNA. *Curr Biol*, **15**; 989-92.
- Bazenet CE and Kazlaukas A.** 1994. The PDGF receptor alpha subunit activates p21ras and triggers DNA synthesis without interacting with rasGAP. *Oncogen*, **9** (2); 517-25.
- Bekker-Jensen S, Lukas C, Melander F, Bartek J and Lukas J.** 2005. Dynamic assembly and sustained retention of 53BP1 at the sites of DNA damage are controlled by Mdc1/NFBD1. *J Cell Biol*, **170**(2); 201-11.
- B  nistant C, Chapuis H and Roche S.** 2000. A specific function for phosphatidylinositol 3-kinase alpha (p85alpha-p110alpha) in cell survival and for phosphatidylinositol 3-kinase beta (p85alpha-p110beta) in de novo DNA synthesis of human colon carcinoma cells. *Oncogene*, **19**(44); 5083-90.
- Bermudez VP, Lindsey-Boltz LA, Cesare AJ, Maniwa Y, Griffith JD, Hurwitz J. and Sancar A.** 2003. Loading of the human 9-1-1 checkpoint complex onto DNA by the checkpoint clamp loader hRad17-replication factor C complex in vitro. *Proc. Natl. Acad. Sci. USA*, **100**; 1633-38.
- Berwanger B, Hartmann O, Bergmann E, Bernard S, Nielsen D, Krause M, Kartal A, Flynn D, Wiedemeyer R, Schwab M, Sch  fer H, Christiansen H and Eilers M.** 2002. Loss of a FYN-regulated differentiation and growth arrest pathway in advanced stage neuroblastoma. *Cancer Cell*, **2**(5); 377-86.
- Bi L, Okabe I, Bernard DJ and Nussbaum RL.** 2002. Early embryonic lethality in mice deficient in the p110beta catalytic subunit of PI 3- kinase. *Mamm Genome*, **13**; 169-172.
- Bi L, Okabe I, Bernard DJ, Wynshaw-Boris A and Nussbaum RL.** 1999. Proliferative defect

and embryonic lethality in mice homozygous for a deletion in the p110 $\alpha$  subunit of phosphoinositide 3-kinase. *J Biol Chem*, **274**; 10963-10968.

**Blain SW, Montalvo E and Massague J.** 1997. Differential interaction of the cyclin-dependent kinase (Cdk) inhibitor p27Kip1 with cyclin A-Cdk2 and cyclin D2-Cdk4. *J. Biol. Chem*, **272**; 25863-25872.

**Bloom J. and Pagano M.** 2003. Deregulated degradation of the cdk inhibitor p27 and malignant transformation, *Semin. Cancer Biol*, **13**; 41-47.

**Blow JJ and A. Dutta.** 2005. Preventing re-replication of chromosomal DNA. *Nat. Rev. Mol. Cell Biol*, **6**; 476-486.

**Brandts CH, Sargin B, Rode M, Biermann C, Lindtner B, Schwäble J, Buerger H, Müller Tidow C, Choudhary C, McMahon M, Berdel WE and Serve H.** 2005. Constitutive activation of Akt by Flt3 internal tandem duplications is necessary for increased survival, proliferation, and myeloid transformation. *Cancer Res*, **65**(21); 9643-50.

**Brazil DP, Hemmings BA.** 2001. Ten years of protein kinase B signalling; a hard Akt to follow. *Trends Biochem. Sci*, **26**; 657-664.

**Brennan P, Babbage JW, Burgering BM, Groner B, Reif K and Cantrell DA.** 1997. Phosphatidylinositol 3-kinase couples the interleukin-2 receptor to the cell cycle regulator E2F. *Immunity*, **7**; 679-689.

**Brehm A, Miska EA, McCance DJ, Reid JL, Bannister AJ and Kouzarides T.** 1998. Retinoblastoma protein recruits histone deacetylase to repress transcription. *Nature*, **391**; 597-601.

**Broderick DK, Di C, Parrett TJ, Samuels YR, Cummins JM, McLendon RE, Fults DW, Velculescu VE, Bigner DD, Yan H.** 2004. Mutations of PIK3CA in anaplastic oligodendrogliomas, high-grade astrocytomas, and medulloblastomas. *Cancer Res*, **64**; 5048-5050.

**Brunet A, Bonni A, Zigmond MJ, Lin MZ, Juo P, Hu LS, Anderson MJ, Arden KC, Blenis J and Greenberg ME.** 1999. Akt promotes cell survival by phosphorylating and inhibiting a Forkhead transcription factor. *Cell*, **96**; 857-68.

**Boronenkov IV, Loijens JC, Umeda M, Anderson RA.** 1998. Phosphoinositide signaling pathways in nuclei are associated with nuclear speckles containing pre-mRNA processing factors. *Mol Biol Cell*, **9**; 3547-60.

**Bouchard C, Marquardt J, Bras A, Medema RH and Eilers M.** 2004. Myc-induced proliferation and transformation require Akt-mediated phosphorylation of FoxO proteins. *EMBO J*, **23**; 2830-2840.

**Bozulic L, Surucu B, Hynx D and Hemmings BA.** 2008. PKB[ $\alpha$ ]/Akt1 Acts Downstream of DNA-PK in the DNA Double-Strand Break Response and Promotes Survival. *Molecular Cell*, **30**; 203-213.

**Brown EJ and Baltimore D.** 2000. ATR disruption leads to chromosomal fragmentation and early embryonic lethality. *Genes Dev*, **14**(4); 397-402.

**Brunet A, Bonni A, Zigmond MJ, Lin LZ, Juo P, Hu LS, Anderson MJ, Arden KC, Burgering BM and Medema RH.** 2002. Cell Cycle Inhibition by FoxO Forkhead Transcription Factors involves downregulation of Cyclin D. *Mol Cell Biol*, **22**; 7842-7852.

- Buchkovich K, Duffy LA and Harlow E.** 1989. The retinoblastoma protein is phosphorylated during specific phases of the cell cycle. *Cell*, **58**; 1097-1105.
- Bulavin DV, Saito S, Hollander MC, Sakaguchi K, Anderson CW, Appella E and Fornace AJ Jr.** 1999. Phosphorylation of human p53 by p38 kinase coordinates N-terminal phosphorylation and apoptosis in response to UV radiation. *EMBO J*, **18**(23); 6845-54.
- Bunney TD, Watkins PA, Beven AF, Shaw PJ, Hernandez LE, Lomonosoff GP, Shanks M, Peart J and Drobak BK.** 2000. Association of phosphatidylinositol 3-kinase with nuclear transcription sites in higher plants. *Plant Cell*, **12**; 1679-88.
- Burma S, Chen BP, Murphy M, Kurimasa A and Chen DJ.** 2001. ATM phosphorylates histone H2AX in response to DNA double-strand breaks. *J Biol Chem*, **276**(45); 42462-7.
- Calzada A, Sanchez M, Sanchez E and Bueno A.** 2000. The stability of the Cdc6 protein is regulated by cyclin-dependent kinase/cyclin B complexes in *Saccharomyces cerevisiae*. *J. Biol. Chem*, **275**; 9734-9741.
- Campbell IG, Russell SE, Choong DY, Montgomery KG, Ciavarella ML, Hooi CS, Cristiano BE, Pearson RB and Phillips WA.** 2004. Mutation of the PIK3CA gene in ovarian and breast cancer. *Cancer Res*, **64**; 7678-7681.
- Cantley LC, Auger KR, Carpenter C, Duckworth B, Graziani A, Kapeller R and Soltoff S.** 1991. Oncogenes and signal transduction. *Cell*, **64**(2); 281-302.
- Cantley LC.** 2002. The phosphoinositide 3-kinase pathway. *Science*, **296**; 1655-1657.
- Cappellini A, Tabellini G, Zweyer M, Bortul R, Tazzari PL, Billi AM, Falà F, Cocco L and Martelli AM.** 2003. The phosphoinositide 3-kinase/Akt pathway regulates cell cycle progression of HL60 human leukemia cells through cytoplasmic relocalization of the cyclin-dependent kinase inhibitor p27Kip1 and control of cyclin D1 expression. *Leukemia*, **17**; 2157-67.
- Carnero A and Hannon G.** 1998. The INK4 family of CDK inhibitors. *Curr. Top. Microbiol. Immunol*, **227**; 43-55.
- Carney JP.** 1998. The hMRE11/hRAD50 protein complex and Nijmegen breakage syndrome; linkage of double-strand break repair to the cellular DNA damage response. *Cell*, **12**; 477-486.
- Casamayor A, Morrice NA and Alessi DR.** 1999. Phosphorylation of Ser-241 is essential for the activity of 3-phosphoinositide-dependent protein kinase-1; identification of five sites of phosphorylation in vivo. *Biochem J*, **342**; 287-92.
- Caspari T.** 2000. How to activate p53. *Curr Biol*, **10**(8); 315-7.
- Chan TO, Rodeck U, Chan AM, Kimmelman AC, Rittenhouse SE, Panayotou G and Tsichlis PN.** 2002. Small GTPases and tyrosine kinases coregulate a molecular switch in the phosphoinositide 3-kinase regulatory subunit. *Cancer Cell*, **1**; 181-191.
- Chen YC, Chiang HY, Yang MH, Chen PM, Chang SY, Teng SC, Vanhaesebroeck B and Wu KJ.** 2008. Activation of phosphoinositide 3-kinase by the NBS1 DNA repair protein through a novel activation motif. *Journal of molecular medicine (Berlin, Germany)* **86**(4); 401-12.
- Cheng M, Olivier P, Diehl JA, Fero M, Roussel MF, Roberts JM and Sherr CJ.** 1999. The p21(Cip1) and p27(Kip1) CDK 'inhibitors' are essential activators of cyclin D-dependent kinases in murine fibroblasts. *EMBO J*, **18**; 1571-1583.

- Chan TO, Rittenhouse SE and Tsichlis PN.** 1999. Akt/PKB and other D3 phosphoinositide-regulated kinases; kinase activation by phosphoinositide-dependent phosphorylation. *Annu. Rev. Biochem.* **68**; 965-1014.
- Ciraolo E, Iezzi M, Marone R, Marengo S, Curcio C, Costa C, Azzolino O, Gonella C, Rubinetto C, Wu H, Dastrù W, Martin EL, Silengo L, Altruda F, Turco E, Lanzetti L, Musiani P, Rückle T, Rommel C, Backer JM, Forni G, Wymann MP and Hirsch E.** Phosphoinositide 3-kinase p110beta activity: key role in metabolism and mammary gland cancer but not development. 2008. *Science Signal*, **1**(36); ra3.
- Cliby WA, Roberts CJ, Cimprich KA, Stringer CM, Lamb JR, Schreiber SL and Friend SH.** 1998. Overexpression of a kinase-inactive ATR protein causes sensitivity to DNA-damaging agents and defects in cell cycle checkpoints. *EMBO J*, **17**(1); 159-69.
- Cortez D, Wang Y, Qin J and Elledge SJ.** 1999. Requirement of ATM-dependent phosphorylation of brca1 in the DNA damage response to double-strand breaks. *Science*, **286**; 1162-66.
- Cortez D, Guntuku S, Qin J and Elledge SJ.** 2001. ATR and ATRIP; partners in checkpoint signaling. *Science*, **294**(5547); 1713-6.
- Cohen P, Alessi DR, Cross DA.** 1997. PDK1, one of the missing links in insulin signal transduction? *FEBS Lett.* **410**; 3-10.
- Cole MD and Nikiforov MA.** 2006. Transcriptional activation by the Myc oncoprotein. *Curr Top Microbiol Immunol*, **302**; 33-50.
- Coverley D, Laman H and Laskey RA.** 2002. Distinct roles for cyclins E and A during DNA replication complex assembly and activation. *Nat. Cell Biol*, **4**; 523-528.
- Cully M, You H, Levine AJ and Mak TW.** 2006. Beyond PTEN mutations; the PI3K pathway as an integrator of multiple inputs during tumorigenesis. *Nat Rev Cancer*, **6**; 184-192.
- Cvetcic CA and Walter JC.** 2006. Getting a grip on licensing; mechanism of stable Mcm2-7 loading onto replication origins. *Mol. Cell*, **21**; 143-144.
- Dang CV.** 1999. c-Myc target genes involved in cell growth, apoptosis and metabolism. *Mol. Cell. Biol*, **19**; 1-11.
- Datta SR, Brunet A and Greenberg ME.** 1999. Cellular survival; a play in three Akts. *Genes Dev*, **13**; 2905-2927.
- Datta SR, Dudek H, Tao X, Masters S, Fu H, Gotoh Y and Greenberg ME.** 1997. Akt phosphorylation of BAD couples survival signals to the cell-intrinsic death machinery. *Cell*, **91**; 231-241.
- Davis AC, Wims M, Spotts GD, Hann SR and Bradley A.** 1993. A null c-myc mutation causes lethality before 10.5 days of gestation in homozygous and reduced fertility in heterozygous female mice. *Genes Dev*, **7**; 671-82.
- del Real G, Jimenez-Baranda S, Mira E, Lacalle RA, Lucas P, Gomez-Mouton C, Alegret M, Pena JM, Rodriguez-Zapata M, Alvarez-Mon M, Martinez AC and Mañes S.** 2004. Statins inhibit HIV-1 infection by down-regulating Rho activity. *J. Exp. Med*, **200**; 541-547.
- de Klein A, Muijtjens M, van Os R, Verhoeven Y, Smit B, Carr AM, Lehmann AR and Hoeijmakers JH.** 2000. Targeted disruption of the cell-cycle checkpoint gene ATR leads to early

embryonic lethality in mice. *Curr Biol*, **10**(8); 479-82.

**Delacroix S, Wagner JM, Kobayashi M, Yamamoto K and Karnitz LM.** 2007. The Rad9-Hus1-Rad1 (9-1-1) clamp activates checkpoint signaling via TopBP1. *Genes Dev*, **21**(12); 1472-7.

**Deng X, Mercer SE, Shah S, Ewton DZ and Friedman E.** 2004. The Cyclin-dependent Kinase inhibitor p27Kip1 is Stabilized in G0 by Mirk/dyrk1B Kinase. *J. Biol. Chem*, **279**; 22498-22504.

**DePamphilis ML.** 2003. The 'ORC cycle'; a novel pathway for regulating eukaryotic DNA replication. *Gene*, **310**; 1-15.

**Dhand R, Hiles I, Panayotou G, Roche S, Fry MJ, Gout I, Totty N F, Truong O, Vicendo P and Yonezawa K.** 1994. PI 3-kinase is a dual specificity enzyme: autoregulation by an intrinsic protein-serine kinase activity. *EMBO J* 13: 522-533.

**Didichenko SA and Thelen M.** 2001. Phosphatidylinositol 3-kinase c2alpha contains a nuclear localization sequence and associates with nuclear speckles. *J Biol Chem*, **276**(51); 48135-42.

**Dijkers PF, Medema RH, Pals C, Banerji L, Thomas NS, Lam EW, Burgering BM, Raaijmakers JA, Lammers JW, Koenderman L and Coffey PJ.** 2000. Forkhead transcription factor FKHR-L1 modulates cytokine-dependent transcriptional regulation of p27(KIP1). *Mol. Cell. Biol*, **20**; 9138-9148.

**DiTullio RA Jr, Mochan TA, Venere M, Bartkova J, Sehested M, Bartek J and Halazonetis TD.** 2002. 53BP1 functions in an ATM-dependent checkpoint pathway that is constitutively activated in human cancer. *Nature Cell Biology*, **4**; 998-1002.

**Domínguez-Cáceres MA, García-Martínez JM, Calcabrini A, González L, Porque PG, León J and Martín-Pérez J.** 2004. Prolactin induces c-Myc expression and cell survival through activation of Src/Akt pathway in lymphoid cells. *Oncogene*, **23**, 7378-7390.

**Downward J.** 2004. PI 3-kinase, Akt and cell survival. *Semin Cell Dev Biol*, **15**; 177-182.

**Downward J.** 2003. Targeting RAS signalling pathways in cancer therapy. *Nature Reviews Cancer*, **3**; 11-22

**Drury LS, Perkins G and Diffley JF.** 2000. The cyclin-dependent kinase Cdc28p regulates distinct modes of Cdc6p proteolysis during the budding yeast cell cycle. *Curr. Biol*, **10**; 231-240.

**Dudek H, Datta SR, Franke TF, Birnbaum MJ, Yao R, Cooper GM, Segal RA, Kaplan DR, and Greenberg ME.** 1997. Regulation of neuronal survival by the serine-threonine protein kinase Akt. *Science*, **275**; 661-665.

**Dupré DJ, Robitaille M, Rebois Rv and Hébert TE.** 2009. The Role of Gβγ Subunits in the Organization, Assembly, and Function of GPCR Signaling Complexes. *Annu. Rev. Pharmacology and Toxicology*, **49**; 31-56.

**Durocher D and Jackson SP.** 2001. DNA-PK, ATM and ATR as sensors of DNA damage; variations on a theme? *Curr. Opin. Cell Biol.*, **13**; 225-31.

**Dutil EM, Toser A and Newton AC.** 1998. Regulation of conventional protein kinase C isozymes by phosphoinositide-dependent kinase 1 (PDK-1). *Curr Biol*, **8**; 1366-75.

**Ekholm-Reed S, Mendez J, Tedesco D, Zetterberg A, Stillman B and Reed SI.** 2004. Deregulation of cyclin E in human cells interferes with prereplication complex assembly. *J. Cell Biol.*, **165**; 789-800.

- Ekholm SV and Reed SI.** 2000. Regulation of G(1) cyclin-dependent kinases in the mammalian cell cycle. *Curr Opin Cell Biol*, **12**; 676-684.
- Elledge SJ, Harper JW.** 1998. The role of protein stability in the cell cycle and cancer. *Biochim Biophys Acta*, **1377**(2); 61-70.
- Engelman JA, Luo J and Cantley LC.** 2006. The evolution of phosphatidylinositol 3-kinases as regulators of growth and metabolism, **7**; 606-619.
- Erisman MD, Rothberg PG, Diehl RE, Morse CC, Spandorfer JM and Astrin SM.** 1985. Deregulation of c-myc gene expression in human colon carcinoma is not accompanied by amplification or rearrangement of the gene. *Mol. Cell. Biol*, **5**; 1969-1976.
- Falck JJ and Jackson SP.** 2005. Conserved modes of recruitment of ATM, ATR and DNA-PK to site of DNA damage. *Nature*, **434**; 605-611.
- Fernandez-Capetillo O, Celeste A and Nussenzweig A.** 2003. Focusing on foci; H2AX and the recruitment of DNA-damage response factors. *Cell Cycle*, **2**(5); 426-7.
- Fornerod M, Ohno M, Yoshida M, and Mattaj IW.** 1997. CRM1 is an export receptor for leucine-rich nuclear exportsignals. *Cell*, **90**; 1051-1060.
- Foukas LC, Claret M, Pearce W, Okkenhaug K, Meek S, Peskett E, Sancho S, Smith A, Withers D and Vanhaesebroeck B.** 2006. Critical role for the p110 phosphoinositide-3-OH kinase in growth and metabolic regulation. *Nature*, **441**; 366-370.
- Foukas LC, Beeton CA, Jensen J, Phillips WA and Shepherd PR.** 2004. Regulation of phosphoinositide 3-kinase by its intrinsic serine kinase activity in vivo. *Mol Cell Biol*, **24**; 966-975.
- Foukas LC and Shepherd PR.** 2004. Phosphoinositide 3-kinase: the protein kinase that time forgot. *Biochem Soc Trans*, **32**; 330-331.
- Franke TF, Hornik CP, Segev L, Shostak GA and Sugimoto C.** 2003. PI3K/Akt and apoptosis; size matters. *Oncogene*, **22**; 8983-8998.
- Franke TF, Kaplan DR, Cantley LC and Toker A.** 1997. Direct regulation of the Akt proto-oncogene product by phosphatidylinositol-3,4-bisphosphate. *Science*, **275**; 665-8.
- Frech M, Andjelkovic M , Ingley E, Reddy KK, Falck JR and Hemmings BA.** 1997. High affinity binding of inositol phosphates and phos- phoinositides to the Pleckstrin homology domain of RAC protein kinase B and their influence on kinase activity. *J. Biol. Chem.*, **272**; 8474-8481.
- Friesner JD, Liu B, Culligan K and Britt AB.** 2005. Ionizing radiation-dependent gamma-H2AX focus formation requires ataxia telangiectasia mutated and ataxia telangiectasia mutated and Rad3-related. *Mol Biol Cell*, **16**(5); 2566-76.
- Frye M, Gardner C, Li ER, Arnold I and Watt FM.** 2003. Evidence that Myc activation depletes the epidermal stem cell compartment by modulating adhesive interactions with the local microenvironment. *Development*, **130**(12); 2793-808.
- Fruman DA.** 2004. Towards an understanding of isoform specificity in phosphoinositide 3-kinase signalling in lymphocytes. *Biochem Soc Tran*, **32**; 315-319.
- Gaestel M.** 2006. MAPKAP kinases-MKs- two's company, three's a crowd. *Nature Reviews Molecular Cell Biology*, **7**; 120 - 130.
- Gaidarov I, Smith ME, Domin J and Keen JH.** 2001. The class II phosphoinositide 3-kinase

- C2alpha is activated by clathrin and regulates clathrin-mediated membrane trafficking. *Mol Cell*, **7**; 443-9.
- Gallo KA and Johnson GL.** 2002. Mixed-lineage kinase control of JNK and p38 MAPK pathways. *Nat. Rev. Mol. Cell Biol.*, **3**; 663-72.
- García Z, Kumar A, Marques M, Cortes I and Carrera AC.** 2006. Phospho-inositide 3-kinase controls early and late events in mammalian cell division. *EMBO J*, **25**; 655-661.
- Gebhardt A, Frye M, Herold S, Benitah SA, Braun K, Samans B, Watt FM, Elsässer HP and Eilers M.** 2006. Myc regulates keratinocyte adhesion and differentiation via complex formation with Miz1. *J Cell Biol*, **172**(1); 139-49.
- Geering B, Cutillas PR, Nock G, Gharbi SI and Vanhaesebroeck B.** 2007. Class IA phosphoinositide 3-kinases are obligate p85-p110 heterodimers. *Proc Natl Acad Sci USA*, **104**; 7809-14.
- Geng Y, Eaton EN, Picón M, Roberts JM, Lunderg AS, Gifford A, Sardet C and Weinberg RA.** 1996. Regulation of cyclin E transcription by E2Fs and retinoblastoma protein. *Oncogene*, **12**; 1173-80.
- Geng Y, Yu Q, Sicinska E, Das M, Schneider JE, Bhattacharya S, Rideout WM, Bronson RT, Gardner H and Sicinski P.** 2003. Cyclin E ablation in the mouse. *Cell*, **114**; 431-443.
- Giman MP and Pirola L.** 1998. Structure and function of phosphoinositide 3-kinases. *Biochim Biophys Acta*, **1436**; 127-50.
- Ginisty H, Sicard H, Roger B and Bouvet P.** 1999. Structure and functions of nucleolin. *J. Cell Sci*, **112**; 761.
- Girard F, Strausfeld U, Fernandez A and Lamb NJ.** 1991. Cyclin A is required for the onset of DNA replication in mammalian fibroblasts. *Cell*, **67**(6); 1169-79.
- Goldberg M, Stucki M, Falck J, D'Amours D, Rahman D, Pappin D, Bartek J and Jackson SP.** 2003. MDC1 is required for the intra-S-phase DNA damage checkpoint. *Nature*, **421**; 952-56.
- Grandori C, Cowley SM, James LP and Eisenman RN.** 2000. The Myc/Max/Mad network and the transcriptional control of cell behavior. *Annu. Rev. Cell Dev. Biol*, **16**; 653-699.
- Graupera M, Guillermet-Guibert J, Foukas LC, Phng LK, Cain RJ, Salpekar A, Pearce W, Meek S, Millan J, Cutillas PR, Smith AJ, Ridley AJ, Ruhrberg C, Gerhardt H and Vanhaesebroeck B.** 2008. Angiogenesis selectively requires the p110alpha isoform of PI3K to control endothelial cell migration. *Nature*, **453**; 662-6.
- Grinberg AV, Hu CD, Kerppola TK.** 2004. Visualization of Myc/Max/Mad family dimers and the competition for dimerization in living cells. *Mol Cell Biol*, **24**(10); 4294-308.
- Griner EM and Kazanietz MG.** 2007. Protein kinase C and other diacylglycerol effectors in cancer. *Nature Reviews Cancer*, **7**; 281-294.
- Harbour JW and Dean DC.** 2000. The Rb/E2F pathway; expanding roles and emerging paradigms. *Genes Dev*, **14**; 2393-2409.
- Harper JW, Elledge SJ, Keyomarsi K, Dynlacht B, Tsai LH, Zhang P, Dobrowolski S, Bai C, Connell-Crowley L and Swindell E.** 1995. Inhibition of cyclin-dependent kinases by p21, *Mol. Biol. Cell*. **6**; 387-400.

- Hatton KS, Mahon K, Chin L, Chiu FC, Lee HW, Peng D, Morgenbesser SD, Horner J and Depinho RA.** 1996. Expression and Activity of L-Myc in Normal Mouse Development. *Mol. Cell. Biol*, **16**;1794-804.
- Hemann MT, Bric A, Teruya-Feldstein J, Herbst A, Nilsson JA, Cordon-Cardo C, Cleveland JL, Tansey WP and Lowe SW.** 2005. Evasion of the p53 tumour surveillance network by tumour-derived MYC mutants. *Nature*, **436**; 807-811.
- Herold S, Wanzel M, Beuger V, Frohme C, Beul D, Hillukkala T, Syvaoja J, Saluz HP, Haenel F and Eilers M.** 2002. Negative regulation of the mammalian UV response by Myc through association with Miz-1. *Mol Cell*, **10**(3); 509-21.
- Hiles ID, Otsu M, Volinia, S, Fry MJ, Gout I, Dhand, R, Panayotou G, Ruiz LF, Thompson A, Totty NF, Hsuan JJ, Courtneidge SA, Parker PJ and Waterfield MD.** 1992. Phosphatidylinositol 3-kinase; structure and expression of the 110 kd catalytic subunit. *Cell*, **70**, 419-429.
- Hirao A, Kong YY, Matsuoka S, Wakeham A, Ruland J, Yoshida H, Liu D, Elledge SJ and Mak TW.** 2000. DNA damage-induced activation of p53 by the checkpoint kinase Chk2. *Science*, **287**; 1824-27.
- Holmes AM and Haber JE.** 1999. Double-strand break repair in yeast requires both leading and lagging strand DNA polymerases. *Cell*, **96**(3); 415-24.
- Hooker CW and Hurlin PJ.** 2006. Of Myc and Mnt. *Journal of Cell Science*, **119**; 208-216.
- Hu P, Mondino A, Skolnik EY and Schlessinger J.** 1993. Cloning of a novel, ubiquitously expressed human phosphatidylinositol 3-kinase and identification of its binding site on p85. *Mol Cell Biol*, **13**; 7677-7688.
- Hua XH and Newport J.** 1998. Identification of a preinitiation step in DNA replication that is independent of origin recognition complex and cdc6, but dependent on cdk2. *J. Cell Biol*, **140**; 271-281.
- Huang CH, Mandelker D, Schmidt-Kittler O, Samuels Y, Velculescu VE, Kinzler KW, Vogelstein B, Gabelli SB and Amzel LM.** 2007. The Structure of a Human p110/p85 Complex Elucidates the Effects of Oncogenic PI3K Mutations. *Science*, **318**; 1744 -1748.
- Hubbard SR and Till JH.** 2000. Protein tyrosine kinase structure and function. *Annu Rev Biochem*, **69**; 373-98.
- Hupfeld CJ and Olefsky JM.** 2007. Regulation of receptor tyrosine kinase signaling by GRKs and beta-arrestins. *Annu. Rev. Physiology* **69**; 561-77
- Irvine RF.** 2003. Nuclear lipid signalling Mixed-lineage kinase control of JNK and p38 MAPK pathways. *Nature Reviews Molecular Cell Biology*, **4**; 349-361.
- Irarrazabal CE, Burg MB, Ward SG and Ferraris JD.** 2006. Phosphatidylinositol 3-kinase mediates activation of ATM by high NaCl and by ionizing radiation: Role in osmoprotective transcriptional regulation. *Proc Natl Acad Sci USA*, **103**(23); 8882-7.
- Jackson SP, Schoenwaelder SM, Goncalves I, Nesbitt WS, Wright CE, Yap CL, Kenche V, Anderson KE, Dopheide SM, Yuan Y, Sturgeon SA, Prabakaran H, Thompson PE, Smith GD, Shepherd PR, Daniele N, Kulkarni S, Abbott B, Saylik D, Jones C, Lu L, Giuliano S, Hughan SC, Angus JA, Robertson AD & Salem HH.** 2005. PI 3-kinase p110; a new target for antithrombotic therapy. *Nat. Med.*, **11**; 507-514.



- Jackson SP, Yap CL and Anderson KE.** 2004. Phosphoinositide 3-kinases and the regulation of platelet function. *Biochemical Society Transactions*, **32**; 387-392.
- Jia S, Liu Z, Zhang S, Liu P, Zhang L, Lee SH, Zhang J, Signoretti S, Loda M, Roberts TM and Zhao JJ.** 2008. Essential roles of PI(3)K-p110beta in cell growth, metabolism and tumorigenesis. *Nature*, **454**(7205); 776-9.
- Jiménez C, Hernandez C, Pimentel B and Carrera AC.** 2002. The p85 regulatory subunit controls sequential activation of phosphoinositide 3-kinase by Tyr kinases and Ras. *J. Biol. Chem*, **277**; 41556-41562.
- Jimenez C, Jones DR, Rodríguez-Viciana P, Gonzalez-García A, Leonardo E, Wennström S, von Kobbe C, Toran JL, R-Borlado L, Calvo V, Copin SG, Albar JP, Gaspar ML, Diez E, Marcos MA, Downward J, Martinez-A C, Mérida I and Carrera AC.** 1998. Identification and characterization of a new oncogene derived from the regulatory subunit of phosphoinositide 3-kinase. *EMBO J*, **17**(3); 743-53.
- Jirmanova L, Afanassieff M, Gobert-Gosse S, Markossian S and Savatier P.** 2002. Differential contributions of ERK and PI3K to the regulation of cyclin D1 expression and to the control of the G1/S transition in mouse ES cells. *Oncogene*, **21**; 5515-5528.
- Johnson A and O'Donnell M.** 2005. Cellular DNA Replicases; Components and Dynamics at the Replication Fork. *Ann. Rev. Biochem.*, **74**; 283-315.
- Joly M, Kazlaukas A, Fay FS and Corvera S.** 1994. Disruption of PDGF receptor trafficking by mutation of its PI-3 kinase binding sites. *Science*, **263**; 684-7.
- Jones SM and Kazlauskas A.** 2000. Connecting signaling and cell cycle progression in growth factor-stimulated cells. *Oncogene*, **19**; 5558 - 5567.
- Jones SM and Kazlauskas A.** 2001. Growth-factor-dependent mitogenesis requires two distinct phases of signalling. *Nat. Cell Biol*, **3**; 165-172.
- Jones SM and Kazlauskas A.** 2001. Growth Factor-Dependent Signaling and Cell Cycle Progression. *Chem. Rev*, **101**; 2413-2424.
- Jones SM, Klinghoffer R, Prestwich GD, Toker A and Kazlauskas A.** 1999. PDGF induces an early and a late wave of PI 3-kinase activity, and only the late wave is required for progression through G1. *Curr. Biol*, **9**; 512-521.
- Jónsson ZO and Hübscher U.** 1997. Proliferating cell nuclear antigen: more than a clamp for DNA polymerases. *Bioessays*. **19**(11); 967-75.
- Kaczmarek L, Hyland JK, Watt R, Rosenberg M and Baserga R.** 1985. Microinjected c-myc as a competence factor. *Science*, **228**(4705); 1313-5.
- Kaffman A and O'Shea EK.** 1999. Regulation of nuclear localization. *Ann. Rev. Cell and Dev. Biol*, **15**; 291-339.
- Kanaar R and Wyman C.** 2008. DNA Repair by the MRN Complex; Break It to Make It. *Cell*, **135**(1); 14-16,
- Kang S, Bader AG and Vogt PK.** 2005. Phosphatidylinositol 3-kinase mutations identified in human cancer are oncogenic. *Proc. Natl. Acad. Sci. USA*, **102**; 802-807
- Kaplan DR, Whitman M, Schaffhausen B, Pallas DC, White M, Cantley L and Roberts TM.**

1987. Common elements in growth factor stimulation and oncogenic transformation; 85 kd phosphoprotein and phosphatidylinositol kinase activity. *Cell*, **50**(7); 1021-9.
- Karn J, Watson JV, Lowe AD, Green SM and Vedeckis W.** 1989. Regulation of cell cycle duration by c-myc levels. *Oncogene*, **4**(6); 773-87.
- Karnoub AE and Weinberg RA.** 2008. Ras oncogenes; split personalities. *Nat Rev Mol Cell Biol.*, **9**(7); 517-31.
- Katso R, Okkenhaug K, Ahmadi K, White S, Timms J and Waterfield MD.** 2001. Cellular function of phosphoinositide 3-kinases; implications for development, homeostasis, and cancer. *Annu. Rev. Cell Dev. Biol.*, **17**; 615-75.
- Kelman Z.** 1997. PCNA; structure, functions and interactions. *Oncogene*, **14**; 629-640.
- Khanna KK and Jackson SP.** 2001. DNA double-strand breaks; signaling, repair and the cancer connection. *Nat Genet*, **27**(3); 247-54.
- Kim ST, Lim DS, Canman CE and Kastan MB.** 1999. Substrate specificities and identification of putative substrates of ATM kinase family members. *J Biol Chem*, **274**(53); 37538-43.
- King KL and Cidlowski JA.** 1998. Cell cycle regulation and apoptosis. *Ann. Rev. Physiol.*, **60**; 601-617.
- Kito S, Shimizu K, Okamura H, Yoshida K, Morimoto H, Fujita M, Morimoto M, Ohba T and Haneji T.** 2003. Cleavage of nucleolin and argyrophilic nucleolar organizer region associated proteins in apoptosis-induced cells. *Biochem. Biophys. Res. Commun*, **300**; 950-6.
- Kleine-Kohlbrecher D, Adhikary S and Eilers M.** 2006. Mechanisms of transcriptional repression by Myc. *Curr Top Microbiol Immunol*, **302**; 51-62.
- Klippel A, Escobedo MA, Wachowicz MS, Apell G, Brown TW, Giedlin MA, Kavanaugh WN and Williams LT.** 1998. Activation of phosphatidylinositol 3-kinase is sufficient for cell cycle entry and promotes cellular changes characteristic of oncogenic transformation. *Mol. Cell. Biol*, **18**; 5699-56711.
- Knight ZA, Gonzalez B, Feldman ME, Zunder ER, Goldenberg DD, Williams O, Loewith R, Stokoe D, Balla A, Toth B, Balla T, Weiss WA, Williams RL and Shokat KM.** 2006. A pharmacological map of the PI3-K family defines a role for p110 $\alpha$  in insulin signaling. *Cell*, **125**; 733-747.
- Knobbe CB and Reifenberger G.** 2003. Genetic alterations and aberrant expression of genes related to the phosphatidylinositol-3'-kinase/protein kinase B (Akt) signal transduction pathway in glioblastomas. *Brain Pathol*, **13**(4); 507-18.
- Knoepfler PS, Cheng PF and Eisenman RN.** 2002. N-myc is essential during neurogenesis for the rapid expansion of progenitor cell populations and the inhibition of neuronal differentiation. *Genes Dev*, **16**(20); 2699-712.
- Kohl NE and Ruley HE.** 1987. Role of c-myc in the transformation of REF52 cells by viral and cellular oncogenes. *Oncogene*, **2**(1); 41-8.
- Konstantinopoulos PA, Karamouzis MV and Papavassiliou AG.** 2007. Post-translational modifications and regulation of the RAS superfamily of GTPases as anticancer targets. *Nat Rev Drug Discov.* **6**(7); 541-55.

- Koyasu S.** 2003. The role of PI3K in immune cells. *Nature Immunology*, **4**; 313 - 319.
- Koundrioukoff S, Jónsson Z, Hasan S, Jong R, van der Vliet P, Hottiger M and Hübscher U.** 2000. A Direct Interaction between Proliferating Cell Nuclear Antigen (PCNA) and Cdk2 Targets PCNA-interacting Proteins for Phosphorylation. *J. Biol. Chem*, **275**; 22882-22887.
- Kudo N, Wolff B, Sekimoto T, Schreiner E, Yoneda Y, Yanagida M, Horinouchi S and Yoshida M.** 1998. Leptomycin B Inhibition of Signal-Mediated Nuclear Export by Direct Binding to CRM1. *Experimental Cell Research*, **242**; 540-47.
- Kumagai A, Lee J, Yoo HY and Dunphy WG.** 2006. TopBP1 activates the ATR-ATRIP complex. *Cell*, **124**(5); 943-55.
- LaBaer J, Garrett MD, Stevenson LF, Slingerland JM, Sandhu C, Chou HS, Fattaey A and Harlow E.** 1997. New functional activities for the p21 family of CDK inhibitors, *Genes Dev*, **11**; 847-862
- Labib K, Diffley JF and Kearsley SE.** 1999. G1-phase and B-type cyclins exclude the DNA-replication factor Mcm4 from the nucleus. *Nat. Cell Biol*, **1**; 415-422.
- Landay M, Oster SK, Khosravi F, Grove LE, Yin X, Sedivy J, Penn LZ and Prochownik EV.** 2000. Promotion of growth and apoptosis in c-myc nullizygous fibroblasts by other members of themyc oncoprotein family. *Cell Death Differ.*, **7**; 697-705.
- Lawlor ER, Soucek L, Brown-Swigart L, Shchors K, Bialucha CU and Evan GI.** 2006. Reversible kinetic analysis of Myc targets in vivo provides novel insights into Myc-mediated tumorigenesis. *Cancer Res*, **66**; 4591-4601.
- Lee J, Kumagai A and Dunphy WG.** 2007. The Rad9-Hus1-Rad1 checkpoint clamp regulates interaction of TopBP1 with ATR. *J Biol Chem*, **282**(38); 28036-44.
- Lee JH and Paull TT.** 2005. ATM Activation by DNA Double-Strand Breaks Through the Mre11-Rad50-Nbs1 Complex. *Science*, **308**; 551-54.
- Lee SH, Kim HS, Park WS, Kim YY, Lee KY, Kim SH, Lee JY and Yoo NJ.** 2002. Non-small cell lung cancers frequently express phosphorylated Akt; an immunohistochemical study. *APMIS*, **110**; 587-592.
- Lee Sb, Nguyen T, Choi J, Lee K, Cho S and Liu Z.** 2008. Nuclear Akt interacts with B23/NPM and protects it from proteolytic cleavage, enhancing cell survival. *Proc. Natl. Acad. Sci. USA*, **105**; 6584-16589.
- Le Good JA, Ziegler WH, Parekh DB, Alessi DR, Cohen P and Parker PJ.** 1998. Protein kinase C isotypes controlled by phosphoinositide 3-kinase through the protein kinase PDK1. *Science*, **281**(5385); 2042-5.
- Leslie NR and Downes CP.** 2004. PTEN function; how normal cells control it and tumour cells lose it. *Biochem J*, **382**; 1-11.
- Li DM and Sun H.** 1997. TEP1, encoded by a candidate tumor suppressor locus, is a novel protein tyrosine phosphatase regulated by transforming growth factor  $\beta$ . *Cancer Res*, **57**; 2124-212.
- Lim MA, Kikani CK, Wick MJ and Dong LQ.** 2003. Nuclear translocation of 3-phosphoinositide-dependent protein kinase 1 (PDK-1); A potential regulatory mechanism for PDK-1 function. *Proc Natl Acad Sci USA*, **100**; 14006-140011.

- Lim DS, Kim ST, Xu B, Maser RS, Lin J, Petrini JH and Kastan MB.** 2000. ATM phosphorylates p95/nbs1 in an S-phase checkpoint pathway. *Nature*, **404**; 613-17.
- Ling LE, Druker BJ, Cantley LC, and Roberts, T. M.** 1992. Transformation defective mutants of polyomavirus middle T antigen associate with phosphatidylinositol 3-kinase (PI 3-kinase) but are unable to maintain wild-type levels of PI 3-kinase products in intact cells. *J Virol*, **66**; 1702-1708.
- Little CD, Nau MM, Carney DN, Gazdar AF and Minna JD.** 1983. Amplification and expression of the c-myc oncogene in human lung cancer cell lines. *Nature*, **306**; 194-196.
- Littlewood TD, Hancock DC, Danielian PS, Parker MG and Evan GI.** 1995. A modified oestrogen receptor ligand-binding domain as an improved switch for the regulation of heterologous proteins. *Nucleic Acids Res*, **23**; 1686-1690.
- Lukas J, Lukas C and Bartek J.** 2004. Mammalian cell cycle checkpoints; signalling pathways and their organization in space and time. *DNA Repair (Amst)*, **3**(8-9); 997-1007.
- Lu PJ, Hsu AL, Wang DS, Yan HY and Yin HL and Chen CS.** 1998. Phosphoinositide 3-kinase in rat liver nuclei. *Biochemistry*, **37**; 5738-5745.
- Lukas J, Parry D, Aagaard L, Mann DJ, Bartkova J, Strauss M, Peters G and Bartek J.** 1995. Retinoblastoma-protein-dependent cell-cycle inhibition by the tumour suppressor p16. *Nature*, **375**; 503-506.
- Maehama T, Dixon JE.** 1998. The tumor suppressor, PTEN/MMAC1, dephosphorylates the lipid second messenger, phosphatidylinositol 3,4,5-trisphosphate. *J Biol Chem*, **273**; 13375-8.
- Madine MA, Swietlik M, Pelizon C, Romanowski P, Mills AD and Laskey RA.** 2000. The roles of the MCM, ORC, and Cdc6 proteins in determining the replication competence of chromatin in quiescent cells. *J. Struct. Biol*, **129**; 198-210.
- Makris C, Voisin L, Giasson E, Tudan C, Kaplan DR and Meloche S.** 2002. The Rb-family protein p107 inhibits translation by a PDK1-dependent mechanism. *Oncogene*, **21**; 7891-7896.
- Malbon CC.** 2004. Insulin signalling; putting the 'G-' in protein-protein interactions. *Biochem J*, **380**(Pt 3); 11-2.
- Malek NP, Sundberg H, McGrew S, Nakayama K, Kyriakides TR and Roberts JM.** 2001. A mouse knock-in model exposes sequential proteolytic pathways that regulate p27Kip1 in G1 and S phase. *Nature*, **413**(6853); 323-7.
- Malynn BA, de Alboran IM, O'Hagan RC, Bronson R, Davidson L, DePinho RA and Alt FW.** 2000. n-Myc can functionally replace c-myc in murine development, cellular growth, and differentiation. *Genes Dev*, **14**; 1390-1399.
- Marqués M, Kumar A, Cortés I, Gonzalez-García A, Hernández C, Moreno-Ortiz MC and Carrera AC.** 2008. Phosphoinositide 3-kinases p110alpha and p110beta regulate cell cycle entry, exhibiting distinct activation kinetics in G1 phase. *Mol Cell Biol*, **28**(8); 2803-14.
- Marqués M, Kumar A, Poveda AM, Zuluaga S, Hernández C, Jackson S, Pasero P and Carrera AC.** 2009. Specific function of phosphoinositide 3-kinase beta in the control of DNA replication. In press, PNAS.
- Mariani-Costantini R, Escot C, Theillet C, Gentile A, Merlo G, Lidereau R and Callahan R.** 1988. In situ c-myc expression and genomic status of the c-myc locus in infiltrating ductal carcinomas of the breast. *Cancer Res*, **48**; 199-205.

- Martelli AM, Capitani S and Neri LM.** 1999. The generation of lipid signaling molecules in the nucleus. *Prog. Lipid Res*, **38**; 273-308.
- Martelli AM, Evangelisti C, Billi A, Manzoli L, PapaV and Cocco L.** 2007. Intracellular 3'-phosphoinositide metabolism and apoptosis protection in PC12 cells. *Acta Biomed*, **78**; 113-119.
- Martínez-Gac L, Marque's M, Garci'a Z, Campanero M and Carrera AC.** 2004. Control of cyclin G2 mRNA expression by forkhead transcription factors; a novel mechanism for cell cycle control by phosphoinositide 3-kinase and forkhead. *Mol. Cell. Biol*, **24**; 2181-2189.
- Mateyak MK, Obaya AJ, Adachi S and Sedivy JM.** 1997. Phenotypes of c-Myc-deficient rat fibroblasts isolated by targeted homologous recombination. *Cell Growth Differ*, **8**; 1039-1048.
- Mateyak MK, Obaya AJ and Sedivy JM.** 1999. c-Myc regulates cyclin D-Cdk4 and -Cdk6 activity but affects cell cycle progression at multiple independent points. *Mol. Cell. Biol*, **19**; 4672-4683.
- Matsuoka S, Rotman G, Ogawa A, Shiloh Y, Tamai K, Elledge SJ.** 2000. Ataxia telangiectasia-mutated phosphorylates Chk2 in vivo and in vitro. *Proc Natl Acad Sci USA*, **97**(19); 10389-94.
- Maya-Mendoza A, Petermann E, Gillespie DA, Caldecott KW and Jackson DA.** 2007. Chk1 regulates the density of active replication origins during the vertebrate S phase. *EMBO J*, **26**(11); 2719-31.
- McGarry TJ and Kirschner MW.** 1998. Geminin, an inhibitor of DNA replication, is degraded during mitosis. *Cell*, **93**(6); 1043-53.
- Medema RH, Kops GJ, Bos JL and Burgering BM.** 2000. AFX-like Forkhead TF mediate cell-cycle regulation by Ras and PKB through p27kip1. *Nature*, **404**; 782-787.
- Meier R, Alessi DR, Cron P, Andjelkovic M and Hemmings BA.** 1997. Mitogenic activation, phosphorylation, and nuclear translocation of protein kinase B. *J. Biol. Chem*, **272**; 30491-97.
- Melo J, Toczyski D.** 2002. A unified view of the DNA-damage checkpoint. *Curr. Opin. Cell Biol*, **14**; 237-45.
- Méndez J and Stillman B.** 2002. Chromatin association of human origin recognition complex, Cdc6, and minichromosome maintenance proteins during the cell cycle; assembly of prereplication complexes in late mitosis. *Mol. Cell. Biol*, **20**; 8602-8612.
- Miele L.** 2004. The biology of cyclins and cyclin-dependent protein kinases: An introduction. *Methods Mol. Biol*, **285**; 3-21.
- Moldovan GL, Pfander B and Jentsch S.** 2007. PCNA, the Maestro of the Replication Fork. *Cell*, **129**; 665-679.
- Munzel P, Marx D, Kochel H, Schauer A and Bock KW.** 1991. Genomic alterations of the c-myc protooncogene in relation to the overexpression of c-erbB2 and Ki-67 in human breast and cervix carcinomas. *J. Cancer Res. Clin. Oncol*, **117**; 603-607.
- Hatton KS, Mahon K, Chin L, Chiu FC, Lee HW, Peng D, Morgenbesser SD, Horner J and DePinho RA.** 1996. Expression and activity of L-Myc in normal mouse development. *Molecular and cellular biology*, **16**(4); 1794-1804.
- Neri LM, Borgatti P, Capitán S and Martelli AM.** 2002. The nuclear phosphoinositide 3-kinase/AKT pathway; a new second messenger system. *Biochim Biophys Acta*, **1584**; 73-80.

- Neri LM, Milani D, Bertolaso L, Strosio M, Bertagnolo V and Capitani S.** 1994. Nuclear translocation of phosphatidylinositol 3-kinase in rat pheochromocytoma PC12 cells after treatment with nerve growth factor. *Cell. Mol. Biol*, **40**; 619-626.
- Neri LM, Martelli AM, Borgatti P, Colamussi ML, Marchisio M and Capitani S.** 1999. Increase in nuclear phosphatidylinositol 3-kinase activity and phosphatidylinositol (3,4,5) trisphosphate synthesis precede PKC-zeta translocation to the nucleus of NGF-treated PC12 cells. *FASEB J*, **13**(15); 2299-310.
- Nguyen H, Gitig DM and Koff A.** 1999. Cell-free degradation of p27Kip1, a G1 cyclin-dependent kinase inhibitor, is dependent on CDK2 activity and the proteasome. *Mol Cell Biol*, **19**; 1190-201.
- Nguyen VQ, Co C and Li JJ.** 2001. Cyclin-dependent kinases prevent DNA rereplication through multiple mechanisms. *Nature*, **411**; 1068-1073.
- Nicholson KM, Streuli CH and Anderson NG.** 2003. Autocrine signalling through erbB receptors promotes constitutive activation of protein kinase B/Akt in breast cancer cell lines. *Breast Cancer Res. Treat*, **81**; 117-28.
- Nigg EA.** 2001. Mitotic kinases as regulators of cell division and its checkpoints. *Nat. Rev. Mol. Cell Biol*, **2**; 21-32.
- Nobukuni T, Joaquin M, Roccio M, Dann SG, Kim SY, Gulati P, Byfield MP, Backer JM, Natt F, Bos JL, Zwartkruis FJ and Thomas G.** 2005. Amino acids mediate mTOR/raptor signaling through activation of class 3 phosphatidylinositol 3OH-kinase. *Proc. Natl. Acad. Sci. USA*, **102**(40); 14238-43.
- Norbury C and Nurse P.** 1992. Animal cell cycles and their control. *Ann. Rev. Biochem.*, **61**; 441-468.
- Nakayama K and Nakayama K.** 1998. Cip/Kip cyclin-dependent kinase inhibitors; Brakes of the cell cycle engine during development. *Bioessays*, **20**; 1020-1029.
- Oskarsson T, Essers MA, Dubois N, Offner S, Dubey C, Roger C, Metzger D, Chambon P, Hummler E, Beard P and Trumpp A.** 2006. Skin epidermis lacking the c-Myc gene is resistant to Ras-driven tumorigenesis but can reacquire sensitivity upon additional loss of the p21Cip1 gene. *Genes Dev*, **20**(15); 2024-9.
- Pacold ME, Suire S, Perisic O, Lara-Gonzalez S, Davis CT, Walker EH, Hawkins PT, Stephens L, Eccleston JF and Williams RL.** 2000. Crystal structure and functional analysis of Ras binding to its effector phosphoinositide 3-kinase gamma. *Cell*, **103**(6); 931-43.
- Pawson T.** 1995. Protein modules and signalling networks. *Nature*, **373**; 573-80.
- Pardee AB.** 1989. G1 events and regulation of cell proliferation. *Science*, **240**; 603-608.
- Parrilla-Castellar ER, Arlander SJ and Karnitz I.** 2004. Dial 9-1-1 for DNA damage; the RAD9-Hus1-Rad1 (9-1-1) clamp complex. *DNA Repair (Amst)*, **3**; 1009-1014.
- Patrucco E, Notte A, Barberis L, Selvetella G, Maffei A, Brancaccio M, Marengo S, Russo G, Azzolino O, Rybalkin SD, Silengo L, Altruda F, Wetzker R, Wymann MP, Lembo G and Hirsch E.** 2004. PI3Kgamma modulates the cardiac response to chronic pressure overload by distinct kinase-dependent and -independent effects. *Cell*, **118**(3); 375-87.
- Pelengaris S, Khan M and Evan G.** 2002. c-MYC more than just a matter of life and death. *Nat. Rev. Cancer*, **2**; 764-776.

- Perez-Roger I, Solomon DL, Sewing A and Land H.** 1997. Myc activation of cyclin E/Cdk2 kinase involves induction of cyclin E gene transcription and inhibition of p27Kip1 binding to newly formed complexes. *Oncogene*, **14**; 2373-2381.
- Pilch DR, Sedelnikova OA, Redon C, Celeste A, Nussenzweig A and Bonner WM.** 2003. Characteristics of gamma-H2AX foci at DNA double-strand breaks sites. *Biochem. Cell Biol*, **81**; 123-29.
- Peterson RT and Schreiber SL.** 1999. Kinase phosphorylation; keeping it all in the family. *Curr. Biol*, **9**; 521-524.
- Planchon SM, Waite KA and Eng C.** 2008. The nuclear affairs of PTEN. *J Cell Sci*, **121**; 249-53.
- Ponzielli R, Katz S, Barsyte-Lovejoy D and Penn LZ.** 2005. Cancertherapeutics; targeting the dark side of Myc. *Eur. J. Cancer*, **41**; 2485-2501.
- Prendergast GC and Ziff EB.** 1991. Methylation-sensitive sequence-specific DNA binding by the c-Myc basic region. *Science*, **251**(4990);186-9.
- Rando OJ, Zhao K, Janmey P and Crabtree GR.** 2002. Phosphatidylinositol-dependent actin-filament binding by the SWI/SWF-like BAF chromatin remodeling complex. *Proc. Natl. Acad. Sci. USA*, **99**; 2824-2829.
- Reif K, Nobes CD, Thomas G, Hall A, and Cantrell DA.** 1996. Phosphatidylinositol 3-kinase signals activate a selective subset of Rac/Rho-dependent effector pathways. *Curr. Biol*, **6**; 1445- 55.
- Reynisdottir I and Massague J.** 1997. The subcellular locations of p15<sup>Ink4b</sup> and p27<sup>Kip1</sup> coordinate their inhibitory interactions with Cdk4 and Cdk2. *Genes & Dev* **11**; 492-503.
- Rhee SG.** 2001. Regulation of Phosphoinositide-Specific Phospholipase C. *Annu Rev Biochem*, **70**; 281-312.
- Robinson DR, Wu YM and Lin SF.** 2000. The protein tyrosine kinase family of the human genome, **19**; 5548-5557.
- Roche S, Koegl M and Courtneidge SA.** 1994. The phosphatidylinositol 3-kinase  $\alpha$  is required for DNA synthesis by some, but not all, growth factors. *Proc Natl Acad Sci USA* **91**;9185-9189.
- Roderick HL and Cook SJ.** 2008. Ca<sup>2+</sup> signalling checkpoints in cancer; remodelling Ca<sup>2+</sup> for cancer cell proliferation and survival. *Nat. Rev. Cancer*, **8**; 361-375.
- Rottmann S and Lüscher B.** 2006. The Mad side of the Max network; antagonizing the function of Myc and more. *Curr Top Microbiol Immunol*, **302**; 63-122.
- Rouse J and Jackson SP.** 2002. Interfaces between the detection, signaling, and repair of DNA damage. *Science*, **297** (5581); 547-51.
- Rowles A, Tada S and Blow JJ.** 1999. Changes in association of the Xenopus origin recognition complex with chromatin on licensing of replication origins. *J Cell Sci*, **112**; 2011-8.
- Ruiz Villarreal, M.** Wikipedia open source. URL. 22-04-2009
- Sancar A, Lindsey-Boltz L, KezibanU'nsal-Kacmaz, and Stuart Linn.** 2004. Molecular mechanisms of mammalian DNA repair and the DNA damage checkpoints. *Annu. Rev. Biochem.* **73**; 39-85

- Saji M, Vasko V, Kada F, Allbritton EH, Burman KD, Ringel MD.** 2005. Akt1 contains a functional leucine-rich nuclear export sequence. *Biochem. Biophys. Res. Commun.*, **332**; 167-73.
- Salmena L, Carracedo A and Pandolfi PP.** 2008. Tenets of PTEN tumor suppression. *Cell*, **133**; 403-414.
- Samuels Y and Ericson K.** 2006. Oncogenic PI3K and its role in cancer. *Curr Opin Oncol* **18**; 77-82.
- Sasaki AT, Chun C, Takeda K, and Firtel RA.** 2004. Localized Ras signaling at the leading edge regulates PI3K, cell polarity, and directional cell movement. *J. Cell Biol.*, **167**; 505-518.
- Schlessinger J and Lemmon MA.** 2003. SH2 and PTB domains in tyrosine kinase signaling. *Sci STKE*, **191**; 12.
- Schlessinger J.** 2000. Cell signaling by receptor tyrosine kinases. *Cell*, **103**; 211-225.
- Schorl C and Sedivy JM.** 2003. Loss of protooncogene c-Myc function impedes G1 phase progression both before and after the restriction point. *Mol. Biol. Cell*, **14**; 823-835.
- Schultz LB, Chehab NH, Malikzay A and Halazonetis TD.** 2000. p53 binding protein 1 (53BP1) is an early participant in the cellular response to DNA double-strand breaks. *J. Cell Biol.*, **151**; 1381-90.
- Schmidt M, Fernandez de Mattos S, van der Horst A, Klompmaker R, Kops GJ, Lam EW, Burgering BM and Medema RH.** 2002. Cell cycle inhibition by FoxO transcription factors involves downregulation of cyclin D. *Mol. Cell. Biol.*, **22**; 7842-7852.
- Sears R, Nuckolls F, Haura E, Taya Y, Tamai K and Nevins JR.** 2000. Multiple Ras-dependent phosphorylation pathways regulate Myc protein stability. *Genes Dev.*, **14**; 2501-2514.
- Seger R and Krebs EG.** 1995. The MAPK signaling cascade. *FASEB J*, **9**(9); 726-35.
- Sengupta TK, Bandyopadhyay S, Fernandes DJ, Spicer EK.** 2004. Identification of nucleolin as an AU-rich element binding protein involved in bcl-2 mRNA stabilization. *J. Biol. Chem.*, **279**; 10855.
- Seoane J, Le HJ and Massagué J.** 2002. Myc suppression of the p21Cip1 Cdk inhibitor influences the outcome of the p53 response to DNA damage. *Nature*, **419**; 729-734.
- Serrano M, Lin AW, McCurrach ME, Beach D and Lowe SW.** 1997. Oncogenic ras provokes premature cell senescence associated with accumulation of p53 and p16INK4a. *Cell*, **88**; 593-602.
- Serunian LA, Auger KR, Roberts TM, Cantley LC.** 1990. Production of novel polyphosphoinositides in vivo is linked to cell transformation by polyomavirus middle T antigen. *J Virol*, **64**; 4718-25.
- Siddhanta, U, McIlroy J, Shah A, Zhang Y and Backer JM.** 1998. Distinct roles for the p110 and hVPS34 phosphatidylinositol 3'-kinases in vesicular trafficking, regulation of the actin cytoskeleton, and mitogenesis. *J. Cell Biol.*, **143**; 1647-1659.
- Sheaff RJ, Groudine M, Gordon M, Roberts JM, Clurman BE.** 1997. Cyclin E-CDK2 is a regulator of p27<sup>Kip1</sup>. *Genes Dev.*, **11**; 1464-1478.
- Sherr CJ and Roberts JM.** 1999. CDK inhibitors; positive and negative regulators of G1-phase progression. *Genes Dev.* **13**; 1501-1512.



- Sherr CJ.** 1994. G1 phase progression; cycling on cue. *Cell*, **79**; 551-555.
- Shtivelman E, Sussman J and Stokoe D.** 2002. A role for PI3K and PKB activity in the G2/M phase of the cell cycle. *Curr Biol*, **12**; 919-924.
- Shi Y, Hutchinson HG, Hall DJ and Zalewski A.** 1993. Downregulation of c-myc expression by antisense oligonucleotides inhibits proliferation of human smooth muscle cells. *Circulation*, **88**(3); 1190-5.
- Skolnik EY, Margolis B, Mohammadi M, Lowenstein E, Fischer R, Drepps A, Ullrich A and Schlessinger J.** 1991. Cloning of PI3 kinase-associated p85 utilizing a novel method for expression/cloning of target proteins for receptor tyrosine kinases. *Cell*, **65**; 83-90.
- Sorrentino V, Drozdoff V, McKinney MD, Zeitz L and Fleissner E.** 1986. Potentiation of growth factor activity by exogenous c-myc expression. *Proc Natl Acad Sci U S A*, **83**(21); 8167-71.
- Staal SP.** 1987. Molecular cloning of the Akt oncogene and its human homologues AKT1 and AKT2; amplification of AKT1 in a primary human gastric adenocarcinoma. *Proc Natl Acad Sci USA*, **84**; 5034 -7.
- Staller P, Peukert K, Kiermaier A, Seoane J, Lukas J, Karsunky H, Möröy T, Bartek J, Massagué J, Hänel F and Eilers M.** 2001. Repression of p15INK4b expression by Myc through association with Miz-1. *Nat Cell Biol*, **3**(4); 392-9.
- Steck PA, Pershouse MA, Jasser SA, Yung WK, Lin H, Ligon AH and Langford LA, Baumgard ML, Hattier T, Davis T, Frye C, Hu R, Swedlund B, Teng DH and Tavtigian SV.** 1997. Identification of a candidate tumor suppressor gene, MMAC1, at chromosome 10q23.3 that is mutated in multiple advanced cancers, *Nat Genet*, **15**; 356-362.
- Stephens L, Smrcka A, Cooke FT, Jackson TR, Sternweis PC and Hawkins PT.** 1994. A novel phosphoinositide 3 kinase activity in myeloid-derived cells is activated by G protein beta gamma subunits. *Cell*, **77**; 83-93.
- Stern DF, Roberts AB, Roche NS, Sporn MB and Weinberg RA.** 1986. Differential responsiveness of myc- and ras-transfected cells to growth factors; selective stimulation of myc-transfected cells by epidermal growth factor. *Mol Cell Biol*, **6**(3); 870-7.
- Stewart GS, Wang B, Bignell CR, Taylor AM and Elledge SJ.** 2003. MDC1 is a mediator of the mammalian DNA damage checkpoint. *Nature*, **421**; 961-66.
- Stiles CD, Capone GT, Scher CD, Antoniades HN, Van Wyk JJ and Pledger WJ.** 1979. *Proc. Natl. Acad. Sci. USA*, **76**; 1279-1283.
- Stoyanov B, Volonia S, Hanck T, Rubio I, Loubtchenkov M, Malek D, Stoyanova S, Vanhaesebroeck B, Dhand R, Nurnberg B, Gierschik P, Seedorf K, Hsuan JJ, Waterfield MD, and Wetzker R.** 1995. Cloning and characterization of a G protein-activated human phosphoinositide 3-kinase. *Science*, **269**; 690-693.
- Su TT.** 2006. Cellular Responses to DNA Damage; One Signal, Multiple Choices. *Annu. Rev. Genet*, **40**; 187-208.
- Syljuåsen RG, Sørensen CS, Hansen LT, Fugger K, Lundin C, Johansson F, Helleday T, Sehested M, Lukas J and Bartek J.** 2005. Inhibition of human Chk1 causes increased initiation of DNA replication, phosphorylation of ATR targets, and DNA breakage. *Mol Cell Biol*, **25**(9); 3553-62.

- Tada S, Li A, Maiorano D, Méchali M and Blow JJ.** 2001. Repression of origin assembly in metaphase depends on inhibition of RLF-B/Cdt1 by geminin. *Nature Cell Biol*, 3; 107-113.
- Takuwa N and Takuwa Y.** 1997. Ras activity late in G1 phase required for p27kip1 downregulation, passage through the restriction point, and entry into S phase in growth factor-stimulated NIH 3T3 fibroblasts. *Mol. Cell. Biol*, 17; 5348-5358.
- Takumwa N and Takuwa Y.** 2001. Regulation of cell cycle molecules by the Ras effector system. *Molecular and Cellular Endocrinology*, 177; 25-33.
- Tamrakar S, Rubin E and Ludlow JW.** 2000. Role of pRB dephosphorylation in cell cycle regulation. *Frontiers in Bioscience*, 5; 121-137.
- Tanaka A and Diffley JF.** 2002. Interdependent nuclear accumulation of budding yeast Cdt1 and Mcm2-7 during G1 phase. *Nat. Cell Biol*, 4; 198-207.
- Thompson EB.** The many roles of c-Myc in apoptosis. 1998. *Annual Review of Physiology*, October, 60; 575-600.
- Tibbetts RS, Brumbaugh KM, Williams JM, Sarkaria JN, Cliby WA, Shieh SY, Taya Y, Prives C and Abraham RT.** 1999. A role for ATR in the DNA damage-induced phosphorylation of p53. *Genes Dev*, 13(2); 152-7.
- Toker A and Cantley LC.** 1997. Signalling through the lipid products of phosphoinositide-3-OH kinase. *Nature*, 387; 673-676.
- Toker A and Newton AC.** 2000. Cellular signaling; pivoting around PDK-1. *Cell*, 103(2); 185-8.
- Torres-Ramos CA, Yoder BL, Burgers PM, Prakash S and Prakash L.** 1996. Requirement of proliferating cell nuclear antigen in RAD6-dependent postreplicational DNA repair. *Proc Natl Acad Sci U S A*, 93(18); 9676-81.
- Tye BK.** 1999. MCM proteins in DNA replication. *Annu. Rev. Biochem*, 68; 649-686.
- Uckun FM, Narla RK, Zeren T, Yanishevski Y, Myers DE, Waurzyniak B, Ek O, Schneider E, Messinger Y, Chelstrom LM, Gunther R and Evans W.** 1998. In vivo toxicity, pharmacokinetics, and anticancer activity of Genistein linked to recombinant human epidermal growth factor. *Clin. Cancer Res*, 4; 1125-1134.
- Valius M and Kazlauskas A.** 1993. Phospholipase C-gamma 1 and phosphatidylinositol 3 kinase are the downstream mediators of the PDGF receptor's mitogenic signal. *Cell*, 73(2); 321-34.
- van den Bosch M, Bree R and Lowndes N.** 2003. The MRN complex; coordinating and mediating the response to broken chromosomes. *EMBO Rep*, 4(9); 844-849.
- Van de Sande T, Roskams T, Lerut E, Joniau S, Poppel HV, Verhoeven G and Swinnen JV.** 2005. High-level expression of fatty acid synthase in human prostate cancer tissues is linked to activation and nuclear localization of Akt/PKB. *J. Pathol*, 206; 214.
- Van de Sande T, Roskams T, Lerut E, Joniau S, Van Poppel H, Verhoeven G and Swinnen JV.** 2005. High-level expression of fatty acid synthase in human prostate cancer tissues is linked to activation and nuclear localization of Akt/PKB. *J Pathol*, 206(2); 214-9.
- Vanhaesebroeck B, Welham MJ, Kotani K, Stein R, Warne PH, Zvelebil MJ, Higashi K, Volinia S, Downward J and Waterfield MD.** 1997. P110δ, a novel phosphoinositide 3-kinase in leukocytes. *Proc Natl Acad Sci USA*, 94; 4330-4335.
- Vanhaesebroeck B and Alessi DR.** 2000. The PI3K-PDK1 connection; more than just a road to PKB. *Biochem J*, 346; 561-76.

- Van Weeren PC, de Bruyn KM, de Vries-Smits AM, van Lint J and Burgering BM.** 1998. Essential role for protein kinase B (PKB) in insulin-induced glycogen synthase kinase 3 inactivation. Characterization of dominant-negative mutant of PKB. *J. Biol. Chem.*, **273**; 13150-13156.
- Varticovski L, Druker B, Morrison D, Cantley L and Roberts T.** 1989. The colony stimulating factor-1 receptor associates with and activates phosphatidylinositol-3 kinase. *Nature*, **342**(6250); 699-702.
- Vasko V, Saji M, Hardy E, Kruhlak M, Larin A, Savchenko V, Miyakawa M, Isozaki O, Murakami H, Tsushima T, Burman KD, De Micco C and Ringel MD.** 2004. Akt activation and localisation correlate with tumour invasion and oncogene expression in thyroid cancer. *J. Med. Genet.*, **41**; 161-70.
- Vennstrom B, Sheiness D, Zabielski J and Bishop JM.** 1982. Isolation and characterization of c-myc, a cellular homolog of the the oncogene (v-myc) of avian myelocytomatosis virus strain 29. *J Virol*, **42**; 773-779.
- Vermeulen K, Bockstaele DRV and Berneman ZN.** 2003. The cell cycle; a review of regulation, deregulation and therapeutic targets in cancer. *Cell Prolif*, **36**; 131-149.
- Vieira OV, Botelho RJ, Rameh L, Brachmann SM, Matsuo T, Davidson HW, Schreiber A, Backer JM, Cantley LC and Grinstein S.** 2001. Distinct roles of class I and class III phosphatidylinositol 3-kinases in phagosome formation and maturation. *J Cell Biol.* **155**(1); 19-25.
- Vlach J, Hennecke S, Alevizopoulos K, Conti D and Amati B.** 1996. Growth arrest by the CDK inhibitor p27Kip1 is abrogated by c-Myc. *EMBO J*, **15**; 6595-6604.
- Vlach J, Hennecke S and Amati B.** 1997. Phosphorylation-dependent degradation of the cyclin-dependent kinase inhibitor p27<sup>Kip1</sup>. *EMBO J*, **16**; 5334-5344.
- Vogt PK, Kang S, Elsliger MA and Gymnopoulos M.** 2007. Cancerspecific mutations in phosphatidylinositol 3-kinase. *Trends Biochem Sci*, **32**; 342-349
- Walker EH, Perisic O, Ried C, Stephens L and Williams RL.** 1999. Structural insights into phosphoinositide 3-kinase catalysis and signalling. *Nature*, **402**(6759); 313-20.
- Wang F, Herzmark P, Weiner O, Srinivasan S, Servant G and Bourne H.** 2002. Lipid products of PI(3)Ks maintain persistent cell polarity and directed motility in neutrophils. *Nat. Cell Biol*, **4**; 513-518.
- Wang B, Matsuoka S, carpenter PB and Elledge SJ.** 2002. 53BP1, a mediator of the DNA damage checkpoint. *Science*, **298**(5597); 1435-8.
- Whitman M, Downes CP, Keeler M, Keller T and Cantley L.** 1988. Type I phosphatidylinositol kinase makes a novel inositol phospholipid, phosphatidylinositol-3-phosphate. *Nature*, **332**, 644-646.
- Whitman M, Kaplan DR, Schaffhausen B, Cantley L and Roberts TM.** 1985. Association of phosphatidylinositol kinase activity with polyoma middle-T competent for transformation. *Nature*, **315**; 239 – 242.
- Wymann MP and Pirola L.** 1998. Structure and function of phosphoinositide 3- kinases. *Biochimica Biophysica Acta*, **1436**; 127-150.
- Wurmser AE and Emr SD.** 2002. Novel PtdIns(3)P-binding protein Etf1 functions as an effector

of the Vps34 PtdIns 3-kinase in autophagy. *J Cell Biol*, **158**(4); 761-72.

**Wick MJ, Ramos FJ, Chen H, Quon MJ, Dong LQ and Liu F.** 2003. Mouse 3-phosphoinositide-dependent protein kinase-1 undergoes dimerization and trans-phosphorylation in the activation loop. *J Biol Chem*, **278**; 42913-42919.

**Wick MJ, Wick KR, Chen H, He H, Dong LQ, Quon MJ and Liu F.** 2002. Substitution of the autophosphorylation site Thr516 with a negatively charged residue confers constitutive activity to mouse 3-phosphoinositide-dependent protein kinase-1 in cells. *J Biol Chem*, **277**; 16632-16638.

**Williams MR, Arthur JS, Balendran A, van der Kaay J, Poli V, Cohen P and Alessi DR.** 2000. The role of 3-phosphoinositide-dependent protein kinase 1 in activating AGC kinases defined in embryonic stem cells. *Curr Biol*, **10**(8); 439-48.

**Wilson A, Murphy MJ, Oskarsson T, Kaloulis K, Bettess MD, Oser GM, Pasche AC, Knabenhans C, Macdonald HR and Trumpp A.** 2004. c-Myc controls the balance between hematopoietic stem cell self-renewal and differentiation. *Genes Dev*, **18**(22); 2747-63.

**Wishart MJ and Dixon JE.** 2002. PTEN and myotubularin phosphatases; from 3-phosphoinositide dephosphorylation to disease. *Trends Cell Biol*, **12**; 579-585.

**Wohlschlegel JA, Dwyer BT, Dhar SK, Cvetic C, Walter JC and Dutta A.** 2000. Inhibition of eukaryotic DNA replication by geminin binding to Cdt1. *Science*, **290**(5500); 2309-12.

**Yamane K, Wu XL and Chen JJ.** 2002. A DNA damage-regulated BRCT-containing protein, TopBP1, is required for cell survival. *Mol. Cell. Biol*, **22**; 555-66,

**Yeh E, Cunningham M, Arnold H, Chasse D, Monteith T, Ivaldi G, Hahn WC, Stukenberg PT, Shenolikar S, Uchida T, Counter CM, Nevins JR, Means AR and Sears RA.** 2004. A signalling pathway controlling c-Myc degradation that impacts oncogenic transformation of human cells. *Nat. Cell Biol*, **6**; 308-318.

**Ye K, Aghdasi B, Luo HR, Moriarity JL, Wu FY, Hong JJ, Hurt KJ, Bae SS, Suh PG and Snyder SH.** 2002. Phospholipase C-g1 is a physiological guanine nucleotide exchange factor for the nuclear GTPase PIKE. *Nature*, **415**; 541-544.

**Ye K, Hurt KJ, Wu FY, Fang M, Luo HR, Hong JJ, Blackshaw S, Ferris CD and Snyder SH.** 2000. Pike. A nuclear gtpase that enhances PI3kinase activity and is regulated by protein 4.1N. *Cell*, **103**; 919-930.

**Yu Q and Sicinski P.** 2004. Mammalian cell cycles without cyclin E-CDK2. *Cell Cycle*, **3**(3); 292-5.

**Zhao JJ, Liu Z, Wang L, Shin E, Loda MF and Roberts TM.** 2005. The oncogenic properties of mutant p110 $\alpha$  and p110 $\beta$  phosphatidylinositol 3-kinases in human mammary epithelial cells. *Proc. Natl. Acad. Sci. USA*, **102**; 18443-18448.

**Zhao K, Wang W, Rando OJ, Xue Y, Swiderek K, Kuo A and Crabtree GR.** 1998. Rapid and phosphoinositol-dependent binding of the SWI/SNF-like BAF complex to chromatin after T lymphocyte receptor signaling. *Cell*, **95**; 625-636.

**Zhou BB and Elledge SJ.** 2000. The DNA damage response; putting checkpoints in perspective. *Nature*, **408**(6811); 433-439

**Zhou G, Seibenhener ML, Wooten MW.** 1997. Nucleolin is a protein kinase C-zeta substrate. Connection between cell surface signaling and nucleus in PC12 cells. *J. Biol. Chem*, **272**; 31130.

- Zhou BB and Bartek J.** 2004. Targeting the checkpoint kinases; chemosensitization versus chemoprotection. *Nat. Rev. Cancer*, **4**(3); 216-25.
- Zhou BB, Chaturvedi P, Spring K, Scott SP, Johanson RA, Mishra R, Mattern MR, Winkler JD and Khanna KK.** 2000. Caffeine abolishes the mammalian G(2)/M DNA damage checkpoint by inhibiting ataxia-telangiectasia-mutated kinase activity. *J Biol Chem*, **275**(14); 10342-8.
- Zhou BP, Liao Y, Xia W, Spohn B, Lee MH and Hung MC.** 2001. Cytoplasmic localization of p21Cip1/WAF1 by Akt-induced phosphorylation in HER-2/neu-overexpressing cells. *Nat. Cell Biol*, **A**; 245-252.
- Zindy F, Knoepfler PS, Xie S, Sherr CJ, Eisenman RN and Roussel MF.** 2006. N-Myc and the cyclin-dependent kinase inhibitors p18Ink4c and p27Kip1 coordinately regulate cerebellar development. *Proc Natl Acad Sci USA*, **103**(31); 11579-83.
- Zini N, Ognibene A, Bavelloni A, Santi S, Sabatelli P, Baldini N, Scotlandi S, Serra M and Maraldi NM.** 1996. Cytoplasmic and nuclear localization sites of phosphatidylinositol 3-kinase in human osteosarcoma sensitive and multidrug-resistant Saos-2 cells. *Histochem. Cell Biol*, **106**; 457-464.
- Zou L, Cortez D and Elledge S J.** 2002. Regulation of ATR substrate selection by Rad17-dependent loading of Rad9 complexes onto chromatin. *Genes Dev*, **16**; 198-208.
- Zou L, Liu D, Elledge SJ.** 2003. Replication protein A-mediated recruitment and activation of Rad17 complexes. *Proc. Natl. Acad. Sci. USA*, **100**; 13827-32

**ARTICLES**

# Specific function of phosphoinositide 3-kinase beta in the control of DNA replication

Miriam Marqués<sup>a,1</sup>, Amit Kumar<sup>a,1</sup>, Ana M. Poveda<sup>b</sup>, Susana Zuluaga<sup>a</sup>, Carmen Hernández<sup>a</sup>, Shaun Jackson<sup>c</sup>, Philippe Pasero<sup>b</sup>, and Ana C. Carrera<sup>a,2</sup>

<sup>a</sup>Department of Immunology and Oncology, Centro Nacional de Biotecnología/Consejo Superior de Investigaciones Científicas, Universidad Autónoma de Madrid, Cantoblanco, Madrid E-28049, Spain; <sup>b</sup>Institute of Human Genetics, Centre National de la Recherche Scientifique Unité Propre de Recherche 1142, 141 Rue de la Cardonille, F-34396 Montpellier, France; and <sup>c</sup>Australian Centre for Blood Diseases, Monash University, Melbourne, Victoria 3004, Australia

Edited by Inder M. Verma, The Salk Institute for Biological Studies, La Jolla, CA, and approved March 20, 2009 (received for review November 25, 2008)

**Class I<sub>A</sub> phosphoinositide 3-kinase (PI3K) are enzymes comprised of a p85 regulatory and a p110 catalytic subunit that induce formation of 3-polyphosphoinositides, which activate numerous downstream targets. PI3K controls cell division. Of the 2 ubiquitous PI3K isoforms,  $\alpha$  has selective action in cell growth and cell cycle entry, but no specific function in cell division has been described for  $\beta$ . We report here a unique function for PI3K $\beta$  in the control of DNA replication. PI3K $\beta$  regulated DNA replication through kinase-dependent and kinase-independent mechanisms. PI3K $\beta$  was found in the nucleus, where it associated PKB. Modulation of PI3K $\beta$  activity altered the DNA replication rate by controlling proliferating cell nuclear antigen (PCNA) binding to chromatin and to DNA polymerase  $\delta$ . PI3K $\beta$  exerted this action by regulating the nuclear activation of PKB in S phase, and in turn phosphorylation of PCNA negative regulator p21<sup>Cip</sup>. Also, p110 $\beta$  associated with PCNA and controlled PCNA loading onto chromatin in a kinase-independent manner. These results show a selective function of PI3K $\beta$  in the control of DNA replication.**

**C**lass I<sub>A</sub> phosphoinositide 3-kinase (PI3K) is an enzyme that controls cell cycle entry. Mutations in this pathway are among the most frequent events in human cancer; a major objective in translational biology is to define PI3K isoform-specific functions. The PI3K are comprised of a p85 regulatory and a p110 catalytic subunit that mediates formation of 3-polyphosphoinositides (1, 2). There are three class I<sub>A</sub> p110 catalytic subunits ( $\alpha$ ,  $\beta$  and  $\delta$ ), but only p110 $\alpha$  and  $\beta$  are ubiquitous and essential for development (3, 4); enhanced p110 $\alpha$  and  $\beta$  activity trigger cell transformation (5). p110 $\alpha$  regulates cell growth and cell cycle entry (6). In the case of p110 $\beta$ , the recent description of p110 $\beta$  conditional knockout mouse phenotype shows that p110 $\beta$  activity is essential for animal growth and tumor development (7). Nonetheless, the cellular events selectively controlled by p110 $\beta$  remain unknown.

DNA replication controls the accurate, timely duplication of the cell genome each time the cell divides. Preparation for replication requires formation of the origin replication complex (ORC) at the DNA replication origin. The ORC acts as a scaffold for assembly of the prereplicative complex that includes Cdc6 and Cdt1, proteins involved in recruitment of the minichromosome maintenance (MCM) complex exhibiting helicase activity. When MCM is loaded into the ORC, the pre-RC is licensed to initiate replication (8–12). After licensing, replication initiation involves formation of the preinitiation complex, which requires activation of Cdk2 and Dbf4/Cdc7 kinases (13). These kinases phosphorylate the MCM and induce binding of DNA polymerase (Pol) $\alpha$ /primase, which triggers primer DNA synthesis (11). Elongation of DNA synthesis requires subsequent binding of the proliferating cell nuclear antigen (PCNA), a homotrimeric factor that triggers Pol $\alpha$  displacement and tethers the processive polymerases ( $\delta$  and  $\epsilon$ ) to the DNA template for rapid, accurate DNA elongation (9, 14). We examine here the function of p110 $\alpha$  and  $\beta$  in DNA replication.

## Results and Discussion

**The p110 $\beta$  Controls S-Phase Progression.** p110 $\alpha$  regulates G1 entry and cell growth (1); both p110 $\alpha$  and  $\beta$  regulate late G1 events and

accelerate G1>S transition (6); however, no p110 $\beta$ -specific function has been described in cell division. To examine the potential p110 $\beta$  action in this process, we compared the division rates of NIH 3T3 stable cell lines expressing p110 $\alpha$  or  $\beta$  active forms (Fig. 1A). Active p110 $\beta$  cells divided more rapidly ( $t_{1/2} \approx 18$  h) than active p110 $\alpha$  cells or controls ( $t_{1/2} \approx 24$  h; Fig. 1B). In addition, although a small fraction of active p110 $\alpha$  and  $\beta$  cells enter cell cycle after serum deprivation (6), only active p110 $\beta$  cells escaped cell contact inhibition in confluence (Fig. S1A). We also compared synchronous cell cycle progression in these cells. Cells were first serum-deprived (G0 arrest) and released by serum addition; using this protocol, NIH 3T3 cells reach S phase at  $\approx 9$  to 12 h postrelease (15). Active p110 $\beta$  cells were faster in terminating S phase than control or active p110 $\alpha$  cells (Fig. 1C; Fig. S1B), as confirmed by calculation of S phase duration ( $4 \pm 0.5$  h for active p110 $\beta$  cells vs. 5.5–6 h for active p110 $\alpha$  cells and  $\approx 6$  h for control cells); three distinct clones behaved similarly.

We also examined the consequences of reducing endogenous p110 $\alpha$  and  $\beta$  activity using inactive K802R-p110 $\alpha$  and K805R-p110 $\beta$  mutants (KR hereafter) (6). Expression of KR mutants in exponentially growing NIH 3T3 cells reduced PKB phosphorylation (pPKB, Fig. 1D) and affected cell division; we were unable to prepare stable KR-p110 $\alpha$  or  $\beta$  lines. We expressed KR mutants by retroviral infection (95% efficiency), which yielded levels similar to endogenous p110 proteins (Fig. 1D). Cell division was significantly slower in KR-p110 $\beta$  cells (Fig. 1E), which remained in S phase for prolonged periods (Fig. 1F; Fig. S1C) and showed a longer S phase ( $\approx 6$  h control cells; 6–6.5 h KR-p110 $\alpha$  cells,  $\approx 8$  h for KR-p110 $\beta$  cells).

p110 $\beta$  expression did not vary appreciably throughout the cell cycle. We examined the consequences of reducing p110 $\beta$  expression using various shRNA and protocols in NIH 3T3 cells and human U2OS cells (Methods). Whereas efficient protocols for p110 $\beta$  deletion interfered with cell viability, partial p110 $\beta$  reduction permitted cell cycle progression studies. To reduce p110 $\beta$  expression in U2OS cells, we stably transfected pTER-shRNA vectors, which allow inducible shRNA expression (16). shRNA reduced p110 $\alpha$  and  $\beta$  levels even before induction, but reduction was greater after doxycycline treatment (Fig. 1G). U2OS cells were synchronized at G1/S boundary by double thymidine block and examined S phase progression after release. We confirmed slower cell cycle entry in cells with reduced p110 $\alpha$  or  $\beta$  levels (6); in addition, only the cells with reduced p110 $\beta$  levels remained in S phase for prolonged periods, showing a Gaussian peak at mid-S phase DNA content at 6–7 h postrelease (Fig. 1G).

Author contributions: A.C.C. designed research; M.M., A.K., A.M.P., S.Z., and C.H. performed research; S.J. contributed new reagents/analytic tools; M.M., A.K., P.P., and A.C.C. analyzed data; and A.C.C. wrote the paper.

The authors declare no conflict of interest.

This article is a PNAS Direct Submission.

<sup>1</sup>M.M. and A.K. contributed equally to this work.

<sup>2</sup>To whom correspondence should be addressed. E-mail: acarrera@cib.csic.es.

This article contains supporting information online at [www.pnas.org/cgi/content/full/0812000106/DCSupplemental](http://www.pnas.org/cgi/content/full/0812000106/DCSupplemental).

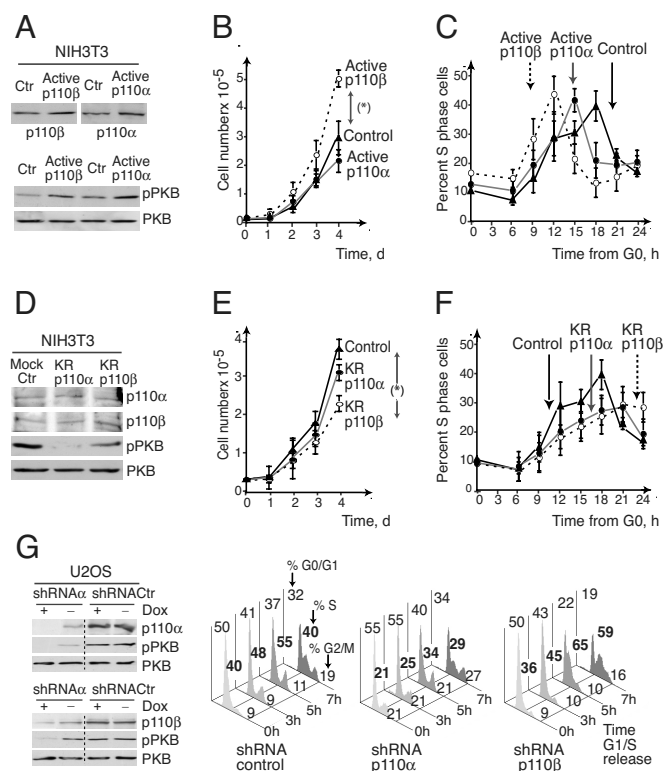


**Fig. 1.** Interference with p110 $\beta$  alters S phase progression. (A) NIH 3T3 stable cell clones expressing active-p110 $\alpha$  or  $\beta$  were examined in Western blotting (WB). (B) Control NIH 3T3 cells, active p110 $\alpha$  and active p110 $\beta$  cells were seeded at similar densities and counted at 24 h intervals (mean  $\pm$  SD,  $n = 6$ ). (C) Percentage of cells with an S phase DNA cell content at different times after release from G0 arrest (mean  $\pm$  SD;  $n = 5$ ). (D) NIH 3T3 cells transfected with KR-p110 $\alpha$  or  $\beta$  were examined in Western blot (WB) at 24 h posttransfection. (E) Cell division time for control or KR-p110 $\alpha$ - and KR-p110 $\beta$ -infected NIH 3T3 cells (mean  $\pm$  SD,  $n = 3$ ) as in B. (F) Percentage of S phase cells (mean  $\pm$  SD,  $n = 5$ ) of control, KR-p110 $\alpha$ - and  $\beta$ -infected cells, as in C. (G) U2OS clones expressing control,  $\alpha$ - or  $\beta$ -shRNA were induced with doxycycline for 48 or 120 h, respectively; p110 $\alpha$  or  $\beta$  expression was examined in WB. Cells were subjected to thymidine block and released for different times, the profiles show cell cycle distribution. \*,  $P < 0.05$ .

We used the selective inhibitors PIK75 and TGX221 to inhibit p110 $\alpha$  and  $\beta$ , respectively (17, 18). We confirmed inhibitor selectivity in NIH 3T3 cells (Fig. S2A–D). Inhibition using 0.5  $\mu$ M PIK resulted in complete blockade of S phase entry and triggered apoptosis (Fig. S2E), showing that p110 $\alpha$  is needed for cell survival (19). p110 $\alpha$  inhibition (0.08  $\mu$ M PIK) near S phase permitted cell cycle entry (Fig. S2F) although it impaired G2/M entry, suggesting that p110 $\alpha$  could be the isoform that acts in mitosis (1). This treatment nonetheless allowed S phase progression, as indicated by the increased proportion of S phase cells and displacement of the S phase population from near-G1 to near-G2 DNA content over the time course (Fig. S2F). In contrast, selective inhibition of p110 $\beta$  permitted G2/M entry but extended S phase compared with controls (Fig. S2F).

**The p110 $\beta$  Activity Controls DNA Elongation.** To compare S phase progression rates more accurately we BrdU-labeled (1 h pulse) newly synthesized DNA in exponentially growing cells and collected cells at various times after BrdU deprivation. While most BrdU<sup>+</sup> control and KR-p110 $\alpha$  cells reached G2/M at 3 to 5 h, the majority of BrdU<sup>+</sup> KR-p110 $\beta$  cells remained in S phase at 5 h (Fig. S3A). We examined the consequences of impaired p110 $\beta$  function on DNA elongation with the DNA combing assay (20, 21). We used PI3K inhibitors, as they permit p110 $\alpha$

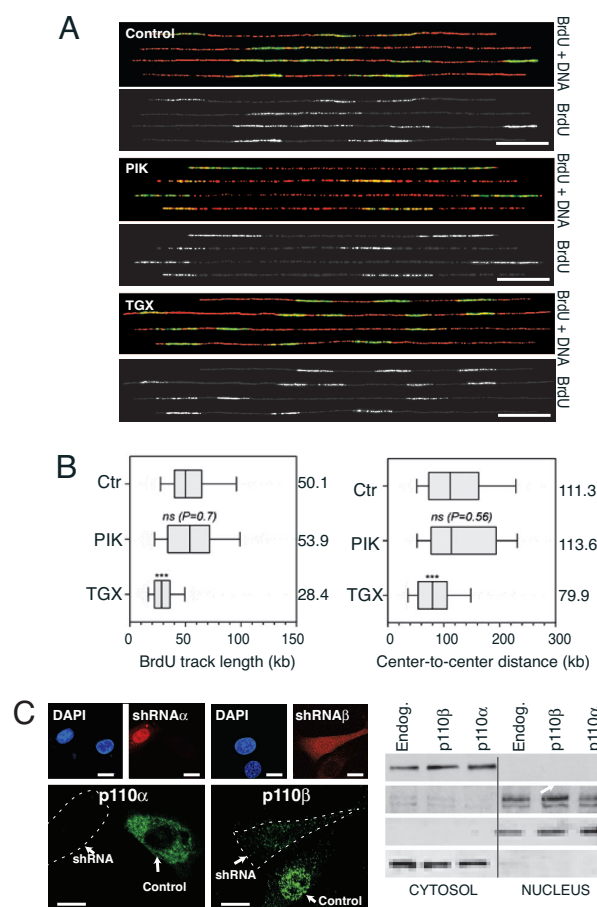


**Fig. 2.** p110 $\beta$  is a nuclear protein and regulates DNA elongation. (A) Single-molecule analysis of DNA replication in synchronized NIH 3T3 cells treated with PIK75 or TGX221 inhibitors at 7 h postserum addition, pulse-labeled (20 min) with BrdU at 12 h postserum addition, and collected immediately for analysis. Genomic DNA fibers were stretched by DNA combing. Newly replicated DNA was detected by immunofluorescence with an anti-BrdU Ab (green); DNA fibers were counterstained with anti-DNA Ab (red). Representative fibers are shown. (Scale bar, 50 Kb.) (B) Distribution of BrdU track length and center-to-center distances between adjacent BrdU tracks. Box: 25–75 percentile range. Whiskers: 10–90-percentile range. [Vertical bar, median value (kb).] \*\*\*, Mann–Whitney rank sum test  $P < 0.0001$ . (C) NIH 3T3 cells were cotransfected with red fluorescence protein (RFP) and control, p110 $\alpha$ , or  $\beta$ -shRNA; p110 localization was examined by immunofluorescence. DAPI nuclear staining is shown in Insets. (Scale bar, 10  $\mu$ m.) NIH 3T3 cells or WT-p110 $\alpha$  or  $\beta$ -transfected cells were fractionated and examined in WB (Right).

or  $\beta$  blockade in late G1 without affecting prior events. G0-synchronized NIH 3T3 cells were serum-released, treated with PIK 75 (0.08  $\mu$ M) or TGX 221 (30  $\mu$ M) at 7 h, BrdU-labeled (20 min) at 12 h, then collected to examine the replication profile (Fig. 2A). For each sample, we analyzed  $\approx 30$  MB of individual DNA fibers ( $>250$  kb). TGX-treated cells showed 43% reduction in the length of BrdU tracks relative to controls, suggesting that p110 $\beta$  is required for normal replication fork progression; in contrast, elongation was not significantly affected by p110 $\alpha$  inhibition (Fig. 2A). Median center-to-center distance between adjacent BrdU tracks, indicative of the initiation rate, was shorter in TGX- than in PIK-treated cells or in controls (Fig. 2B), consistent with cell activation of additional replication origins to compensate slow fork progression (21). The percentage of replication of individual DNA fibers was lower in TGX- (20.7%) than in control or PIK-treated cells (33.0 and 32.3%). These





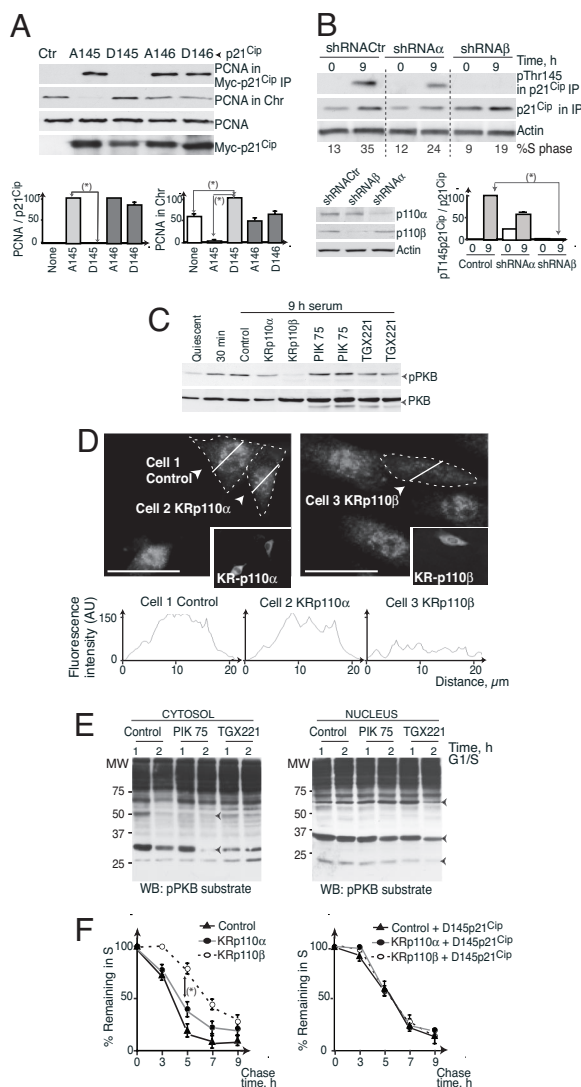


**Fig. 4.** p110 $\beta$  controls nuclear PKB. (A) NIH 3T3 cells transfected with A145, A146, D145, or D146 p21<sup>Cip</sup> mutants were fractionated. PCNA levels were measured in p21<sup>Cip</sup> immunoprecipitates, chromatin-containing and -free fractions; p21<sup>Cip</sup> expression was also examined in chromatin-free fractions. Graphs show the percentage PCNA signal (mean  $\pm$  SD) in p21<sup>Cip</sup> immunoprecipitates and that of PCNA in chromatin fractions, compared with the maximum PCNA signal in each case ( $n = 3$ ). (B) NIH 3T3 transfected with control, p110 $\alpha$ , or  $\beta$  shRNA were synchronized in G0 and released (9 h). WB shows pT145-p21<sup>Cip</sup> immunoprecipitates from chromatin extracts; graphs show the pT145-p21<sup>Cip</sup> signal (percentage  $\pm$  SD) normalized to p21<sup>Cip</sup> levels and compared with the signal at 9 h in controls (100%;  $n = 3$ ). WB (bottom left) shows p110 expression levels. (C) NIH 3T3 cells transfected with KR-p110 mutants were synchronized after 24 h and other cells were treated at 7 h with TGX221 (30  $\mu$ M) or PIK75 (0.08  $\mu$ M); cells were collected at 9 h. pPKB levels were measured in WB. (D) pPKB localization examined by immunofluorescence in cells cotransfected with KR-p110 mutants and RFP, fixed 9 h after G0 release. Graphs show fluorescence intensity in arbitrary units (AU) examined along the line in the images. Insets show expression of KR mutants. (Scale bar, 50  $\mu$ m.) (E) Phosphorylation of PKB substrates was examined by WB in fractionated extracts of U2OS cells that were thymidine-arrested, then released (1 and 2 h). (F) NIH 3T3 cells expressing KR-p110 $\beta$  or  $\alpha$  mutants alone or in combination with D145-p21<sup>Cip</sup> were BrdU-labeled and chased at different times. Graph shows the cell percentage remaining in S phase (mean  $\pm$  SD,  $n = 3$ ). \*,  $P < 0.05$ .

S phase PKB kinase activity in vitro (Fig. S6A and B). Western blot analysis of pPKB in extracts from synchronized NIH 3T3 cells expressing KR-p110 $\beta$  or treated near S phase with TGX221 confirmed that p110 $\beta$  regulates S phase pPKB, whereas p110 $\alpha$

inhibition had a lesser effect (Fig. 4C); results were similar in U2OS cells (Fig. S6C). As an alternative approach, we examined pPKB by immunofluorescence. At 1 h postserum addition (G1 phase) pPKB concentrated at the cell membrane and was reduced by KR-p110 $\alpha$  (Fig. S7A), whereas in S phase pPKB concentrated in the nucleus and was notably reduced by KR-p110 $\beta$  and p110 $\beta$  inhibition (Fig. 4D; Fig. S7B). Cell fractionation confirmed TGX inhibition of S phase nuclear pPKB (Fig. S7C).

We examined other PKB substrates in S phase; GSK3 $\beta$  phosphorylation was reduced by p110 $\beta$  inhibition, whereas FKHRL1 phosphorylation was p110 $\alpha$  activity-dependent (Fig. S7D), as is the case in G1 phase (6). WB using anti-pPKB substrate Ab showed that p110 $\beta$  inhibition reduced phosphorylation of some PKB substrates in S phase cells (such as p21<sup>Cip</sup>, Fig. S7C), while others were p110 $\alpha$ -regulated (Fig. S7D). Results were similar using S phase U2OS cells treated with PI3K inhibitors and then fractionated (Fig. 4E); this assay also showed that p110 $\alpha$  inhibition affected mainly cytosolic substrates and p110 $\beta$  nuclear substrates, suggesting that p110 $\alpha$  and  $\beta$  control distinct PKB pools. p110 $\beta$  thus governs nuclear S phase PKB activity. Since p110 $\alpha$  is activated at the G1/S boundary (6), the early timing of phosphorylation of some PKB substrates or their cytosolic localization might determine a p110 $\alpha$  activity requirement for phosphorylation.

Based on p110 $\beta$  regulation of S phase nuclear pPKB-mediated p21<sup>Cip</sup> phosphorylation, expression of the phosphomimetic D145-p21<sup>Cip</sup> mutant in cells with impaired p110 $\beta$  activity could replace p110 $\beta$  activity in S phase. BrdU labeling of newly-synthesized DNA in exponentially growing cells expressing KR-p110 $\beta$  alone or in combination with D145-p21<sup>Cip</sup> showed that D145-p21<sup>Cip</sup> expression accelerated S phase progression in KR-p110 $\beta$  cells (Fig. 4F). D145-p21<sup>Cip</sup> expression also increased PCNA-Pol $\delta$  association and reduced PCNA-p21<sup>Cip</sup> complexes in KR-p110 $\beta$  cells (Fig. S8A). Accordingly, A145-p21<sup>Cip</sup> expression corrected PCNA-Pol $\delta$  complexes in active p110 $\beta$  cells (Fig. S8B). Thus, expression of phosphomimetic p21<sup>Cip</sup> mutants corrects the S phase defects of cells with altered p110 $\beta$  activity.

**PI3K $\beta$  Protein Regulates PCNA Loading onto Chromatin.** The recently described conditional p110 $\beta$ <sup>-/-</sup> mouse phenotype and that of inactive p110 $\beta$  knock-in mice (7, 30) indicate that p110 $\beta$  kinase activity regulates mouse growth and tumor development and also that p110 $\beta$  has a kinase-independent function in embryonic development. Kinase-independent functions often reflect the ability of a protein to associate a necessary partner, as is the case for PI3K $\gamma$  in the control of cardiac stress response (31). We examined whether p110 $\beta$  expression (independent of its kinase activity) regulates DNA elongation, studying the extent of PCNA binding to chromatin after p110 $\beta$  inhibition or p110 $\beta$  knockdown. To improve p110 $\beta$  deletion, we transfected cells with puromycin-shRNA-encoding vectors, selected them for 48 h and immediately analyzed these asynchronous cultures (synchronization requires longer culture times) before reduction of cell viability. Pulse-chase BrdU analysis in exponentially growing NIH 3T3 cells showed that p110 $\beta$  inhibition reduced S phase progression, but p110 $\beta$  knockdown had a greater effect in decelerating S phase (Fig. 5A). PCNA loading onto chromatin was also reduced by p110 $\beta$  or PKB inhibition, but was drastically diminished by p110 $\beta$  knockdown (Fig. 5B).

We also analyzed asynchronous cultures of p110 $\beta$ <sup>-/-</sup> immortalized mouse embryonic fibroblasts (MEF) reconstituted with WT or KR-p110 $\beta$  (7). KR-p110 $\beta$  MEF progressed through S phase more slowly than WT p110 $\beta$  MEF, although p110 $\beta$ <sup>-/-</sup> MEF showed the slowest S phase progression (Fig. 5A). KR-p110 $\beta$  MEF had less chromatin-bound PCNA than controls, but PCNA loading was lowest in p110 $\beta$ <sup>-/-</sup> MEF (Fig. 5B). These results suggest that PCNA loading onto chromatin and in turn S phase progression rate is further regulated via a kinase-independent p110 $\beta$  function.

pPKB was little affected by p110 $\beta$  deletion in asynchronous cultures (7). To define whether p110 $\beta$  controls nuclear PKB in S





a kinase-independent manner. Since PCNA loading onto chromatin is essential for DNA duplication, this kinase-independent function explains the greater division defects in cells with reduced p110 $\beta$  expression. The role of p110 $\beta$  in DNA replication could contribute to cause the early lethality (E2–3, ref.4) of p110 $\beta$ -deficient mice.

## Materials and Methods

**Complementary DNA and shRNA.** pSG5-p110 $\alpha$ CAAX (active p110 $\alpha$ ), pSG5-HA-wt-PKB and -gag-PKB were described (5, 35). pCEF2-hp110 $\beta$ CAAX (active p110 $\beta$ ) was a gift of Dr. Murga (Centro de Biología Molecular/CSIC, Madrid, Spain). PcDNA-Myc-WT and p21<sup>Cip</sup> mutants were donated by Dr. Rössig (28). pcDNA Myc-S146A/T145A double mutant was generated using Quick Change Site-Directed mutagenesis (Stratagene). Myc-K802R-hp110 $\alpha$  and myc-K805R-hp110 $\beta$  mutants were subcloned into pSG5 and pRV-IRES-GFP for retroviral infection (6). We used several specific short hairpin RNA (shRNA) directed to human or murine p110 sequences, each assay was performed at least with two shRNA, with similar results. These shRNA (6) were subcloned in pBluescript/U6 or in pTER vector; we used control shRNA that did not reduce p110 $\alpha$  or  $\beta$  expression. We also used Pik3cb shRNA (Origene; Fig. 5). To prepare NLS-p85, the PKKKRKV sequence was inserted 3' of the p85 sequence.

**Cell Lines, Cell Culture, and Retroviral Transduction.** Active p110 $\alpha$  and active p110 $\beta$  NIH 3T3 cells lines were described (6). KR-p110 $\alpha$  and  $\beta$  mutations were transduced by transient transfection or retroviral infection. We generated pTER-p110 $\alpha$  or pTER-p110 $\beta$  U2OS clones according to manufacturer's protocol (Invitrogen); shRNA expression was induced for 2 days (p110 $\alpha$ ) or 5 days (p110 $\beta$ ) in medium plus doxycycline (6  $\mu$ g/mL, Sigma). NIH 3T3 murine fibroblasts, U2OS and COS7 cells were cultured as described (6). For retrovirus production, Phoenix cells were transfected using JetPei-NaCl (Qbiogene). MEF were donated by Drs. Zhao and Roberts (7) (Dana Farber Cancer Institute, Boston, MA).

**Cell Cycle, BrdU Labeling, Immunofluorescence, and Dynamic Molecular Combing.** Immunofluorescence and NIH 3T3 G0 synchronization were as reported (15). Briefly, cells were incubated in serum-free medium (19 h) and released by serum addition. Cell cycle distribution was examined by DNA staining with propidium

iodide and analyzed by flow cytometry (Beckman-Coulter) using Multicycle AV (Phoenix Flow Systems). Cells were synchronized at G1/S by double thymidine block (6) or using aphidicolin (22). To determine cell division time ( $t_{1/2}$ ), cells were seeded at similar densities and counted at 24 h intervals. S phase duration was calculated considering  $t_{1/2}$  (mean of  $n = 6$ ) and the proportion of cells in S phase in exponential growth (mean of  $n = 12$ ). S phase progression rates were examined in exponentially growing cultures incubated with 20  $\mu$ M bromodeoxyuridine (BrdU; 1 h), chased at different times and stained with BrdU-FITC Ab (BD Biosciences), then examined by three-dimensional FACS.

For dynamic molecular combing, synchronized NIH 3T3 cells were treated with 0.08  $\mu$ M PIK75 or 30  $\mu$ M TGX221 at 7 h postserum addition; 20 min before harvest (12 h postserum addition), cells were treated with 20  $\mu$ M BrdU. After harvest, cells were embedded in LMP agarose plugs ( $3 \times 10^6$  cells/plug) and DNA fibers were purified and stretched on silanized coverslips as described (21). BrdU tracks were detected with rat monoclonal Ab (clone BU1/75; AbCys) and an Alexa 488-conjugated secondary Ab (Molecular Probes). DNA fibers were counterstained with mouse anti-ssDNA (MAB3034, Chemicon) and Alexa 546-secondary Ab (Molecular Probes). Signals were analyzed with MetaMorph.

Statistical analyses were performed using StatView 512+ (Calabasas, CA). Gel bands and fluorescence intensity were quantitated with ImageJ software. Statistical significance was calculated using Student's  $t$  test. For DNA combing, statistical analysis was performed with GraphPad Prism 5.0 (GraphPad Software).

For description of antibodies and reagents, cell lysis, subcellular fractionation, Western blotting, immunoprecipitation, and kinase assays, see *SI Methods*.

**ACKNOWLEDGMENTS.** We thank Drs. Roberts and Zhao for sharing p110 $\beta$ <sup>-/-</sup> immortal MEF, M. White for the myc-p110 plasmid, C. Murga for pCEF2-p110 $\beta$ CAAX, B. Vanhaesebroeck for His-p110 $\beta$ , M. van de Wetering for the pTER vector, Y. Shi for the pBlue/U6 plasmid, A. Klippel for anti-p110 $\alpha$ , J. Méndez for help in chromatid purification, as well as E. Schwob and the DNA combing facility (Montpellier) for silanized coverslips, and C. Mark for editorial assistance. M.M. has a predoctoral Formación de Profesorado Universitario fellowship from the Spanish Ministry of Science and Innovation, and A.M.P. a postdoctoral fellowship from the Fondation Recherche Médicale. This work was supported in part by grants from the American Institute for Cancer Research Foundation, the Fundación Ramón Areces, the Asociación Española de la Lucha Contra el Cáncer, the Centre National de la Recherche Scientifique, and the Spanish Dirección General de Ciencia y Desarrollo Tecnológico Grants SAF2004-05955 and SAF2007-63624.

- García Z, Kumar A, Marques M, Cortes I, Carrera AC (2006) PI3K controls early and late events in mammalian cell division. *EMBO J* 25:655–661.
- Fruman DA, Meyers RE, Cantley LA (1998) Phosphoinositide kinases. *Annu Rev Biochem* 67:481–507.
- Bi L, Okabe I, Bernard DJ, Wynshaw-Boris JA, Nussbaum RL (1999) Proliferative defect and embryonic lethality in mice homozygous for a deletion in the p110-alpha subunit of PI3K. *J Biol Chem* 274:10963–10968.
- Bi L, Okabe I, Bernard DJ, Nussbaum RL (2002) Early embryonic lethality in mice deficient in the p110beta catalytic subunit of PI3K. *Mamm Genome* 13:169–172.
- Kang S, Denley A, Vanhaesebroeck B, Vogt PK (2006) Oncogenic transformation induced by the p110b, g and d isoforms of class I PI3K. *Proc Natl Acad Sci USA* 103:1289–1294.
- Marqués M, et al. (2008) PI3K p110alpha and p110beta regulate cell cycle entry, exhibiting distinct activation kinetics in G1 phase. *Mol Cell Biol* 28:2803–2814.
- Jia S, et al. (2008) Essential roles of PI(3)K-p110beta in cell growth, metabolism and tumorigenesis. *Nature* 454:776–779.
- Cvetcic C, Walter JC (2006) Getting a grip on licensing: Mechanism of stable Mcm2–7 loading onto replication origins. *Mol Cell* 21:143–144.
- Frouin I, et al. (2002) Cell cycle-dependent dynamic association of cyclin/Cdk complexes with human DNA replication proteins. *EMBO J* 21:2485–2495.
- Sasaki T, Gilbert DM (2007) The many faces of the origin recognition complex. *Curr Opin Cell Biol* 19:337–343.
- Hübscher U, Maga G, Spadari S (2002) Eukaryotic DNA polymerases. *Annu Rev Biochem* 71:133–163.
- Nishitani H, Lygerou Z (2002) Control of DNA replication licensing in a cell cycle. *Genes Cells* 7:523–534.
- Sclafani RA, Tecklenburg M, Pierce A (2002) The mcm5-bob1 bypass of Cdc7p/Dbf4p in DNA replication depends on both Cdk1-independent and Cdk1-dependent steps in *Saccharomyces cerevisiae*. *Genetics* 161:47–57.
- Waga S, Stillman B (1994) Anatomy of a DNA replication fork revealed by reconstitution of SV40 DNA replication in vitro. *Nature* 369:207–212.
- Martínez-Gac L, Marqués M, García Z, Campanero M, Carrera AC (2004) Control of cyclin G2 mRNA expression by forkhead transcription factors: A novel mechanism for cell cycle control by PI3K and forkhead. *Mol Cell Biol* 24:2181–2189.
- Van de Wetering M, et al. (2003) Specific inhibition of gene expression using a stably integrated, inducible small-interfering-RNA vector. *EMBO Rep* 4:609–615.
- Madson S, et al. (2005) PI 3-kinase p110beta: A new target for antithrombotic therapy. *Nat Med* 11:507–514.
- Knight ZA, et al. (2006) A pharmacological map of the PI3-K family defines a role for p110alpha in insulin signaling. *Cell* 125:733–747.
- Downward J (2004) PI 3-kinase, Akt and cell survival. *Semin Cell Dev Biol* 15:177–182.
- Michalet X, et al. (1997) Dynamic molecular combing: Stretching the whole human genome for high-resolution studies. *Science* 277:1518–1523.
- Tourrière H, Versini G, Cordon-Preciado V, Alabert C, Pasero P (2005) Mrc1 and top1 promote replication fork progression and recovery independently of Rad53. *Mol Cell* 19:699–706.
- Riva F, et al. (2004) Distinct pools of proliferating cell nuclear antigen associated to DNA replication sites interact with the p125 subunit of DNA polymerase delta or DNA ligase I. *Exp Cell Res* 293:357–367.
- Mendez J, Stillman B (2000) Chromatin Association of Human Origin Recognition Complex, Cdc6, and Minichromosome Maintenance Proteins during the Cell Cycle: Assembly of Pre-replication Complexes in Late Mitosis. *Mol Cell Biol* 20:8602–8612.
- Cazzalini O, et al. (2003) p21<sup>CDKN1A</sup> does not interfere with loading of PCNA at DNA replication sites, but inhibits subsequent binding of DNA polymerase delta at the G1/S phase transition. *Cell Cycle* 2:596–603.
- Scott MT, Morrice N, Ball KL (2000) Reversible phosphorylation at the C-terminal regulatory domain of p21<sup>Waf1/Cip1</sup> modulates proliferating cell nuclear antigen binding. *J Biol Chem* 275:11529–11537.
- Walker JL, Castagnino P, Chung BM, Kazanietz MG, Assoian RK (2006) Post-transcriptional destabilization of p21<sup>Cip1</sup> by protein kinase C in fibroblasts. *J Biol Chem* 281:38127–38132.
- Zhou BP, et al. (2001) Cytoplasmic localization of p21<sup>Cip1</sup>/WAF1 by Akt-induced phosphorylation in HER-2/neu-overexpressing cells. *Nat Cell Biol* 3:245–252.
- Rössig L, et al. (2001) Akt-dependent phosphorylation of p21<sup>Cip1</sup> regulates PCNA binding and proliferation of endothelial cells. *Mol Cell Biol* 21:5644–5657.
- Toutou R, et al. (2001) A degradation signal located in the C-terminus of p21<sup>Cip1</sup> is a binding site for the C8 alpha-subunit of the 20S proteasome. *EMBO J* 20:2367–2375.
- Ciavola E, et al. (2008) PI3-kinase p110beta activity: Key role in metabolism and mammary gland cancer but not development. *Sci Signal* 1:ra3.
- Patrucco E, et al. (2004) PI3K modulates the cardiac response to chronic pressure overload by distinct kinase-dependent and -independent effects. *Cell* 118:375–387.
- Carrera AC, Li P, Roberts TM (1991) Characterization of an active, non myristylated, cytoplasmic form of the lymphoid protein Tyr kinase pp56lck. *Int Immunol* 3:673–682.
- Qu L, et al. (2004) Endoplasmic reticulum stress induces p53 cytoplasmic localization and prevents p53-dependent apoptosis by a pathway involving glycogen synthase kinase-3beta. *Genes Dev* 18: 261–277.
- Bakkenist CJ, Kastan MB (2004) Initiating cellular stress responses. *Cell* 118:9–17.
- Álvarez B, Martínez AC, Burgering BM, Carrera AC (2001) Forkhead TFs contribute to execution of the mitotic programme in mammals. *Nature* 413:744–747.

## Phosphoinositide 3-Kinases p110 $\alpha$ and p110 $\beta$ Regulate Cell Cycle Entry, Exhibiting Distinct Activation Kinetics in G<sub>1</sub> Phase<sup>▽</sup>

Miriam Marqués, Amit Kumar, Isabel Cortés, Ana Gonzalez-García, Carmen Hernández, M. Carmen Moreno-Ortiz, and Ana C. Carrera\*

*Department of Immunology and Oncology, Centro Nacional de Biotecnología/CSIC, Campus de Cantoblanco, Madrid E-28049, Spain*

Received 28 September 2007/Returned for modification 9 November 2007/Accepted 29 January 2008

**Phosphoinositide 3-kinase (PI3K) is an early signaling molecule that regulates cell growth and cell cycle entry. PI3K is activated immediately after growth factor receptor stimulation (at the G<sub>0</sub>/G<sub>1</sub> transition) and again in late G<sub>1</sub>. The two ubiquitous PI3K isoforms (p110 $\alpha$  and p110 $\beta$ ) are essential during embryonic development and are thought to control cell division. Nonetheless, it is presently unknown at which point each is activated during the cell cycle and whether or not they both control S-phase entry. We found that p110 $\alpha$  was activated first in G<sub>0</sub>/G<sub>1</sub>, followed by a minor p110 $\beta$  activity peak. In late G<sub>1</sub>, p110 $\alpha$  activation preceded that of p110 $\beta$ , which showed the maximum activity at this time. p110 $\beta$  activation required Ras activity, whereas p110 $\alpha$  was first activated by tyrosine kinases and then further induced by active Ras. Interference with p110 $\alpha$  and - $\beta$  activity diminished the activation of downstream effectors with different kinetics, with a selective action of p110 $\alpha$  in blocking early G<sub>1</sub> events. We show that inhibition of either p110 $\alpha$  or p110 $\beta$  reduced cell cycle entry. These results reveal that PI3K $\alpha$  and - $\beta$  present distinct activation requirements and kinetics in G<sub>1</sub> phase, with a selective action of PI3K $\alpha$  at the G<sub>0</sub>/G<sub>1</sub> phase transition. Nevertheless, PI3K $\alpha$  and - $\beta$  both regulate S-phase entry.**

The exposure of quiescent cells to growth factors (GF) activates a number of early signaling pathways that trigger cell cycle entry. Class I phosphoinositide 3-kinase (PI3K) represents one of the GF-stimulated pathways that regulate G<sub>0</sub>/G<sub>1</sub> and G<sub>1</sub>/S transitions. There are four class I PI3K enzymes, composed of a regulatory subunit and a conserved p110 catalytic subunit that triggers phosphatidylinositol (3,4)-biphosphate and phosphatidylinositol (3,4,5)-triphosphate (PIP<sub>3</sub>) production. Class I PI3K enzymes are further classified as the GF receptor-controlled class I<sub>A</sub> enzymes and the G protein-coupled receptor-regulated p110 $\gamma$  (class I<sub>B</sub> PI3K) (12, 42). Three genes encode class I<sub>A</sub> catalytic subunits (p110 $\alpha$ , p110 $\beta$ , and p110 $\delta$ ) (12, 14, 42). Class I<sub>A</sub> enzymes are activated by tyrosine kinases (TyrK) and Ras and regulate cell growth and DNA synthesis (5, 14, 17). Of the three class I<sub>A</sub> catalytic subunits, p110 $\delta$  is expressed mainly in hematopoietic cells and regulates the immune response (30), whereas p110 $\alpha$  and - $\beta$  are ubiquitous and they might control cell division. Mice deficient in p110 $\alpha$  or - $\beta$  isoforms are embryonic lethal, suggesting that at least in development, these two isoforms have nonredundant functions (3, 4).

PI3K activity increases within minutes after GF receptor (GFR) stimulation (first peak) and again in advanced G<sub>1</sub> phase (second peak) (18, 19, 24). PI3K has been implicated in the induction of cell growth and regulation of Cdk activity. Pharmacological inhibition of PI3K at the time of GFR stimulation blocks cell division (2). In addition, enhanced PIP<sub>3</sub> production

after GFR binding accelerates cell cycle entry, whereas PIP<sub>3</sub> reduction diminishes this process (1). PI3K regulates cell mass increase by activating p70S6 kinase (p70S6K) and mTOR (9, 10, 23, 34, 35). The upregulation of PI3K activity also enhances Cdk2 activation (21). The mechanisms by which PI3K controls Cdk activity include the induction of cyclin D synthesis and inhibition of cyclin D degradation, an effect mediated by protein kinase B (PKB)-induced glycogen synthase kinase 3 $\beta$  inactivation (31, 33, 41). PI3K also regulates cell cycle entry through PKB-mediated FoxO transcription factor (TF) phosphorylation, which reduces FoxO TF-controlled cyclin G2 and p27<sup>INK</sup> expression (25, 27). Finally, the late G<sub>1</sub> PI3K activity stabilizes c-Myc, an event required for correct cyclin A expression and Cdk2 activation (24).

Although it is well established that PI3K activation regulates progression through early and late G<sub>1</sub> phase and cell cycle entry (18, 24), it is unclear which of the two ubiquitous catalytic subunits, p110 $\alpha$  or - $\beta$ , is activated and whether or not they both regulate cell cycle entry. Here we analyzed p110 $\alpha$  and - $\beta$  activation patterns during G<sub>1</sub>-phase progression, their activation requirements, and their potential contributions to G<sub>1</sub>-phase progression and cell cycle entry.

### MATERIALS AND METHODS

**Plasmids.** pSG5-myc-p110 $\alpha$  and -p110 $\alpha$ CAAX have been described previously (1). pCEF2-hp110 $\beta$ CAAX was a gift from C. Murga (Centro de Biología Molecular/CSIC, Madrid, Spain). The plasmid pAC-CMV encoding Myc-tagged full-length wild-type human p110 $\alpha$  (hp110 $\alpha$ ) was donated by M. White (Howard Hughes Medical Institute, Chevy Chase, MD), and His-tagged wild-type hp110 $\beta$  by B. Vanhaesebroeck (Ludwig Institute for Cancer Research, London, United Kingdom). The mutants myc-K802R-hp110 $\alpha$  and myc-K805R-hp110 $\beta$  were generated by using a QuikChange site-directed mutagenesis kit (Stratagene, La Jolla, CA) with appropriate oligonucleotides and were subcloned into pSG5 and pRV-IRES-GFP (for retroviral infection). Julian Downward donated the cDNAs

\* Corresponding author. Mailing address: Department of Immunology and Oncology, Centro Nacional de Biotecnología/CSIC, Darwin 3, Cantoblanco, Madrid E-28049, Spain. Phone: (34) 91-585-4849. Fax: (34) 91-372-0493. E-mail: acarrera@cnb.uam.

<sup>▽</sup> Published ahead of print on 19 February 2008.



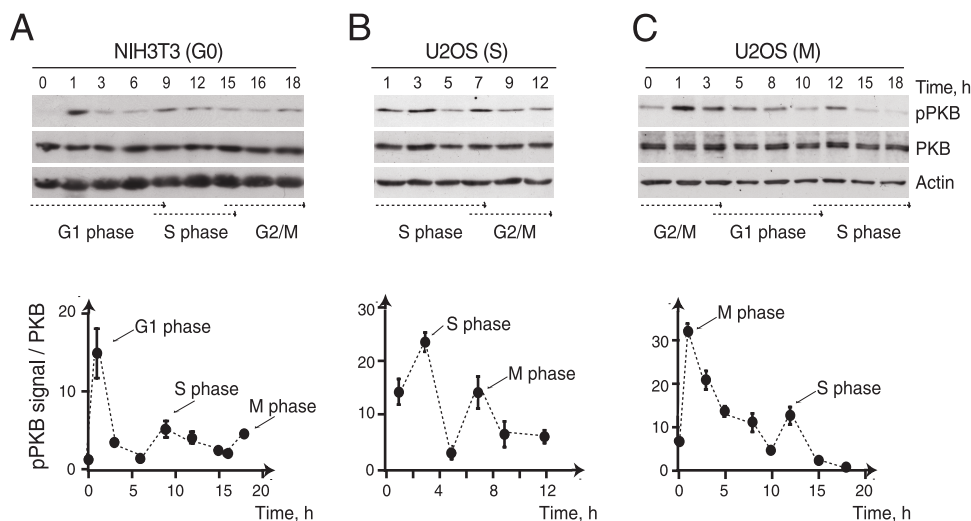


FIG. 1. PI3K is activated at S-phase entry in different cell lines. (A) NIH 3T3 cells were arrested in  $G_0$ ; (B and C) U2OS cells were synchronized at the  $G_1$ /S boundary (B) or in metaphase (C) and released for different times. Extracts were examined with WB by using the indicated Ab. Cell cycle distribution was examined in parallel; transits through  $G_1$ , S, or  $G_2$ /M are indicated (arrows). Graphs represent the means  $\pm$  standard deviations of the p-PKB signals in arbitrary units, normalized in comparison to control PKB levels ( $n = 3$ ).

encoding yellow fluorescent protein–N17-Ras and V12-Ras (London Research Institute, London, United Kingdom). Murine short hairpin RNAs (shRNA) were subcloned in pBluescript/U6 (39). Human shRNA were cloned in the pTER vector as described previously (40). The following target sequences were efficient in reducing target mRNA expression: human/murine p110 $\alpha$ 1 (h/mp110 $\alpha$ 1), 5'-GGCATCCACCTTGATGCC; h/mp110 $\alpha$ 2, 5'-GGGAGAACCAGACATCATGTCA; h/mp110 $\beta$ 2, 5'-AAAGCTGGACTACTAAAGTGA; h/mp110 $\beta$ 7, 5'-TTGCTCAGCTTCAGGCGCTGC; hp110 $\alpha$ 7, 5'-CTGTGGGGCATCCACTTGA; and h/mp110 $\beta$ 15, 5'-CTGGAATTGATATTAATAT. The different  $\alpha$  shRNA and  $\beta$  shRNA gave similar results. For controls, we used shRNA that did not reduce p110 $\alpha$  or  $\beta$  expression. The following sequences were used for controls: 5'-GGAATGAACCACTGGAATTT (control  $\beta$ ) and 5'-CCCAGACATCATGTCAGAG (control  $\alpha$ ).

**Ab and reagents.** Transfections were performed by using Lipofectamine (Invitrogen, Carlsbad, CA). Blots were probed with the following antibodies (Ab): cyclin E (M-20), c-Myc (C-19), p110 $\beta$  (S-19), and p70S6K (C-18) (Santa Cruz Biotechnology, CA). Anti-cyclin D3, anti-phospho-PKB (anti-p-PKB) (Ser-473), anti-Myc (9B11), and anti-p-p70S6K (Thr-389) Ab were from Cell Signaling (Beverly, MA); anti-cyclin A, anti-retinoblastoma protein (anti-RB), and anti-six-His from BD Biosciences (San Jose, CA); and anti-Akt1/PKB $\alpha$  and anti-p-Thr32-FKHRL1 (p-FoxO3a) from Upstate Biotechnology (Millipore, Billerica, MA). Anti- $\beta$ -actin was from Sigma (St. Louis, MO), anti-Ras was from Oncogene (Merck, Germany), and anti-p110 $\alpha$  was donated by A. Klippel (Merck, Boston, MA). [ $\gamma$ - $^{32}$ P]ATP was from Amersham (United Kingdom); lovastatin and herbamycin were from Calbiochem.

**Cell lines, cell culture, and retroviral transduction.** Murine embryonic fibroblasts (MEF) were prepared as reported previously (13). The cells were maintained in Dulbecco's modified Eagle's medium supplemented with 10% fetal bovine serum, 2 mM glutamine, 10 mM HEPES, 100 U/ml penicillin, and 100  $\mu$ g/ml streptomycin. Stable NIH 3T3 p110 $\alpha$ CAAX (p110 $\alpha$ \*) lines were previously described (1). NIH 3T3 p110 $\beta$ CAAX (p110 $\beta$ \*) cell lines were prepared by transfecting NIH 3T3 cells with 3  $\mu$ g pCEF2-hp110 $\beta$ CAAX plus 1  $\mu$ g p-Pur (Clontech, Mountain View, CA). We failed to obtain stable cell lines expressing K802R-p110 $\alpha$  and K805R-p110 $\beta$  mutations; analyses using these mutants were performed by transient transfection or retroviral infection (cultured for 1 week). We expressed pTER-p110 $\alpha$ 7 or pTER-p110 $\beta$ 15 in U2OS cells as described previously (40).

**Cell cycle and immunofluorescence analysis.** Cells were synchronized in  $G_0$  by serum starvation as reported previously (25). Synchronous cell cycle entry was induced by the addition of serum. Cell cycle distribution was examined by DNA staining using propidium iodide and analyzed by flow cytometry (Beckman-Coulter, Fullerton, CA). U2OS cell cultures were synchronized at the  $G_1$ /S boundary by double-thymidine block (11) or were synchronized in metaphase with colcemid (13). For retrovirus production, Phoenix cells were transfected by

using JetPei-NaCl according to the manufacturer's protocols (Qbiogene, Irvine, CA). Retroviral infection and immunofluorescence analysis were performed as described previously (24).

**WB, in vitro transcription and translation, immunoprecipitation, and PI3K assays.** Total cell extracts were prepared in radioimmunoprecipitation buffer (20 mM Tris-HCl, pH 8.0, 137 mM NaCl, 1 mM MgCl $_2$ , 1 mM CaCl $_2$ , 10% glycerol, 1% NP-40, 0.5% sodium deoxycholate, 0.1% sodium dodecyl sulfate [SDS]) containing protease and phosphatase inhibitors (1 mM Na $_3$ VO $_4$ , 5 mM NaF, 1 mM phenylmethylsulfonyl fluoride, 10  $\mu$ g/ml aprotinin, 10  $\mu$ g/ml leupeptin, 10 nM okadaic acid). Western blotting (WB) and immunoprecipitation were performed as described previously (25). For PI3K assays, cells were transfected with empty vector (pSG5) or with a combination of pSG5–myc-tagged p110 $\alpha$  and pSG5–His-tagged p110 $\beta$  and were then synchronized as described above. In some samples, 10  $\mu$ M lovastatin or 0.3  $\mu$ g/ml herbamycin was added 1 h before harvest. In vitro transcription and translation and subsequent PI3K activity analysis were performed as reported previously (17). PI3K was immunoprecipitated by using anti-Myc or anti-six-His Ab; the kinase assays were performed as described previously (24).

**Quantitation of gel bands and statistical analyses.** Statistical analyses were performed by using StatView 512+ (Calabasas, CA). Gel bands and fluorescence intensities were quantitated with ImageJ software and were normalized according to the fluorescence intensity of the loading control band. Cell cycle profiles were analyzed with multicycle AV for Windows (Phoenix Flow Systems, CA).

## RESULTS

**p110 $\alpha$  and  $\beta$  contribute differently to downstream signaling.** We investigated specific functions of p110 $\alpha$  and  $\beta$  PI3K catalytic subunits in  $G_1$  phase by comparing the consequences of interfering with their activation for the induction of different effectors. We examined several PI3K downstream targets, including PKB, FoxO3a, and p70S6K. To synchronize the cells, we arrested immortal nontransformed murine NIH 3T3 cells in  $G_0$  phase by serum deprivation and then released them by low-density replating in serum-containing medium for different time periods, as described previously (25). We confirmed that the PI3K effector PKB is activated at  $G_0$ / $G_1$ , in late  $G_1$ , and at M-phase entry (Fig. 1A), as reported previously (7, 38). We also synchronized human U2OS cells at the  $G_1$ /S boundary or in metaphase (Fig. 1B and C), as these cells fail to arrest in  $G_0$

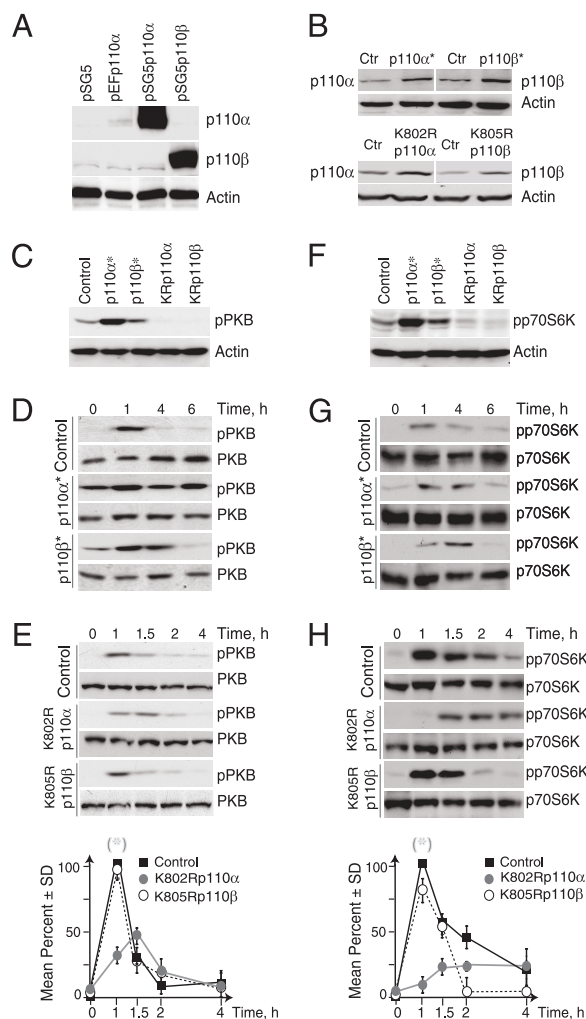


FIG. 2. Interference with p110 $\alpha$  or - $\beta$  activity differentially affects downstream signaling cascades. (A) Extracts (30  $\mu$ g) from COS cells transfected with pSG5, pEFp110 $\alpha$ , pSG5-p110 $\alpha$ , or pSG5-p110 $\beta$  were analyzed by WB using anti-p110 $\alpha$ , anti-p110 $\beta$ , or actin Ab. (B, C, and F) NIH 3T3 cells were transfected with vectors encoding p110 $\alpha^*$  or p110 $\beta^*$  or the K802R-p110 $\alpha$  (KRp110 $\alpha$ ) or K805R-p110 $\beta$  (KRp110 $\beta$ ) mutant, and extracts were examined with WB as described above. (D, E, G, and H) Synchronous p110 $\alpha^*$ - and p110 $\beta^*$ -expressing NIH 3T3 clones (D and G) or NIH 3T3 cells transfected with the K802R-p110 $\alpha$  or K805R-p110 $\beta$  mutant (E and H) were lysed, and extracts (30  $\mu$ g) were examined with WB using the Ab indicated on the left. Graphs (E and H) show the mean percentages  $\pm$  standard deviations (SD) of the p-Ser-473-PKB (pPKB) or p-Thr-389-p70S6K (pp70S6K) signals normalized in comparison to those of loading controls and compared to the maximum signal (control cells at 1 h, 100%) ( $n = 3$ ).  $P$  values compare results for control cells and those expressing the K802R-p110 $\alpha$  mutant at 1 h. (\*),  $P < 0.05$ ; Student's  $t$  test. Ctr, control.

(7, 38). We confirmed PI3K activation at G<sub>1</sub>/S transition and M-phase entry in U2OS cells (Fig. 1B and C).

We confirmed the specificities of the p110 Ab used for this study by transfection of wild-type p110 $\alpha$  and p110 $\beta$  under the control of the simian virus 40 promoter (pSG5 vector) in COS cells, which gives rise to high levels of overexpression of recombinant proteins (Fig. 2A). Anti-p110 $\alpha$  Ab selectively detected p110 $\alpha$  despite the high expression levels of recombinant

p110 $\beta$ ; similarly, anti-p110 $\beta$  Ab only detected endogenous and recombinant p110 $\beta$  (Fig. 2A). To interfere with p110's cellular activity, we first used the active p110 $\alpha^*$  (1) and p110 $\beta^*$  forms, as well as the kinase-inactive myc-K802R-p110 $\alpha$  and myc-K805R-p110 $\beta$  mutants (see Materials and Methods). The interference activities of the mutants were tested by transient transfection of these PI3K forms in asynchronous cultures of NIH 3T3 cells. The expression levels of exogenous p110 were approximately double those of the endogenous proteins (Fig. 2B). Transient transfection of the mutants showed that K802R-p110 $\alpha$  and K805R-p110 $\beta$  reduced and p110 $\alpha^*$  and - $\beta^*$  increased (p110 $\alpha^*$  had a greater effect) the p-PKB cellular levels (Fig. 2C). Thus, these mutants interfere with endogenous PI3K pathway activation.

We then examined PKB, FoxO, and p70S6K activities during early G<sub>1</sub> (until 6 h following serum addition) in synchronized populations of stable p110 $\alpha^*$  and p110 $\beta^*$  transfectants (see Materials and Methods). In these cells, the exogenous p110 expression levels were similar to the levels of endogenous proteins (1) (data not shown). In synchrony, p110 $\alpha^*$ -expressing cell lines showed sustained p-PKB activation (1) and p110 $\beta^*$ -expressing cells showed a minor increase in basal levels of p-PKB and an increase in the p-PKB signal at  $\sim$ 4 h (Fig. 2D). We failed to stably maintain cells expressing inactive mutants; these mutants were transduced by transient transfection (or infection) of NIH 3T3 cells, which yielded expression levels similar to those of endogenous proteins (Fig. 2B). The expression of the K802R-p110 $\alpha$  mutant, but not of the K805R-p110 $\beta$  mutant, reduced p-PKB activation in early G<sub>1</sub> ( $\sim$ 1 h) (Fig. 2E), as p110 $\alpha$  activity is greater at this point (see below).

We also examined p70S6K activation. In asynchronous cultures, the transient expression of p110-interfering forms decreased and p110-activating mutations enhanced (p110 $\alpha^*$  had a greater effect than p110 $\beta^*$ ) p-p70S6K cellular levels (Fig. 2F). In synchronized populations, however, p110 $\alpha^*$  enhanced p70S6K activation even in G<sub>0</sub>, whereas p110 $\beta^*$  increased p-p70S6K levels most notably at  $\sim$ 4 h after the addition of serum (Fig. 2G). This suggested a selective action of p110 $\alpha$  at the first PI3K activity peak; accordingly, the expression of the K802R-p110 $\alpha$  mutant selectively inhibited the initial p-p70S6K peak ( $\sim$ 1 h), whereas the K805R-p110 $\beta$  mutant moderately reduced late p-p70S6K levels (Fig. 2H). The K805R-p110 $\beta$  mutant did not reduce p70S6K activation at 1 h, probably because p110 $\beta$  exhibits a notably lower activity than p110 $\alpha$  in early G<sub>1</sub> (see below). Quantitation of the gel bands in several assays confirmed the selective effect of the K802R-p110 $\alpha$  mutant on the early p-PKB and p-p70S6K activity peaks following the addition of GF (Fig. 2E and H). The reduction of p110 $\alpha$  and - $\beta$  levels with shRNA yielded consistent results (not shown). These results indicate that both p110 $\alpha$  and p110 $\beta$  modified PKB and p70S6K activation but that only p110 $\alpha$  regulated their early G<sub>1</sub> ( $\sim$ 1 h) activity peaks.

**p110 $\alpha$  regulates FoxO3a phosphorylation.** We also examined FoxO3a (FKHRL1), whose PKB-dependent phosphorylation is required for G<sub>0</sub>/G<sub>1</sub> transition (27). We examined the consequences of reducing the expression of p110 $\alpha$  and - $\beta$  by using interfering mutants or specific shRNA (see Materials and Methods). The expression of p110 $\alpha$  shRNA only affected p110 $\alpha$  levels; similarly, p110 $\beta$  shRNA reduced only p110 $\beta$ , and not p110 $\alpha$ , expression (Fig. 3A). p110 $\beta$  shRNA required

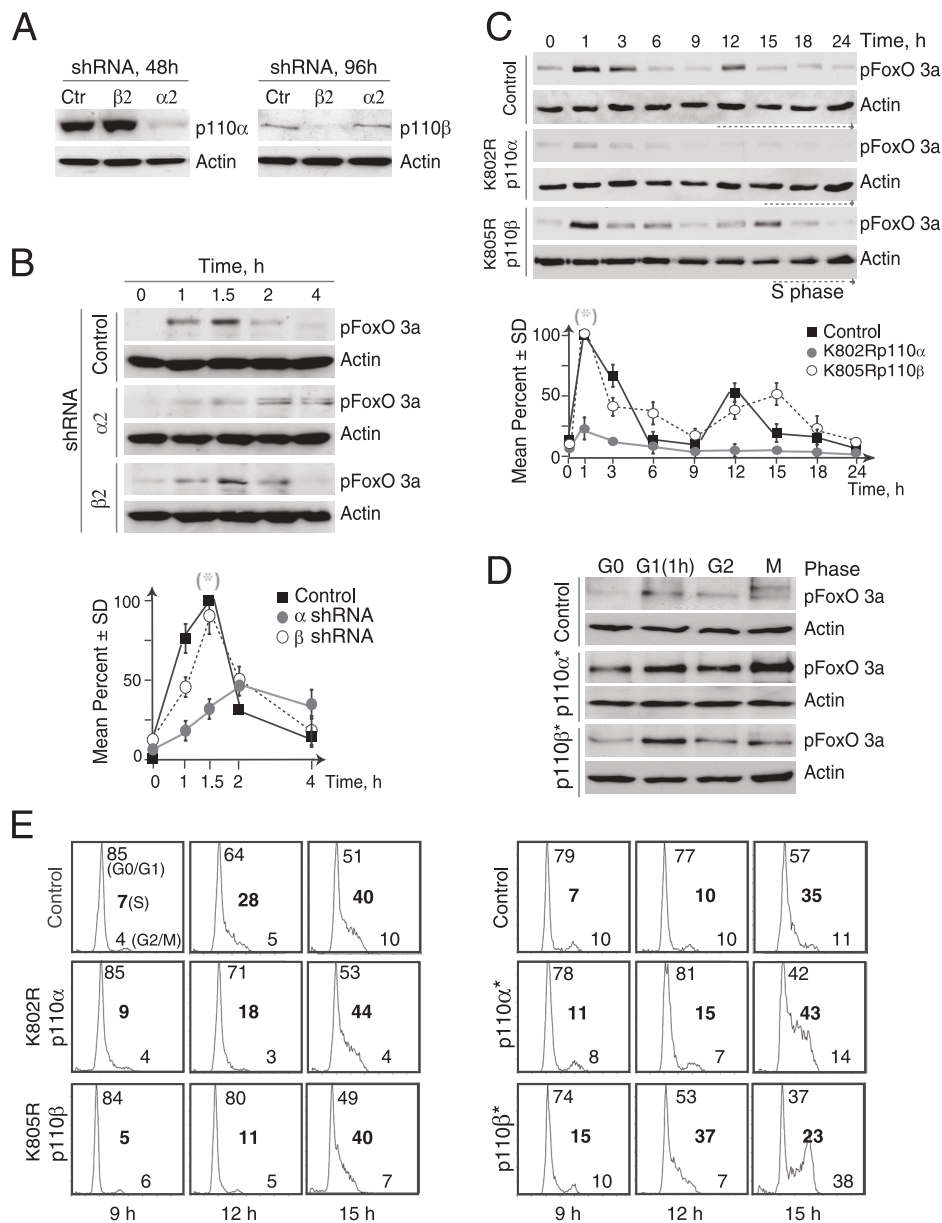


FIG. 3. Selective action of p110 $\alpha$  on FoxO3a phosphorylation. (A and B) NIH 3T3 cells were transfected with pB/U6- $\alpha$ 2 ( $\alpha$ 2) or pB/U6- $\beta$ 2 ( $\beta$ 2) shRNA; WB was used to analyze p110 $\alpha$  or - $\beta$  expression at 48 and 96 h posttransfection (A). A cell fraction was arrested in G<sub>0</sub> and incubated for different times with serum; p-Thr-32-FoxO3a (pFoxO 3a) levels were analyzed with WB (B). The graph represents the mean percentages  $\pm$  standard deviations (SD) of the signal normalized with those of the actin loading control and compared to the maximum signal in control cells (100%) ( $n = 3$ ). (C) Extracts (30  $\mu$ g) from synchronized NIH 3T3 cells transfected with the K802R-p110 $\alpha$  or K805R-p110 $\beta$  mutant were examined with WB as described above. Data were quantitated as described for panel B ( $n = 3$ ); arrows indicate S-phase progression. (D) Extracts from control or stable p110 $\alpha$ \*- or p110 $\beta$ \*-expressing NIH 3T3 cells synchronized in different phases were examined with WB as described above. (E) Representative cell cycle distributions of the indicated synchronized cells.  $x$  axis represents DNA content, and  $y$  axis represents cell number. Percentages of cells in G<sub>0</sub>/G<sub>1</sub>, S, and G<sub>2</sub>/M are indicated. (\*),  $P < 0.05$  for comparison of results for control cells with results for cells expressing p110 $\alpha$  shRNA or the K802R-p110 $\alpha$  mutant at 1.5 h. Ctr, control.

longer incubation periods than p110 $\alpha$  shRNA (minimum 96 h versus 48 h for p110 $\alpha$  shRNA), probably due to the greater stability of the p110 $\beta$  protein (unpublished data). In control cells, the p-FoxO3a signal peaked at 1 to 1.5 h and was reduced by 2 h after GF addition (Fig. 3B). p110 $\alpha$  shRNA greatly decreased p-FoxO3a levels at 1 to 1.5 h, whereas p110 $\beta$  shRNA had only a moderate effect on FoxO3a phosphorylation (Fig. 3B). Similar results were obtained by using a differ-

ent set of shRNA (see Materials and Methods) or the K802R-p110 $\alpha$  or K805R-p110 $\beta$  mutant (Fig. 3C). Control cells showed two peaks of increased p-FoxO3a content in cells in G<sub>1</sub> phase, an early G<sub>1</sub> peak and another peak coincident with the PI3K activity peak in late G<sub>1</sub> (Fig. 3C). Whereas the K802R-p110 $\alpha$  mutant significantly reduced p-FoxO3a levels throughout G<sub>1</sub>, the K805R-p110 $\beta$  mutant moderately diminished the duration of the early G<sub>1</sub> peak and slightly postponed late G<sub>1</sub> FoxO3a



phosphorylation. Accordingly, stable p110 $\alpha^*$ -expressing cell lines exhibited sustained and high p-FoxO3a levels (1) (Fig. 3D), whereas p110 $\beta^*$  only moderately and transiently increased FoxO3a phosphorylation (Fig. 3D and data not shown). The more-prominent action of p110 $\alpha$  in FoxO TF control in early G<sub>1</sub> was confirmed by examining cyclin D (see below). Thus, p110 $\alpha$  plays a dominant role in FoxO phosphorylation in early G<sub>1</sub>. The parallel examination of cell cycle profiles in these assays showed that both the K802R-p110 $\alpha$  and the K805R-p110 $\beta$  mutant reduced cell cycle entry (Fig. 3E); the levels of inhibition varied in different assays (see below) but were of similar magnitudes for interference with p110 $\alpha$  or p110 $\beta$ . Accordingly, p110 $\alpha^*$ -expressing cells entered cell cycle earlier (1, 21) (Fig. 3E) and p110 $\beta^*$ -expressing cells entered S phase even more efficiently than p110 $\alpha^*$ -expressing cells (Fig. 3E).

**p110 $\alpha$  and - $\beta$  control cyclin E and A levels, but only p110 $\alpha$  regulates cyclin D.** Early signaling pathways promote cell growth and the expression of G<sub>1</sub> cyclins (14). We subsequently examined the consequences for G<sub>1</sub> cyclin expression of interfering with p110 $\alpha$  and - $\beta$  activity. Comparison of synchronous stable p110 $\alpha^*$ - and p110 $\beta^*$ -expressing cells showed that enhanced activation of p110 $\alpha$ , but not - $\beta$ , increased cyclin D3 levels (Fig. 4A and B). In contrast, both p110 $\alpha^*$ - and p110 $\beta^*$ -expressing cells upregulated cyclin E levels even before the addition of serum, and p110 $\alpha^*$ , but not - $\beta^*$ , prolonged cyclin E expression (Fig. 4A and B). Neither p110 $\alpha^*$  nor - $\beta^*$  expression was sufficient to induce cyclin A expression in G<sub>0</sub>, but cyclin A appeared earlier in these cells than in controls, and its expression was greater and more prolonged in p110 $\alpha^*$ -expressing cells (Fig. 4A and B). In p110 $\alpha^*$ -expressing cells, the higher cyclin D3 levels (Fig. 4A) correlated with their greater p-FoxO3a content (Fig. 3) (1), as p-FoxO3a controls cyclin D synthesis (36).

We performed a complementary analysis and examined the effects of interfering with p110 $\alpha$  and - $\beta$  expression on G<sub>1</sub> cyclin expression. We examined the effect of reducing p110 $\alpha$  and - $\beta$  expression levels by shRNA in murine NIH 3T3 cells (not shown) and human U2OS cells synchronized at the G<sub>1</sub>/S border (Fig. 5). hp110 $\alpha$  shRNA selectively reduced p110 $\alpha$  expression, and p110 $\beta$  shRNA acted only on p110 $\beta$  (Fig. 5A). Nonetheless, p110 $\alpha$ , but not - $\beta$ , shRNA reduced cyclin D3 expression (Fig. 5B and C). In contrast, both shRNA (for p110 $\alpha$  or - $\beta$ ) delayed the expression of cyclins E and A (Fig. 5B and C). Thus, p110 $\alpha$  and p110 $\beta$  regulate the expression of cyclins E and A, but only p110 $\alpha$  controls cyclin D levels.

**p110 $\alpha$  and - $\beta$  control late G<sub>1</sub> c-Myc levels and RB phosphorylation.** Late G<sub>1</sub> PI3K activation stabilizes c-Myc (24); we attempted to determine which of the two ubiquitous isoforms regulated c-Myc levels in late G<sub>1</sub>. Stable p110 $\alpha^*$ - and p110 $\beta^*$ -expressing NIH 3T3 cell lines, as well as NIH 3T3 cells infected with retroviruses expressing the K802R-p110 $\alpha$  or K805R-p110 $\beta$  mutant, were synchronized as described above. The control cells exhibited two peaks of increased c-Myc levels (Fig. 6A and B), as reported previously (24). In p110 $\alpha^*$ -expressing cells, the c-Myc levels were higher and peaked earlier but the cells still showed the two peaks of c-Myc expression (Fig. 6A and B). p110 $\beta^*$  expression also moderately enhanced c-Myc stability, but only in late G<sub>1</sub> (Fig. 6A and B). The effect of p110 $\alpha^*$  at increasing c-Myc levels is consistent with its ac-

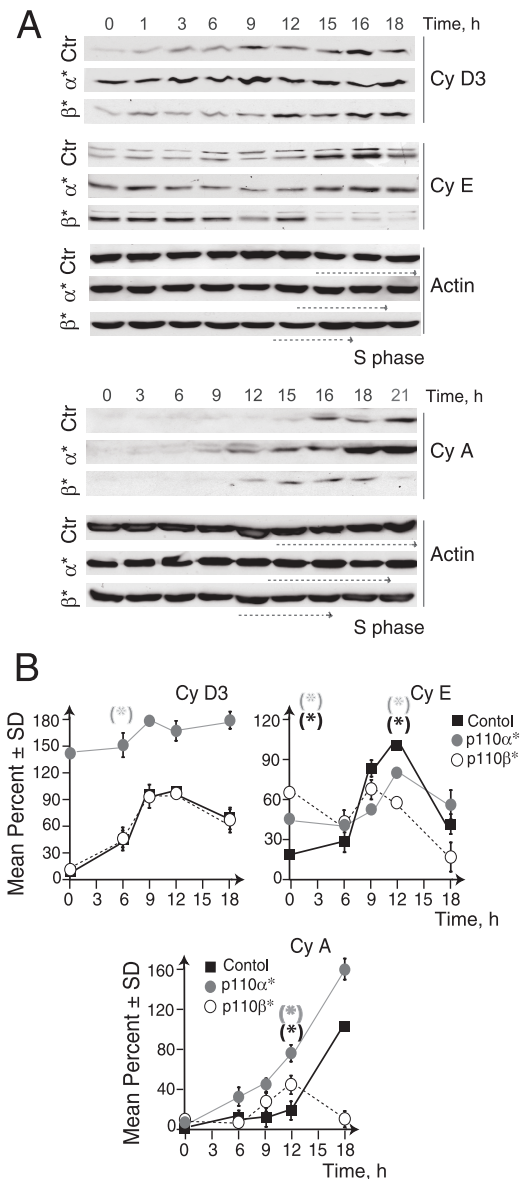


FIG. 4. Enhanced p110 $\alpha$  and - $\beta$  activities upregulate G<sub>1</sub> cyclins. (A) Levels of cyclins D3, E, and A, as well as actin levels, were examined by WB in synchronous cultures of stable p110 $\alpha^*$ - or p110 $\beta^*$ -expressing NIH 3T3 cells. Transits through S phase are indicated (arrows). Ctr, control. (B) The graphs represent the mean percentages  $\pm$  standard deviations (SD) of the signals for cyclins normalized with those of loading controls and compared to the maximum signal (100%) in wild-type cells ( $n = 3$ ).  $P$  values ( $P < 0.05$ ) for the data from some time points are indicated by asterisks. Gray asterisks show comparisons between control and p110 $\alpha^*$ -expressing cells; black asterisks show comparisons between control and p110 $\beta^*$ -expressing cells. Cy, cyclin.

tion on FoxO TF, since FoxO TF represses c-Myc expression (8); it also concurs with the higher cyclin A levels observed in these cells, as c-Myc regulates cyclin A expression (26). Nonetheless, both p110 $\alpha^*$  and p110 $\beta^*$  prolonged c-Myc stability in late G<sub>1</sub>. Interference with either p110 $\alpha$  or - $\beta$  postponed or reduced, respectively, the c-Myc expression levels in late G<sub>1</sub> (Fig. 6C and D), suggesting that both isoforms control c-Myc levels in advanced G<sub>1</sub>, although they do so differently.

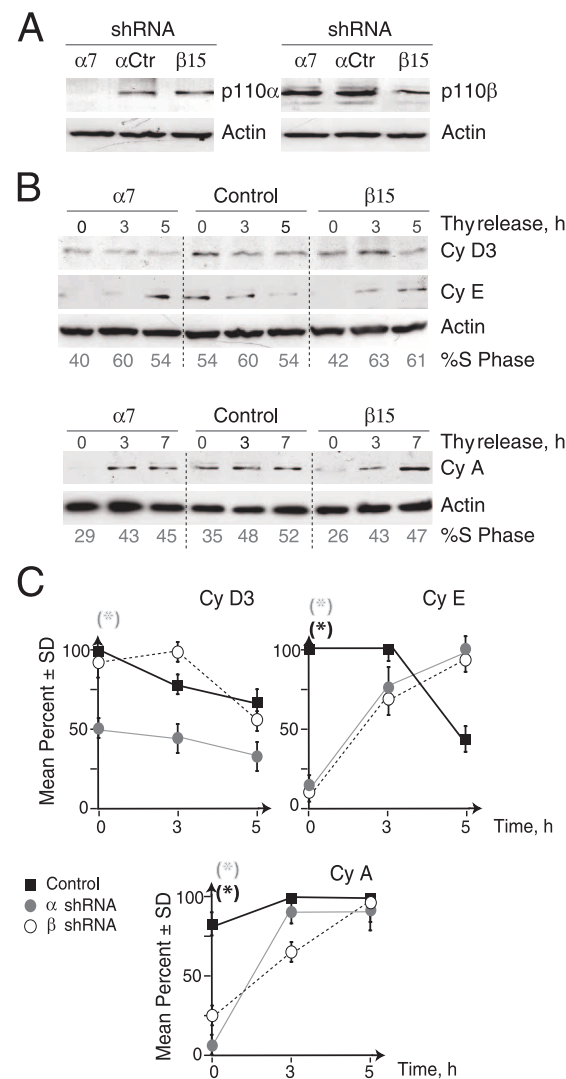


FIG. 5. p110 $\alpha$  and - $\beta$  control expression of G<sub>1</sub> cyclins. (A and B) Expression levels of p110 $\alpha$  and p110 $\beta$  in extracts of U2OS cells transfected with pTER-p110 $\alpha$ 7 ( $\alpha$ 7) and pTER-p110 $\beta$ 15 ( $\beta$ 15) shRNA (for 48 and 96 h, respectively) (A), and a fraction of the cells was synchronized at the G<sub>1</sub>/S boundary, and expression levels of cyclins D3, E, and A were examined by WB at different times after serum addition (B). The percentages of cells in S phase are indicated. (C) Graphs show the mean percentages  $\pm$  standard deviations (SD) of the signals for each cyclin compared to the maximum signal in wild-type cells (100%), normalized with the signals for loading controls ( $n = 3$ ).  $P$  values ( $P < 0.05$ ) for data at the 0 time point, prior to release, are shown by asterisks. Gray asterisks show comparisons between control and p110 $\alpha$  shRNA-expressing cells; black asterisks show comparisons between cells expressing p110 $\beta$  shRNA and cells expressing control shRNA. Ctr, control; Cy, cyclin; Thy, thymidine.

We also examined the consequences of interfering with p110 $\alpha$  and - $\beta$  activities for the phosphorylation of RB, a major Cdk2/cyclin substrate (37). In synchronized NIH 3T3 control cells, RB was hyperphosphorylated at  $\sim 12$  h after GF addition (Fig. 7A). Both p110 $\alpha$ \* and - $\beta$ \* expression affected RB phosphorylation, which was observed at low levels even in quiescent cells; in late G<sub>1</sub>, p110 $\alpha$ \* and - $\beta$ \* also increased and accelerated (p110 $\beta$ \* more so) the appearance of hyperphosphorylated RB

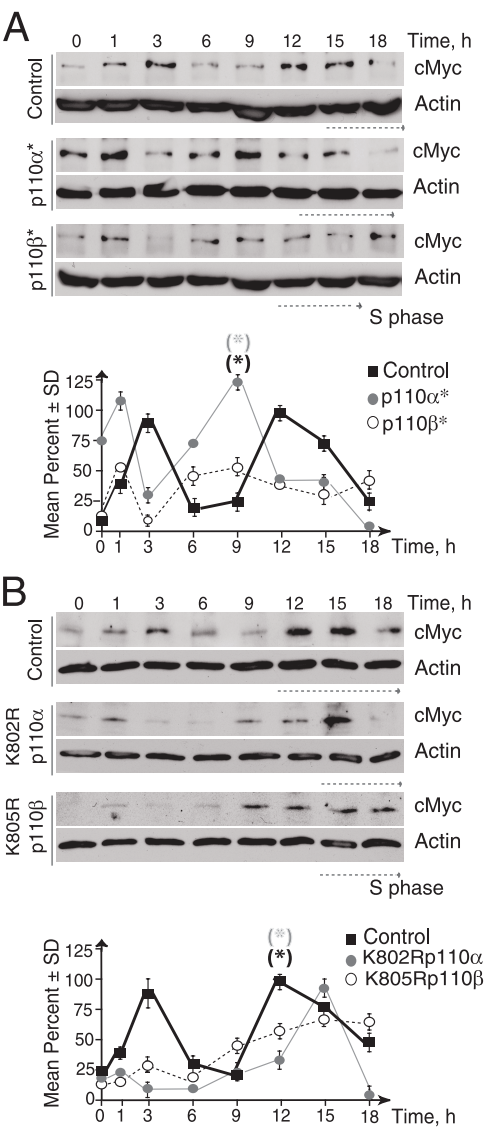


FIG. 6. p110 $\alpha$  and - $\beta$  regulate c-Myc levels. (A and B) Stable NIH 3T3 cells expressing p110 $\alpha$ \* or p110 $\beta$ \* (A) or NIH 3T3 cells infected with viruses expressing the K802R-p110 $\alpha$  or K805R-p110 $\beta$  mutant (B) were arrested in G<sub>0</sub> and incubated for different times after serum addition; c-Myc expression levels were analyzed by WB. Graphs show the mean percentages  $\pm$  standard deviations (SD) of the c-Myc signals compared to the maximum signal in wild-type cells at 12 h after GF addition (100%) and normalized with the signals of loading controls ( $n = 3$ ). Transits through S phase are indicated (arrows).  $P$  values ( $P < 0.05$ ; Student's  $t$  test) for comparisons of data at 9 and 12 h are shown by asterisks. Gray asterisks show comparisons between control and p110 $\alpha$  mutant-expressing cells; black asterisks show comparisons between controls and p110 $\beta$  mutant-expressing cells.

(Fig. 7A). Accordingly, interference with p110 $\alpha$  or - $\beta$  activity by the expression of the K802R-p110 $\alpha$  or K805R-p110 $\beta$  mutant delayed RB phosphorylation (the K805R-p110 $\beta$  mutant had a greater effect) (Fig. 7B), suggesting that both p110 $\alpha$  and - $\beta$  activities regulate RB phosphorylation. **Distinct activation kinetics of p110 $\alpha$  and - $\beta$  during G<sub>1</sub> phase.** The distinct contributions of p110 $\alpha$  and - $\beta$  to early G<sub>1</sub> events suggested that p110 $\alpha$  and - $\beta$  might present different

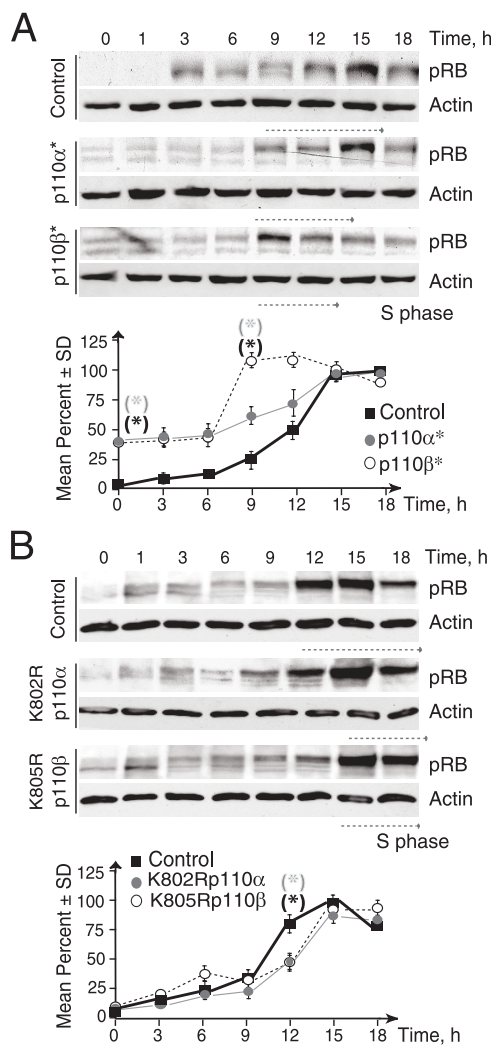


FIG. 7. p110 $\alpha$  and - $\beta$  control RB phosphorylation. (A and B) Stable NIH 3T3 cells expressing p110 $\alpha^*$  or p110 $\beta^*$  or infected with viruses encoding the K802R-p110 $\alpha$  (p110 $\alpha$ ) or K805R-p110 $\beta$  (p110 $\beta$ ) mutant were treated as described in the Fig. 6 legend; RB expression levels were analyzed by WB. Graphs represent the mean percentages  $\pm$  standard deviations (SD) of the signals for p-RB (pRB) compared to the maximum p-RB signal in wild-type cells at 15 h (100%) ( $n = 3$ ). Quantitation was as described in the Fig. 6 legend. (\*),  $P < 0.05$ .

activation kinetics. To determine the PI3K isoform(s) activated in early and late G<sub>1</sub>, we examined NIH 3T3 cells that permit the synchronization of the cultures in G<sub>0</sub> phase (25). To isolate p110 $\alpha$  and - $\beta$ , we could not use p85 Ab as it brings down both catalytic subunits, nor we could use anti-p110 $\alpha$  and - $\beta$  Ab, since most of them reduce PI3K activity (unpublished observations). Thus, to evaluate specific isoform activation through G<sub>1</sub> phase, we cotransfected NIH 3T3 cells simultaneously with cDNA encoding wild-type p110 $\alpha$  and - $\beta$  fused to two different tags. Recombinant Myc-tagged p110 $\alpha$  and His-tagged p110 $\beta$  were expressed at slightly above basal levels (Fig. 8A). p110 $\alpha$  and p110 $\beta$  were efficiently immunoprecipitated by using Myc-tagged or His-tagged Ab, as determined by WB using the specific p110 $\alpha$  or p110 $\beta$  Ab, respectively (Fig. 8B). Moreover, p110 $\alpha$ -p85 and p110 $\beta$ -p85 complexes were at similar levels, as

estimated by comparison of the amounts of p85 present in p110 $\alpha$  and p110 $\beta$  immunoprecipitates (Fig. 8B, bottom).

We immunopurified p110 $\alpha$  and - $\beta$  with the corresponding anti-tag Ab and tested their enzyme activities *in vitro*. After the addition of serum, p110 $\alpha$  activated early, at 5 to 10 min following serum addition; this activity increased at 1 h and then diminished to basal levels, increasing again at  $\sim$ 7 h (Fig. 8C). p110 $\beta$  exhibited modest activity peaks at 1 and 4 h and a maximum activity at  $\sim$ 8 h after the addition of serum (Fig. 8C). In NIH 3T3 cells, part of p110 $\beta$ , but not p110 $\alpha$ , localizes in the nuclei (our unpublished results); nuclear PI3K activity peaked at  $\sim$ 8 h after the addition of serum, confirming maximum endogenous p110 $\beta$  activity in late G<sub>1</sub> (not shown). We checked that similar amounts of p85 were associated with either p110 $\alpha$  or p110 $\beta$  at different time points (Fig. 8D). Therefore, most PI3K activity in early G<sub>1</sub> corresponds to that of p110 $\alpha$ ; p110 $\beta$  exhibits another minor peak by 4 h. In late G<sub>1</sub>, both p110 $\alpha$  and - $\beta$  are activated and p110 $\beta$  exhibits its maximum activity.

**p110 $\alpha$  and - $\beta$  have different activation requirements.** The different activation kinetics of p110 $\alpha$  and - $\beta$  suggested that they exhibit distinct activation requirements. Since TyrK and Ras regulate class I<sub>A</sub> PI3K activation (17), we tested whether the p110 $\alpha$  and - $\beta$  activities in G<sub>1</sub> phase were affected by treatment with inhibitors of TyrK (herbamycin) and Ras (lovastatin). We first checked the selective action of these inhibitors in reducing p-Tyr or active Ras levels (24 and data not shown).

Herbamycin treatment, but not treatment with lovastatin, reduced p110 $\alpha$  activity at 7 min. Both herbamycin and lovastatin inhibited p110 $\alpha$  activation at 1 and 7 h (Fig. 8C). This suggests that the first increase in the activity of p110 $\alpha$  is TyrK dependent, but TyrK and Ras contribute to p110 $\alpha$  activation at 1 and 7 h. In contrast, the modest p110 $\beta$  activity at 1 h was sensitive to lovastatin, but not to herbamycin, although both inhibitors blocked later p110 $\beta$  activation peaks (at 4 and 8 h) (Fig. 8C and F). The results of these assays illustrate the distinct activation requirements for p110 $\alpha$  and - $\beta$  activities. The maximum p110 $\alpha$  (at 1 h) and p110 $\beta$  (at 8 h) activities, nonetheless, were herbamycin and lovastatin sensitive, suggesting that TyrK and Ras activation contribute to optimal p110 $\alpha$  and p110 $\beta$  activities.

To confirm the distinct activation requirements of p110 $\alpha$  and p110 $\beta$ , we examined whether the response of purified p85-p110 $\beta$  complex to activated TyrK and Ras is similar to that of p85-p110 $\alpha$  (17). We used Tyr-phosphorylated platelet-derived growth factor receptor (PDGF-R) peptide and purified active Ras *in vitro*; this analysis confirmed that the Tyr-phosphorylated peptide activates p110 $\alpha$ , that active Ras alone exerts a moderate activation effect, and that Ras synergizes with p-Tyr phosphopeptides to enhance p110 $\alpha$  activity (Fig. 9B and C) (17). In contrast, although p110 $\beta$  activity also increased with the phosphopeptides and with active Ras and together they induced a greater activation effect (Fig. 9B and C), there was a consistent difference between p110 $\alpha$  and p110 $\beta$  activation. Whereas p110 $\alpha$  responds better to Tyr phosphopeptides than to V12-Ras alone, Ras consistently induced a greater activating effect than phosphopeptides on p110 $\beta$  (Fig. 9B and C). These assays confirmed the TyrK activation requirement for p110 $\alpha$  induction (17) and demonstrated the greater intrinsic Ras dependence for p110 $\beta$  activation.

Since p110 $\alpha$  activation is greater than that of p110 $\beta$  in early



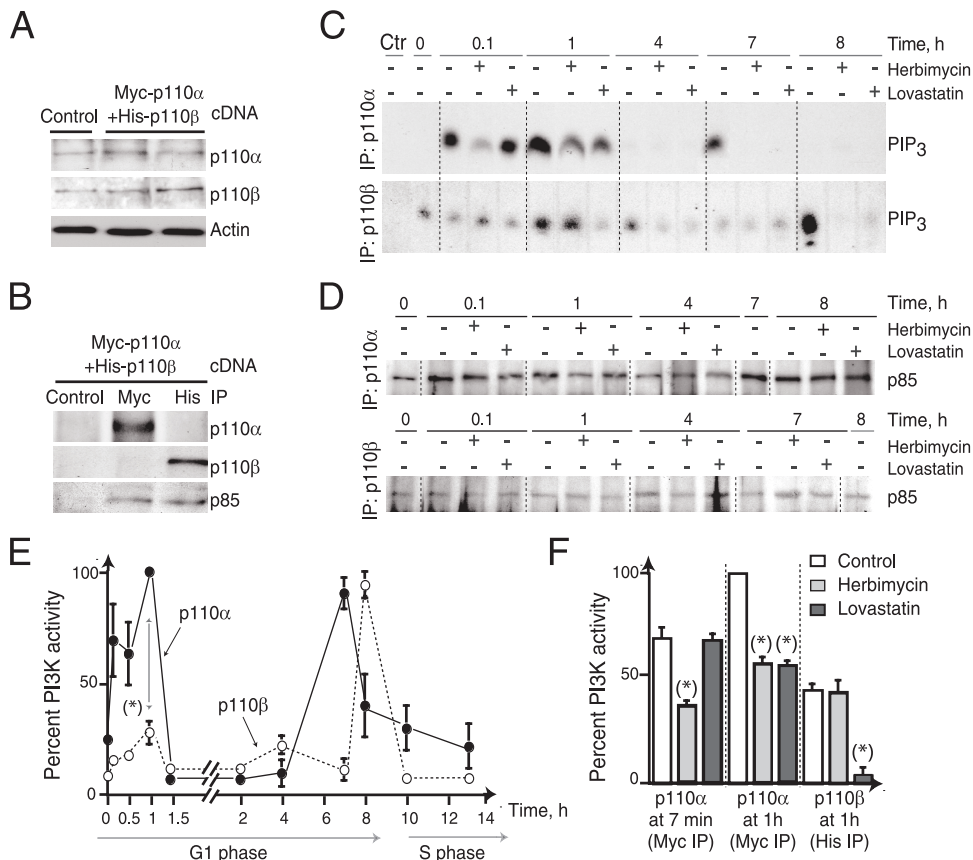


FIG. 8. p110 $\alpha$  and - $\beta$  show distinct activation kinetics. (A) WB analysis of total p110 $\alpha$  and p110 $\beta$  levels in NIH 3T3 cells transfected with empty vector or with cDNA encoding Myc-tagged p110 $\alpha$  plus His-tagged p110 $\beta$ ; expression levels of recombinant proteins are within the range of expression of endogenous p110. (B) NIH 3T3 cell extracts as described for panel A were immunoprecipitated (IP) using anti-Myc-tagged or anti-His-tagged Ab. WB showed p110 $\alpha$  or - $\beta$  expression and the amount of p85 in complex with p110. (C) NIH 3T3 cells transfected with Myc-p110 $\alpha$  plus His-p110 $\beta$  were incubated (24 h), arrested in G<sub>0</sub>, and released in serum alone or with herbimycin or lovastatin at the indicated times. p110 $\alpha$  or - $\beta$  was immunoprecipitated as described for panel B, and kinase activity was assayed in vitro. (D) Immunoprecipitates as described for panel C were resolved by SDS-polyacrylamide gel electrophoresis, and associated p85 was assayed by WB. (A to D) Each assay result shown is representative of five assays with similar results. (E and F) Graphs show the mean percentages  $\pm$  standard deviations (SD) ( $n \geq 4$ ) of p110 $\alpha$  and - $\beta$  activities (as shown in panel C) compared to the activity of p110 $\alpha$  at 1 h (100%). The double-headed arrow in panel E indicates the time point for which the  $P$  value was calculated. (\*),  $P < 0.05$ ; Student's  $t$  test. Ctr, control; +, present; -, absent.

G<sub>1</sub> (at 7 min to 1 h), we compared the binding of p110 $\alpha$  and - $\beta$  to PDGF-R at early time points. Both isoforms associated with the PDGF-R at 7 min after the addition of serum (not shown), arguing against a selective binding of p110 $\alpha$  as the cause for its selective activation at this point. To gain insight into the mechanisms of p110 $\alpha$  and - $\beta$  activation in early G<sub>1</sub>, we considered the greater Ras dependence of p110 $\beta$  in vitro and postulated that the activation of p110 $\beta$  in vivo might also rely more on active Ras than that of p110 $\alpha$  does. To determine the relative Ras dependence for p110 $\alpha$  and - $\beta$ , we examined the sensitivities of p110 $\alpha$  and - $\beta$  to interference with Ras activation induced by the coexpression of N17-Ras with Myc-tagged versions of p110 $\alpha$  and - $\beta$ . Whereas the first p110 $\alpha$  activity peak at 7 min decreased only partially in the presence of N17-Ras (approximately one-third), p110 $\beta$  activation, which was lower than that of p110 $\alpha$ , occurred later and was drastically reduced (more than 90%) following the expression of N17-Ras (Fig. 9D and E). These observations show that both in vitro and in vivo, the activation of p110 $\beta$  is more Ras dependent than that of p110 $\alpha$ . Considering that Ras activation is moderate at 1 h and

maximal in late G<sub>1</sub> (24), the greater Ras dependence of p110 $\beta$  explains its activation kinetics in G<sub>1</sub> phase.

**Interference with p110 $\alpha$  or - $\beta$  expression/activity results in cell cycle entry defects.** During the course of the experiments using synchronized populations, we noticed that cells expressing p110 $\alpha$ \* and - $\beta$ \* showed an earlier S-phase entry (Fig. 3E, 4, 6A, and 7A). Accordingly, the expression of K802R-p110 $\alpha$  and K805R-p110 $\beta$  mutants (Fig. 3E, 6B, and 7B) or the reduction of p110 $\alpha$  and - $\beta$  levels by shRNA in U2OS cells (Fig. 5B) induced a delayed G<sub>1</sub>/S transition. We also interfered with p110 $\alpha$  or - $\beta$  expression in NIH 3T3 cells by using p110 $\alpha$  or - $\beta$  shRNA, as described above. p110 $\alpha$  shRNA selectively reduced p110 $\alpha$  expression and p110 $\beta$  shRNA diminished only p110 $\beta$  levels (Fig. 10A). Despite partial reductions in p110 $\alpha$  and - $\beta$  expression, both shRNA delayed S-phase entry (Fig. 10A).

We also examined cell cycle entry by the incorporation of bromodeoxyuridine (BrdU). Interference with endogenous p110 $\alpha$  and - $\beta$  kinase activity in COS cells by the transfection of the inactive K802R-p110 $\alpha$  or K805R-p110 $\beta$  mutants reduced BrdU incorporation (Fig. 10B). We also analyzed primary

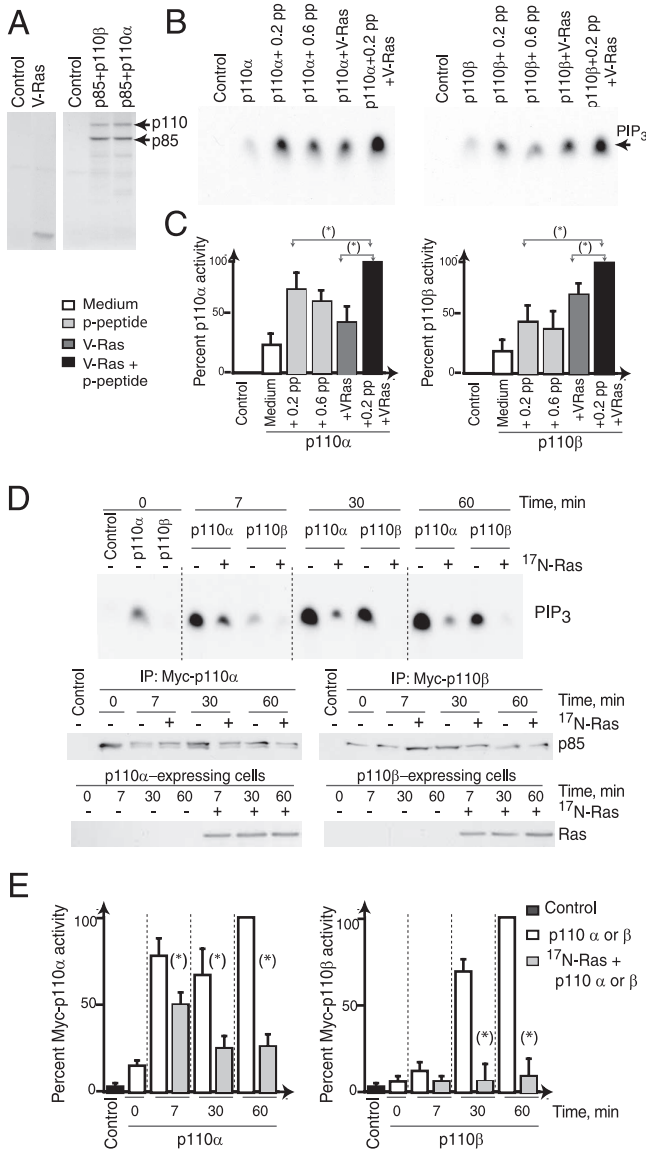


**FIG. 9.** Activation of p110 $\beta$  requires Ras. (A) Control vector or cDNAs encoding V12-Ras or p85 combined with p110 $\alpha$  or p110 $\beta$  were transcribed and translated *in vitro* and then analyzed by SDS-polyacrylamide gel electrophoresis. (B) The activities of purified p85/p110 $\alpha$  or p85/p110 $\beta$  complexes were assayed *in vitro*, alone or in the presence of a PDGF-R phosphopeptide (pp) at the indicated dose ( $\mu$ M), V12-Ras, or both. The panels show the results of representative experiments ( $n = 3$ ). (C) The graphs compare PIP<sub>3</sub> spot intensities for three experiments (as in panel B) to maximum p110 $\alpha$  or - $\beta$  activities (pp + VRas [V12-Ras], 100%) ( $n = 3$ ). Double-ended arrows indicate the two values being compared. (D) NIH 3T3 cells were transfected with empty vector or cotransfected with cDNAs encoding p85 and Myc-p110 $\alpha$  or Myc-p110 $\beta$ . p85-p110 cDNAs were transfected alone or with a vector encoding N17-Ras. After 36 h, cells were synchronized in G<sub>0</sub> and released by serum addition for different times. p110 $\alpha$  or p110 $\beta$  was immunoprecipitated, and their activities assayed *in vitro*. We examined the amount of p85 in the p85-p110 complexes by WB (middle panels). The different samples expressed similar N17-Ras levels (bottom), as determined by WB. +, present; -, absent; IP, immunoprecipitate. (E) Graphs compare the mean percentages  $\pm$  standard deviations (SD) of p110 $\alpha$  and - $\beta$  activities of three different assays as described for panel C to the activity of p110 $\alpha$  or p110 $\beta$  at 1 h (100%), normalized in comparison with the p85 loading control. (\*),  $P < 0.05$ . V-Ras/VRas, V12-Ras; N-Ras/<sup>17</sup>N-Ras, N17-Ras.

cells. Homozygous deletion of p110 $\alpha$  or - $\beta$  causes embryonic lethality (3, 4). We thus examined MEF from p110 $\alpha$  and - $\beta$  heterozygous mice. Since G<sub>0</sub> arrest by serum deprivation or growth to confluence is inefficient in MEF, we analyzed S-phase entry by measuring BrdU incorporation in exponentially growing cultures. Both heterozygous deletions reduced the fraction of BrdU-positive cells compared to the BrdU-positive fraction of wild-type fibroblasts (Fig. 10C). These results demonstrate that both p110 $\alpha$  and - $\beta$  control cell cycle entry.

## DISCUSSION

The activation of PI3K is essential for cell division. We examined which one of the two ubiquitous PI3K isoforms (p110 $\alpha$  and - $\beta$ ) regulates cell cycle entry. We describe results showing that p110 $\alpha$  activated before p110 $\beta$  at the G<sub>0</sub>/G<sub>1</sub> transition exerts a selective action in inducing G<sub>1</sub> entry events. In fact, the first activity peak of p110 $\alpha$  had already occurred at 5 to 10 min following the addition of GF and it required TyrK activation; p110 $\alpha$  further increased its activity at  $\sim$ 1 h in a TyrK- and Ras-dependent manner and activated again in advanced G<sub>1</sub>. In contrast, p110 $\beta$  displayed low activity in early G<sub>1</sub>, with a moderate increase at  $\sim$ 1 h; Ras induction was essential for p110 $\beta$  activation. p110 $\beta$  displayed another low activity peak in mid-G<sub>1</sub> and maximal activation in late G<sub>1</sub>. p110 $\alpha$  and - $\beta$  activate in a sequential manner in late G<sub>1</sub>. This concurs with their distinct sensitivities to TyrK and Ras since, also in late G<sub>1</sub>, the activation of TyrK precedes that of Ras, which is maximal at this point (24). In agreement with the greater activation of p110 $\alpha$  in early G<sub>1</sub>, this isoform regulated early G<sub>1</sub> events (such as cyclin D levels and FoxO phosphorylation) more than p110 $\beta$  did. Nonetheless, interference with either p110 $\alpha$  or p110 $\beta$  reduced S-phase entry, showing that both isoforms control the G<sub>1</sub>→S transition. p110 $\alpha$  and - $\beta$  regulated the expression of c-Myc and cyclins E and A, RB phosphorylation, and, in turn, S-phase entry.

The critical role of p110 $\alpha$  and - $\beta$  in the control of cell division was taken into account during the preparation of the cell lines for this study. We used stable cell lines expressing low levels of p110 $\alpha^*$  and p110 $\beta^*$ , since the transient overexpression of high levels of p110 $\alpha^*$  impairs progression through the G<sub>2</sub>/M phases (1). p110 $\alpha^*$ -expressing cells entered cell cycle faster than controls, and p110 $\beta^*$ -expressing cells divided at a lower half-life than both p110 $\alpha^*$ -expressing cells and controls. For the analysis of the consequences of reducing the p110 $\alpha$  and p110 $\beta$  activities, we had to use transient transfection or infection, as cell lines of kinase-inactive mutants or shRNA were unstable, showing that p110 $\alpha$  and p110 $\beta$  activities control cell survival and/or division.

An open question regarding the select functions of class I<sub>A</sub> PI3K isoforms is how the specificities of the different isoforms are acquired, as p110 catalytic subunits produce the same lipid products and all class I<sub>A</sub> p110s associate with p85 molecules, which bring p110 to activated receptors (42, 12). p110 $\delta$ 's specificity seems related to its tissue-specific expression pattern (30). However, in the case of p110 $\alpha$  and - $\beta$ , they are ubiquitous and still they exhibit distinct functions in development (3, 4) and cell division (Fig. 2 and 3). The observations presented here illustrate mechanisms for the p110 $\alpha$  and - $\beta$  functional

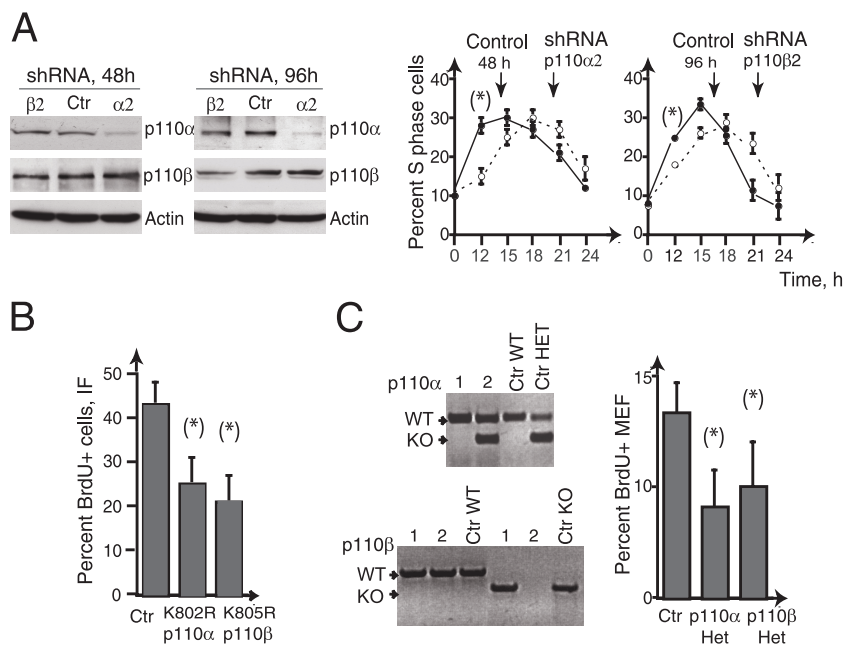


FIG. 10. Interference with p110 $\alpha$  or - $\beta$  results in cell cycle defects. (A) NIH 3T3 cells were transfected with the indicated shRNA; at 48 or 96 h posttransfection, cells were collected and lysates (30  $\mu$ g) examined by WB using anti-p110 $\alpha$ , anti-p110 $\beta$ , and antiactin Ab (left panels). A fraction of the cells were synchronized, and cell cycle distribution examined at indicated times. The proportion of cells in S phase is represented (mean  $\pm$  standard deviation) ( $n = 3$ ) (right panels).  $P$  values for comparisons of the data at 12 h are shown. (B) COS cells were transfected with cDNA encoding the K802R-p110 $\alpha$  or K805R-p110 $\beta$  mutant; at 24 h posttransfection, the cells were incubated with BrdU (1 h). The percentages of cells incorporating BrdU were examined by immunofluorescence (IF) (means  $\pm$  standard deviations) ( $n = 3$ ). (C) Heterozygous (HET/HET) p110 $\alpha$  and p110 $\beta$  MEF were screened by specific PCR (left). We show percent BrdU incorporation in exponentially growing heterozygous MEF compared to that in wild-type (WT) MEF from littermate embryos. (\*),  $P < 0.05$ ; Student's  $t$  test. Ctrl, control; 1 and 2, mice 1 and 2; KO, knockout.

specificities that are delimited by the different activation requirements determining when these isoforms are activated.

The phenotype of mice expressing a Ras-resistant p110 $\alpha$  mutant supports the observation that, physiologically, p110 $\alpha$  activity is partially independent of Ras. These mice present a number of defects, including reduced cell proliferation and diminished Ras-dependent tumor formation (15); however, they exhibit a milder phenotype than p110 $\alpha$ -deficient mice (3). This shows that despite the fact that K227A p110 $\alpha$  is not activated by Ras, it still exerts some of the p110 $\alpha$  actions in vivo (15). Interestingly, the expression of wild-type p110 $\beta$ , - $\delta$ , and - $\gamma$  is sufficient to induce chicken embryo fibroblast focus formation; in contrast, p110 $\alpha$  requires an activating mutation to trigger transformation (20). The crystal structure analysis of the inter-Src homology 2 domain of p85 in complex with the N-terminal part of p110 $\alpha$  suggests that activation by Tyr kinases releases p110 $\alpha$  from the inhibition exerted by p85; it is possible that the p85-mediated p110 structural constraint is stronger in the case of p110 $\alpha$  (16, 29). The H1047R mutant activates p110 $\alpha$ ; following the additional K227E mutation, this mutant no longer binds Ras but contributes to cell transformation. In contrast, wild-type p110 $\beta$  loses its transforming activity when Ras binding is impaired (20). It is possible that in the absence of Ras binding, p110 $\beta$  simply exhibits low enzymatic activity, since we show that purified p110 $\beta$  shows a higher Ras dependence for activation than p110 $\alpha$  (Fig. 9). In this regard, although late G<sub>1</sub> p110 $\beta$  activation was greatly inhibited by the addition of herbamycin at 7 h (Fig. 8C), this treatment reduced late G<sub>1</sub> Ras activity (not shown). Future

studies will attempt to determine which residues in the p110 Ras-binding site determine the greater Ras dependence of p110 $\beta$ .

Whereas the results of our studies support the existence of activation specificities for p110 $\alpha$  and - $\beta$ , downstream of p110 $\alpha$  and - $\beta$  we find that they are both capable of regulating the same substrates. In fact, both the mutants interfering with p110 $\alpha$  and those interfering with p110 $\beta$  affected PKB and p70S6K activities, illustrating that these p110 isoforms have the potential of regulating the same effectors. The distinct kinetics of p110 $\alpha$  activation in early G<sub>1</sub> phase explains the specific function for p110 $\alpha$  at this point. In fact, in synchronized cells, p110 $\alpha$  selectively controlled the first activation wave of PKB and p70S6K and, in turn, FoxO3a phosphorylation and the expression of its effector, cyclin D. Since p110 $\beta$ 's activity was low in early G<sub>1</sub>, interference with its kinase activity affected PKB and p70S6K activities at this point only slightly, although it modulated their activities at later time points (Fig. 2). In contrast, in late G<sub>1</sub>, both p110 $\alpha$  and p110 $\beta$  exhibited remarkable increases in activity and regulated c-Myc and cyclin E and A levels, as well as RB phosphorylation. Therefore, both the p110 $\alpha$  and - $\beta$  isoforms controlled cell cycle regulators at the G<sub>1</sub>/S boundary, offering a mechanism for the involvement of these isoforms in the control of cell cycle entry.

The expression of p110 $\alpha$  shRNA inhibits carcinoma cell growth (28), supporting the role of p110 $\alpha$  in cell division. Selective interference with p110 $\alpha$  inhibited the early activation of the cell growth regulator p70S6K (Fig. 2). Since cell cycle entry cannot occur without cell growth (35), p110 $\alpha$  mutations



in human cancer might facilitate G<sub>0</sub> exit by upregulating protein synthesis and inhibiting FoxO TF-controlled cell cycle inhibitors. Later in the cell cycle, p110 $\alpha$  and - $\beta$  contribute to enhancing c-Myc stability and Cdk2 activation (24). p110 $\alpha$  is thus a potential target for cancer treatment; nonetheless, the inhibition of p110 $\alpha$  interferes with glucose metabolism (22). Alternatively, interference with p110 $\beta$  might also be considered a promising approach, since although no activating mutations in p110 $\beta$  in human cancer have been described, the overexpression of the wild-type p110 $\beta$  does promote cell transformation (20). In fact, shRNA for p110 $\beta$  show an antiproliferative effect in tumor cell lines (6, 32) and interference with p110 $\beta$  blocks S-phase entry (Fig. 10).

Altogether, we report that p110 $\alpha$  and - $\beta$  are activated with distinct kinetics during G<sub>1</sub> phase, as they respond differently to the activation of TyrK and Ras. p110 $\alpha$  primarily controls early G<sub>1</sub> events, such as FoxO TF inactivation and cyclin D expression, whereas both p110 $\alpha$  and - $\beta$  regulate later G<sub>1</sub> events and G<sub>0</sub>/G<sub>1</sub> transition.

#### ACKNOWLEDGMENTS

M.M. has a predoctoral FPU fellowship from the Spanish Ministry of Education and Science. This work was financed in part by grants from the AICR Foundation, the Fundación Ramón Areces, the AECC, and the Spanish DGcyDT (SAF2004-05955). The Department of Immunology and Oncology was founded and is supported by the Spanish National Research Council (CSIC) and by Pfizer.

We thank M. White for the myc-p110 plasmid, C. Murga for pCEF2-p110 $\beta$ -CAAX, B. Vanhaesebroeck for His-p110 $\beta$ , M. van de Wetering for the pTer vector, and Y. Shi for the pBlue/U6 plasmid. We also thank R. L. Nussbaum for the kind donation of p110 $\alpha$ - and p110 $\beta$ -deficient mice, A. Klippel for anti-p110 $\alpha$  Ab, and C. Mark for editorial assistance.

#### REFERENCES

- Álvarez, B., C. Martínez-A., B. M. Burgering, and A. C. Carrera. 2001. Forkhead transcription factors contribute to execution of the mitotic programme in mammals. *Nature* **413**:744–747.
- Álvarez, B., E. Garrido, J. A. García-Sanz, and A. C. Carrera. 2003. Phosphoinositide 3-kinase activation regulates cell division time by coordinated control of cell mass and cell cycle progression rate. *J. Biol. Chem.* **278**:26466–26473.
- Bi, L., I. Okabe, D. J. Bernard, A. Wynshaw-Boris, and R. L. Nussbaum. 1999. Proliferative defect and embryonic lethality in mice homozygous for a deletion in the p110 $\alpha$  subunit of phosphoinositide 3-kinase. *J. Biol. Chem.* **274**:10963–10968.
- Bi, L., I. Okabe, D. J. Bernard, and R. L. Nussbaum. 2002. Early embryonic lethality in mice deficient in the p110 $\beta$  catalytic subunit of PI3K. *Mamm. Genome* **13**:169–172.
- Chan, T. O., U. Rodeck, A. M. Chan, A. C. Kimmelman, S. E. Rittenhouse, G. Panayotou, and P. N. Tsichlis. 2002. Small GTPases and tyrosine kinases coregulate a molecular switch in the phosphoinositide 3-kinase regulatory subunit. *Cancer Cell* **1**:181–191.
- Czauderna, F., M. Fechtner, H. Aygun, W. Arnold, A. Klippel, K. Giese, and J. Kaufmann. 2003. Functional studies of the PI(3)-kinase signalling pathway employing synthetic and expressed shRNA. *Nucleic Acids Res.* **31**:670–682.
- Dangi, S., H. Cha, and P. Shapiro. 2003. Requirement for PI3K activity during progression through S-phase and entry into mitosis. *Cell Signal.* **15**:667–675.
- Dominguez-Cáceres, M. A., J. M. García-Martínez, A. Calcabrini, L. González, P. G. Porque, J. León, and J. Martín-Pérez. 2004. Prolactin induces c-Myc expression and cell survival through activation of Src/Akt pathway in lymphoid cells. *Oncogene* **23**:7378–7390.
- Fingar, D. C., S. Salama, C. Tsou, E. Harlow, and J. Blenis. 2002. Mammalian cell size is controlled by mTOR and its downstream targets S6K1 and 4EBP1/eIF4E. *Genes Dev.* **16**:1472–1487.
- Foukas, L. C., M. Claret, W. Pearce, K. Okkenhaug, S. Meek, E. Peskett, S. Sancho, A. J. Smith, D. J. Withers, and B. Vanhaesebroeck. 2006. Critical role for the p110 $\alpha$  phosphoinositide-3-OH kinase in growth and metabolic regulation. *Nature* **441**:366–370.
- Frouin, I., A. Montecucco, G. Biamonti, U. Hubscher, S. Spadari, and G. Maga. 2002. Cell cycle-dependent dynamic association of cyclin/Cdk complexes with human DNA replication proteins. *EMBO J.* **21**:2485–2495.
- Fruman, D. A., R. E. Meyers, and L. A. Cantley. 1998. Phosphoinositide kinases. *Annu. Rev. Biochem.* **67**:481–507.
- García, Z., V. Silió, M. Marqués, I. Cortés, A. Kumar, C. Hernández, A. I. Checa, A. Serrano, and A. C. Carrera. 2006. A PI3K activity-independent function of p85 regulatory subunit in control of mammalian cytokinesis. *EMBO J.* **25**:4740–4751.
- García, Z., A. Kumar, M. Marques, I. I. Cortes, and A. C. Carrera. 2006. PI3K controls early and late events in mammalian cell division. *EMBO J.* **25**:655–661.
- Gupta, S., A. R. Ramjaun, P. Haiko, Y. Wang, P. H. Warne, B. Nicke, E. Nye, G. Stamp, K. Alitalo, and J. Downward. 2007. Binding of Ras to phosphoinositide 3-kinase p110 $\alpha$  is required for Ras-driven tumorigenesis in mice. *Cell* **129**:957–968.
- Jimenez, C., D. R. Jones, P. Rodríguez-Viciano, A. Gonzalez-García, E. Leonardo, S. Wennström, C. von Kobbé, J. L. Toran, L. R.-Borlado, V. Calvo, S. G. Copin, J. P. Albar, M. L. Gaspar, E. Díez, M. A. Marcos, J. Downward, C. Martínez-A., I. Mérida, and A. C. Carrera. 1998. Identification and characterization of a new oncogene derived from the regulatory subunit of phosphoinositide 3-kinase. *EMBO J.* **17**:743–753.
- Jiménez, C., C. Hernández, B. Pimentel, and A. C. Carrera. 2002. The p85 subunit controls activation of PI3K by Tyr kinases and Ras. *J. Biol. Chem.* **277**:41556–41562.
- Jones, S. M., R. Klinghoffer, G. D. Prestwich, A. Tokar, and A. Kazlauskas. 1999. PDGF induces an early and a late wave of PI 3-kinase activity, and only the late wave is required for progression through G<sub>1</sub>. *Curr. Biol.* **9**:512–521.
- Jones, S. M., and A. Kazlauskas. 2001. Growth-factor-dependent mitogenesis requires two distinct phases of signalling. *Nat. Cell Biol.* **3**:165–172.
- Kang, S., A. Denley, B. Vanhaesebroeck, and P. K. Vogt. 2006. Oncogenic transformation induced by the p110 $\beta$ ,  $\gamma$  and  $\delta$  isoforms of class I PI3K. *Proc. Natl. Acad. Sci. USA* **103**:1289–1294.
- Klippel, A., M. A. Escobedo, M. S. Wachowicz, G. Apell, T. W. Brown, M. A. Giedlin, W. M. Kavanaugh, and L. T. Williams. 1998. Activation of phosphatidylinositol 3-kinase is sufficient for cell cycle entry and promotes cellular changes characteristic of oncogenic transformation. *Mol. Cell. Biol.* **18**:5699–5711.
- Knight, Z. A., B. Gonzalez, M. E. Feldman, E. R. Zunder, D. D. Goldenberg, O. Williams, R. Loewith, D. Stokoe, A. Balla, B. Toth, T. Balla, A. W. Weiss, R. L. Williams, and K. M. Shokat. 2006. A pharmacological map of the PI3-K family defines a role for p110 $\alpha$  in insulin signaling. *Cell* **125**:733–747.
- Kozma, S. C., and G. Thomas. 2002. Regulation of cell size in growth, development and human disease: PI3K, PKB and S6K. *Bioessays* **24**:65–71.
- Kumar, A., M. Marqués, and A. C. Carrera. 2006. Phosphoinositide 3-kinase activation in late G<sub>1</sub> is required for c-Myc stabilization and S phase entry. *Mol. Cell. Biol.* **26**:9116–9125.
- Martínez-Gac, L., M. Marqués, Z. García, M. R. Campanero, and A. C. Carrera. 2004. Control of cyclin G2 mRNA expression by forkhead transcription factors: novel mechanism for cell cycle control by phosphoinositide 3-kinase and forkhead. *Mol. Cell. Biol.* **24**:2181–2189.
- Mateyak, M. K., A. J. Obaya, and J. M. Sedivy. 1999. c-Myc regulates cyclin D-Cdk4 and -Cdk6 activity but affects cell cycle progression at multiple independent points. *Mol. Cell. Biol.* **19**:4672–4683.
- Medema, R. H., G. J. Kops, J. L. Bos, and B. M. Burgering. 2000. AFX-like forkhead transcription factors mediate cell-cycle regulation by Ras and PKB through p27<sup>Kip1</sup>. *Nature* **404**:782–787.
- Meng, Q., C. Xia, J. Fang, Y. Rojanasakul, and B. H. Jiang. 2006. Role of PI3K and AKT specific isoforms in ovarian cancer cell migration, invasion and proliferation through the p70S6K1 pathway. *Cell Signal.* **18**:2262–2271.
- Miled, N., Y. Yan, W. C. Hon, O. Perisic, M. Zvebil, Y. Inbar, D. Schneidman-Duhovny, H. J. Wolfson, J. M. Backer, and R. L. Williams. 2007. Mechanism of two classes of cancer mutations in the PI3K catalytic subunit. *Science* **317**:239–242.
- Okkenhaug, K., A. Bilancio, G. Farjot, H. Priddle, S. Sancho, E. Peskett, W. Pearce, S. E. Meek, A. Salpekar, M. D. Waterfield, A. J. Smith, and B. Vanhaesebroeck. 2002. Impaired B and T cell antigen receptor signaling in p110 $\delta$  PI 3-kinase mutant mice. *Science* **297**:1031–1034.
- Olson, M. F., A. Ashworth, and A. Hall. 1995. An essential role for Rho, Rac and Cdc42 GTPases in cell cycle progression through G<sub>1</sub>. *Science* **269**:1270–1272.
- Pu, P., C. Kang, Z. Zhang, X. Liu, and H. Jiang. 2006. Downregulation of PIK3CB by siRNA suppresses malignant glioma cell growth in vitro and in vivo. *Technol. Cancer Res. Treat.* **5**:271–280.
- Ryves, W. J., and A. J. Harwood. 2003. The interaction of glycogen synthase kinase-3 (GSK-3) with the cell cycle. *Prog. Cell Cycle Res.* **5**:489–495.
- Sarbassov, D. D., S. M. Ali, and D. M. Sabatini. 2005. Growing roles for the mTOR pathway. *Curr. Opin. Cell Biol.* **17**:596–603.
- Saucedo, L. J., and B. A. Edgar. 2002. Why size matters: altering cell size. *Curr. Opin. Genet. Dev.* **12**:565–571.
- Schmidt, M., S. Fernandez de Mattos, A. van der Horst, R. Klompaker,

- G. J. P. L. Kops, E. W.-F. Lam, B. M. T. Burgering, and R. H. Medema. 2002. Cell cycle inhibition by FoxO forkhead transcription factors involves down-regulation of cyclin D. *Mol. Cell. Biol.* **22**:7842–7852.
37. Sherr, C. J., and J. M. Roberts. 1999. CDK inhibitors: positive and negative regulators of G<sub>1</sub>-phase progression. *Genes Dev.* **13**:1501–1512.
38. Shtivelman, E., J. Sussman, and D. Stokoe. 2002. A role for PI3K and PKB activity in the G<sub>2</sub>/M phase of the cell cycle. *Curr. Biol.* **12**:919–924.
39. Sui, G., C. Soohoo, B. el Affar, F. Gay, Y. Shi, W. C. Forrester, and Y. Shi. 2002. A DNA vector-based RNAi technology to suppress gene expression in mammalian cells. *Proc. Natl. Acad. Sci. USA* **99**:5515–5520.
40. van de Wetering, M., I. Oving, V. Muncan, M. T. Pon Fong, H. H. Brantjes, D. van Leenen, F. C. Holstege, T. R. Brummelkamp, R. Agami, and H. Clevers. 2003. Specific inhibition of gene expression using a stably integrated, inducible small-interfering-RNA vector. *EMBO Rep.* **4**:609–615.
41. Van Weeren, P. C., K. M. de Bruyn, A. M. de Vries-Smits, J. van Lint, and B. M. Burgering. 1998. Essential role for protein kinase B (PKB) in insulin-induced glycogen synthase kinase 3 inactivation. Characterization of dominant-negative mutant of PKB. *J. Biol. Chem.* **273**:13150–13156.
42. Wymann, M. P., and L. Pirola. 1998. Structure and function of phosphoinositide 3-kinases. *Biochim. Biophys. Acta* **1436**:127–150.



## Perspective

# New Functions for PI3K in the Control of Cell Division

Amit Kumar

Ana C. Carrera\*

Department of Immunology and Oncology; Centro Nacional de Biotecnología/CSIC; Universidad Autónoma de Madrid; Cantoblanco, Madrid Spain

\*Correspondence to: Ana C. Carrera; Department of Immunology and Oncology; Centro Nacional de Biotecnología/CSIC; Universidad Autónoma de Madrid; Darwin 3; Cantoblanco, Madrid E-28049 Spain; Tel.: +34.91.585.4846; Fax: 34.91.3720493; Email: [acarrera@cnb.uam.es](mailto:acarrera@cnb.uam.es)

Original manuscript submitted: 02/20/07

Manuscript accepted: 05/25/07

Previously published online as a *Cell Cycle* E-publication:

<http://www.landesbioscience.com/journals/cc/abstract.php?id=4492>

## KEY WORDS

phosphoinositide 3-kinase, c-Myc, p85, cell cycle, cytokinesis

## ABSTRACT

Although cell lipids were initially envisioned as structural components of the cell, their essential contribution to initiation and regulation of cell responses is now clearly established. Among the different lipids that regulate cell responses, those produced by class I phosphoinositide 3-kinase (PI3K), phosphatidylinositol (3,4)P<sub>2</sub> (PIP<sub>2</sub>) and phosphatidylinositol (3,4,5)P<sub>3</sub> (PIP<sub>3</sub>), have concentrated much attention in recent years. PIP<sub>2</sub> and PIP<sub>3</sub> are involved in cell division and survival control, and mutations in the PI3K pathway are linked to autoimmunity and cancer. Here we discuss two novel observations: a PI3K function in the late-G<sub>1</sub> phase of the cell cycle and the contribution of the p85 PI3K regulatory subunit in the control of cytokinesis.

The phosphoinositide 3-kinases (PI3K) are a family of enzymes that phosphorylate the 3-position in the inositol ring of membrane phosphoinositides. The family is classified according to sequence homology and substrate specificity into three different types: class I, class II and class III. Class I PI3K produce PIP<sub>2</sub> and PIP<sub>3</sub> rapidly and transiently following receptor stimulation. These enzymes are further subdivided in class I<sub>A</sub> PI3K, activated by receptor-activated tyrosine kinases (Tyr K), and class I<sub>B</sub> PI3K, activated by G protein-coupled receptors. The class I<sub>B</sub> PI3K catalytic subunit is encoded by a single gene, p110 $\gamma$ , and is regulated by two subunits, p101 and p87.<sup>1,2</sup> For class I<sub>A</sub>, three different genes encode regulatory subunits (p85 $\alpha$ , p85 $\beta$  and p55 $\gamma$ ) that have different alternative splice forms; there are also three catalytic subunits (p110 $\alpha$ , p110 $\beta$  and p110 $\delta$ ). We will focus on class I<sub>A</sub> p85/p110 enzymes, as they are clearly involved in control of cell division.<sup>2</sup>

Growth factor addition to quiescent cells triggers a number of early signaling cascades, including activation of Tyrosine kinases (Tyr K), Ras, and phospholipase C, among others. Tyr K and Ras trigger class I<sub>A</sub> PI3K activation.<sup>3</sup> PIP<sub>2</sub> and PIP<sub>3</sub> act as docking sites for proteins containing pleckstrin homology (PH) domains, such as protein kinase B (PKB or Akt), phosphoinositide-dependent kinase (PDK1), and some GTPase exchange factors (GEF). These enzymes subsequently activate secondary effectors including small GTPases, the target of rapamycin (mTOR), glycogen synthase-3 kinase (GSK3 $\beta$ ), ribosomal S6 kinase (p70S6K), etc. PI3K/PKB also regulate transcription factors such as c-Myc and FoxO.<sup>2</sup> By inducing these cascades, PI3K controls cell responses including survival, motility and division.

Symmetrical cell division is the process in which DNA and protein content duplicate to give rise to two daughter cells with conserved genetic content and cell size. This process requires induction of protein synthesis (highly active during the G<sub>1</sub> phase) and of DNA replication, controlled by the Cyclin-dependent kinases (Cdk). PI3K regulates cell growth through effectors such as mTOR and p70S6K, which control protein synthesis. PI3K regulates the nuclear cell cycle by controlling the stability of Cdk regulatory proteins including GSK3 $\beta$ , c-Myc, Cyclin D and p27<sup>Kip</sup>. In addition to affecting G<sub>0</sub>/G<sub>1</sub> transition, PI3K activates again in late-G<sub>1</sub>, an event required for S phase entry.<sup>4</sup> The second G<sub>1</sub> PI3K activity peak parallels activation of other signaling molecules including Tyr K, MAPK and Ras, some of which are required for late-G<sub>1</sub> PI3K activation.<sup>3,5,6</sup> In fact, the prolonged exposure to growth factors required for cell cycle entry and commitment to completion, can be replaced by two short mitogens pulses at G<sub>0</sub>  $\rightarrow$  G<sub>1</sub> and late-G<sub>1</sub> (~8 h after the first pulse).<sup>4</sup>

We recently reported that expression of c-Myc substitutes for the late-G<sub>1</sub> PI3K activity peak, resulting in ~80% recovery of G<sub>1</sub>-S transition.<sup>5</sup> Increased c-Myc protein levels correlates with PI3K induction in early-G<sub>1</sub> and late-G<sub>1</sub> of the cell cycle. It is nonetheless puzzling that late-G<sub>1</sub> PI3K can be replaced by c-Myc, as PI3K and c-Myc have otherwise unrelated functions. In contrast to the functions described for PI3K, the role of c-Myc is

linked to its transcription factor activity, required for its transforming capacity.<sup>7-9</sup> c-Myc regulates transcription in complex with the Max protein. c-Myc/Max-regulated gene expression involves several mechanisms that include chromatin remodeling as well as recruitment of RNA polymerases and transcription elongation factors.<sup>8,10</sup>

The requirement for c-Myc for cell cycle entry is based on several observations. Under certain conditions, c-Myc alone drives cell cycle entry and G<sub>1</sub> phase progression.<sup>11,12</sup> c-Myc overexpression shortens G<sub>1</sub> phase promoting Cyclin D transcription and p27<sup>kip</sup> downregulation, which enhances Cyclin D-associated kinase activities in early-G<sub>1</sub>;<sup>9</sup> c-Myc also regulates Cyclin E and A expression in late-G<sub>1</sub>.<sup>8</sup> Accordingly, c-Myc depletion leads to lengthening of G<sub>1</sub> to almost double the time compare to wild type cells.<sup>13</sup>

c-Myc cooperates with Ras and PI3K to trigger cell transformation.<sup>14</sup> In nontransformed quiescent cells, expression of c-Myc and of active Mek1 (an activator of MAPK) synergize with PIP<sub>3</sub> to promote cell cycle entry, but Mek1 and PIP<sub>3</sub> are insufficient for the cells to enter S phase, showing that c-Myc, MAPK and PI3K regulate different events in cell cycle.<sup>4</sup> Accordingly, we find that inhibition of PI3K activity during the first 6 h following growth factor addition is not compensated by c-Myc induction, confirming that PI3K and c-Myc exhibit nonredundant functions in early-G<sub>1</sub>.<sup>5</sup>

Despite their different functions, we find that c-Myc expression reconstitutes S phase entry (~80%) when PI3K is inhibited in late-G<sub>1</sub>. Expression of c-Myc mRNA is regulated by Src kinases, Ras/Raf signaling, and positive feedback regulation, as in the case of E2F-1-induced c-Myc expression.<sup>15-17</sup> Nonetheless, as c-Myc mRNA and protein, both have very short half-lives (~20–30 min),<sup>9</sup> c-Myc must be stabilized during G<sub>1</sub> to guarantee its function.<sup>18</sup> The PI3K/PKB/GSK3 $\beta$  cascade controls c-Myc stability function.<sup>19,20</sup> Regulation of c-Myc stability involves phosphorylation of two key residues, T58 and S62. MAPK mediates S62 phosphorylation, required for subsequent T58 phosphorylation by GSK3 $\beta$ , which targets c-Myc for degradation (reviewed in ref. 19). Phosphorylation of T58, which is regulated by the PI3K pathway, is a key-destabilizing event, as it represents a major mutation hotspot in Burkitt's lymphomas.<sup>20</sup> Thus, besides the role of PI3K at G<sub>0</sub>–G<sub>1</sub> entry, the second G<sub>1</sub> PI3K activity peak is essential for c-Myc stabilization, which in turn affects Cyclin A expression, Cdk2 activity, and licensing of the DNA replication complex.<sup>5</sup>

Apart from contributing to the initiation of cell division, PI3K is an essential manager of cell survival by regulating PKB (reviewed in ref. 21). PI3K also regulates cell migration.<sup>22</sup> PI3K activity-dependent c-Rac activation and p85-regulated Cdc42 activation are both essential events for remodeling the Actin cytoskeleton. Remarkably, this p85 function in cytoskeletal remodeling is also important for cytokinesis (see below).

Following S phase entry, PI3K exhibits basal activity during S–G<sub>2</sub> phases.<sup>23,24</sup> PI3K activates again at mitosis entry, which contributes to trigger Cdk1 activation and mitosis initiation.<sup>25-27</sup> As mitosis progresses, however, PI3K activity reduces; reaching basal levels by the time cells are ready to divide their cytosol.<sup>27</sup> We found that deletion of p85 $\alpha$ , the ubiquitous, most abundant p85 regulatory isoform, impairs cytosolic separation.<sup>27</sup> As in the case of migrating cells,<sup>22</sup> p85 appears to control Cdc42 activity in cytokinesis, as well as its localization to the cleavage furrow.<sup>27</sup> Defective Cdc42 localization to the cleavage furrow in p85 $\alpha$ -deficient cells results in impaired Septin 2 localization and defective cytokinesis (20% of these cells are binucleated, ref. 27). Cdc42-controlled Septin action in cytokinesis was described in *Saccharomyces cerevisiae*,<sup>28,29</sup>

but not in mammals. In fact, in mammals, the Septins and Cdc42 regulate microtubule-to-chromosome attachment in metaphase,<sup>30-33</sup> making difficult to examine posterior cell cycle defects. At least for the Septins their cytokinesis function in mammals was envisioned by microinjection of anti-Septin 2 antibodies as well as using shRNA for the Septin MSF.<sup>34,35</sup> We found that metaphase is unaffected by p85 deletion, suggesting that Cdc42 and Septin 2 actions in this phase are virtually p85-independent. In contrast, the role of Cdc42 and Septin 2 in controlling cytosolic separation involves p85 $\alpha$ , making possible to unmask the function of p85 $\alpha$   $\rightarrow$  Cdc42  $\rightarrow$  Septin2 in cytokinesis, without apparent effects in metaphase. p85 $\alpha$  regulates this pathway through the simultaneous binding of Cdc42 and Septin 2 via the N-terminal Bcr region and a C-terminal region (around the SH2-iSH2 domains), respectively.<sup>27</sup> This action of p85 is restricted to vertebrates, as the invertebrate PI3K regulatory subunit lacks the N-terminal SH3-Bcr region (i.e., *Drosophila* Acc No Y12498). We suggest that p85 brings Cdc42 to the cleavage furrow through microtubules, an aspect that remains to be studied. Once in the cleavage furrow, Cdc42 may contact a GTP exchange factor such as ECT-2,<sup>36</sup> which localizes in this position; this would explain the local activation of Cdc42. Cdc42 activation in the furrow then fosters the changes in Septin polymerization that regulate cytosolic division.

Formation of a Septin ring is essential for cytosolic separation in the budding yeast *S. cerevisiae* as it regulates new membrane formation; Septin ring formation in this organism is regulated by Cdc42 activation and deactivation cycles.<sup>28,29</sup> We show that Septins, regulated by Cdc42, are also important in mammalian cytokinesis, but their action remains to be examined. The Rho GTPase controls Actin polymerization in the cleavage furrow;<sup>37</sup> it is therefore possible that Cdc42 and Rho cooperate for cytoskeletal reorganization in cytokinesis, as they do during wound healing.<sup>38</sup>

It is now clearly established that symmetrical division begins by growth factor-triggered activation of early signaling molecules. Early-G<sub>1</sub> PI3K activity is crucial for cell growth,<sup>23,24</sup> as well as for inactivation of the FoxO transcription factors.<sup>39,40</sup> In addition, PI3K, c-Myc and MAPK trigger Cyclin D synthesis and/or stabilization.<sup>9,10,14,41-43</sup> When Cyclin D reaches optimal levels and cell cycle entry inhibitors expression decrease, Cyclin D/Cdk complexes drive phosphorylation of retinoblastoma protein (Rb), facilitating E2F-mediated Cyclin E synthesis.<sup>44</sup> The initial signaling wave is transient, probably due to the action of phosphatases on Tyr K, Ras, MAPK and PI3K. Nonetheless, these enzymes reactivate in late-G<sub>1</sub> and they enhance Cdk2 activity through upregulation of c-Myc and other events.<sup>44</sup> During this second signaling wave, PI3K is necessary for c-Myc stabilization. c-Myc in turn triggers Cyclin A synthesis, reduces p27<sup>kip</sup> binding to Cdk2 complexes, and increases Cyclin E/Cdk2 and Cyclin A/Cdk2 activities. All of these events are essential for DNA synthesis induction, explaining why PI3K activity requirement in late-G<sub>1</sub> for S phase entry.

PI3K activity is basal during S–G<sub>2</sub> phases; which contributes to correct activation of Forkhead transcription factors in G<sub>2</sub> phase, required for mitosis progression.<sup>23</sup> PI3K reactivates at mitosis entry, when it regulates Cdk1 activation,<sup>25,26</sup> however PI3K activity decreases during mitosis progression, and reach basal levels in telophase. In this phase, the action of the p85 PI3K regulatory subunit contributes to Cdc42 activation in the cleavage furrow, Septin accumulation at this site and subsequent execution of cytokinesis.<sup>27</sup> Thus, PI3K, and most likely other signaling pathways, not only regulate G<sub>0</sub> phase exit and G<sub>1</sub> progression, but also later phases of the cell cycle, contributing to promote the complex process of cell division.

## References

1. Vanhaesebroeck B, Ali K, Bilancio A, Geering B, Foukas LC. Signalling by PI3K isoforms: Insights from gene-targeted mice. *Trends Biochem Sci* 2005; 30:194-204.
2. Garcia Z, Kumar A, Marques M, Cortes I, Carrera AC. Phosphoinositide 3-kinase controls early and late events in mammalian cell division. *EMBO J* 2006; 25:655-61.
3. Jimenez C, Hernandez C, Pimentel B, Carrera AC. The p85 regulatory subunit controls sequential activation of phosphoinositide 3-kinase by Tyr kinases and Ras. *J Biol Chem* 2002; 277:41556-62.
4. Jones SM, Kazlauskas A. Growth-factor-dependent mitogenesis requires two distinct phases of signalling. *Nat Cell Biol* 2001; 3:165-72.
5. Kumar A, Marques M, Carrera AC. Phosphoinositide 3-kinase activation in late-G<sub>1</sub> is required for c-Myc stabilization and S phase entry. *Mol Cell Biol* 2006; 26:9116-25.
6. Stacey D, Kazlauskas A. Regulation of Ras signaling by the cell cycle. *Curr Opin Genet Dev* 2002; 12:44-46.
7. Dang CV. *c-Myc* target genes involved in cell growth, apoptosis and metabolism. *Mol Cell Biol* 1999; 19:1-11.
8. Vlach J, Hennecke S, Alevizopoulos K, Conti D, Amati B. Growth arrest by the CDK inhibitor p27<sup>Kip1</sup> is abrogated by c-Myc. *EMBO J* 1996; 15:6595-604.
9. Mateyak MK, Obaya AJ, Sedivy JM. c-Myc regulates Cyclin D-Cdk4 and Cdk6 activity but affects cell cycle progression at multiple independent points. *Mol Cell Biol* 1999; 19:4672-83.
10. Jirmanova L, Afanasieff M, Gobert-Gosse S, Markossian S, Savatier P. Differential contributions of ERK and PI3K to the regulation of Cyclin D1 expression and to the control of the G<sub>1</sub>/S transition in mouse ES cells. *Oncogene* 2002; 21:5515-28.
11. Littlewood TD, Hancock DC, Danielian PS, Parker MG, Evan GI. A modified oestrogen receptor ligand-binding domain as an improved switch for the regulation of heterologous proteins. *Nucleic Acids Res* 1995; 23:1686-90.
12. Eilers M, Schirm S, Bishop JM. The MYC protein activates transcription of the alpha-prothymosin gene. *EMBO J* 1991; 10:133-41.
13. Shichiri M, Hanson KD, Sedivy JM. Effects of c-myc expression on proliferation, quiescence, and the G<sub>0</sub> to G<sub>1</sub> transition in nontransformed cells. *Cell Growth Differ* 1993; 4:93-104.
14. Bouchard C, Marquardt J, Bras A, Medema RH, Eilers M. Myc-induced proliferation and transformation require Akt-mediated phosphorylation of FoxO proteins. *EMBO J* 2004; 23:2830-40.
15. Bowman T, Broome MA, Sinibaldi D, Wharton W, Pledger WJ, Sedivy JM, Irby R, Yeatman T, Courtneidge SA, Jove R. Stat3-mediated Myc expression is required for Src transformation and PDGF-induced mitogenesis. *Proc Natl Acad Sci USA* 2001; 98:7319-24.
16. Kerkhoff E, Houben R, Löffler S, Troppmair J, Lee JE, Rapp UR. Regulation of *c-myc* expression by Ras/Raf signalling. *Oncogene* 1998; 16:211-16.
17. Matsumura I, Tanaka H, Kanakura Y. E2F1 and c-myc in cell growth and death. *Cell Cycle* 2003; 2:333-38.
18. Ponzilli R, Katz S, Barsyte-Lovejoy D, Penn LZ. Cancer therapeutics: Targeting the dark side of Myc. *Eur J Cancer* 2005; 41:2485-501.
19. Sears RC. The life cycle of C-Myc. *Cell cycle* 2004; 3:1133-37.
20. Hemann MT, Bric A, Teruya-Feldstein J, Herbst A, Nilsson JA, Cordon-Cardo C, Cleveland JL, Tansey WP, Lowe SW. Evasion of the p53 tumour surveillance network by tumour-derived MYC mutants. *Nature* 2005; 436:807-11.
21. Vivanco I, Sawyers CL. The PI3K AKT pathway in human cancer. *Nat Rev Cancer* 2002; 2:489-501.
22. Jimenez C, Portela RA, Mellado M, Rodriguez-Frade JM, Collard J, Serrano A, Martinez-A C, Avila J, Carrera AC. Role of the PI3K regulatory subunit in the control of Actin organization and cell migration. *J Cell Biol* 2000; 151:249-62.
23. Álvarez B, Martínez AC, Burgering BM, Carrera AC. Forkhead transcription factors contribute to execution of the mitotic programme in mammals. *Nature* 2001; 413:744-47.
24. Álvarez B, Garrido F, Garcia-Sanz JA, Carrera AC. PI3K activation regulates cell division time by coordinated control of cell mass and cell cycle progression rate. *J Biol Chem* 2003; 278:26466-73.
25. Shivelman E, Sussman J, Stokoe D. A role for PI3K and PKB activity in the G<sub>2</sub>/M phase of the cell cycle. *Curr Biol* 2002; 12:919-24.
26. Dangi S, Cha H, Shapiro P. Requirement for PI3K activity during progression through S-phase and entry into mitosis. *Cell Signal* 2003; 15:667-75.
27. Garcia Z, Silio V, Marques M, Cortes I, Kumar A, Hernandez C, Checa AI, Serrano A, Carrera AC. A PI3K activity-independent function of p85 regulatory subunit in control of mammalian cytokinesis. *EMBO J* 2006; 25:4740-51.
28. Caviston JP, Longtine M, Pringle JR, Bi E. The role of Cdc42p GTPase-activating proteins in assembly of the Septin ring in yeast. *Mol Biol Cell* 2003; 14:4051-66.
29. Kinoshita M. The Septins. *Genome Biol* 2003; 4:236-45.
30. Yasuda S, Ocegüera-Yanez F, Kato T, Okamoto M, Yonemura S, Terada Y, Ishizaki T, Narumiya S. Cdc42 and mDia3 regulate microtubule attachment to kinetochores. *Nature* 2004; 428:767-771.
31. Spiliotis ET, Kinoshita M, Nelson WJ. A mitotic Septin scaffold required for Mammalian chromosome congression and segregation. *Science* 2005; 307:1781-85.
32. Yoshizaki H, Ohba Y, Kurokawa K, Itoh RE, Nakamura T, Mochizuki N, Nagashima K, Matsuda M. Activity of Rho-family GTPases during cell division as visualized with FRET-based probes. *J Cell Biol* 2003; 162:223-32.
33. Ocegüera-Yanez F, Kimura K, Yasuda S, Higashida C, Kitamura T, Hiraoka Y, Haraguchi T, Narumiya S. Ect2 and MgcRacGAP regulate the activation and function of Cdc42 in mitosis. *J Cell Biol* 2005; 168:221-232.
34. Surka MC, Tsang CW, Trimble WS. The mammalian Septin MSF localizes with microtubules and is required for completion of cytokinesis. *Mol Biol Cell* 2002; 13:3532-45.
35. Kinoshita M, Kumar S, Mizoguchi A, Ide C, Kinoshita A, Haraguchi T, Hiraoka Y, Noda M. Nedd5, a mammalian Septin, is a novel cytoskeletal component interacting with Actin-based structures. *Genes Dev* 1997; 11:1535-47.
36. Morita K, Hirono K, Han M. The *Caenorhabditis elegans* ect-2 *RhoGEF* gene regulates cytokinesis and migration of epidermal P cells. *EMBO Rep* 2005; 6:1163-68.
37. Mishima M, Kaitna S, Glotzer M. Central spindle assembly and cytokinesis require a kinesin-like protein/RhoGAP complex with microtubule bundling activity. *Dev Cell* 2002; 2:41-54.
38. Benink HA, Bement WM. Concentric zones of active RhoA and Cdc42 around single cell wounds. *J Cell Biol* 2005; 168:429-39.
39. Medema RH, Kops GJ, Bos JL, Burgering BM. AFX-like Forkhead TF mediate cell-cycle regulation by Ras and PKB through p27<sup>Kip1</sup>. *Nature* 2000; 404:782-87.
40. Martinez-Gac L, Marques M, Garcia Z, Campanero MR, Carrera AC. Control of Cyclin G<sub>2</sub> mRNA expression by forkhead transcription factors: Novel mechanism for cell cycle control by PI3K and forkhead. *Mol Cell Biol* 2004; 24:2181-89.
41. Yeh E, Cunningham M, Arnold H, Chasse D, Monteith T, Ivaldi G, Hahn WC, Stukenberg PT, Shenolikar S, Uchida T, Counter CM, Nevins JR, Means AR, Sears RA. A signalling pathway controlling c-Myc degradation that impacts oncogenic transformation of human cells. *Nat Cell Biol* 2004; 6:308-18.
42. van Weeren PC, de Bruyn KM, de Vries-Smits AM, van Lint J, Burgering BM. Essential role for PKB in insulin-induced GSK3 inactivation: Characterization of dominant-negative mutant of PKB. *J Biol Chem* 1998; 273:13150-56.
43. Ryves WJ, Harwood AJ. The interaction of glycogen synthase kinase-3 (GSK-3) with the cell cycle. *Prog Cell Cycle Res* 2003; 5:489-95.
44. Sherr CJ, Roberts JM. CDK inhibitors: Positive and negative regulators of G<sub>1</sub>-phase progression. *Genes Dev* 1999; 13:1501-12.



## Phosphoinositide 3-Kinase Activation in Late G<sub>1</sub> Is Required for c-Myc Stabilization and S Phase Entry<sup>▽</sup>

Amit Kumar, Miriam Marqués, and Ana C. Carrera\*

*Department of Immunology and Oncology, Centro Nacional de Biotecnología/CSIC, Universidad Autónoma de Madrid, Cantoblanco, Madrid E-28049, Spain*

Received 4 May 2006/Returned for modification 16 June 2006/Accepted 18 September 2006

**Phosphoinositide 3-kinase (PI3K) is one of the early-signaling molecules induced by growth factor (GF) receptor stimulation that are necessary for cell growth and cell cycle entry. PI3K activation occurs at two distinct time points during G<sub>1</sub> phase. The first peak is observed immediately following GF addition and the second in late G<sub>1</sub>, before S phase entry. This second activity peak is essential for transition from G<sub>1</sub> to S phase; nonetheless, the mechanism by which this peak is induced and regulates S phase entry is poorly understood. Here, we show that activation of Ras and Tyr kinases is required for late-G<sub>1</sub> PI3K activation. Inhibition of late-G<sub>1</sub> PI3K activity results in low c-Myc and cyclin A expression, impaired Cdk2 activity, and reduced loading of MCM2 (minichromosome maintenance protein) onto chromatin. The primary consequence of inhibiting late-G<sub>1</sub> PI3K was c-Myc destabilization, as conditional activation of c-Myc in advanced G<sub>1</sub> as well as expression of a stable c-Myc mutant rescued all of these defects, restoring S phase entry. These results show that Tyr kinases and Ras cooperate to induce the second PI3K activity peak in G<sub>1</sub>, which mediates initiation of DNA synthesis by inducing c-Myc stabilization.**

Exposure of quiescent cells to growth factors (GF) activates a number of early-signaling cascades involved in triggering cell cycle entry (32). Class I<sub>A</sub> phosphoinositide 3-kinase (PI3K) is a heterodimer composed of a p110 catalytic subunit and a p85 regulatory subunit, which induces phosphatidylinositol(3,4)P<sub>2</sub> [PtdIns(3,4)P<sub>2</sub>] and PtdIns(3,4,5)P<sub>3</sub> formation. Class I<sub>A</sub> PI3K is one the GF-stimulated pathways that trigger S phase entry (12, 19); it is activated by Tyr kinases (Tyr-K) and Ras (15) and aids in initiating cell division by inducing cell growth and activating protein kinase B (PKB) (12). PKB inhibits glycogen synthase kinase 3 (GSK3 $\beta$ ) and FoxO transcription factors, which in turn control cell cycle regulators (1, 22, 25, 37, 41). In addition, the expression of a constitutively active PI3K mutant augments Cdk2 activity (19). PI3K activity increases not only within minutes of GF receptor stimulation (first peak), but also in advanced G<sub>1</sub> phase (second peak) (1, 17, 38). Late-G<sub>1</sub> PI3K activity is essential for S phase entry (18, 38), but its mechanism of action remains unknown.

c-Myc also regulates cell cycle entry (3, 23, 34), and its levels are frequently increased in human cancers (30). c-Myc controls the expression of a large number of genes, including cyclin D and E and more markedly cyclin A (9, 24). c-Myc also controls Cdk kinase activity by regulating p27<sup>kip</sup> expression and its association with cyclin E/Cdk2 and cyclin A/Cdk2 (29, 42). c-Myc is very unstable; its stability must be precisely regulated during the cell cycle. Phosphorylation-dependent regulation of c-Myc stability involves two key residues, T58 and S62. S62 phosphorylation is mediated by microtubule-associated protein kinase (MAPK) and that of T58 by GSK3 $\beta$ , which targets c-Myc for degradation (43).

DNA replication requires the establishment of a replication fork. This is initiated by formation of a prereplication complex (pre-RC) that assembles when the origin replication complex is bound to the DNA replication origin, and minichromosome maintenance proteins (MCM2 to MCM7) load onto chromatin via a Cdt1- and Cdc6-dependent mechanism (4, 8, 21, 27). Binding of MCM to the origin is restricted to late mitosis and to the end of G<sub>1</sub> (in cells exiting G<sub>0</sub>); following MCM loading, the origin replication complex is “licensed” for replication (21).

Activation of Cdk2 (cyclin E/Cdk2 and cyclin A/Cdk2) and Ddk (Cdc7) kinases at the G<sub>1</sub>-S boundary initiates replication by recruiting Cdc45 and DNA polymerases to the origin (27). The helicase activity of the MCM complex is then required to unwind the DNA double helix (4, 8, 27). Cdc7 and Cdk2 functions are not completely defined, although many initiation components have consensus phosphorylation sites for these kinases (27). Cyclin E/Cdk2 is crucial for loading of MCM2 onto chromatin, as it cooperates with Cdc6 in pre-RC assembly; cells lacking cyclin E fail to form the pre-RC on exit from G<sub>0</sub> (11, 13). In addition, cyclin A/Cdk2 activates initiation of replication and blocks pre-RC reassembly (7).

Here, we examined the mechanism involved in PI3K activation in late G<sub>1</sub> and its role in S phase entry. To distinguish the first and second PI3K activity peaks, NIH 3T3 cells were driven into quiescence by serum deprivation and then released into G<sub>1</sub> by serum addition. This protocol allows synchronous cell cycle progression through G<sub>1</sub> and entry into S phase at approximately 9 to 12 h after serum stimulation. We show that Ras and Tyr-K activation are responsible for PI3K activation in late G<sub>1</sub>. Inhibition of the late-G<sub>1</sub> PI3K activity peak did not markedly affect cyclin E levels but reduced c-Myc and cyclin A levels, Cdk2 activity, and loading of MCM2 onto chromatin. Here, we present evidence that the primary role of PI3K activity in late G<sub>1</sub> is c-Myc stabilization.

\* Corresponding author. Mailing address: Department of Immunology and Oncology, Centro Nacional de Biotecnología/CSIC, Darwin 3, Campus de Cantoblanco, Madrid E-28049, Spain. Phone: (34) 91/585-4846. Fax: (34) 91/372-0493. E-mail: acarrera@cnb.uam.es.

<sup>▽</sup> Published ahead of print on 2 October 2006.

## MATERIALS AND METHODS

**Plasmids and reagents.** The retroviral vectors encoding wild-type (WT) c-Myc-internal ribosome entry site-green fluorescent protein (GFP) or T58Ac-Myc-internal ribosome entry site-GFP (14) were kindly provided by S. Lowe (Cold Spring Harbor Laboratory, NY). pBabePuro encoding c-MycER (20) was generously donated by G. Evan (Cancer Research Institute, University of California at San Francisco, CA). Antibodies to c-Myc (C-19), cyclin E (M-20), and estrogen receptor alpha (ER $\alpha$ ) (MC-20) were obtained from Santa Cruz Biotechnology; anti-pan-Ras and - $\alpha$ -tubulin were from Oncogene Research; anti-p-PKB(473) was from Cell Signaling Technologies; and anti-cyclin D3, -p27<sup>Kip</sup>, and -MCM2 were obtained from BD Biosciences. Anti-Rb antibody was from Zymed Laboratories, anti-phospho(T58/S62)-c-Myc and anti-c-Myc (9B11) were from Cell Signaling Technologies, and anti-cyclin A and -phosphotyrosine were from Upstate Biotechnology. Monoclonal anti- $\beta$ -actin antibody was from Sigma and anti-histone from Chemicon International. Horseradish peroxidase-conjugated secondary antibodies were purchased from Dako Cytomations. Enhanced chemiluminescence, L-[<sup>35</sup>S]methionine, [ $\alpha$ -<sup>32</sup>P]dCTP, and [ $\gamma$ -<sup>32</sup>P]ATP were from Amersham Biosciences. Lovastatin, herbimycin, and Ly294002 were from Calbiochem.

**Cell lines and cell cycle analysis.** NIH 3T3 and Phoenix cells were maintained in Dulbecco's modified Eagle's medium (DMEM; Gibco-BRL) supplemented with 10% (vol/vol) fetal bovine serum (FBS), 2 mM glutamine, 10 mM HEPES, 100 U/ml penicillin, and 100  $\mu$ g/ml streptomycin in a humidified atmosphere (5% CO<sub>2</sub>, 37°C). To monitor the G<sub>0</sub>-to-S transition accurately, we established a standard time course protocol for all experiments. Exponentially growing cells were seeded into dishes and rendered quiescent by incubation in DMEM-0.1% FBS (19 h). Under these conditions, cells exhibited a G<sub>0</sub> phenotype, examined as previously described (22). Quiescent cultures were rinsed with serum-free medium, and synchronous cell cycle entry was stimulated by readdition of serum (10% final concentration). Some samples were harvested immediately before serum addition (time zero). Cells were harvested at various times after serum stimulation. DNA synthesis was studied by DNA staining with propidium iodide and analyzed with a flow cytometer (Beckman-Coulter) as described previously (1) or by bromodeoxyuridine (BrdU) incorporation.

**BrdU incorporation.** Cells were incubated with 10  $\mu$ M BrdU for 90 min and harvested at indicated time points by using trypsin-EDTA (see Fig. 4). Cells were washed twice with phosphate-buffered saline (PBS)-1% FBS and fixed in ice-cold 80% methanol overnight. Cells were then washed twice and resuspended in PBS containing 1% FBS and 0.1 mg/ml RNase (30 min, room temperature). To extract histones and denature cellular DNA, we incubated cells with 1.5 N HCl and 0.5% Triton X-100 (30 min, room temperature). For direct immunofluorescence staining, cells were incubated (1 h) with fluorescein isothiocyanate-conjugated anti-BrdU antibody (Becton Dickinson). After being washed (in PBS-1% FBS), cells were resuspended in 500  $\mu$ l PBS (containing 0.1 mg/ml RNase, 0.1% NP-40, and 5  $\mu$ g/ml propidium iodide) and analyzed by flow cytometry.

**Pulse-chase assay.** NIH 3T3 cells were incubated in DMEM-0.1% FBS for 19 h (as described above), and then the medium was replaced with Met-free RPMI medium (Gibco) containing 10% dialyzed FBS for 9 h, with 0.75 mCi [<sup>35</sup>S]Met (each p100 dish) included for the last 6 h. At 8.5 h after serum addition, some of the samples were treated with Ly294002 (10  $\mu$ M). After the 9-h incubation period described above (pulse), the [<sup>35</sup>S]Met-containing medium was washed and replaced by DMEM-10% FBS containing 200  $\mu$ M of cold Met and Cys alone or with Ly294002 (10  $\mu$ M) and maintained until 12 h and 16 h after serum addition (chase).

**Inhibitor treatments and retroviral transduction.** To activate c-MycER, we added 4-hydroxytamoxifen (4-OHT) (200 nM; Sigma) 6.5 h after serum stimulation. In some cases, cells were treated with 0.1% dimethyl sulfoxide (control), lovastatin (10  $\mu$ M), herbimycin (2  $\mu$ M), or Ly294002 (10  $\mu$ M). When samples were collected at time zero, inhibitors were added 30 min before serum addition; otherwise, inhibitors were added after 4, 6, or 7 h after serum stimulation.

Phoenix cells were transfected using Jet Pei-NaCl (Poly plus transfection) according to the manufacturer's protocols; after 10 h, cells were washed and placed in DMEM-10% FBS. Retroviral gene transduction was performed as described previously (35). Infected NIH 3T3 (c-MycER) cells were selected for 2 days in medium containing 2  $\mu$ g/ml puromycin (Sigma).

**Cell lysis, immunoprecipitation, PI3K assay, WB, pull-down assay, subcellular fractionation, Northern blotting, and Cyclin/Cdk kinase assays.** Lysates were prepared in Triton X-100 lysis buffer (50 mM HEPES, pH 8.0, 150 mM NaCl, 1% Triton X-100) containing protease and phosphatase inhibitors (1 mM Na<sub>3</sub>VO<sub>4</sub>, 5 mM NaF, 1 mM phenylmethylsulfonyl fluoride, 1  $\mu$ g/ml aprotinin, and 10  $\mu$ g/ml leupeptin). Immunoprecipitation, PI3K assays, and Western blotting (WB) were performed as described previously (15). For the PI3K assay, the cells

were transfected with pSG5-myc-tagged-p110 $\alpha$  (15), and the cells were synchronized 24 h later, as described above; PI3K was immunoprecipitated using anti-Myc-tag antibody. Ras-GTP was purified from cell extracts on Sepharose-Gex2T-RBD (the Ras-binding domain of Raf-1). Briefly, NIH 3T3 cells were harvested, lysed with glutathione S-transferase fluorescent in situ hybridization buffer (50 mM Tris-HCl, pH 7.5, 2 mM EDTA, 100 mM NaCl, 2 mM MgCl<sub>2</sub>, 1% [vol/vol] NP-40, 5 mM NaF, 10% [vol/vol] glycerol, 1 mM phenylmethylsulfonyl fluoride, 1  $\mu$ g/ml aprotinin, and 10  $\mu$ g/ml leupeptin). Protein concentration, examined using the Micro bicinchoninic acid assay (Pierce), was normalized, and lysates were incubated (1 h, 4°C) with glutathione-Sepharose beads precoupled with glutathione S-transferase-RBD. Beads were washed three times in lysis buffer, and bound Ras-GTP was solubilized in 30  $\mu$ l Laemmli buffer. Ras-GTP content was analyzed by WB. Total cell extracts, nuclear extracts, and chromatin fractions were isolated as described previously (26). Northern blot and cyclin/Cdk kinase assays were performed as described previously (22, 26, 35).

## RESULTS

**PI3K activity in late G<sub>1</sub> induces PKB activation that correlates with increased c-Myc protein levels.** PI3K is activated in late G<sub>1</sub>; this activity peak is essential for S phase entry, since late-G<sub>1</sub> PI3K inhibition blocks S phase entry and PtdIns (3,4,5)P<sub>3</sub> addition in late G<sub>1</sub> induces cell cycle entry in the absence of serum (17, 18). To study the role of PI3K in late G<sub>1</sub>, NIH 3T3 cells were driven into quiescence by serum deprivation and then released into G<sub>1</sub> by serum addition. Cells were committed to enter S phase at about 9 h after serum addition, with no further GF requirement (not shown). S phase began between 9 and 12 h after serum addition (Fig. 1A). In cells entering the cell cycle synchronously, we detected early-G<sub>1</sub> (1 h) and late-G<sub>1</sub> (~9 to 15 h) PI3K activity peaks (Fig. 1B), as determined by examining the phosphorylation of the PI3K effector PKB (p-PKB) (1). c-Myc expression levels paralleled the PI3K activity peaks (Fig. 1C).

**Ras and Tyr kinases activate PI3K in late G<sub>1</sub>.** PI3K activation at G<sub>0</sub>-to-G<sub>1</sub> transition is dependent on Tyr-K and Ras activities (6, 15); Ras is also activated in late G<sub>1</sub> (38). We examined Tyr-K activation by WB using an anti-pTyr antibody and Ras activity by pull-down assays. After GF addition, total Tyr-K activity increased transiently at 1 h and again between 6 and 16 h (Fig. 1D). Some of the Tyr-phosphorylated bands that appeared at 1 h differed from those visible at ~9 h, suggesting that more than one Tyr-K is activated during G<sub>1</sub> (Fig. 1D). Ras-GTP increased at ~1 h and again at 9 to 12 h after serum stimulation (Fig. 1E).

To determine whether Tyr-K or Ras stimulation is required for late-G<sub>1</sub> PI3K activation, we used small molecule inhibitors and examined the effects on p-PKB and c-Myc levels. Addition of the Ras inhibitor lovastatin (10) at 0, 4, or 6 h after serum stimulation reduced p-PKB levels at 9 and 12 h (Fig. 2A), suggesting that Ras activation is involved in late-G<sub>1</sub> PI3K activation. Addition of mevalonate, a lovastatin substrate, restored PKB phosphorylation (Fig. 2A). Herbimycin, a Src Tyr-K inhibitor (39), also reduced PKB activation at 9 and 12 h (Fig. 2A), whereas genistein, an inhibitor with high specificity for the epidermal GF receptor (40), did not affect the second G<sub>1</sub> PI3K activity peak (not shown). Combination of lovastatin and herbimycin treatments yielded a larger p-PKB reduction (Fig. 2A). The decrease in p-PKB levels correlated with a reduction in both c-Myc content and S phase entry at 12 h (Fig. 2A). The activities of the inhibitors in blocking Tyr-K and Ras activation were confirmed by WB; herbimycin reduced phos-

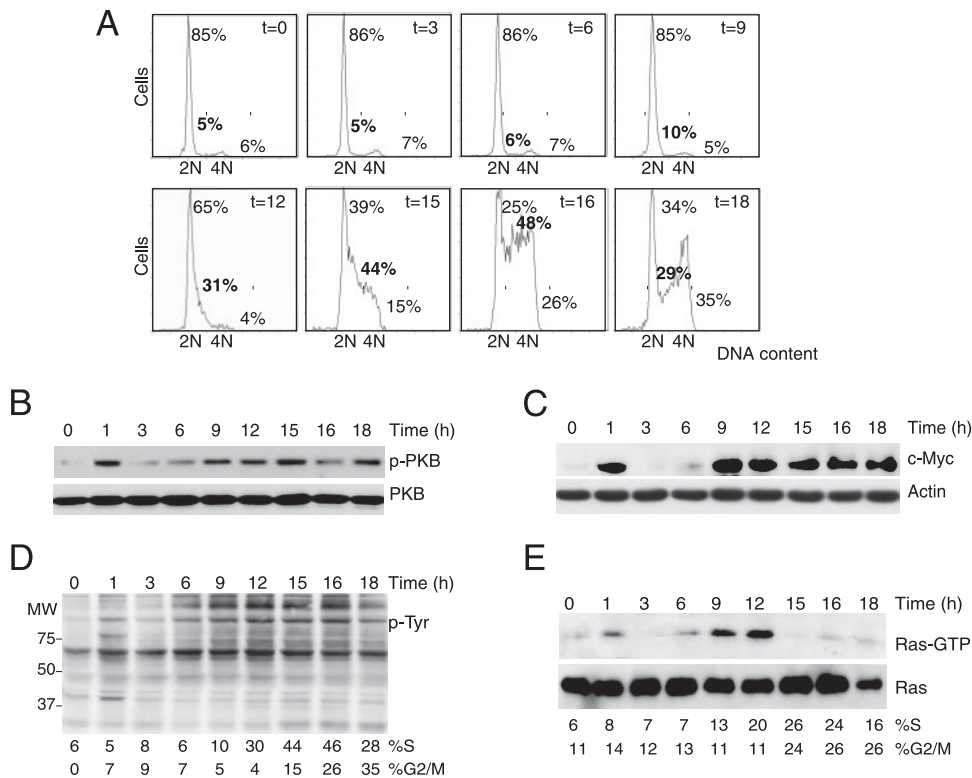


FIG. 1. Late-G<sub>1</sub> PI3K activity peak induces PKB activation that correlates with Tyr-K and Ras activation. (A) DNA content cell cycle profiles of NIH 3T3 cells arrested in G<sub>0</sub> by serum deprivation and then released for different periods (indicated) to allow synchronous cell cycle entry. Percentages of cells in G<sub>0</sub>/G<sub>1</sub>, S (in bold), or G<sub>2</sub>/M phases are indicated. (B and C) WB analysis of the cells used for panel A, using anti-phospho-S473-PKB (p-PKB), -PKB, -c-Myc, and -actin antibodies. (D) Activation of Tyr-K in cells entering cycle entry as examined by WB using anti-p-Tyr antibody. (E) Ras-GTP content was examined in cell extracts prepared as described for panel D. Total Ras and Ras-GTP were examined by WB. The figure shows data representative of at least four experiments with similar results.

pho-Tyr cellular content (Fig. 2B), and lovastatin reduced the active-Ras fraction, an effect that was reversed by mevalonate addition (Fig. 2C).

To confirm that late-G<sub>1</sub> PI3K activation requires Tyr-K and Ras, we examined PI3K activity in extracts from synchronous-cell cultures (as described above). Addition of lovastatin, herbimycin, or both at 4 h after serum addition resulted in reduced PI3K activity at 7 to 8 h after serum addition (Fig. 2D). As PI3K activity regulates cyclin levels (see below), we also examined whether lovastatin and herbimycin affected cyclin D3, E, and A levels. Tyr-K and Ras inhibition reduced the levels of these cyclins, most markedly those of cyclin A (Fig. 2E). Thus, Tyr-K and Ras cooperate in the induction of the second PI3K activity peak, which in turn regulates c-Myc and G<sub>1</sub> cyclin levels as well as S phase entry.

**Late-G<sub>1</sub> PI3K inhibition reduces c-Myc and cyclin A levels as well as Cdk2 activity.** As late-G<sub>1</sub> PI3K activation correlates with increased c-Myc expression levels, we examined the consequences of inhibiting late-G<sub>1</sub> PI3K on *c-myc* mRNA levels by Northern blotting. Cells were synchronized as described above, and the PI3K inhibitor Ly294002 was added at 7 h after serum stimulation; cells were harvested at 9 h. This analysis showed that late-G<sub>1</sub> PI3K inhibition induces a reduction of *c-myc* mRNA levels of about 15% ± 5% (at 9 h, the mean value for three experiments) (Fig. 3A), whereas c-Myc protein reduction was systematically greater than 50%. In fact, late-G<sub>1</sub> PI3K

inhibition markedly reduced c-Myc protein levels at 9 to 18 h poststimulation (Fig. 3A and B).

PI3K/PKB inhibits GSK3β (41), a kinase that phosphorylates c-Myc at Thr 58, thereby triggering Myc degradation (43). PI3K inhibition notably enhanced Thr 58-c-Myc phosphorylation, an event that correlated with c-Myc level reduction (Fig. 3B). The decrease in c-Myc protein levels correlated with the diminished expression of the Myc-transcriptional effectors cyclin D2 and Cdk4 (Fig. 3B). c-Myc stability was further examined in pulse-chase assays. Inhibition of PI3K activity in early G<sub>1</sub> (3 h after serum stimulation) blocked protein synthesis (not shown). Thus, for pulse-chase, we synchronized cells, labeled them with [<sup>35</sup>S]Met between 3 and 9 h after serum addition, and harvested them at 9 h. At this time, the medium was replaced with nonradiolabeled Met/Cys-rich medium, alone or with Ly294002, and cells were collected at 12 and 16 h (Fig. 3C). For the sample treated with Ly294002 at the 9-h time point, the inhibitor was added 30 min before cell harvesting. PI3K inhibition greatly reduced c-Myc stability, an effect that was already evident 30 min after enzyme inhibition (Fig. 3C).

To further define the role of the second G<sub>1</sub> PI3K activity peak in S phase entry, cells were synchronized in G<sub>0</sub>/G<sub>1</sub> and PI3K was inhibited at 7 h after serum stimulation; we examined the consequences for G<sub>1</sub>-phase cyclin levels at different time points. Inhibition of late-G<sub>1</sub> PI3K activity greatly reduced cyclin A protein levels at 9 h, whereas cyclin D3 and E levels were



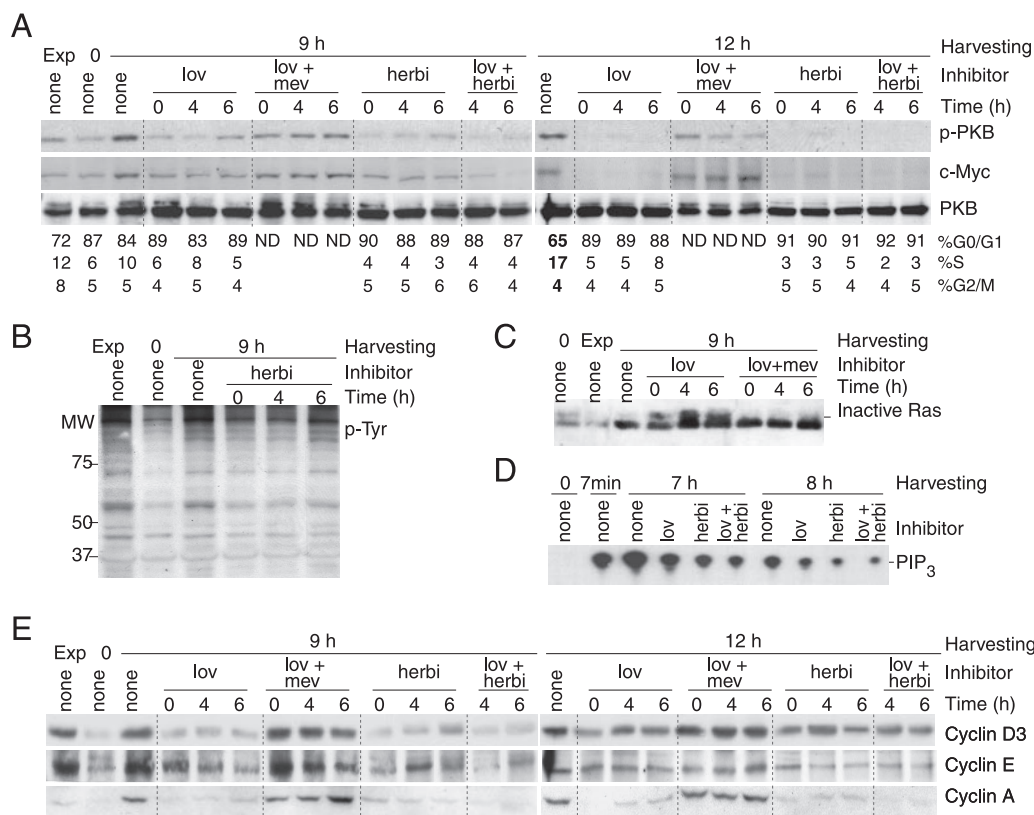


FIG. 2. Ras and Tyr kinases contribute to late-G<sub>1</sub> PI3K activation. (A) p-PKB levels in serum-starved cells, cells in exponential growth, or cells arrested in G<sub>0</sub> and then released in the presence of serum for 9 or 12 h. Lovastatin (lov), lovastatin plus mevalonate (lov+mev), or herbimycin (herbi) was added to some samples at the time of serum addition (time zero) or at 4 or 6 h after serum addition. Cell extracts were examined by WB using anti-p-PKB, -PKB, or -c-Myc antibodies. The percentages of cells in G<sub>0</sub>/G<sub>1</sub>, S, and G<sub>2</sub>/M phases are indicated. (B and C) The efficiencies of the inhibitors were tested in samples prepared as described for panel A by WB using either anti-p-Tyr (B) or anti-pan-Ras (C) antibodies. The slower-migrating, inactive Ras form is indicated. (D) PI3K was immunoprecipitated from cell extracts (see Materials and Methods) and its activity assayed in vitro. Inhibitors were added at 4 h after serum addition and cell extracts collected at the indicated time points. (E) Extracts of the cells used for panel A were examined by WB using anti-cyclin-D3, -E, and -A antibodies. (A to E) Data for one representative experiment (Exp) of four with similar results.

more affected when Ly294002 had been present for prolonged periods (Fig. 3D). The Ras inhibitor lovastatin had a greater effect than Ly294002 in reducing cyclin D3 levels (Fig. 2E and 3D); this is likely due to the Ras/MAPK dependence for cyclin D synthesis (16).

We next tested the effect of inhibiting PI3K on Cdk2 activity. The Cdk2 substrate retinoblastoma protein (Rb) was hypophosphorylated following late- $G_1$  PI3K inhibition (Fig. 3D). Consistently, both cyclin E/Cdk2 and cyclin A/Cdk2 activities decreased after PI3K inhibition (Fig. 3E). The decrease in cyclin A expression paralleled the reduction of cyclin A/Cdk2 activity. Nonetheless, late- $G_1$  PI3K inhibition affected cyclin E/Cdk2 activity more markedly than cyclin E levels. We thus examined whether PI3K inhibition reduced cyclin E/Cdk2 activity by enhancing its association with the Cdk2 inhibitor p27<sup>kip</sup>. PI3K inhibition increased the amount of p27<sup>kip</sup> bound to Cdk2 (see below), explaining the reduction of cyclin E/Cdk2 activity by late- $G_1$  PI3K inhibition. Cyclin E/Cdk2 activity is required for loading of MCM2 onto chromatin (11, 13); PI3K inhibition in advanced  $G_1$  resulted in a notable reduction in the amount of chromatin-bound MCM2 (Fig. 3F).

**Conditional c-Myc-ER activation rescues S phase entry in PI3K inhibitor-treated cells.** PI3K inhibition reduced cyclin A levels and Cdk2 activity. c-Myc regulates G<sub>1</sub> cyclin expression, especially that of cyclin A, and the association of p27<sup>kip</sup> with cyclin/Cdk2 (24, 29, 42). We thus hypothesized that the main function of late-G<sub>1</sub> PI3K activity may be to regulate c-Myc levels. To test this possibility, we used a c-Myc–estrogen receptor fusion protein (c-Myc-ER) that translocates to the nucleus after addition of an estrogen analogue such as 4-OHT (20). We examined whether the S phase entry defects induced by late-G<sub>1</sub> PI3K inhibition were counteracted by c-Myc-ER induction. Cells were infected with c-Myc-ER-expressing viruses (Fig. 4A), arrested in G<sub>0</sub>, and released by serum addition. Some of the cells were treated with 4-OHT alone (at 6.5 h), with Ly294002 (at 7 h after serum addition), or with both. We collected cells at different times and examined S phase entry.

c-Myc-ER expression did not trigger S phase entry in the absence of serum (Fig. 4B and C). After serum addition, c-Myc-ER expression caused a slight increase in S phase entry compared to that in control cells, which was moderately enhanced upon 4-OHT addition (Fig. 4C). We found no notable

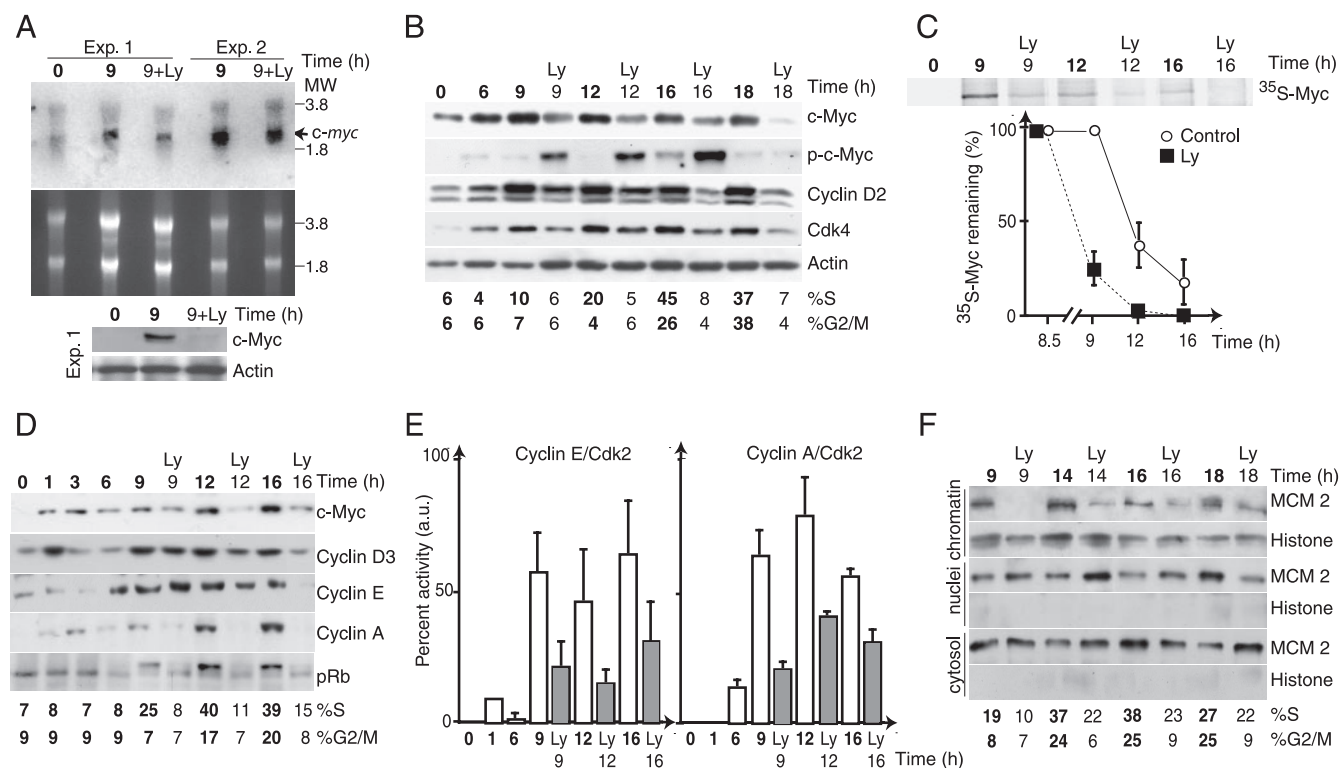


FIG. 3. Late- $G_1$  PI3K inhibition reduces c-Myc and cyclin A expression as well as Cdk2 activity. (A) Total RNA and protein extracts were prepared from cells entering the cell cycle synchronously. Ly294002 was added at 7 h after serum addition; cell harvesting was at 0 and 9 h. Samples were examined by Northern blotting (see Materials and Methods) or by WB, using a c-myc probe or anti-Myc antibody, respectively. The Northern blot corresponds to two different experiments (Exp.). (B) Cell extracts were prepared from cells entering the cell cycle synchronously. Ly294002 was added at 7 h after serum addition. Western blots show the expression of c-Myc, phospho-c-Myc, cyclin D2, Cdk4, and actin. The percentages of cells with sub- $G_1$ ,  $G_0/G_1$ , S, or  $G_2/M$  DNA content are indicated. (C) Synchronized cells were [ $^{35}$ S]Met labeled during the first 9 h after serum addition, and then the medium was replaced with nonlabeled Met/Cys-rich medium alone or with Ly294002 (10  $\mu$ M), and cells were collected at 12 and 16 h. For the sample treated with Ly294002 at 9 h, the inhibitor was added 30 min before harvesting. [ $^{35}$ S]c-Myc was examined by autoradiography. Quantitative-analysis data for three experiments are shown below the blots. (D) The cell extracts used for panel B were examined by WB using anti-c-Myc, -cyclin-D3, -E, -A, and -Rb antibodies. The percentages of cells in S and  $G_2/M$  phases are indicated. (E) Cyclin E/Cdk2 and cyclin A/Cdk2 kinase activities in cyclin E and cyclin A immunoprecipitates, respectively, from cell extracts prepared as described for panel B. Histone H1 (5  $\mu$ g) was used as a substrate.  $^{32}$ P-histone was quantitated, and the activities are represented (in arbitrary units [a.u.]). Data show means  $\pm$  standard deviations for three experiments. (F) Cells entering the cell cycle synchronously, treated as described for panel B, were fractionated into cytosolic, nuclear, and chromatin fractions and were examined by WB using anti-MCM2 and anti-histone antibodies. Panels A to D and F show data for one representative experiment of three with similar results.

differences when 4-OHT was added at 0 or 6.5 h (not shown). Ly294002 treatment reduced the proportion of cells in S phase by 50%, in both c-Myc-ER- and control ER vector-expressing cells (Fig. 4C). Nonetheless, c-Myc-ER induction at 6.5 h in cells treated with Ly294002 in advanced  $G_1$  (7 h) showed almost normal S phase entry levels ( $\sim 85\%$  recovery) compared to what was found for Ly294002-treated control cells (Fig. 4B and C). Induction of c-Myc-ER failed to compensate for the action of PI3K in S phase entry when PI3K was inhibited in early  $G_1$  (0 to 4 h poststimulation) (Fig. 4C and data not shown). Examination of BrdU incorporation confirmed that c-Myc induction at 6.5 h counteracts S phase entry defects in cells treated with Ly294002 in advanced  $G_1$  (Fig. 4D). Comparable results were obtained using the PI3K inhibitor wortmannin (not shown). These data suggest that the main function of late- $G_1$  PI3K activity is to regulate c-Myc protein levels.

**Expression of a GSK3 $\beta$ -resistant c-Myc mutant rescues the cell cycle entry defects induced by inhibiting late- $G_1$  PI3K activity.** PI3K/PKB inactivate GSK3 $\beta$ , an enzyme that targets

c-Myc for degradation (43). To confirm that c-Myc stabilization is the main role of PI3K activity in late  $G_1$ , we examined the effect of inhibiting PI3K in cells expressing the c-Myc $_{T58A}$  substitution mutant, which is resistant to GSK3 $\beta$  action (14).

Cells were transfected with GFP control vector or with cDNAs encoding GFP fused to wild-type (WT) c-Myc or c-Myc $_{T58A}$  (Fig. 5A). Transfected cells were sorted, and cultures were synchronized, released from arrest, and treated with Ly294002 at 7 h after serum addition. Cells were harvested at different time points. Overexpression of either WT c-Myc or c-Myc $_{T58A}$  induced apoptosis and cell cycle entry in the absence of serum (Fig. 5B). Late- $G_1$  PI3K inhibition reduced cell cycle entry in control cells and to a lesser extent in cells overexpressing WT c-Myc; c-Myc $_{T58A}$  expression, however, largely restored cell cycle entry (Fig. 5B). To reduce c-Myc expression levels, cells were infected with viruses encoding c-Myc $_{T58A}$ . Under these conditions, c-Myc $_{T58A}$  did not significantly induce cell cycle entry in the absence of serum (Fig. 5C). Synchronous-cell-infected cultures were treated with Ly294002 at 7 h



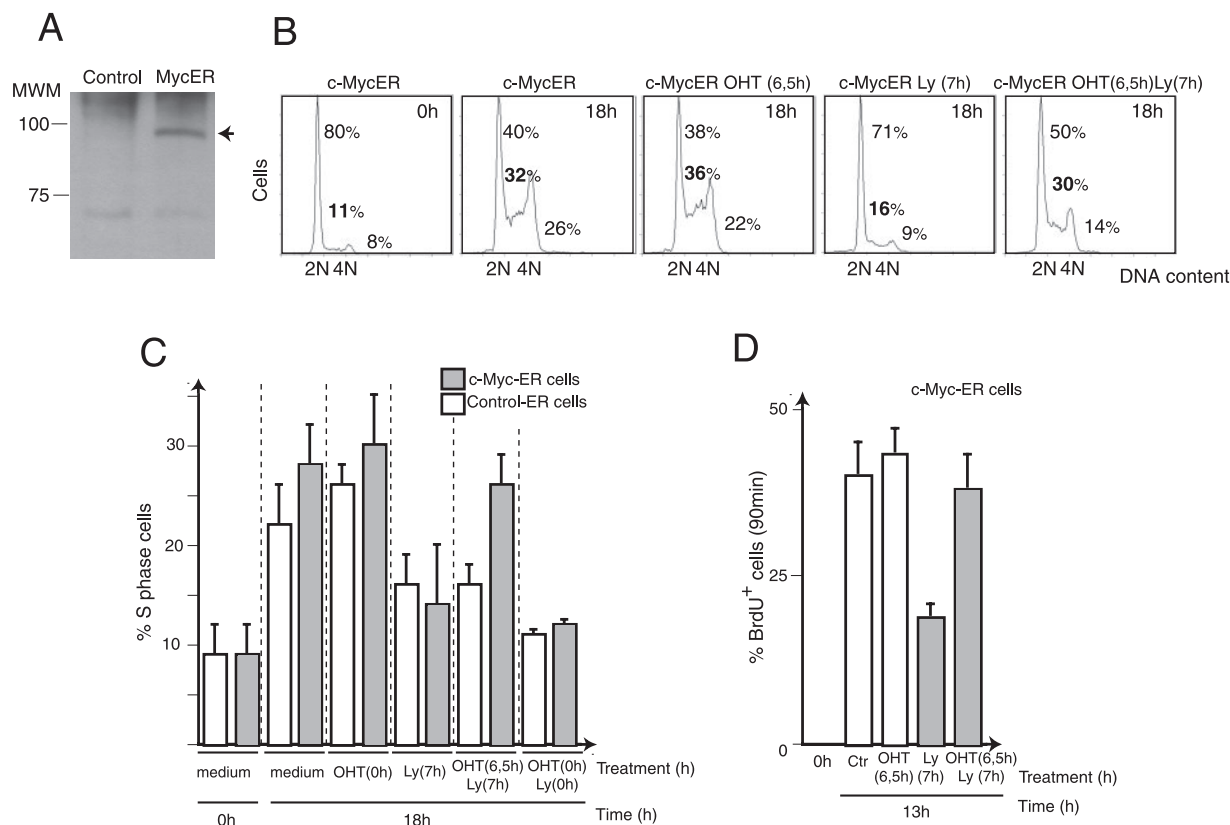


FIG. 4. Conditional activation of c-Myc-ER rescues S phase entry blockade induced by late- $G_1$  PI3K inhibition. (A) c-Myc-ER expression was examined in NIH 3T3 c-Myc-ER-infected cells by WB using anti-Myc antibody. (B) Cell cycle profiles of c-Myc-ER cells in quiescence (time zero) or at 18 h after serum addition, alone or in the presence of OHT (200 nM; added at 6.5 h after serum addition) and/or Ly294002 (10  $\mu$ M; added at 7 h after serum addition). The figure shows results for one representative experiment of three performed. (C) Percentages of c-Myc-ER and control cells in S phase. Cells were treated as described for panel B. Data for a sample of cells treated with OHT (200 nM) and Ly294002 (10  $\mu$ M) at the time of serum addition (time zero) are included. Data shown are mean values for three experiments. (D) BrdU incorporation in NIH 3T3 c-Myc-ER-infected cells entering the cell cycle synchronously as in panel B and collected at 13 h after serum addition. BrdU (10  $\mu$ M) was present for the last 90 min. Data shown are means  $\pm$  standard deviations for three experiments.

after serum addition and harvested at different time points. PI3K inhibition blocked cell cycle entry in control cells, but cell cycle entry was nearly normal in cells expressing c-Myc<sub>T58A</sub> (Fig. 5D). These results indicate that a stable form of c-Myc substitutes for PI3K action in late  $G_1$ .

**c-Myc<sub>T58A</sub> expression rescues cyclin A expression, Cdk2 activity, and MCM2 loading defects induced by late- $G_1$  PI3K inhibition.** To confirm that the primary effect of PI3K activity in advanced  $G_1$  is to stabilize c-Myc, we examined whether c-Myc<sub>T58A</sub> expression compensated for the cell cycle entry defects induced by late- $G_1$  PI3K inhibition. PI3K inhibition moderately affected cyclin D3 and E expression levels (see above). Similarly, c-Myc<sub>T58A</sub> expression did not markedly alter cyclin D3 (not shown) or cyclin E levels (Fig. 6A). In contrast, cyclin A expression levels were greatly reduced upon late- $G_1$  PI3K inhibition (Fig. 6A). c-Myc<sub>T58A</sub> expression increased cyclin A expression in Ly294002-treated cells and moderately increased basal cyclin A levels (Fig. 6A). Moreover, whereas hyperphosphorylated Rb levels, cyclin E/Cdk2, and cyclin A/Cdk2 kinase activities were reduced by late- $G_1$  PI3K inhibition in control cells, they were virtually unaffected in c-Myc<sub>T58A</sub>-expressing cells (Fig. 6A to C). As c-Myc controls the levels of Cdk2 bound to p27<sup>kip</sup> (29, 42), we tested whether

p27<sup>kip</sup>-Cdk2 association was affected by c-Myc<sub>T58A</sub> expression. Ly294002 treatment at 7 h in synchronous-cell cultures increased the association of p27<sup>kip</sup> with cyclin E/Cdk2 in controls, but association was lower and resistant to PI3K inhibition in c-Myc<sub>T58A</sub>-expressing cells (Fig. 6D). Similar results were obtained using c-Myc-ER-expressing cells treated with 4-OHT (at 6.5 h), Ly294002 (at 7 h), or both simultaneously (Fig. 6E and data not shown). In fact, c-Myc-ER induction corrected the defects in S phase entry, cyclin A expression, and Rb phosphorylation induced by late- $G_1$  PI3K inhibition (Fig. 6E).

We also examined the consequences of expressing c-Myc<sub>T58A</sub> on the loading of MCM2 onto chromatin. In control cells, MCM2 loading was still low at 9 h (similar to that observed at 0 h), increased at 12 to 16 h, and was blocked by PI3K inhibition. In contrast, in c-Myc<sub>T58A</sub> cells, MCM2 loading increased by 9 h and remained insensitive to late- $G_1$  PI3K inhibition (Fig. 7).

## DISCUSSION

Activation of PI3K in late  $G_1$  is essential for cell cycle entry (1, 12, 17). We examined the signals involved in late- $G_1$  PI3K activation and the mechanisms by which this event controls the  $G_1$ -to-S transition. We report that tyrosine kinase and Ras

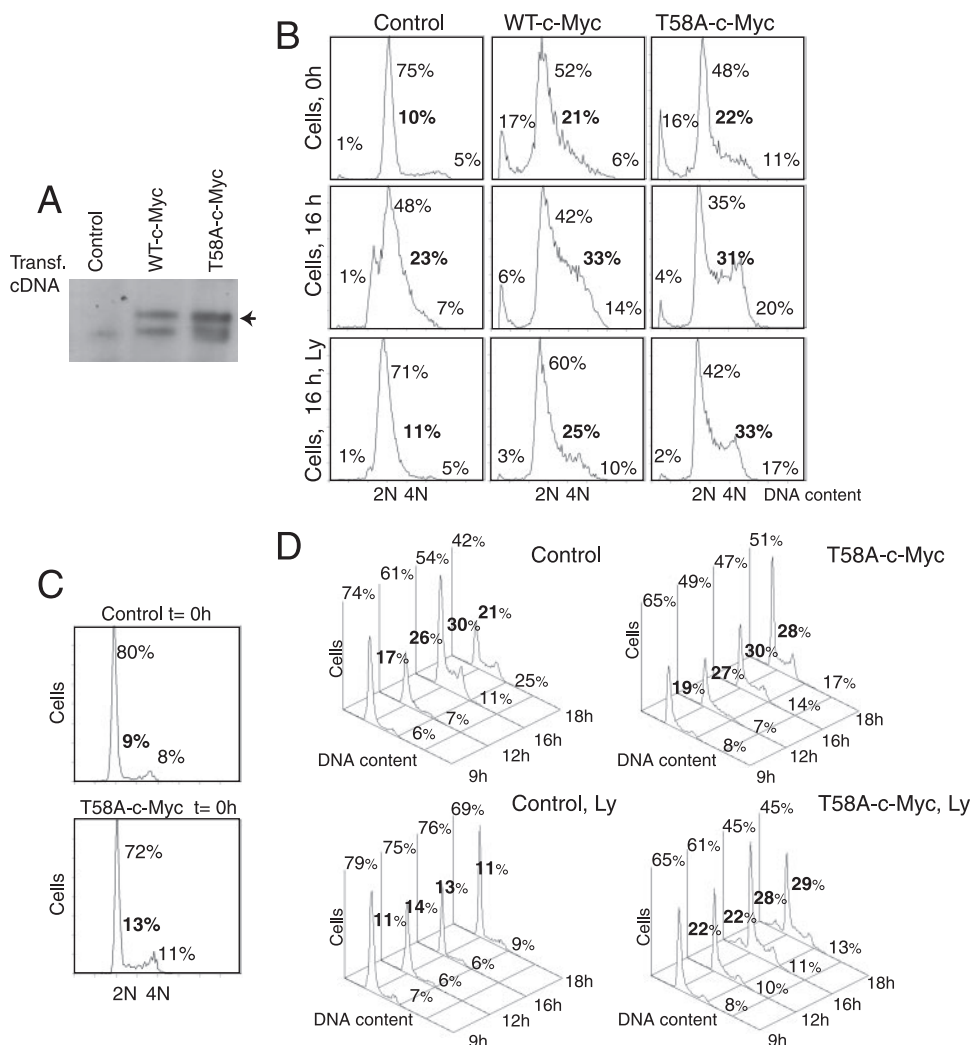
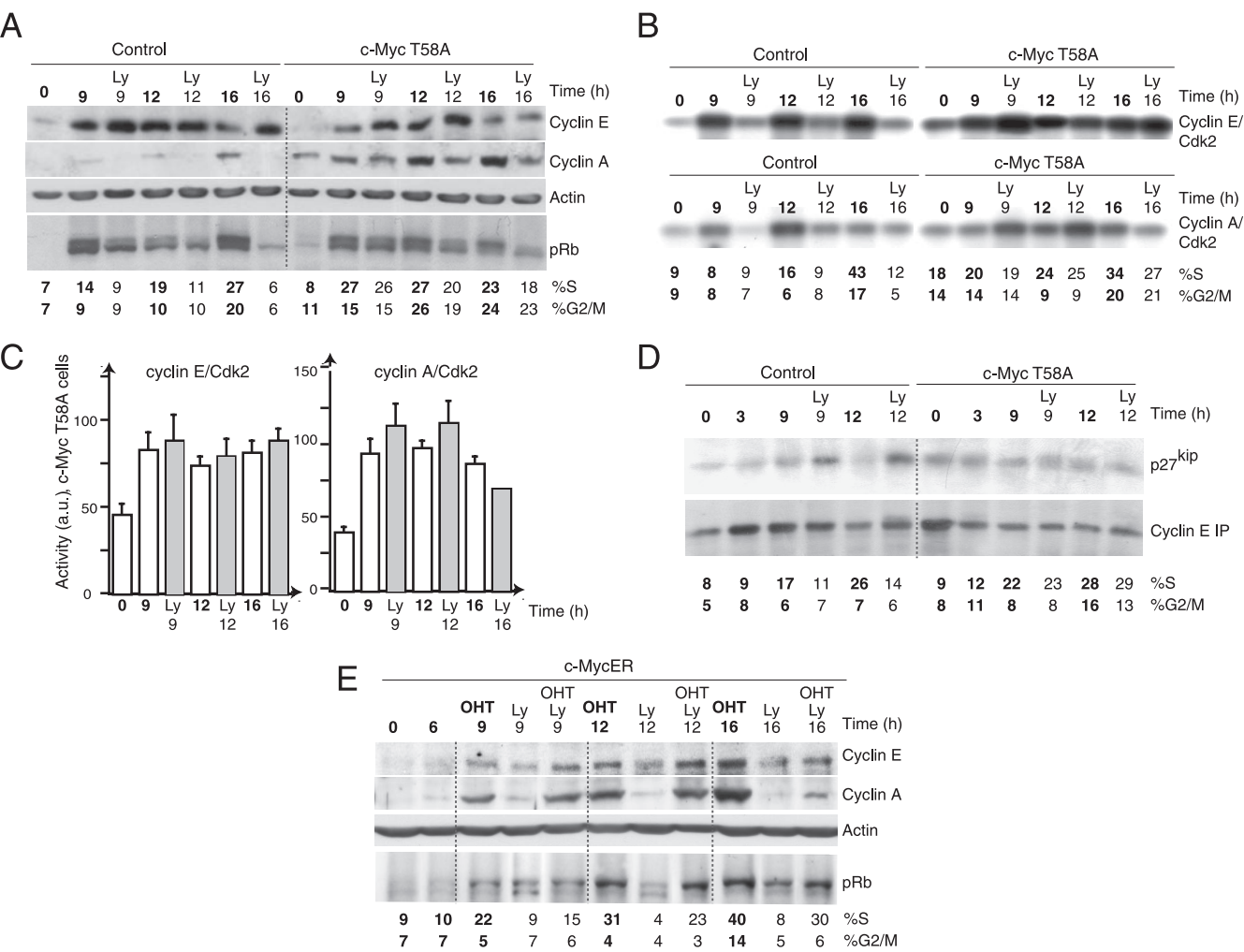


FIG. 5. Expression of c-Myc T58A rescues cell cycle entry defects induced by late- $G_1$  PI3K inhibition. (A) WT c-Myc and c-Myc<sub>T58A</sub> expression in NIH 3T3 cells, tested by WB using anti-Myc antibody. (B) DNA content in representative NIH 3T3 cells transfected (Transf.) with a control vector or cDNA encoding WT c-Myc or c-Myc<sub>T58A</sub>. Cells were arrested by serum deprivation (time zero) and released by serum addition for 16 h. Some samples were incubated with Ly294002 added 7 h after serum stimulation. (C and D) DNA content in representative NIH 3T3 cells infected with a control virus or a virus encoding c-Myc<sub>T58A</sub>. Infected cells were arrested by serum deprivation (C) or first arrested and then released by serum addition for 9, 12, 16, and 18 h (D). Some samples were incubated with Ly294002 added 7 h after serum stimulation. (A to D) Data representative of one experiment of four with similar results. Percentages of cells in  $G_0/G_1$ , S (in bold), and  $G_2/M$  phases are indicated.

activation are required to induce the PI3K/PKB pathway in late  $G_1$ . Since PI3K/PKB inactivates GSK3 $\beta$ , the enzyme that targets c-Myc for degradation (41, 43), we hypothesized that late- $G_1$  PI3K activation may be essential for c-Myc stabilization. We observed that PI3K inhibition in advanced  $G_1$  decreases c-Myc and cyclin A levels, reduces cyclin E/Cdk2 and cyclin A/Cdk2 activity, and increases the fraction of p27<sup>kip</sup> bound to cyclin E/Cdk2; c-Myc-deficient cells show these defects (23, 24, 42). Moreover, c-Myc induction in late  $G_1$  and the expression of a c-Myc mutant (c-Myc<sub>T58A</sub>) (14) that does not require PI3K/PKB for stabilization counteract the cell cycle entry defects induced by PI3K inhibition in late  $G_1$ , including those related to DNA synthesis, cyclin A expression, cyclin E/Cdk2 and cyclin A/Cdk2 activity, and the association of p27<sup>kip</sup> with cyclin E/Cdk2. We conclude that c-Myc stabilization is a major role for PI3K activation in late  $G_1$ .

c-myc mRNA and protein both have very short half-lives (20 to 30 min). To achieve the c-Myc expression levels required for cell cycle entry, c-Myc stability must be regulated during  $G_1$  (9, 30); we show that late- $G_1$  PI3K activation stabilizes c-Myc. This conclusion is further supported by our in-progress studies using interfering RNA and constitutive active mutants of class I<sub>A</sub> PI3K isoforms. Although these tools do not allow distinction between the first and second PI3K activity peaks in  $G_1$ , they confirm the role of PI3K in cell cycle entry and in c-Myc expression control. Whereas activation of PI3K accelerates cell cycle entry and increases c-Myc levels, decrease of PI3K levels reduces S phase entry and c-Myc content (not shown).

Phosphorylation-dependent regulation of c-Myc stability involves two key residues, T58 and S62. MAPK mediates S62 phosphorylation, which stabilizes c-Myc, but is required for subsequent T58 phosphorylation by GSK3 $\beta$ , which then in-



**FIG. 6.** c-Myc<sub>T58A</sub> expression counteracts the cyclin A expression, Cdk2 activity, and MCM2 chromatin loading defects induced by late-G<sub>1</sub> PI3K inhibition. (A) Control and c-Myc<sub>T58A</sub>-expressing cells were arrested in G<sub>0</sub> and then released and treated with Ly294002 at 7 h after serum addition. Cells were harvested at different time points (indicated) and extracts examined by WB using anti-cyclin E, -cyclin A, -actin, and -Rb antibodies. (B) Cyclin E/Cdk2 and cyclin A/Cdk2 kinase activities in cyclin E and cyclin A immunoprecipitates, respectively, of cell extracts from control and c-Myc<sub>T58A</sub>-expressing cells treated as described for panel A. Cdk2 activity was measured as described in the legend to Fig. 3. (C) Cyclin E/Cdk2 and cyclin A/Cdk2 activities in c-Myc<sub>T58A</sub>-expressing cells were examined by *in vitro* kinase assays performed as described for panel B. Data shown are means  $\pm$  standard deviations for three experiments. (D) The cells used for panel A were lysed, and cyclin E was immunoprecipitated from lysates (200  $\mu$ g). Samples were resolved and examined by WB using anti-p27<sup>kip</sup> or anti-cyclin E antibody. (E) Synchronized c-Myc-ER-expressing cells were treated with 4-OHT (at 6.5 h), Ly294002 (at 7 h), or both simultaneously; cells were collected at different time points (indicated). Cyclin E, cyclin A, pRb, and actin levels were examined by WB. (A, B, D, and E) Data for one representative experiment of three with similar results. Percentages of cells in S and G<sub>2</sub>/M phases are indicated.

duces c-Myc degradation (43). T58 phosphorylation nonetheless appears to be the key destabilizing event, as it represents a major mutation hot spot in Burkitt's lymphomas (14). Since S62 phosphorylation is a prerequisite for T58 phosphorylation, c-Myc might also be phosphorylated in late G<sub>1</sub> by MAPK, as we observed concomitant activations of MAPK and PI3K at this point (not shown).

c-Myc function is linked to its transcription factor activity, which is required for its transforming capacity (3, 9, 30). c-Myc regulates transcription by association with the Max protein. Gene expression regulated by c-Myc/Max involves several mechanisms that include chromatin remodeling as well as recruitment of RNA polymerases and transcription elongation factors (9, 28). c-Myc regulates the expression of a number of

target genes, including cyclins D and E and, to a large extent, cyclin A (30). The first c-Myc expression peak in G<sub>1</sub> occurs at  $\sim$ 1 h after serum stimulation. Since c-Myc promotes cyclin D and E expression (24), the first c-Myc expression peak may trigger the expression of these cyclins in early/mid-G<sub>1</sub>. Later on, c-Myc is essential for cyclin A expression, as well as for inhibiting the association of p27<sup>kip</sup> with Cdk2 complexes (24, 29, 42). The kinetics of cyclin A expression, its reduction following c-Myc destabilization (by late-G<sub>1</sub> PI3K inhibition), and the association of p27<sup>kip</sup> with cyclin E/Cdk2 complexes suggest that the second c-Myc expression peak regulates cyclin A induction and Cdk2 activity by controlling its association with p27<sup>kip</sup> (29, 42).

Although late-G<sub>1</sub> PI3K action is nearly identical to that of

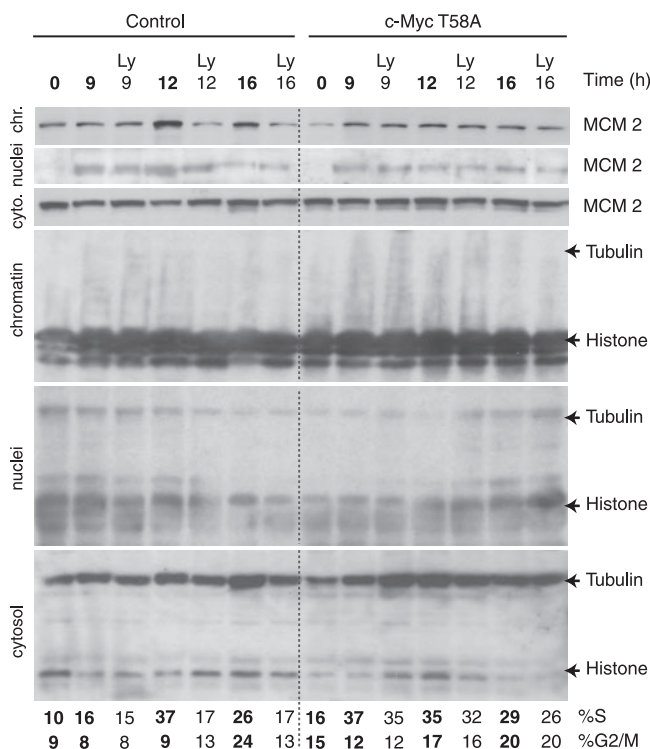


FIG. 7. c-Myc<sub>T58A</sub> expression counteracts the reduced MCM2 chromatin loading induced by PI3K inhibition in late G<sub>1</sub>. Western blots documenting MCM2 protein levels in different subcellular fractions (as shown in Fig. 3F) of cells treated as described in the legend to Fig. 6A are shown. WB analyses using anti-tubulin and -histone antibodies were used as controls for fraction purity.

c-Myc, PI3K and c-Myc have otherwise unrelated functions and appear to cooperate for cell cycle entry (17), suggesting distinct functions. PI3K/PKB activation is required for inactivation of FoxO transcription factors, which inhibit the expression of several c-Myc targets, providing a mechanism for the cooperative action of c-Myc and PI3K in early G<sub>1</sub> (5). In fact, inhibition of PI3K in early G<sub>1</sub> (during the first 6 h) impaired cell growth and cycle entry, and this blockade was not counteracted by c-Myc-ER induction (Fig. 4C). In early G<sub>1</sub>, PI3K regulates cell growth, FoxO transcription factor inactivation, and GSK3 $\beta$  inhibition, events that in turn control cyclin D levels (1, 2, 22, 25, 31, 33, 36). Nonetheless, Tyr-K and Ras are reactivated in mid-/late G<sub>1</sub>, driving PI3K activation (Fig. 2). We show that the main role of late-G<sub>1</sub> PI3K activity is to stabilize c-Myc. Stabilized c-Myc in turn triggers cyclin A synthesis, reduces the binding of p27<sup>kip</sup> to Cdk2 complexes, and induces cyclin E/Cdk2 (which regulates MCM2 loading) and cyclin A/Cdk2 activities. These events are crucial for DNA synthesis induction, explaining the requirement for PI3K activity in late G<sub>1</sub> for cell cycle entry.

#### ACKNOWLEDGMENTS

We thank J. León and S. Mañes for continuous advice, L. Roman for checking RNA stability, S. Lowe for the c-Myc<sub>T58A</sub> cDNA, G. Evan for c-MycER plasmid, and C. Mark for editorial assistance.

A.K. received a predoctoral fellowship associated with a project financed by the Fundación Ramón Areces, and M.M. received a predoctoral FPU fellowship from the Spanish Ministry of Education and

Science. This work was financed in part by grants from the AICR Foundation, the Fundación Ramón Areces, the European Union (QLRT2001-02171), and the Spanish DGCyT (SAF2004.05955). The Department of Immunology and Oncology was founded and is supported by the Spanish National Research Council (CSIC) and by Pfizer.

#### REFERENCES

- Alvarez, B., A. C. Martinez, B. M. Burgering, and A. C. Carrera. 2001. Forkhead transcription factors contribute to execution of the mitotic programme in mammals. *Nature* **413**:744–747.
- Alvarez, B., F. Garrido, J. A. Garcia-Sanz, and A. C. Carrera. 2003. Phosphoinositide 3-kinase activation regulates cell division time by coordinated control of cell mass and cell cycle progression rate. *J. Biol. Chem.* **278**:26466–26473.
- Amati, B., K. Alevizopoulos, and J. Vlach. 1998. Myc and the cell cycle. *Front. Biosci.* **3**:250–268.
- Blow, J. J., and A. Dutta. 2005. Preventing re-replication of chromosomal DNA. *Nat. Rev. Mol. Cell Biol.* **6**:476–486.
- Bouchard, C., J. Marquardt, A. Bras, R. H. Medema, and M. Eilers. 2004. Myc-induced proliferation and transformation require Akt-mediated phosphorylation of FoxO proteins. *EMBO J.* **23**:2830–2840.
- Chan, T. O., U. Rodeck, A. M. Chan, A. C. Kimmelman, S. E. Rittenhouse, G. Panayotou, and P. N. Tsichlis. 2002. Small GTPases and tyrosine kinases coregulate a molecular switch in the phosphoinositide 3-kinase regulatory subunit. *Cancer Cell* **1**:181–191.
- Coverley, D., H. Laman, and R. A. Laskey. 2002. Distinct roles for cyclins E and A during DNA replication complex assembly and activation. *Nat. Cell Biol.* **4**:523–528.
- Cvetc, C. A., and J. C. Walter. 2006. Getting a grip on licensing: mechanism of stable Mcm2-7 loading onto replication origins. *Mol. Cell* **21**:143–144.
- Dang, C. V. 1999. c-Myc target genes involved in cell growth, apoptosis and metabolism. *Mol. Cell. Biol.* **19**:1–11.
- del Real, G., S. Jimenez-Baranda, E. Mira, R. A. Lacalle, P. Lucas, C. Gomez-Mouton, M. Alegret, J. M. Pena, M. Rodriguez-Zapata, M. Alvarez-Mon, A. C. Martinez, and S. Manes. 2004. Statins inhibit HIV-1 infection by down-regulating Rho activity. *J. Exp. Med.* **200**:541–547.
- Eklholm-Reed, S., J. Mendez, D. Tedesco, A. Zetterberg, B. Stillman, and S. I. Reed. 2004. Deregulation of cyclin E in human cells interferes with prereplication complex assembly. *J. Cell Biol.* **165**:789–800.
- García, Z., A. Kumar, M. Marques, I. Cortes, and A. C. Carrera. 2006. Phospho-inositide 3-kinase controls early and late events in mammalian cell division. *EMBO J.* **25**:655–661.
- Geng, Y., Q. Yu., E. Sicinska, M. Das, J. E. Schneider, S. Bhattacharya, W. M. Rideout, R. T. Bronson, H. Gardner, and P. Sicinski. 2003. Cyclin E ablation in the mouse. *Cell* **114**:431–443.
- Hemann, M. T., A. Bric, J. Teruya-Feldstein, A. Herbst, J. A. Nilsson, C. Cordon-Cardo, J. L. Cleveland, W. P. Tansey, and S. W. Lowe. 2005. Evasion of the p53 tumour surveillance network by tumour-derived MYC mutants. *Nature* **436**:807–811.
- Jiménez, C., C. Hernandez, B. Pimentel, and A. C. Carrera. 2002. The p85 regulatory subunit controls sequential activation of phosphoinositide 3-kinase by Tyr kinases and Ras. *J. Biol. Chem.* **277**:41556–41562.
- Jirmanova, L., M. Afanassieff, S. Gobert-Gosse, S. Markossian, and P. Savatier. 2002. Differential contributions of ERK and PI3K to the regulation of cyclin D1 expression and to the control of the G1/S transition in mouse ES cells. *Oncogene* **21**:5515–5528.
- Jones, S. M., and A. Kazlauskas. 2001. Growth-factor-dependent mitogenesis requires two distinct phases of signalling. *Nat. Cell Biol.* **3**:165–172.
- Jones, S. M., R. Klinghoffer, G. D. Prestwich, A. Toker, and A. Kazlauskas. 1999. PDGF induces an early and a late wave of PI 3-kinase activity, and only the late wave is required for progression through G1. *Curr. Biol.* **9**:512–521.
- Klippel, A., M. A. Escobedo, M. S. Wachowicz, G. Apell, T. W. Brown, M. A. Giedlin, W. N. Kavanaugh, and L. T. Williams. 1998. Activation of phosphatidylinositol 3-kinase is sufficient for cell cycle entry and promotes cellular changes characteristic of oncogenic transformation. *Mol. Cell. Biol.* **18**:5699–5711.
- Littlewood, T. D., D. C. Hancock, P. S. Danielian, M. G. Parker, and G. I. Evan. 1995. A modified oestrogen receptor ligand-binding domain as an improved switch for the regulation of heterologous proteins. *Nucleic Acids Res.* **23**:1686–1690.
- Madine, M. A., M. Swietlik, C. Pelizon, P. Romanowski, A. D. Mills, and R. A. Laskey. 2000. The roles of the MCM, ORC, and Cdc6 proteins in determining the replication competence of chromatin in quiescent cells. *J. Struct. Biol.* **129**:198–210.
- Martínez-Gac, L., M. Marqués, Z. García, M. Campanero, and A. C. Carrera. 2004. Control of cyclin G<sub>2</sub> mRNA expression by forkhead transcription factors: a novel mechanism for cell cycle control by phosphoinositide 3-kinase and forkhead. *Mol. Cell. Biol.* **24**:2181–2189.
- Mateyak, M. K., A. J. Obaya, S. Adachi, and J. M. Sedivy. 1997. Phenotypes



- of c-Myc-deficient rat fibroblasts isolated by targeted homologous recombination. *Cell Growth Differ.* **8**:1039–1048.
24. **Mateyak, M. K., A. J. Obaya, and J. M. Sedivy.** 1999. c-Myc regulates cyclin D-Cdk4 and -Cdk6 activity but affects cell cycle progression at multiple independent points. *Mol. Cell. Biol.* **19**:4672–4683.
  25. **Medema, R. H., G. J. Kops, J. L. Bos, and B. M. Burgering.** 2000. AFX-like Forkhead TF mediate cell-cycle regulation by Ras and PKB through p27<sup>Kip1</sup>. *Nature* **404**:782–787.
  26. **Méndez, J., and B. Stillman.** 2002. Chromatin association of human origin recognition complex, Cdc6, and minichromosome maintenance proteins during the cell cycle: assembly of prereplication complexes in late mitosis. *Mol. Cell. Biol.* **20**:8602–8612.
  27. **Nishitani, H., and Z. Lygerou.** 2002. Control of DNA replication licensing in a cell cycle. *Genes Cells* **7**:523–534.
  28. **Pelengaris, S., M. Khan, and G. Evan.** 2002. c-MYC more than just a matter of life and death. *Nat. Rev. Cancer* **2**:764–776.
  29. **Perez-Roger, I., D. L. Solomon, A. Sewing, and H. Land.** 1997. Myc activation of cyclin E/Cdk2 kinase involves induction of cyclin E gene transcription and inhibition of p27<sup>Kip1</sup> binding to newly formed complexes. *Oncogene* **14**:2373–2381.
  30. **Ponzielli, R., S. Katz, D. Barsyte-Lovejoy, and L. Z. Penn.** 2005. Cancer-therapeutics: targeting the dark side of Myc. *Eur. J. Cancer* **41**:2485–2501.
  31. **Ryves, W. J., and A. J. Harwood.** 2003. The interaction of glycogen synthase kinase-3 (GSK-3) with the cell cycle. *Prog. Cell Cycle Res.* **5**:489–495.
  32. **Schlessinger, J.** 2000. Cell signaling by receptor tyrosine kinases. *Cell* **103**:211–225.
  33. **Schmidt, M., S. Fernandez de Mattos, A. van der Horst, R. Klompaker, G. J. Kops, E. W. Lam, B. M. Burgering, and R. H. Medema.** 2002. Cell cycle inhibition by FoxO transcription factors involves downregulation of cyclin D. *Mol. Cell. Biol.* **22**:7842–7852.
  34. **Schorl, C., and J. M. Sedivy.** 2003. Loss of protooncogene c-Myc function impedes G1 phase progression both before and after the restriction point. *Mol. Biol. Cell* **14**:823–835.
  35. **Serrano, M., A. W. Lin, M. E. McCurrach, D. Beach, and S. W. Lowe.** 1997. Oncogenic *ras* provokes premature cell senescence associated with accumulation of p53 and p16<sup>INK4a</sup>. *Cell* **88**:593–602.
  36. **Sherr, C. J., and J. M. Roberts.** 1999. CDK inhibitors: positive and negative regulators of G1-phase progression. *Genes Dev.* **13**:1501–1512.
  37. **Shin, I., F. M. Yakes, F. Rojo, N. Y. Shin, A. V. Bakin, J. Baselga, and C. L. Arteaga.** 2002. PKB/Akt mediates cell-cycle progression by phosphorylation of p27<sup>Kip1</sup> at threonine 157 and modulation of its cellular localization. *Nat. Med.* **8**:1145–1152.
  38. **Stacey, D., and A. Kazlauskas.** 2002. Regulation of Ras signaling by the cell cycle. *Curr. Opin. Genet. Dev.* **12**:44–46.
  39. **Taylor, C. C.** 2000. Platelet-derived growth factor activates porcine thecal cell PI3K-Akt/PKB and Ras-extracellular signal-regulated kinase-1/2 kinase signaling pathways via the platelet-derived growth factor- $\beta$  receptor. *Endocrinology* **141**:1545–1553.
  40. **Uckun, F. M., R. K. Narla, T. Zeren, Y. Yanishevski, D. E. Myers, B. Waurzyniak, O. Ek, E. Schneider, Y. Messinger, L. M. Chelstrom, R. Gunther, and W. Evans.** 1998. In vivo toxicity, pharmacokinetics, and anti-cancer activity of Genistein linked to recombinant human epidermal growth factor. *Clin. Cancer Res.* **4**:1125–1134.
  41. **Van Weeren, P. C., K. M. de Bruyn, A. M. de Vries-Smits, J. van Lint, and B. M. Burgering.** 1998. Essential role for protein kinase B (PKB) in insulin-induced glycogen synthase kinase 3 inactivation. Characterization of dominant-negative mutant of PKB. *J. Biol. Chem.* **273**:13150–13156.
  42. **Vlach, J., S. Hennecke, K. Alevizopoulos, D. Conti, and B. Amati.** 1996. Growth arrest by the CDK inhibitor p27<sup>Kip1</sup> is abrogated by c-Myc. *EMBO J.* **15**:6595–6604.
  43. **Yeh, E., M. Cunningham, H. Arnold, D. Chasse, T. Monteith, G. Ivaldi, W. C. Hahn, P. T. Stukenberg, S. Shenolikar, T. Uchida, C. M. Counter, J. R. Nevins, A. R. Means, and R. A. Sears.** 2004. A signalling pathway controlling c-Myc degradation that impacts oncogenic transformation of human cells. *Nat. Cell Biol.* **6**:308–318.